DESIGN MANUAL
FOR
BUOYANT SCREW PROPULSION

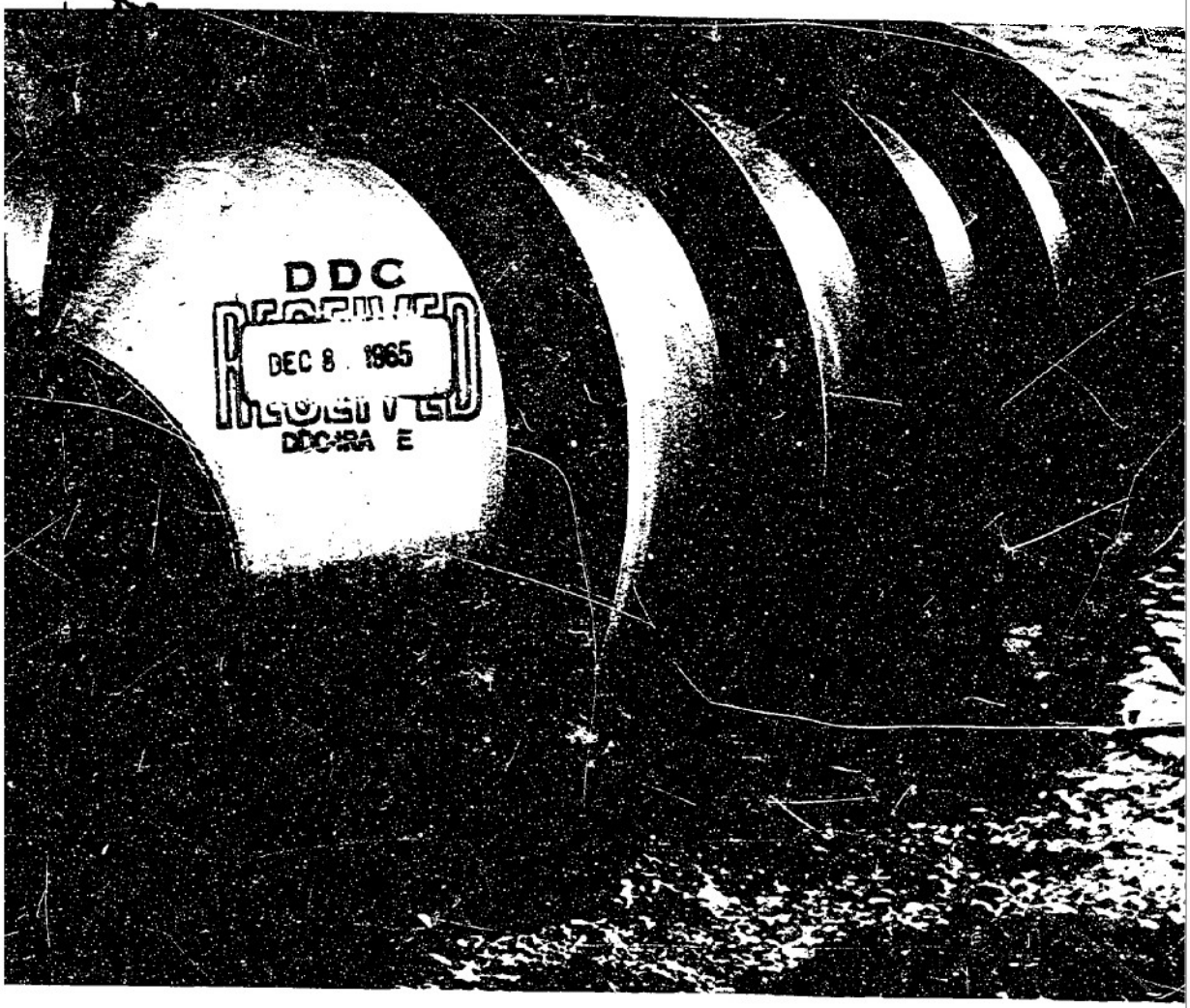

DEFENSE OPERATIONS DIVISION
CHRYSLER CORPORATION
DETROIT, MICHIGAN

DESIGN MANUAL

FOR

BUOYANT SCREW PROPULSION

SUBMITTED TO

CHIEF, BUREAU OF SHIPS

CODE 529V

PREPARED BY

R.F KRESS

STAFF NAVAL ARCHITECT

APPROVED BY

M. J. NEUMEYER

PROGRAM MANAGER

DECEMBER 2, 1965

DEFENSE OPERATIONS DIVISION CHRYSLER CORPORATION

DEFENSE ENGINEERING

P.O. BOX 757 DETROIT, MICH., 48231

NTIS DISCLAIMER

PREFACE

Propulsion by the buoyant screw principle is not new but, the projection of quantified vehicle mobility requirements using this principle by model testing is a new field. This manual represents a significant advance in buoyant screw technology and is published under Contract NObs 4633, a contract between the U.S. Navy, Bureau of Ships and the Chrysler Corporation.

Chrysler Corporation has been engaged in buoyant screw propulsion activity since 1961, gaining considerable experience with two "Marsh Screw Amphibians". These vehicles were operated for approximately 500 hours in a variety of terrain including:

- Mud flats, bayous, and heavily vegetated swamps in Louisiana.
- Silt, clay and sand in Mississippi.
- Ocean beaches and tidal basins in California.
- Swamp, snow, lakes and beaches in Michigan.
- Muskeg in Canada.

Now, under NObs 4633, full scale experience has been complemented by extensive model testing to establish rational design guides for future screw vehicles. The data contained in this manual represents many hours of model testing, a single graph representing as many as 50 runs down a 300 foot water test basin. For water tests it is estimated that 2500 runs were made in the test basin. For soil propulsion, approximately 1000 runs were made in the test bin.

CONTENTS

CONTENTS

ILLUSTRATIONS

ILLUSTRATIONS - Continued

ILLUSTRATIONS – Continued

ILLUSTRATIONS - Continued

ILLUSTRATIONS - Continued

ILLUSTRATIONS - Continued

APPENDIX C

CHAPTER I

SUMMARY

This manual contains the charts, graphs, and calculations necessary to establish design criteria for buoyant screw propulsion. The manual was developed from a study performed under contract NObs 4633 sponsored by the Department of Defense, ARPA, and administered through the Bureau of Ships.

In the past century numerous systematic propeller series and systematically varied hull forms have been tested, and specialized design techniques based on such data developed. Numerous model tests of tracks and wheels have also been conducted in many soil conditions. Testing, however, has not been performed on the unique propulsion system of the Marsh Screw Amphibian with the intent of establishing data and a related design technique.

Since design data for a buoyant screw concept was not available, additional basic research was conducted with the intent of obtaining a technique for predicting performance in water and over various terrains. Model tests appeared to be the most practical method for obtaining the large amount of data required. The validity of these model tests could be established by comparison with full-size vehicle data.

Two model test programs were conducted. The water tests were performed at the naval architecture water basin of the University of

Michigan, and the soil tests at Davidson Laboratories at Stevens Institute of Technology. Two phases of tests were conducted at both laboratories. The first was the testing of a systematically varied series of buoyant screw models and the second was the testing of certain miscellaneous configurations.

The first test in water was one which established the optimum length/diameter ratio. These tests were performed at various speeds with the model free to pitch and heave. All other motions were prevented. When the preferred length/diameter ratio was established, a systematic series of rotor configurations were investigated. This investigation established the blade height and helix angle desired for optimum water performance.

The next phase of tests investigated miscellaneous configurations merely to indicate trends in horsepower requirements. Tests on a progressive helix angle along the length of the rotor and on a tapered rotor body were performed. The progressive helix configuration continuously accelerates flow rearward over the entire length of the rotor. The tapered rotor is an attempt to counteract the bow-up attitude of constant section rotors while continuously accelerating flow rearward. An investigation of rotor tail configuration, aft strut configuration, and shrouded rotors was made to obtain the relative merit of each. Tests to determine the interference and interaction effects for various rotor spacings were

performed. Tests on rotors of a different scale were conducted to establish the scaling factors to be used in a final design.

The results obtained from the water model tests were then compared with those results obtained from extensive tests on the Marsh Screw Amphibian.

The second model test program was conducted in various soils representing typical land operating conditions. The first tests in the various soil conditions chosen established the optimum length/diameter ratio. These tests were performed in a manner similar to the water tests. Since the length/diameter ratio was established by the water performance requirement, any length/diameter ratio differing from that previously determined in water provided an estimate of the additional power required. A systematic series of rotor configurations with the length/diameter ratio established by the water performance was investigated in various soil conditions. This data furnished the power requirements for various rotor configurations and provided a means for determining what blade height and helix angle provides the maximum thrust for a given amount of power.

The results obtained from the model soil test program were compared with data obtained from tests on the Marsh Screw Amphibians in corresponding soils.

Exact evaluation of model data and development of a design is dictated by the performance criteria specified by the functional specifications of a proposed vehicle.

Generally, a length/diameter ratio of six would be selected for maximum water and mud performance. In sand a length/diameter ratio of four would be selected. It is obvious that the design is a compromise and penalties in certain regions of performance will result.

A helix angle of approximately 50 degrees will usually result in the best water performance. The higher blade heights are also advantageous for maximum water performance and necessary for maximum thrust in mud or sand. Generally, a 30-degree helix angle is preferred for mobility over these terrains.

Rotor centerline spacing equivalent to four rotor diameters results in the most efficient system in water. Over various terrains centerline spacing would be determined by maneuverability requirements.

To illustrate practical application of the test data, a design technique was developed and the technique applied to three design examples. The examples place primary emphasis on detailed rotor information and performance.

This manual, then, reflects an initial investigation, the limitations of which are indicated throughout the text.

CHAPTER 2

ESSENTIALS OF TESTING A MODEL BUOYANT SCREW

The theory of similitude is the basis for all model testing. The buoyant screw rotor is a unique concept of propulsion since it contributes to a vehicle's buoyancy while providing the thrust. Because of this uniqueness, this chapter will:

- Provide an analysis of the basis laws used in testing a model of the buoyant screw rotor
- Establish the non-dimensional parameters used throughout the report
- Examine some actual data with regards to the laws of similitude and the method of model data extrapolation

The chapter is divided into two sections, the essentials of model testing in water and in soils, the latter being a relatively new field of study.

Section I

MODEL TESTING IN WATER

Those familiar with model test realize the advantages of such tests and consider such tests common engineering practice. A vehicle model study furnishes useful qualitative and quantitative indications of the characteristics of the prototype vehicle. The numerical value that is obtained by a test of a model depends on the values of the influential variables in the problem. A dimensional analysis of the relationship invariably leads to an equation of the form,

$$\pi = f(\pi_1, \pi_2, \ldots \pi_i)$$

where the π_i's are dimensionless products. A particular value of π may be obtained by means of a model, provided that the dimensionless products have the same value for model as for full scale. This implies geometrical as well as dynamic similarity.

In the case of the buoyant screw, a dimensional analysis of torque on the rotor leads to an equation of the form,

$$K_Q = f\left(\frac{Dn}{V}, \frac{\mu}{DV\rho}, \frac{\sigma}{DV^2}, \frac{Dg}{V^2}\right)$$

The mathematical manipulation of this analysis can be found in Appendix B. Since the models are tested in water, the following constraints are imposed,

$$\sigma_p = \sigma_m$$

$$\rho_p = \rho_m$$

$$g_p = g_m$$

$$\mu_p = \mu_m$$

and it is important to test at equivalent slips which implies,

$$\left(\frac{V}{nD}\right)_p = \left(\frac{V}{nD}\right)_m$$

making exact similitude impossible. To be more specific, if the Froude number, which is the ratio of the inertial forces to the gravity forces and is associated with the wave-making resistance, is scaled properly, then it becomes impossible to scale the Reynolds number which is the ratio of the inertial forces with the frictional forces. The same problem is encountered with the Weber number which is the ratio of inertia forces to surface tension forces.

However, it is not usually feasible to impose complete similarity in a model test. Therefore, some of the independent dimensionless variables, which are believed to have secondary influences or which affect the phenomenon in a known manner, are allowed to deviate from their correct values. Yet, any departure from complete similarity or any application of theoretical or emperical corrections to compensate for such departures must be justified.

It is important to remember that in a scale model test, only the net forces are measurable. If force components must be separated, and

each component expanded by a different ratio because of the inequality of corresponding and important dimensionless parameters, then some sort of empirical division is required would be based on extensive experiment and correlation. It is not the intent in this discussion to imply that the problem is insurmountable, but rather to point out the difficulty of obtaining the empirical data necessary.

Since all model data obtained from water tests is generally extrapolated to full size vehicle data based on Froude's law, justification of departing from exact similitude should be established. This can be accomplished by either compensating empirically as previously explained or by proving such a departure results in a negligible effect on the data.

If it were then possible to define a frictional torque line analogous to a flat plate friction line as used for extrapolation in the ship model case, as well as properly determine the spray scale effect, expansion of rotor torque could be handled in a manner similar to extrapolation of model resistance. The problems of deriving such a frictional torque line can be easily anticipated since large accelerations and decelerations of the flow occur on the immersed portion of the rotor. Certainly other flow phenomena would be dissimilar between sheering flow on a flat plate and the flow on rotor. An analytical approach to this problem was investigated and the results are noted in Appendix C.

Figures 2-1 through 2-4 shows that correlation between two sets of data, obtained from models approximately 1/6 and 1/3 the size of those rotors on the Marsh Screw Amphibian, is not exact. These plots will not provide a means for correcting for the inequality of the dimensionless parameters, since the difference noticed on each graph is due to both testing at unequivalent Reynolds number and Weber number. These plots do establish the fact that the effect is negligible since the slope of the curves is small. It is the slope of the curve rather than the magnitude which is important. The non-dimensional torque constant is practically independent of both Reynolds number and Weber number. This is also apparent for the advance coefficient. Therefore, if these negligible effects are disregarded and extrapolation performed based upon Froude's law, the prototype data will tend to be somewhat conservative.

One precaution must be mentioned with regard to the neglecting of dimensionless products. It may happen that forces that have practically no effect on the behavior of the prototype, significantly affect the behavior of the model. For example, surface tension does not influence large rotors, but for smaller rotors visible dissimilarities in spray patterns are apparent. Therefore, the Weber number for a small model is important, although it is negligible for the prototype. Disturbing influences of this type are called scale effects. Scale

effects occur, to some extent, in nearly all model tests, and the best method of preventing the effects is to build models as large as feasible.

With this in mind, again look at the previous graphs (Figures 2-1 through 2-4). Correlation between the 1/6 scale rotor results and 1/3 scale rotor results is unsatisfactory. A series of eight tests were run, four tests of 1/3 scale rotors of two different configurations at two displacements and four of 1/6 scale rotors of the same configurations at similar displacements.

The problem of scale effects was not previously anticipated. The lack of correlation between the two sets of data was due to the inconsistent extent to which turbulence was established in the boundary friction layers of the models at low Reynolds numbers and low speed/length ratios. Thus, it was concluded that the 1/6 scale rotors were too small to avoid scale effects due to partial laminar flow, and testing of these rotors was discontinued in favor of a model twice the original size.

LEGEND FOR FIGURES 2-1, 2-2, 2-3, AND 2-4

Curve	Helix Angle	Blade Height	Percent Displacement	
1	40°	0.78	25%	
2	40°	0.78	50%	
3	50°	0.78	25%	1/6 Scale
4	50°	0.78	50%	
5	40°	1.56	25%	
6	40°	1.56	50%	1/3 Scale
7	50°	1.56	25%	
8	60°	1.56	50%	

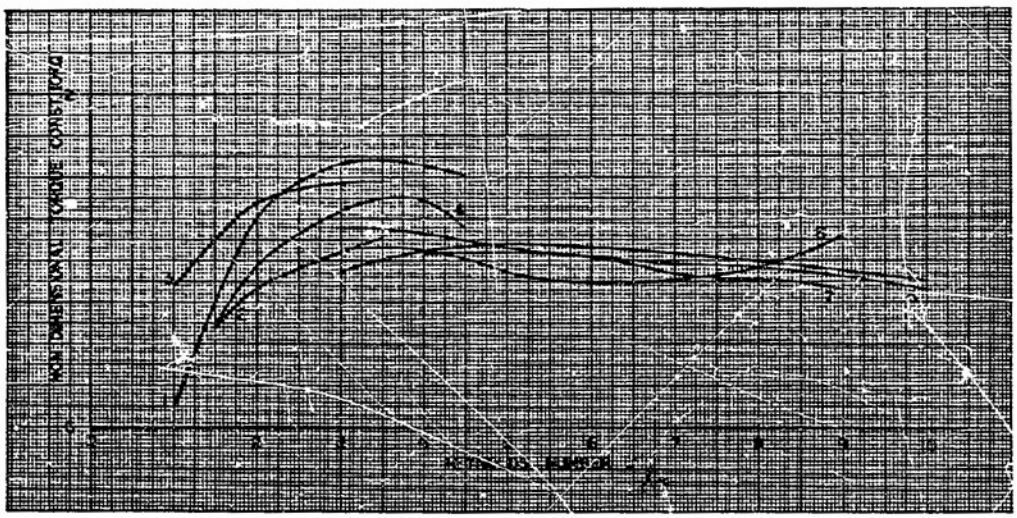

Figure 2-1 Non-Dimensional Torque Constant vs Reynolds Number for 1/6 and 1/3 Scale Models

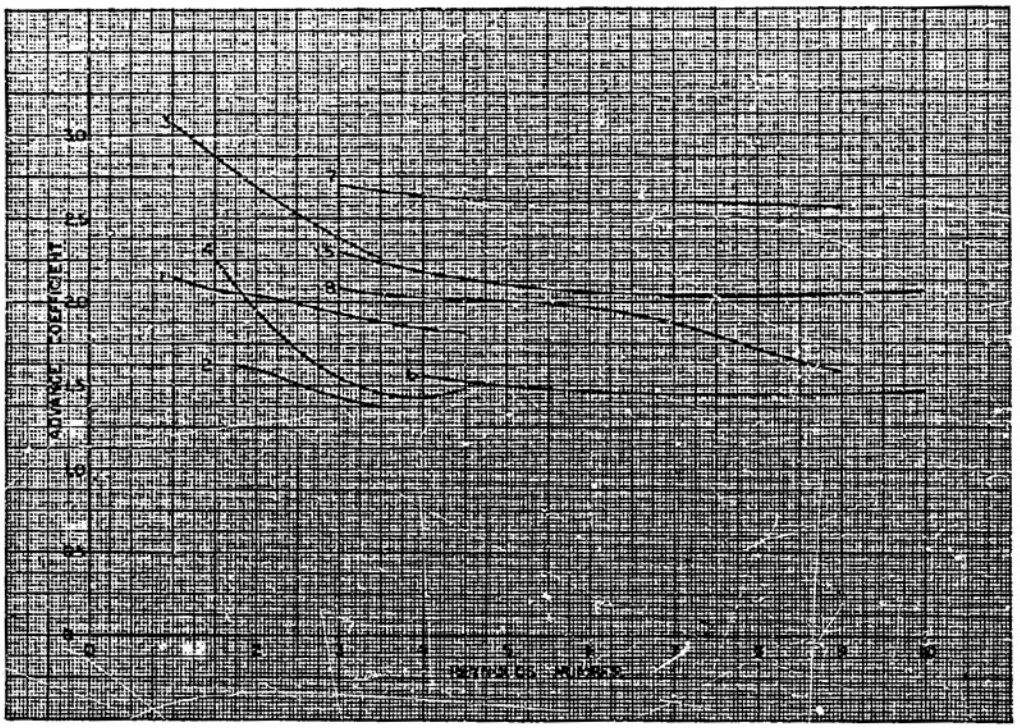

Figure 2-2 Advance Coefficient vs Reynolds Number for 1/6 and 1/3 Scale Models

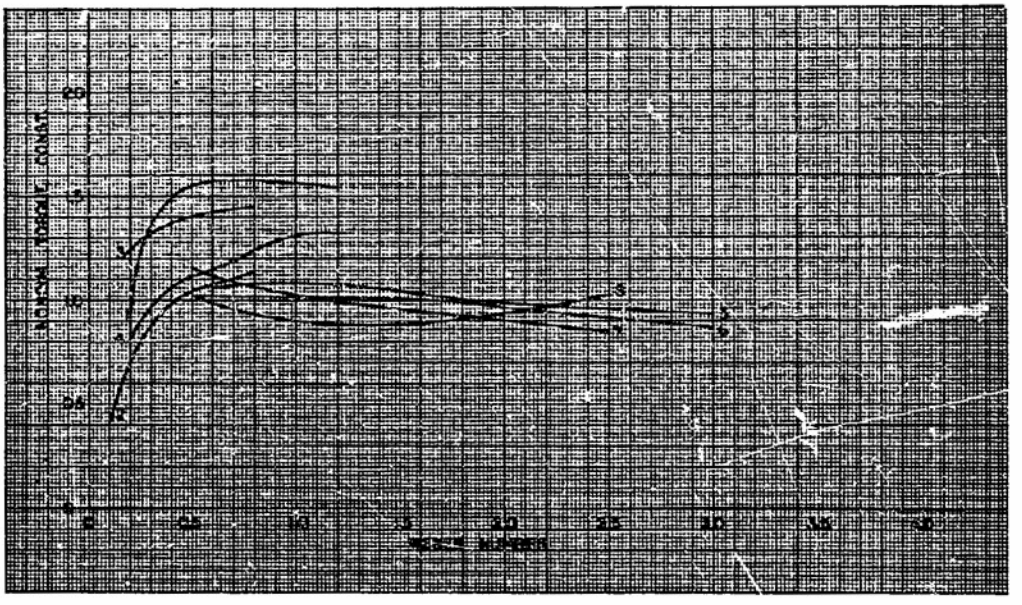

Figure 2-3 Non-Dimensional Torque Constant vs Weber Number for 1/6 and 1/3 Scale Models

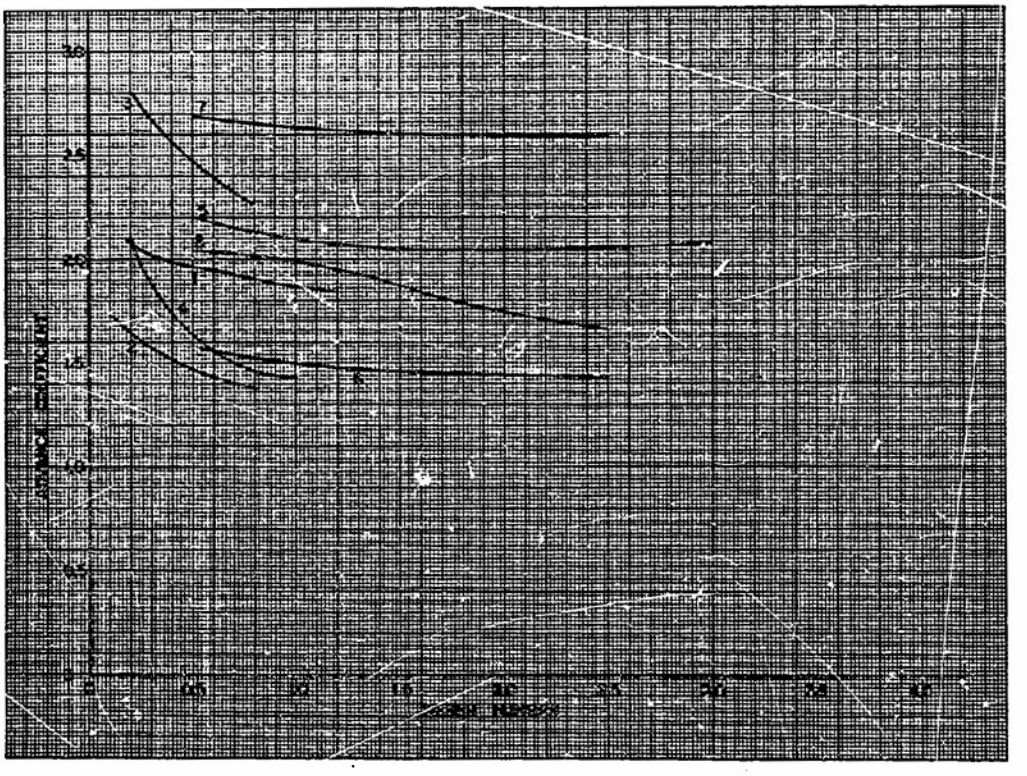

Figure 2-4 Advance Coefficient vs Weber Number for 1/6 and 1/3 Scale Model

Section II

MODEL TESTING IN SOILS

In the case of soil-vehicle mechanics, the performance characteristics are not well understood, and model tests are an excellent means of isolating the effects of various vehicle parameters. The use of models in studying vehicle action in soils is, however, relatively new. Difficulties arise in soil testing in that the media is far from being homogeneous and soil properties are not isotropic as are the properties of most fluids. As explained in the preceding section a dimensional analysis is a prerequisite if scale model systems are to be properly understood. Thus a dimensional analysis of drawbar pull on the rotor leads to an equation of the form,

$$\frac{DBP}{W} = f\left(\frac{cD^2}{W}, \frac{Dn}{V}, \frac{Dg}{V2}, \phi, f\right).$$

The mathematical manipulation is found in Appendix B. Since two of the constraints imposed are,

$$c_p = c_m$$

$$g_p = g_m$$

and it is important to test at equivalent slips which implies,

$$\left(\frac{V}{nD}\right)_p = \left(\frac{V}{nD}\right)_m$$

making exact similitude impossible.

The theory of model testing in soils is not well developed and means of compensating for departures by either theoretical or emperical corrections have not been developed. Certainly an analysis of the factors involved in conducting model tests to determine what data distortion can be expected is possible, and the effect upon the predicted performance of the prototype can be estimated.

At first glance, this inability to make exact predictions would appear to be a major stumbling block in the conduct of soil model tests. However, experience indicates that direct absolute correlation, while highly desirable, is not absolutely necessary. Properly set up and properly run model tests are superior to full-scale model tests for many purposes. Comparative tests of different configurations, as well as tests of a given model under various operating conditions, can be made with a much higher degree of confidence. Since model tests are much easier to control, comparison in models tend to be more sensitive and more accurate than full-size tests.

For those not familiar with the theory of land locomotion, it should be pointed out that soil properties may be divided into two categories, vertical and horizontal deformations. The motions which are being investigated are, however, neither pure vertical or pure horizontal, but rather a combination of both. Because of this uniqueness the dimensional analysis previously performed is further discussed.

Geometric similarity is presupposed. Practical limitations dictate that the densities of the materials be constant and obviously the acceleration of gravity must be equivalent. This then implies that the horizontal and vertical forces scale by λ^3. But if soil cohesion is equal in both model and prototype, then the cohesive forces will scale by λ^2, thus the frictional component of thrust or the horizontal tractive forces scale by λ^3 while the cohesive component scales by λ^2.

It is interesting to note that the horizontal tractive force is independent of velocity. There has been no indications in data for the past several years of any marked effect of vehicle speed upon performance for various soil conditions. This is apparent over a range of rather slow speeds at which quantitative tests have been run. Model tests to verify this indication were conducted in the sand and wet mud. The results shown on Figures 2-5 through 2-8 indicate that the values measured are independent of speed.

In dry mason sand, used for model tests, the cohesive component of thrust was insignificant in comparison with the friction component. Extrapolation based upon Froude's law would be appropriate even though justification of extrapolation by this cube relationship is not theoretically valid. This would result in a representative estimate which would be somewhat conservative.

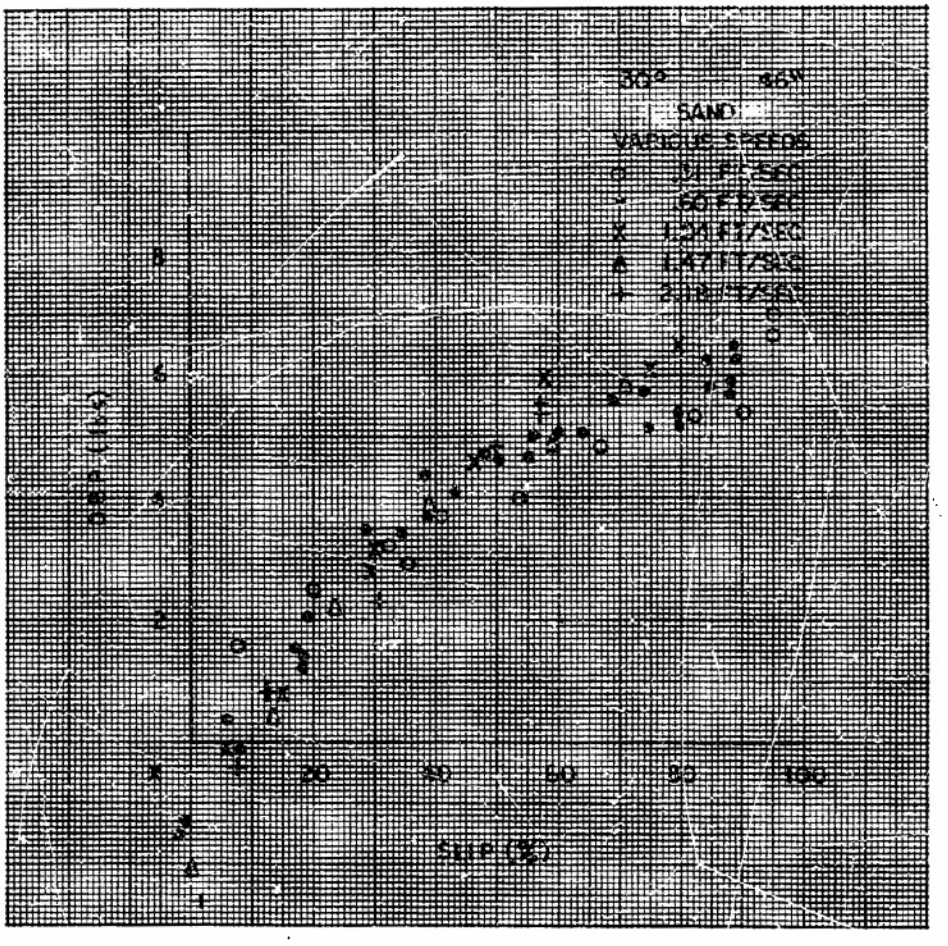

Figure 2-5 Drawbar Pull vs. Slip - Sand (30 Degree Helix, 0.460 Inch Blade Height)

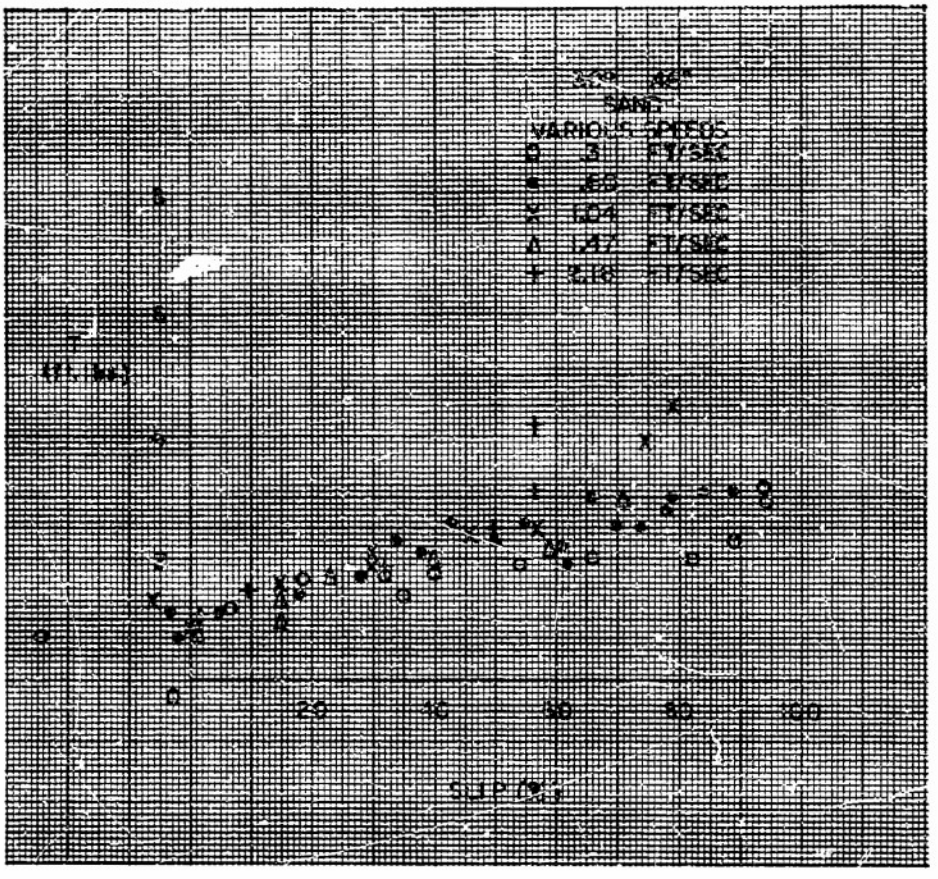

Figure 2-6 Torque vs. Slip – Sand (30 Degree Helix, 0.460 Inch Blade Height)

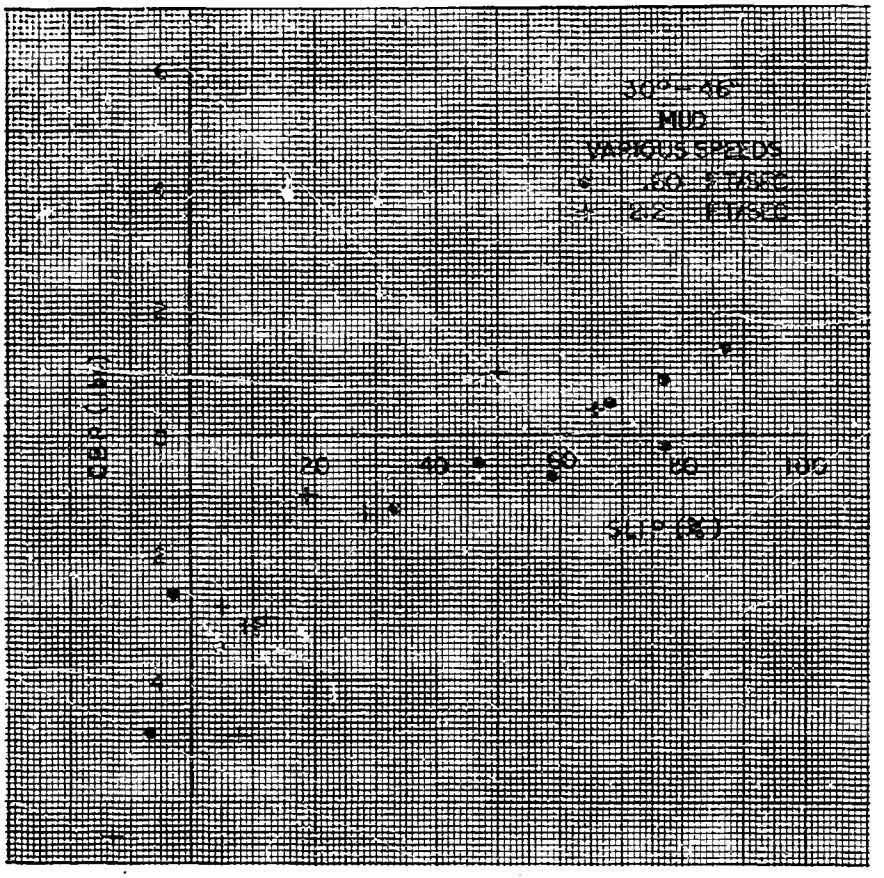

Figure 2-7 Drawbar Pull vs. Slip – Mud (30 Degree Helix, 0.460 Inch Blade Height)

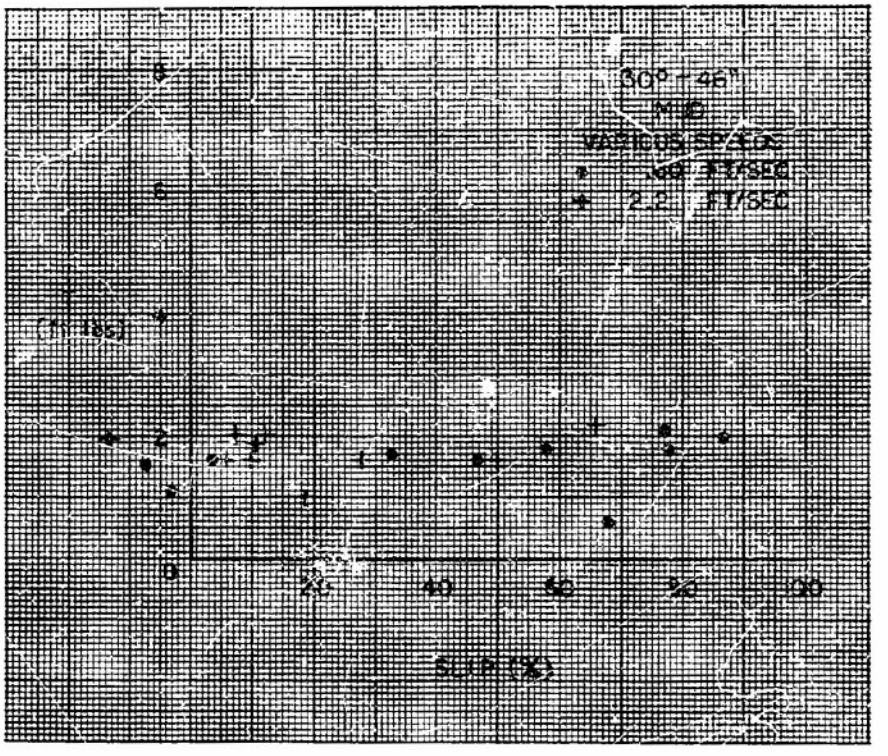

Figure 2-8 Torque vs. Slip - Mud (30 Degree Helix, 0.460 Inch Blade Height)

The rest of the model tests were conducted in an extremely wet organic silt procured from a marsh in Michigan where Marsh Screw Amphibian data has been obtained. Since the frictional component of thrust was insignificant in comparison to the cohesive component, extrapolation based upon the square relationship would be more nearly correct. An additional problem was apparent during the tests conducted in this mud. The soil was in a completely worked state and measurements were not at all indicative of those expected. Certainly these results then are only qualitative and extrapolation of data should not be attempted.

Tests on an intermediate scale model, twice the size of those used throughout the test program, were conducted to establish scaling effects. As mentioned previously, the tractive forces will not scale properly since the friction forces scale as λ^3 while the cohesive forces scale as λ^2, if the same soil is used for model and prototype test. Therefore, the force generated in the model by cohesion, which equals the area times the coefficient of cohesion, will be too great by the factor λ when compared to the frictional forces. Concurrently, the drawbar pull/weight in a cohesive soil will be somewhat greater than that experienced in the prototype or a larger scale model.

In a like manner, the specific torque (T/Wr) required of a model in a cohesive soil would also be somewhat greater than that required for its prototype.

In a purely frictional soil such as sand, the cohesion is equal to or near zero, hence this problem will not exist and the tractive force should scale correctly by λ^3.

Unfortunately, the test rig was designed for the 1/6 scale rotor and was not capable of the higher torque required by the 1/3 scale rotor. Positive drawbar pull was not experienced. The data from Figures 2-9 through 2-11 is inadequate and the characteristics anticipated above could not be verified.

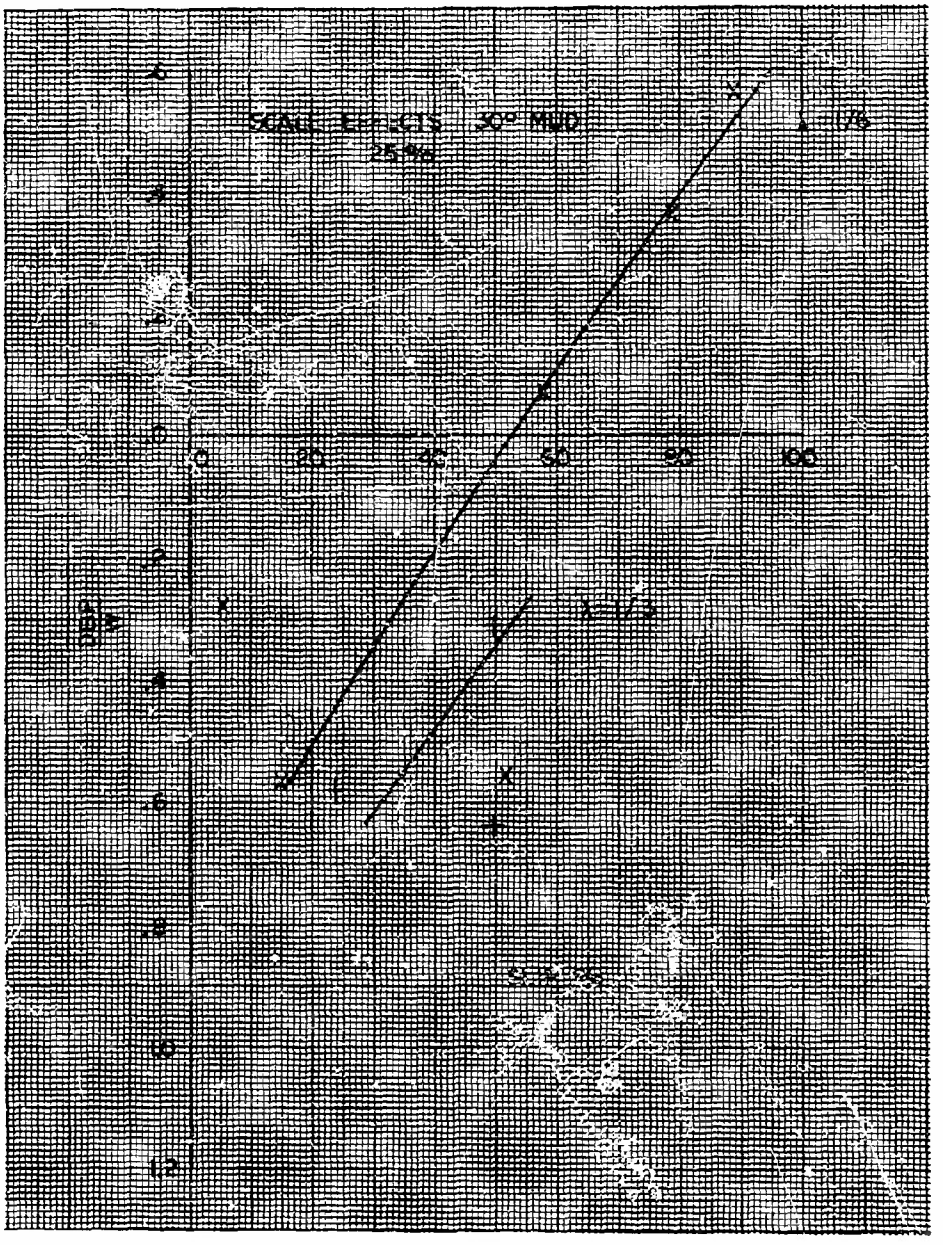

Figure 2-9 Drawbar Pull vs. Slip - Scale Effects, Mud (25 Percent Displacement)

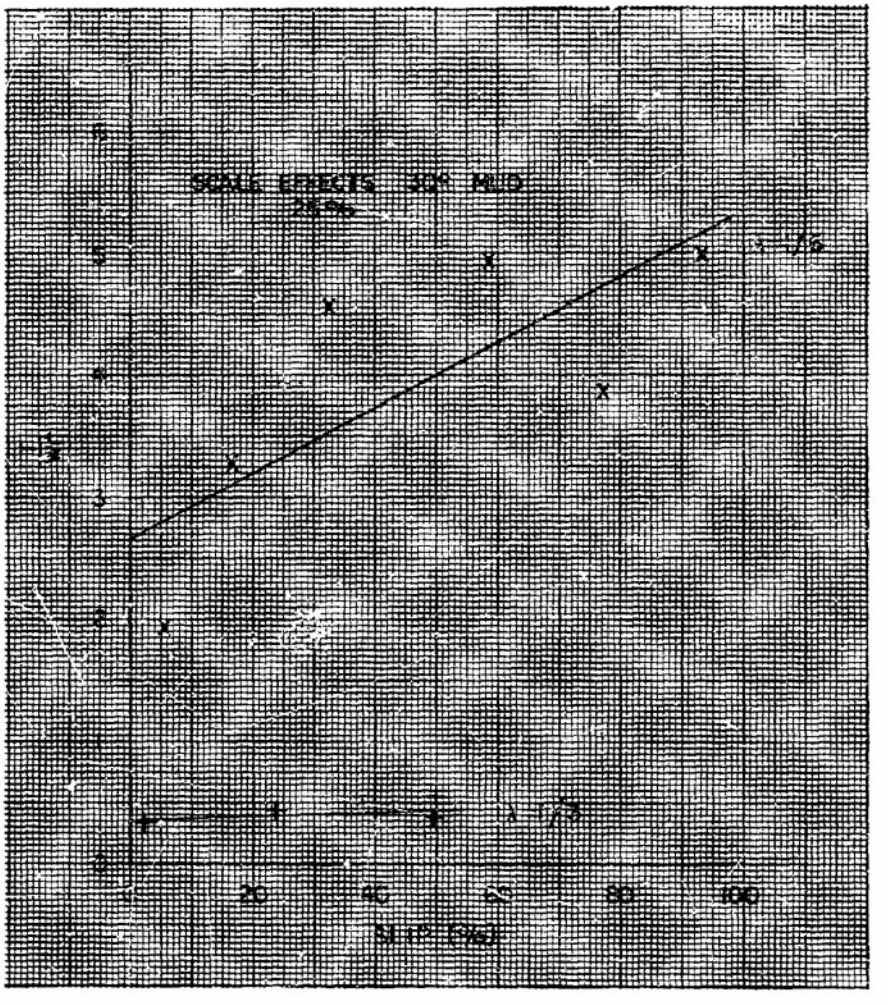

Figure 2-10 Torque vs. Slip - Scale Effects, Mud (25 Percent Displacement)

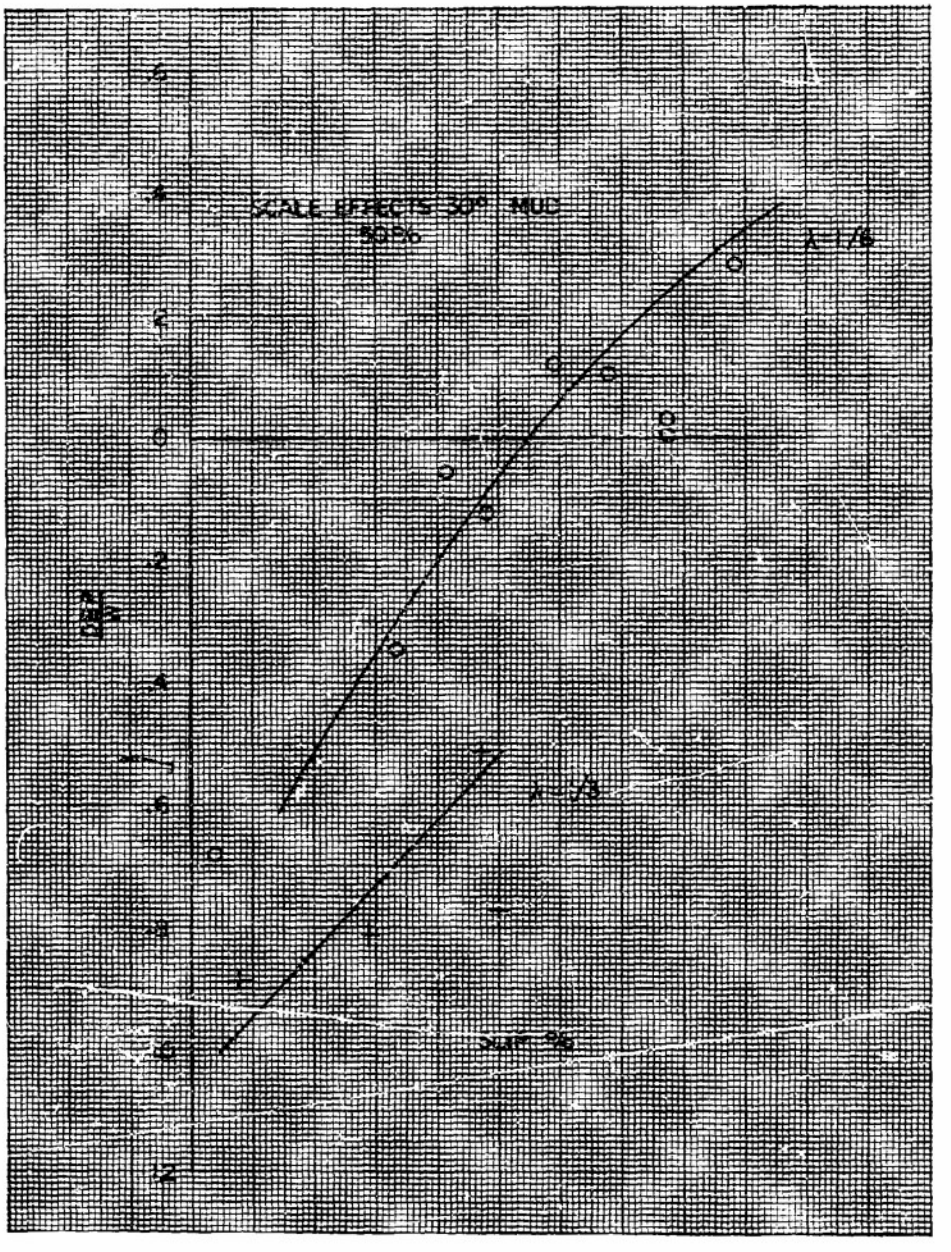

Figure 2-11 Drawbar Pull vs. Slip – Scale Effects, Mud (50 Percent Displacement)

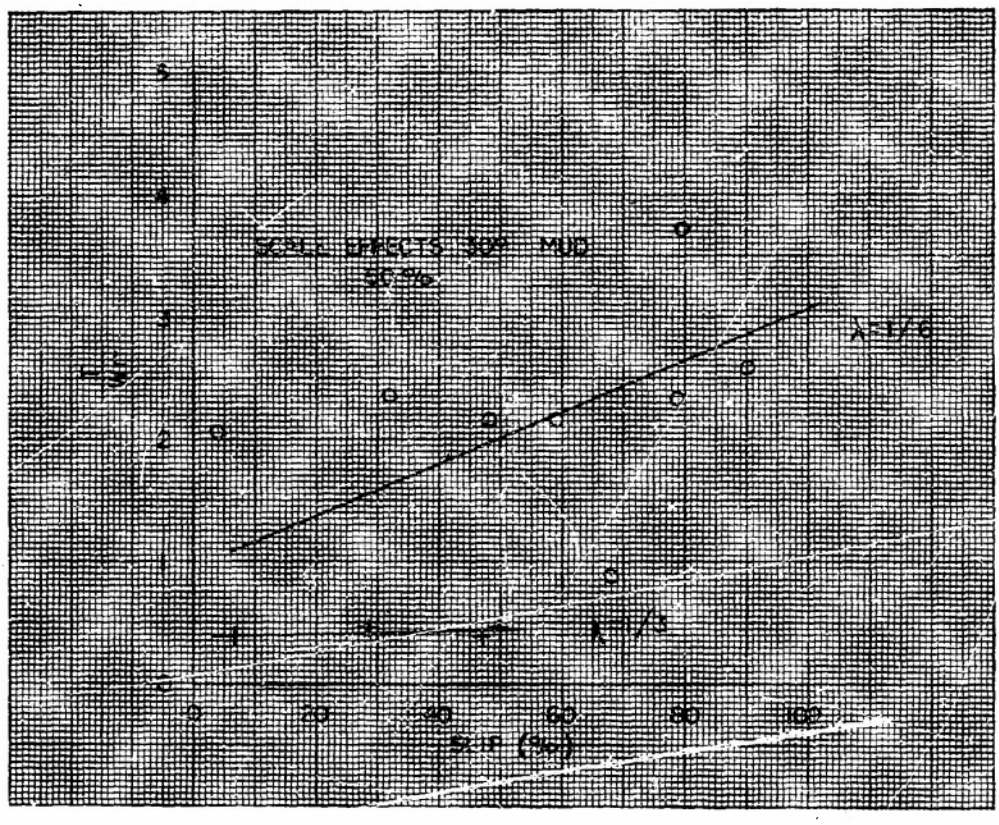

Figure 2-12 Torque vs. Slip - Scale Effects, Mud (50 Percent Displacement)

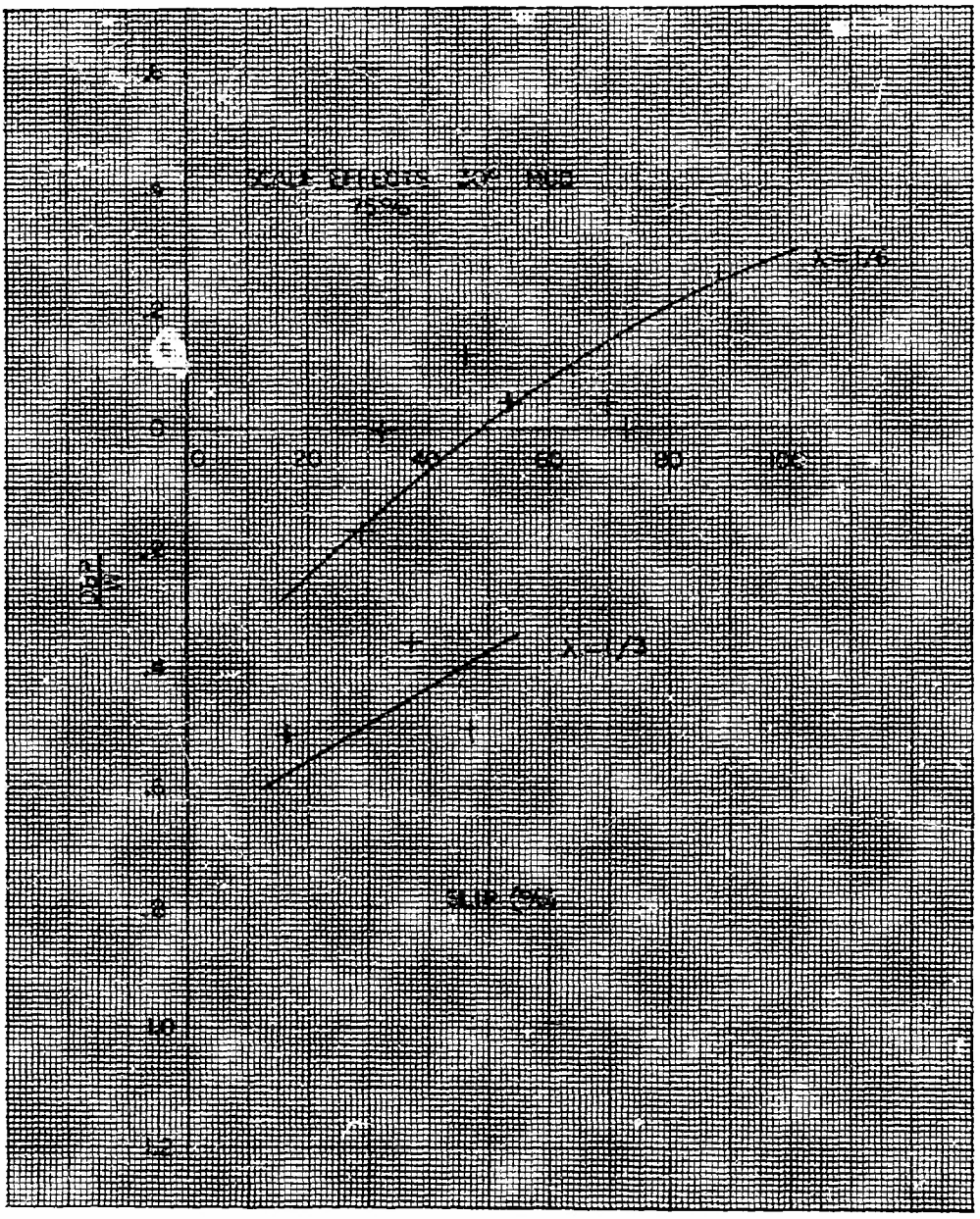

Figure 2-13 Drawbar Pull vs. Slip - Scale Effects, Mud (75 Percent Displacement)

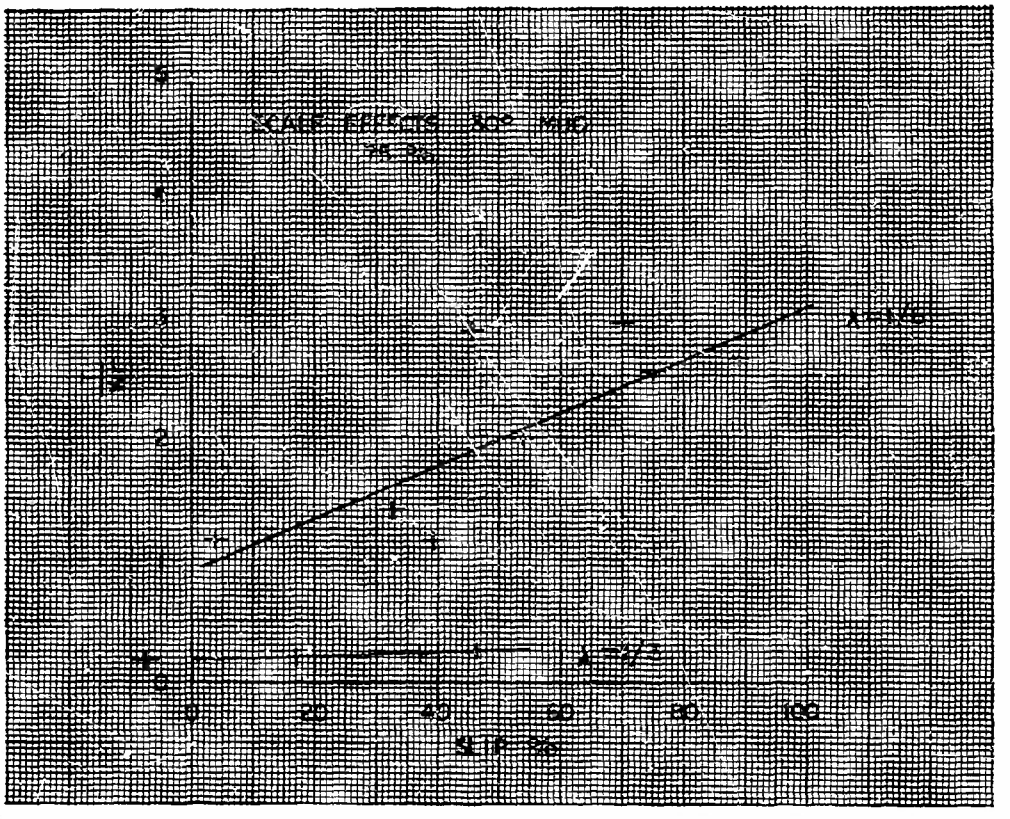

Figure 2-14 Torque vs. Slip - Scale Effects, Mud (75 Percent Displacement)

CHAPTER 3

WATER TESTS

The water test program, conducted by the University of Michigan's Hydrodynamics Laboratory under contract to Chrysler Corporation Defense Engineering, consisted of two categories of investigation. These categories are:

- The testing of a systematic series of buoyant screw rotors
- The testing of miscellaneous configurations of buoyant screw rotors

The following sections describe the apparatus and test procedures, and presents test results in graphical representation. Full-scale vehicle performance data are provided at the end of the chapter for comparison with model test results.

Section I

DESCRIPTION OF APPARATUS

Initially all model tests were to be conducted on 24 inch long models. These models, approximately 1/6 the size of the rotors on the Marsh Screw Amphibian, revealed inconsistent data. Larger models, 48 inches long, of identical configuration, helix angle and blade height, were tested at loadings which represented the same percentage of immersed volume. Test results disclosed a lack of correlation. It was concluded that the 1/6 scale rotors were too small to avoid the scale effects as explained in this manual. All remaining tests were conducted using the 1/3 scale rotors.

Typical photographs of the earlier tests are included at the end of this section in order to familiarize the reader with the running attitude, spray patterns, and other characteristics observed during the test program.

The test apparatus used for the model tests in water, consisting of a rotor and dynamometer, is shown schematically in Figure 3-1. Two degrees of freedom, trim and sinkage, were allowed by the apparatus. That is, in the running condition the rotors were allowed to seek their equilibrium trim angle and vertical position. Measurements were made of:

- Torque
- RPM

- Trim
- Sinkage
- Speed of Advance (Carriage Speed)

Test runs were made at the model propulsion point. With the towing carriage at constant speed, the drive motor speed was varied until thrust output balanced the hydrodynamic drag. The balance was indicated by a zero output from the force transducer.

The maximum speed at which any given rotor was run was limited by one of two factors. The first was the maximum load which the electric motor would absorb. The second was with regard to the degree of freedom in trim. Generally, except for these two limiting factors, all tests were run up to about 16 feet per second.

As shown in Figure 3-1, in order to allow trim, the horizontal distance between the two sliding rods was allowed to vary by means of a small sub-carriage. Due to the mechanical arrangement, the carriage travel was limited such that approximately 14 degrees bow up was the maximum trim possible. In the designing of the test rig, allowance for higher angles of trim was not anticipated since these angles would be unrealistic for any proposed vehicle operation. There were cases where, as speed increased, trim would have exceeded 14 degrees within the normally run speed range.

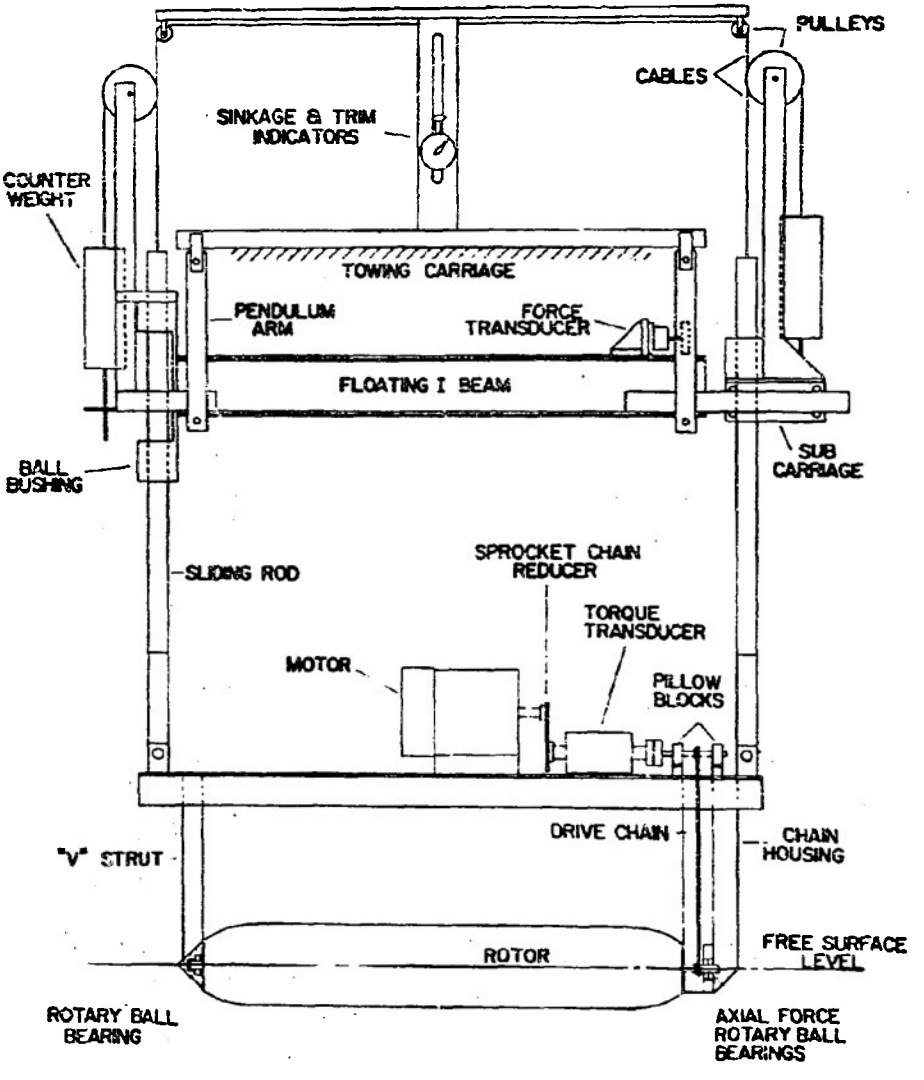

Figure 3-1 Buoyant Screw Rotor Test Fixture

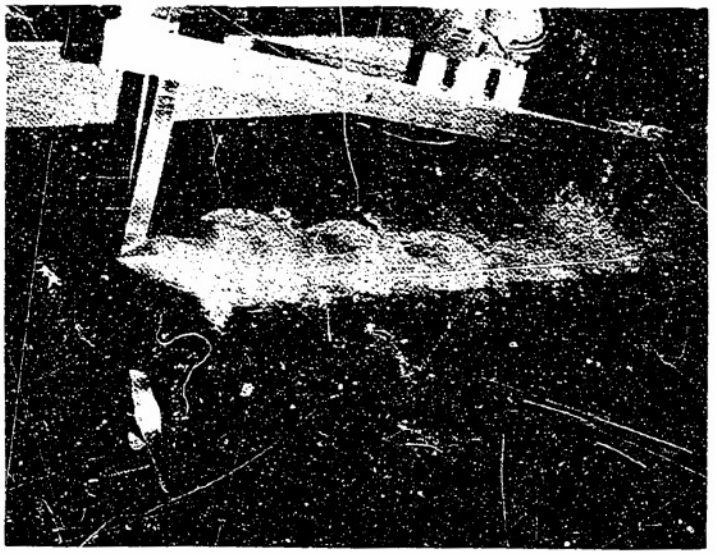

Helix angle	40 deg.
Blade height	1.560 inches
Hub diameter	8.000 inches
% Displacement	50% of rotor hub
Velocity	8.0 ft/sec
Initial trimming angle	4.0 deg. bow up
Running trimming angle	9.3 deg. bow up
Running full scale sinkage	0.95 inch down

Figure 3-2 Buoyant Screw Rotor Model Test Characteristics (1 of 5)

Helix angle	40 deg.
Blade height	1.560 inches
Hub diameter	8.000 inches
% Displacement	50% of rotor hub
Velocity	8.0 ft/sec
Initial trimming angle	2.2 deg. bow up
Running trimming angle	8.2 deg. bow up
Running full scale sinkage	0.71 inch down

Figure 3-2 Buoyant Screw Rotor Model Test Characteristics (2 of 5)

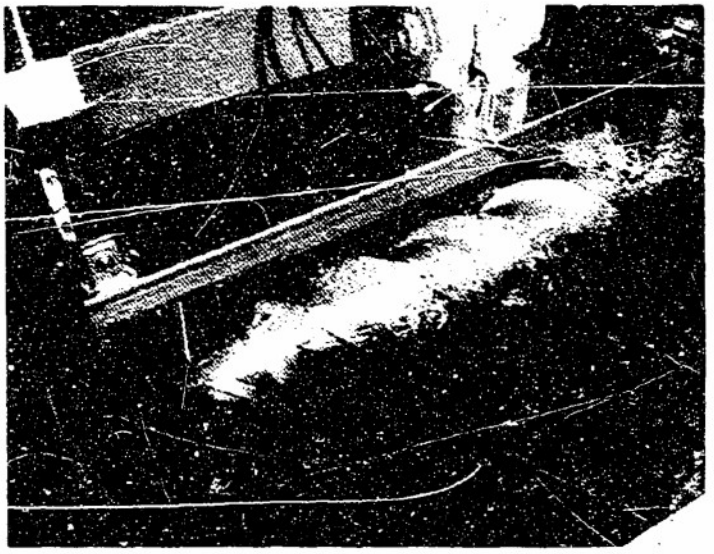

Helix angle	40 deg.
Blade height	1.560 inches
Hub diameter	8.000 inches
% Displacement	75% of rotor hub
Velocity	5.5 ft/sec
Initial trimming angle	0
Running trimming angle	0
Running full scale sinkage	5.68 inches down

Figure 3-2 Buoyant Screw Rotor Model Test Characteristics (3 of 5)

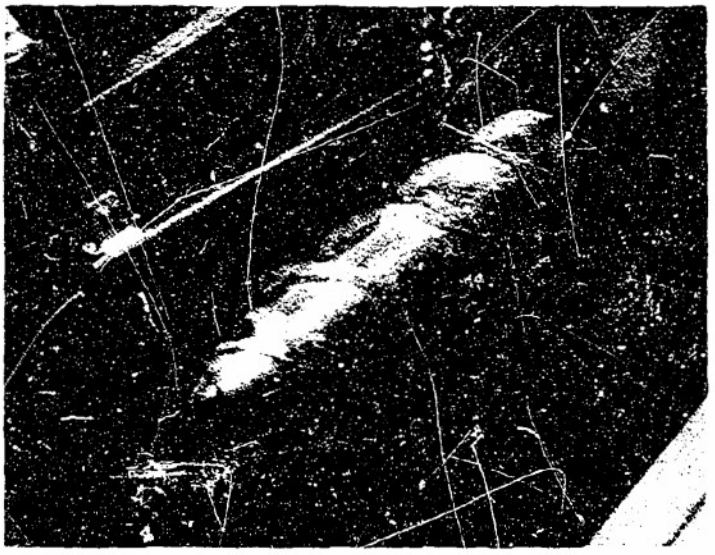

Helix angle	40 deg.
Blade height	1.875 inches
Hub diameter	8.00 inches
% Displacement	25% of rotor hub
Velocity	8.0 ft/sec
Initial trimming angle	2.3 deg. bow up
Running trimming angle	10.8 deg. bow up
Running full scale sinkage	0.47 inch down

Figure 3-2 Buoyant Screw Rotor Model Test Characteristics (4 of 5)

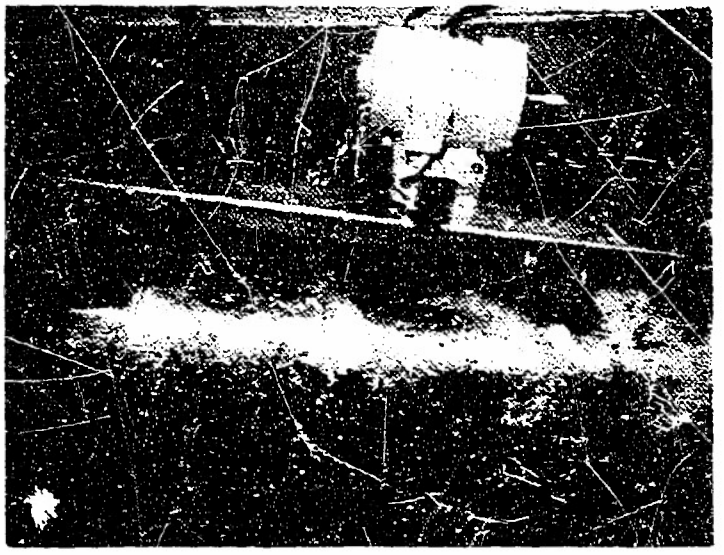

Helix angle	50 deg.
Blade height	1.875 inches
Hub diameter	8.000 inches
% Displacement	50% of rotor hub
Velocity	8.0 ft/sec
Initial trimming angle	2.2 deg. bow up
Running trimming angle	11.4 deg. bow up
Running full scale sinkage	0.59 inch up

Figure 3-2 Buoyant Screw Rotor Model Test Characteristics (5 of 5)

Section II

SYSTEMATIC SERIES OF BUOYANT SCREWS

A thorough investigation of water performance for a systematic series of rotors was undertaken to provide a rational basis for determining optimum buoyant screw configuration. A systematic series is one where the screw models differ only in one particular characteristic. The fundamental parameter for each group is the pitch angle or helix angle. Other parameters are blade width and displacement. The matrix of models tested is indicated in the following table.

HELIX ANGLE, degrees

BLADE HEIGHT inches	30	40	50	60
0.920	X		X	
1.250		X	X	
1.560	X	X	X	X
1.875		X	X	

Other model characteristics were:

Length	48.0 inches
Hub Diameter	8.0 inches
Hub Volume	1.3247 cubic feet

Each rotor was tested at a displacement corresponding to 25, 50 and 75 percent of the total hub volume. Buoyancy of the blades was neglected. All data is contingent on one degree bow up static trim.

The highest speeds possible were dependent on test apparatus limitations.

Most curves representing experimental data are not always expressible by simple mathematical expressions. The mathematical method sacrifices either simplicity or accuracy. Data can be presented without a sacrifice in accuracy in the form of simple graphs which facilitate data use. Thus, with the raw data collected, a convenient non-dimensional form for presentation was sought. An IBM 7090 computer was used to compute numerous pertinent parameters in their various forms. Certain parameters lead to a more satisfactory representation of the data. The use of these non-dimensional parameters was most desirable to cross-plotting the data. This enabled a complex matrix of buoyant screw configurations to be represented even though a few model configurations were not tested. The non-dimensional parameters selected were:

$$\text{Torque Coefficient, } K_Q = Q/[\rho V^2 \nabla]$$

$$\text{Advance Coefficient, } J = V/[n\nabla^{1/3}]$$

$$\text{Froude Volume Number, } F_\nabla = V/[g\nabla^{1/3}]^{1/2}$$

V = Advance Velocity ft/sec

∇ = Initial immersed hub volume ft^3

n = Revolutions per second

Q = Torque ft-lbs

ρ = Density of water $lb\text{-}sec^2/ft^4$

g = Acceleration of gravity 32.2 ft/sec

After all cross-plotting of the data had been accomplished the final graphs were prepared (Figure 3-3 through 3-26). The plots are the non-dimensional torque constant - vs - Froude volume number and advance coefficient - vs - Froude volume number. The use of this non-dimensional data enables analysis and extrapolation to be done accurately since transition from one curve to another is systematic and gradual.

A few curves of typical running sinkage and running trim are plotted versus Froude volume number for those models tested and are included at the end of this section (Figures 3-27 and 3-28). Values for slip are not indicated but may be calculated.

What is not obvious from this non-dimensional data is "what is an optimum rotor configuration". An optimum rotor configuration is a function of the rotor loading and speed. Therefore a particular configuration is best for a particular set of conditions. Generally a rotor with a helix angle of approximately 50 degrees and the highest blade height is best. The method for determining this optimum configuration for an exact set of conditions is outlined in Chapter 5.

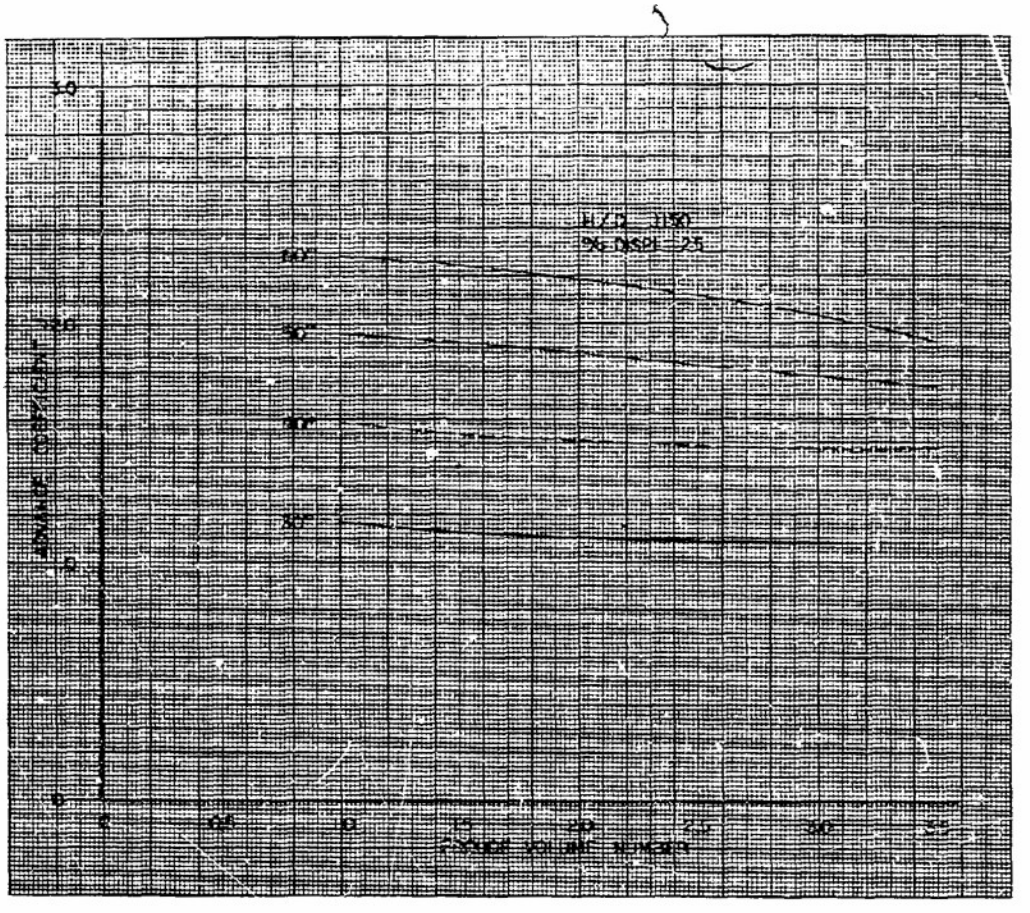

Figure 3-3 Advance Coefficient vs Froude Volume Number (H/D = 0.1150, 25 Percent Displacement)

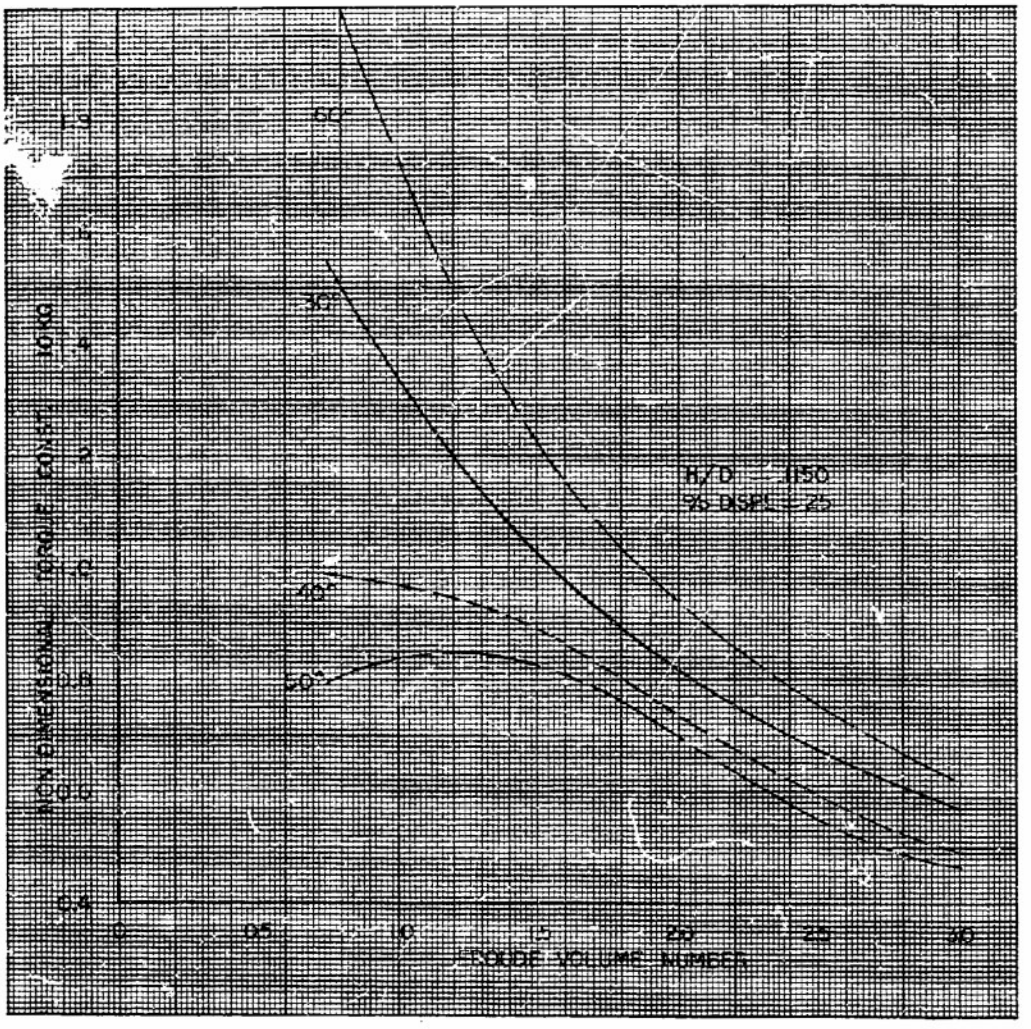

Figure 3-4 Non-Dimensional Torque Constant vs Froude Volume Number (H/D = 0.150, 25 Percent Displacement)

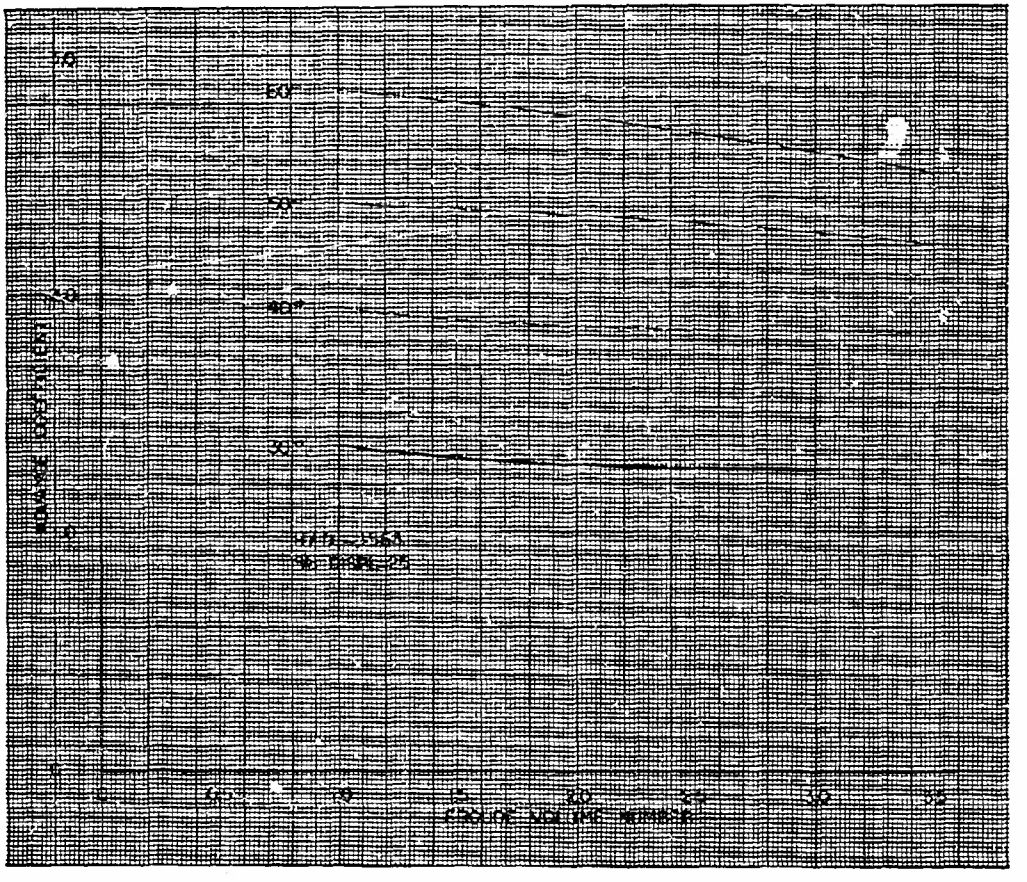

Figure 3-5 Advance Coefficient vs Froude Volume Number (H/D = Q.1563, 25 Percent Displacement)

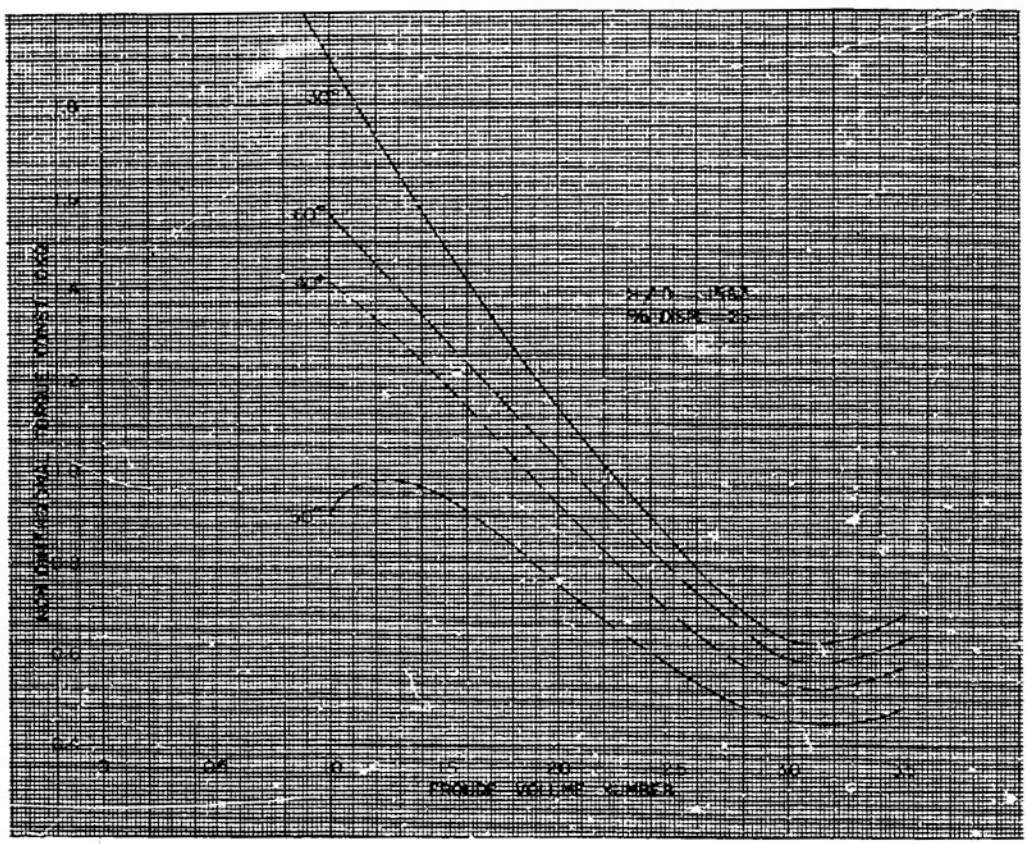

Figure 3-6 Non-Dimensional Torque Constant vs Froude Volume Number (H/D = 0.1563, 25 Percent Displacement)

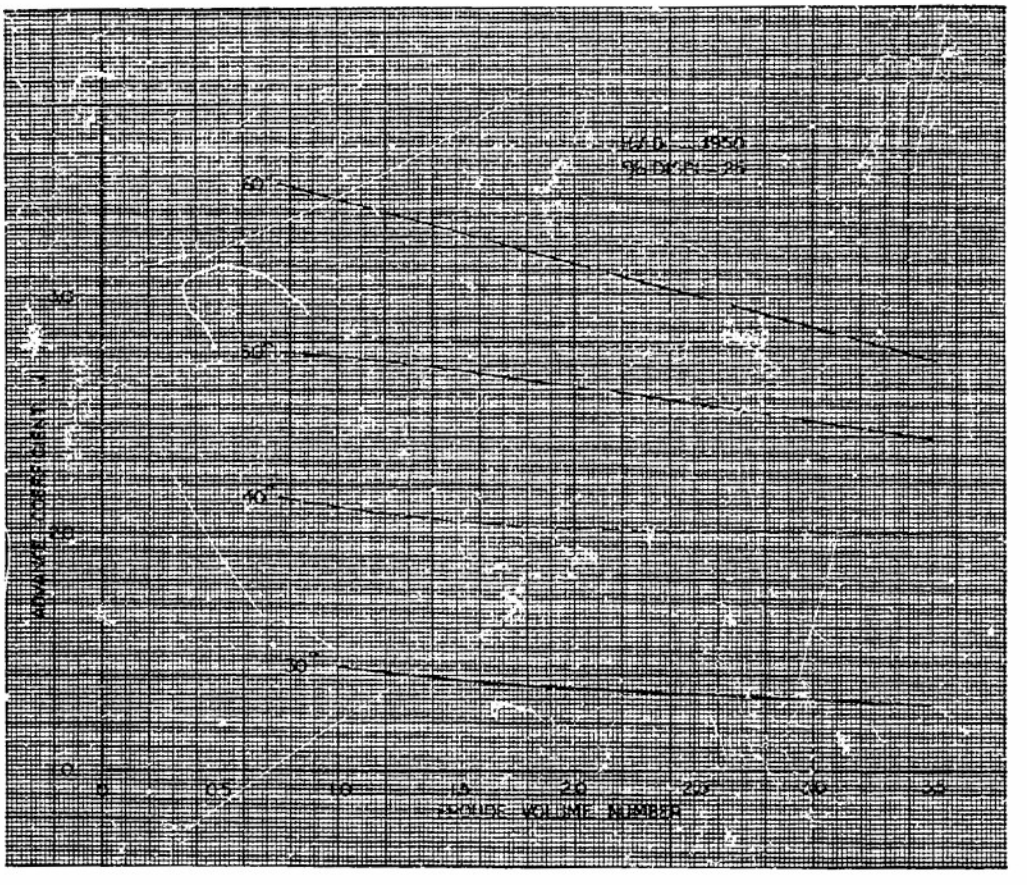

Figure 3-7 Advance Coefficient vs Froude Volume Number
(H/D = 0.1950, 25 Percent Displacement)

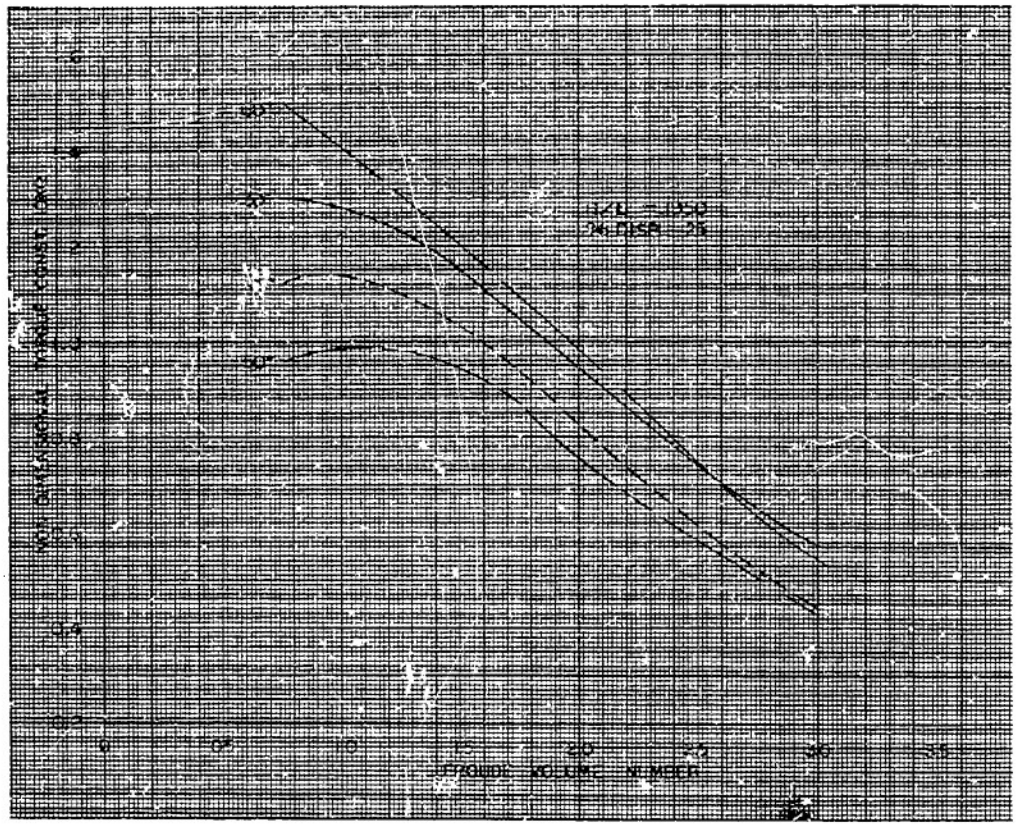

Figure 3-8 Non-Dimensional Torque Constant vs Froude Volume Number
(H/D = 0.1950, 25 Percent Displacement)

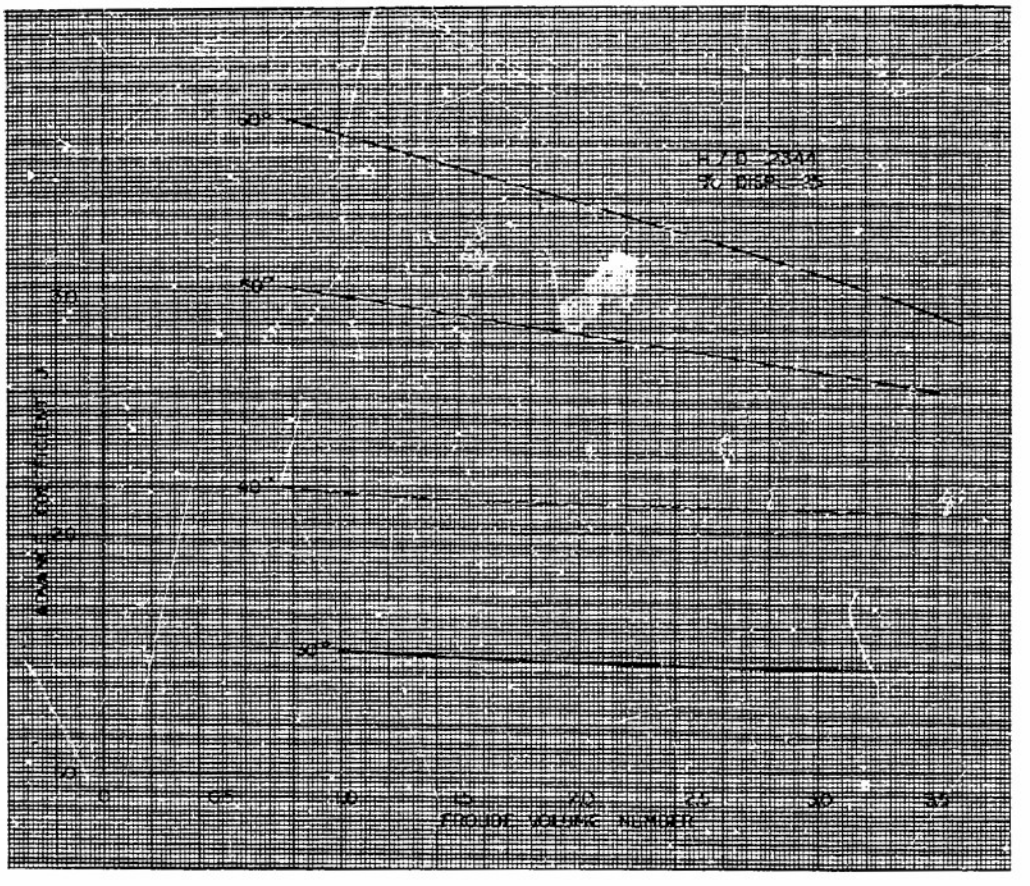

Figure 3-9 Advance Coefficient vs Froude Volume Number
(H/D = 0.2344, 25 Percent Displacement)

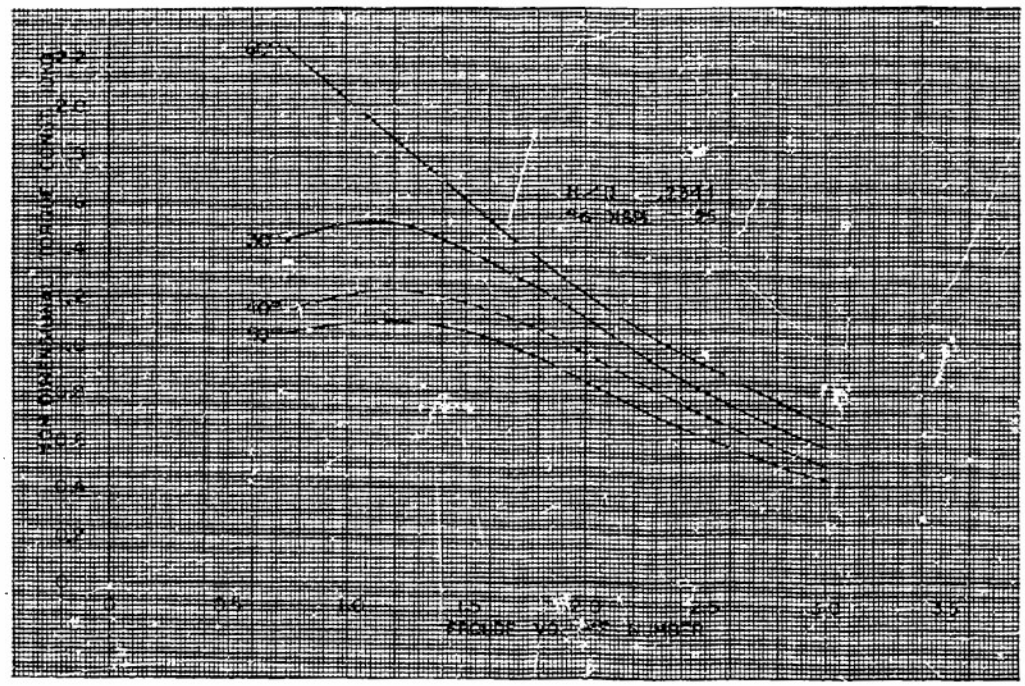

Figure 3-10 Non-Dimensional Torque Constant vs Froude Volume Number (H/D = 0.2344, 25 Percent Displacement)

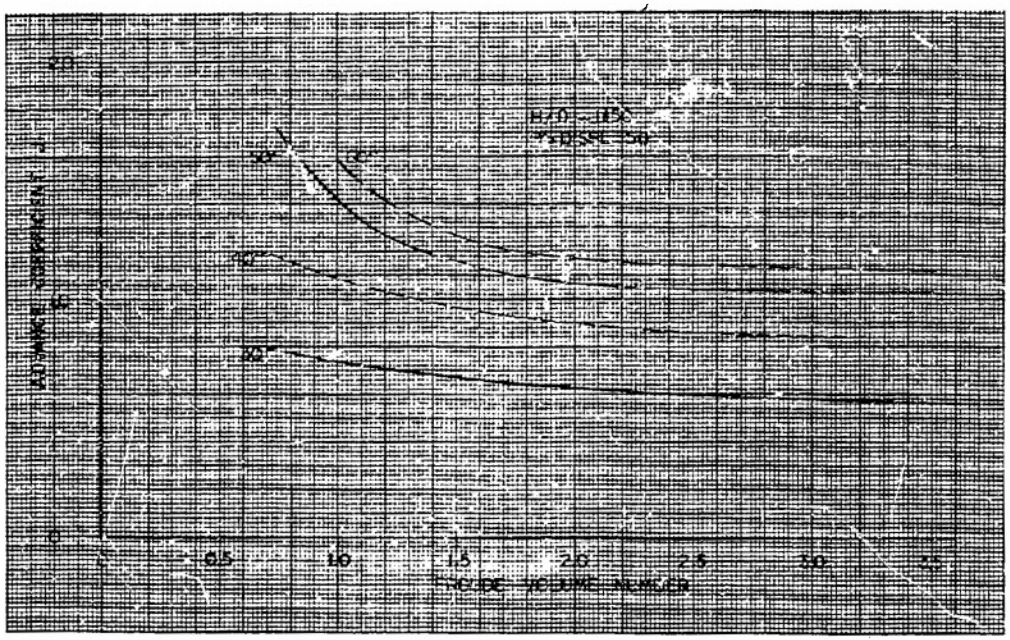

Figure 3-11 Advance Coefficient vs Froude Volume Number
(H/D = 0.1150, 50 Percent Displacement)

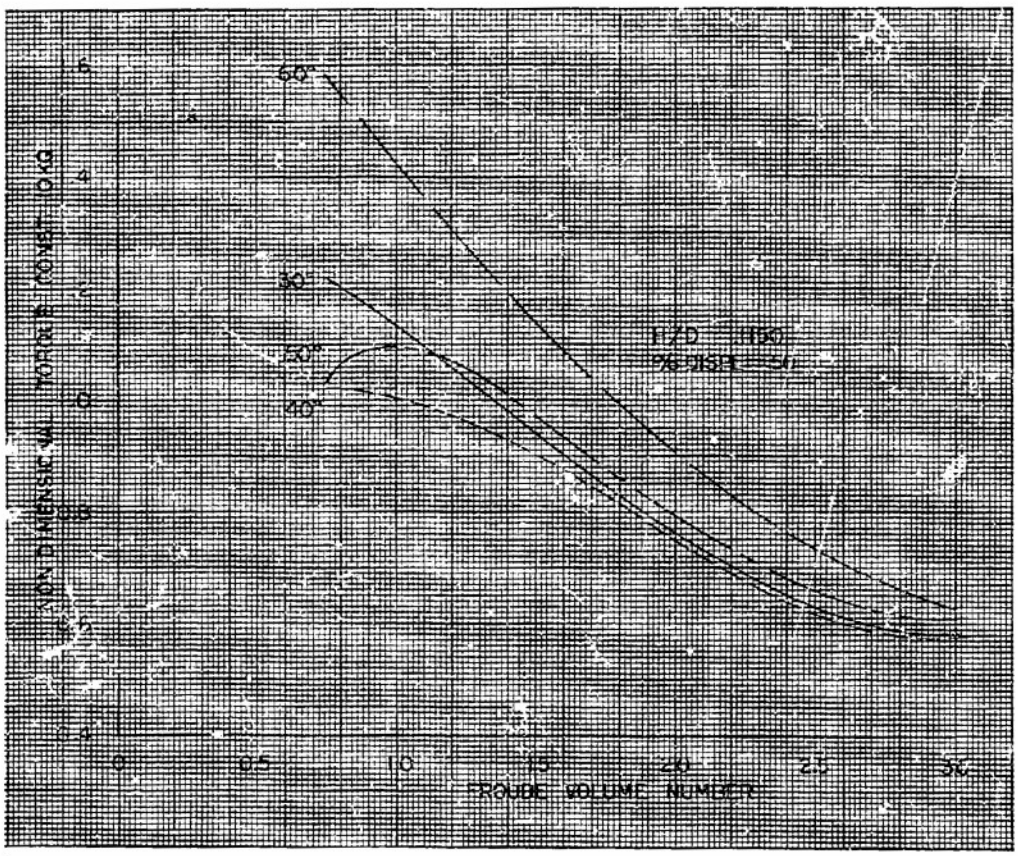

Figure 3-12 Non-Dimensional Torque Constant vs Froude Volume Number (H/D = 0.1150, 50 Percent Displacement)

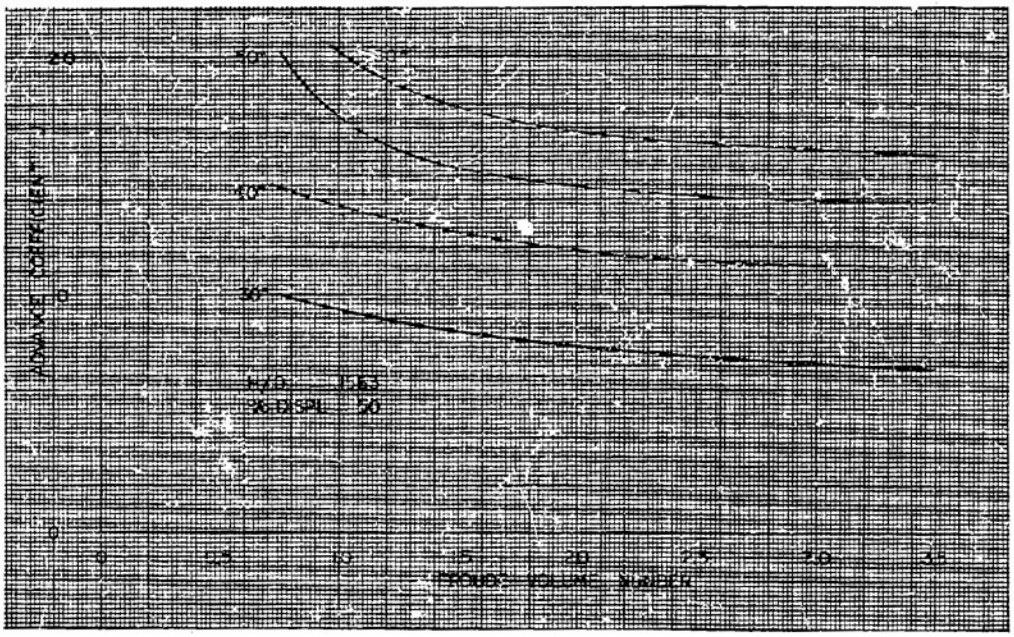

Figure 3-13 Advance Coefficient vs Froude Volume Number
(H/D = 0.1563, 50 Percent Displacement)

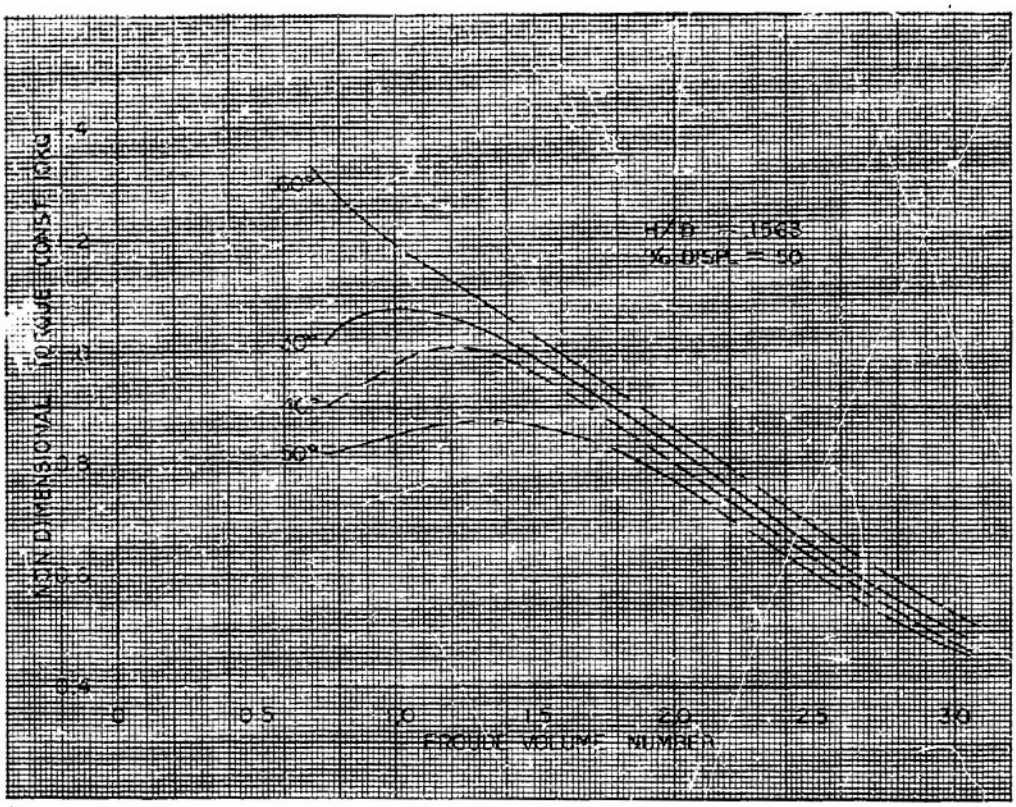

Figure 3-14 Non-Dimensional Torque Constant vs Froude Volume Number (H/D = 0.1563, 50 Percent Displacement)

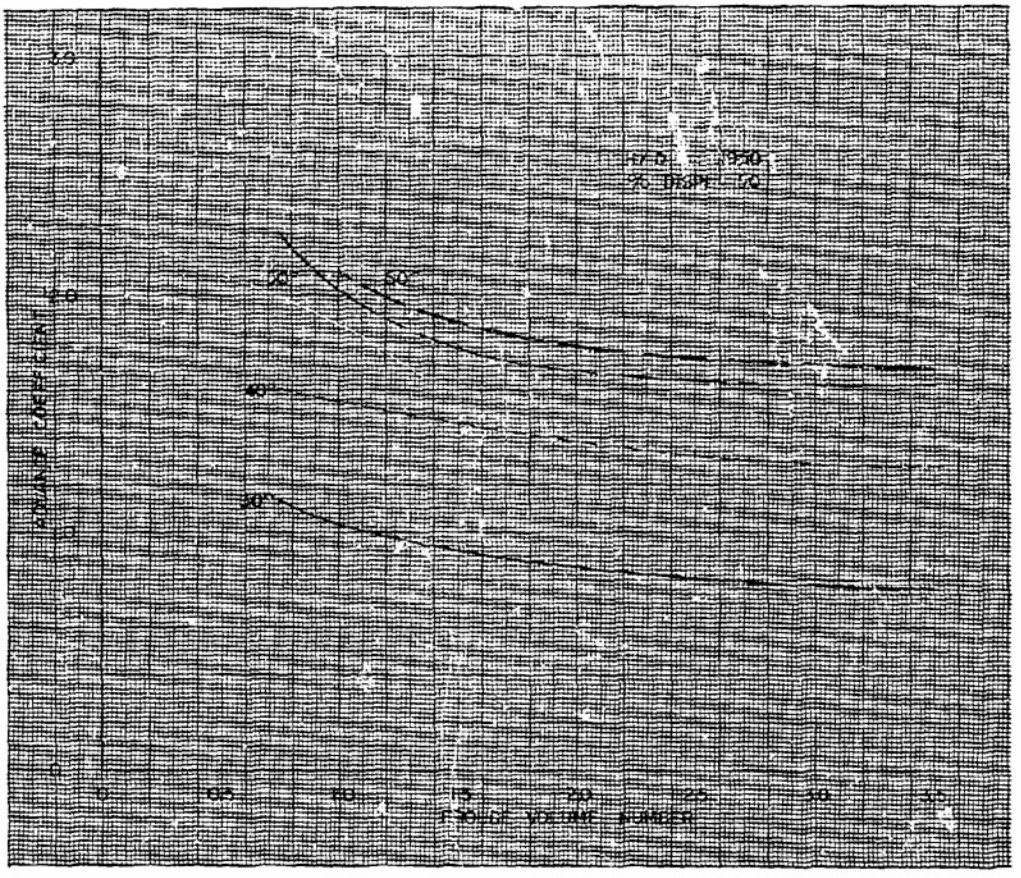

Figure 3-15 Advance Coefficient vs Froude Volume Number
(H/D = 0.1950, 50 Percent Displacement)

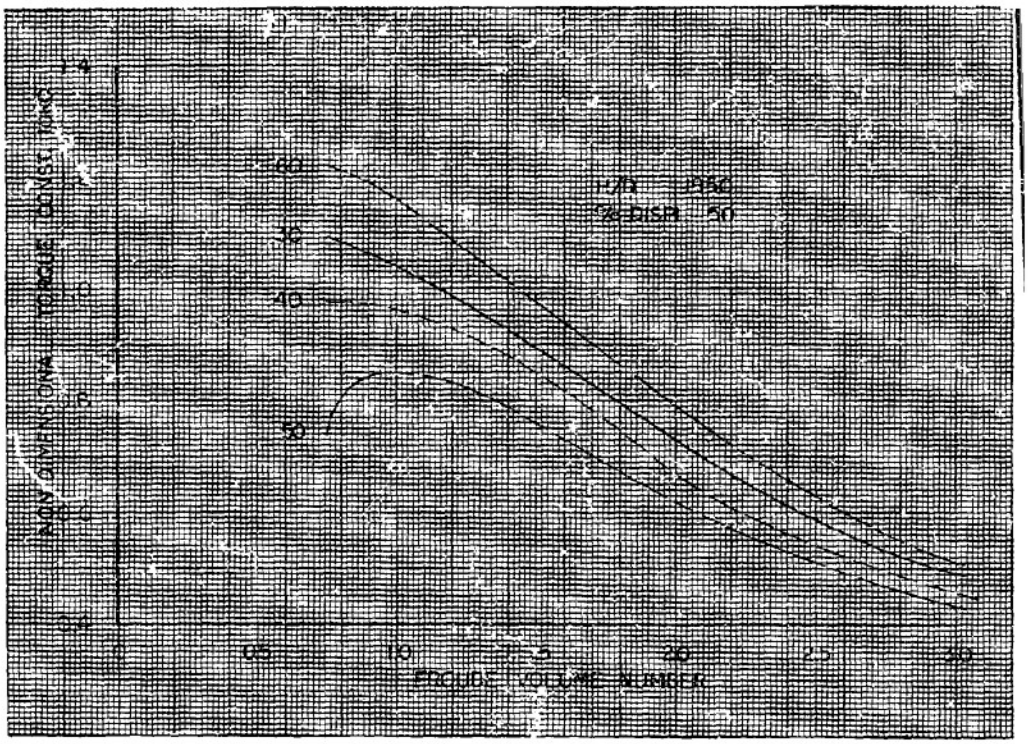

Figure 3-16 Non-Dimensional Torque Constant vs Froude Volume Number (H/D = 0.1950, 50 Percent Displacement)

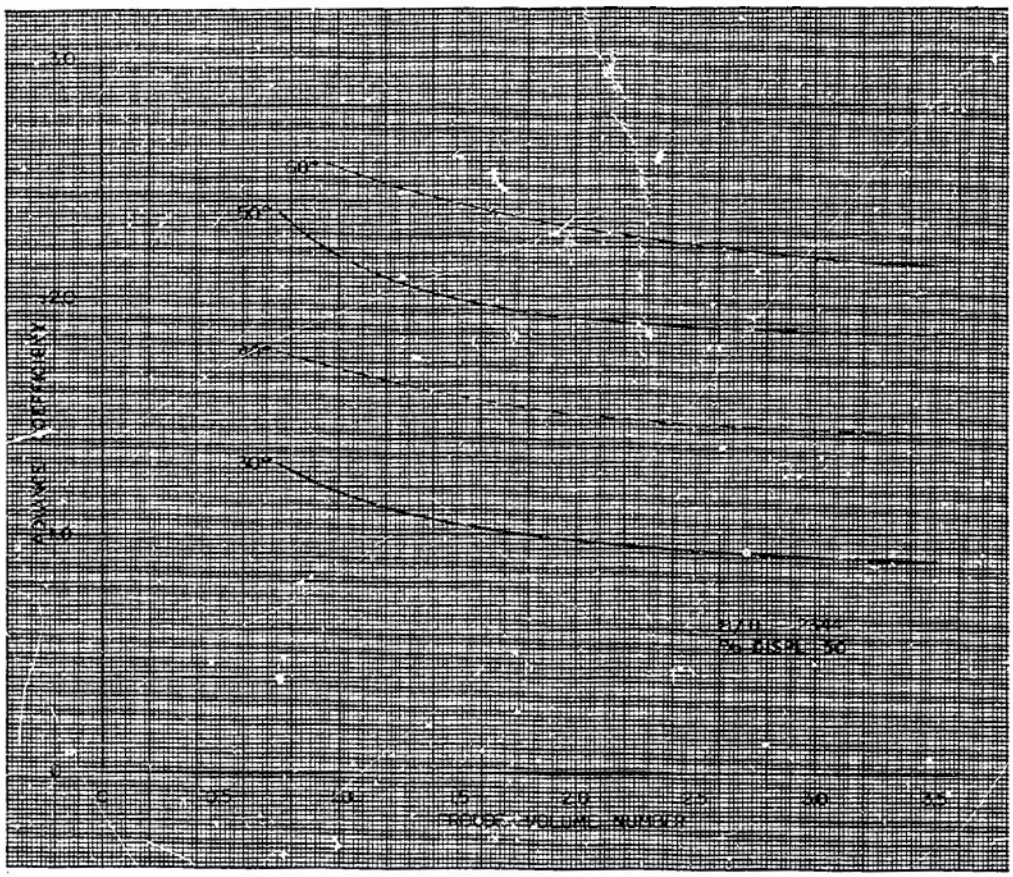

Figure 3-17 Advance Coefficient vs Froude Volume Number
(H/D = 0.2344, 50 Percent Displacement)

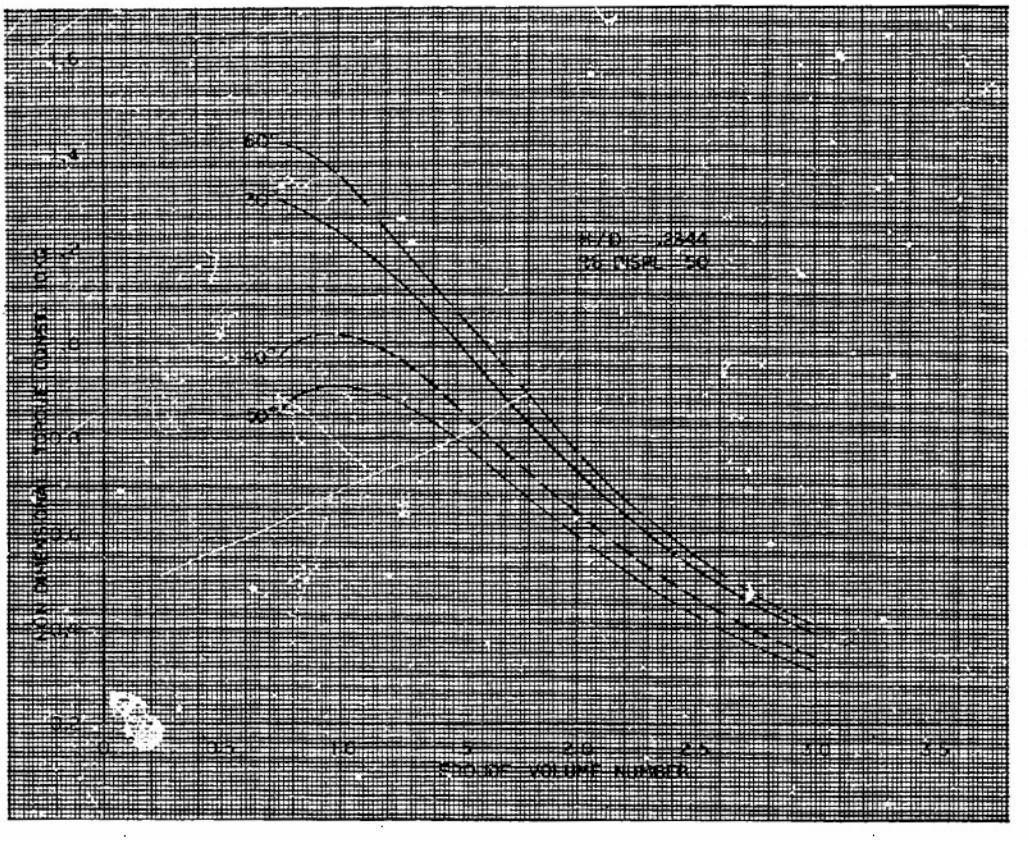

Figure 3-18 Non-Dimensional Torque Constant vs Froude Volume Number (H/D = 0.2344, 50 Percent Displacement)

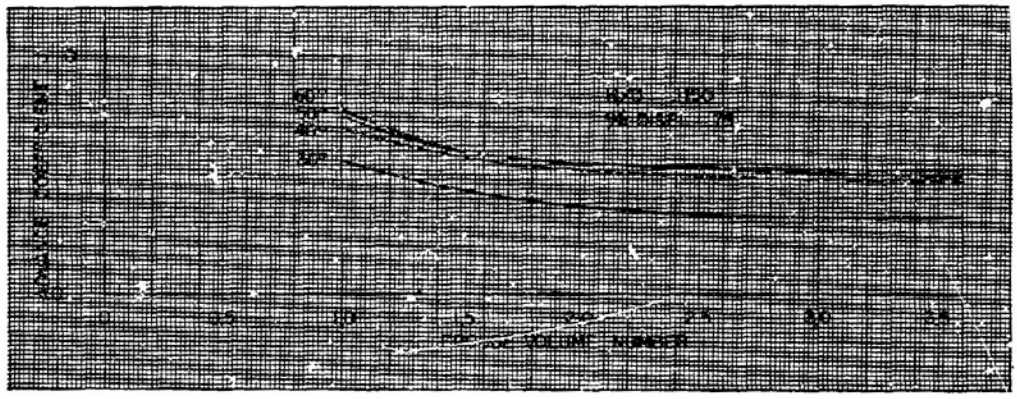

Figure 3-19 Advance Coefficient vs Froude Volume Number
(H/D = 0.1150, 75 Percent Displacement)

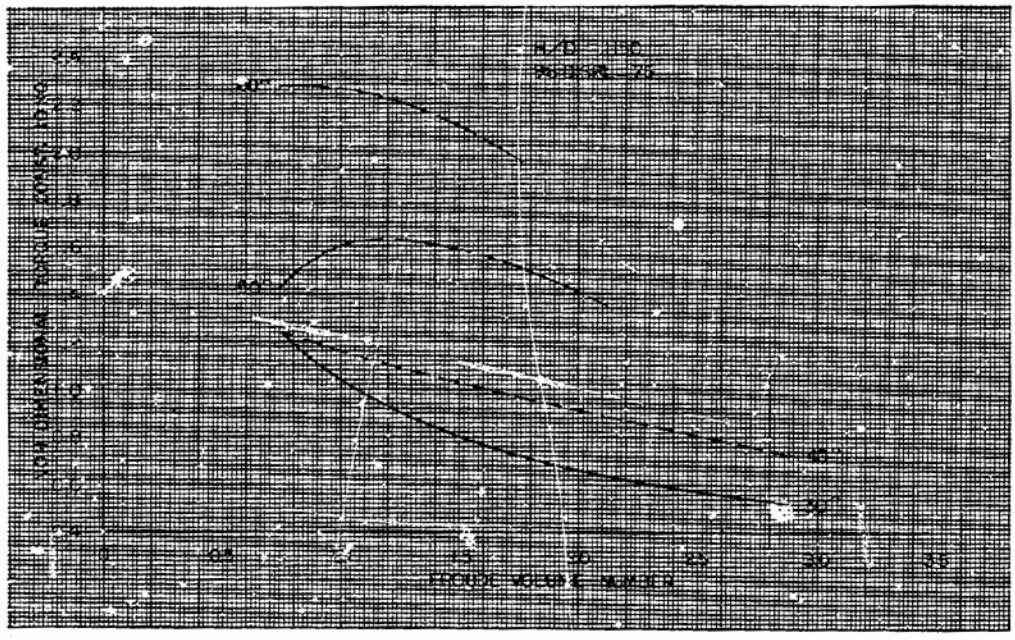

Figure 3-20 Non-Dimensional Torque Coefficient vs Froude Volume Number (H/D = 0.1150, 75 Percent Displacement)

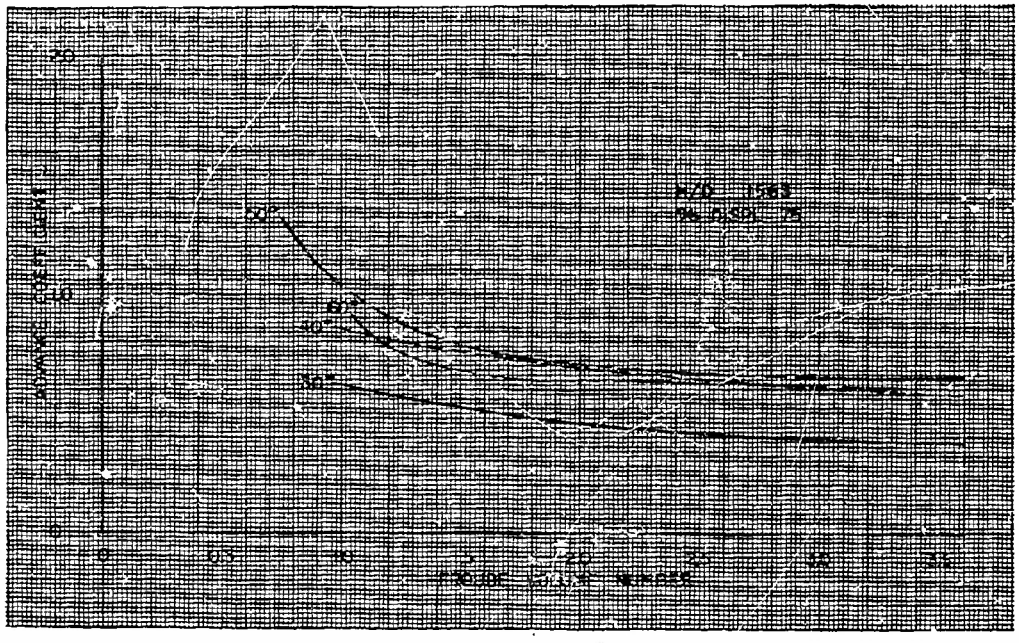

Figure 3-21 Advance Coefficient vs Froude Volume Number
(H/D = 0.1563, 75 Percent Displacement)

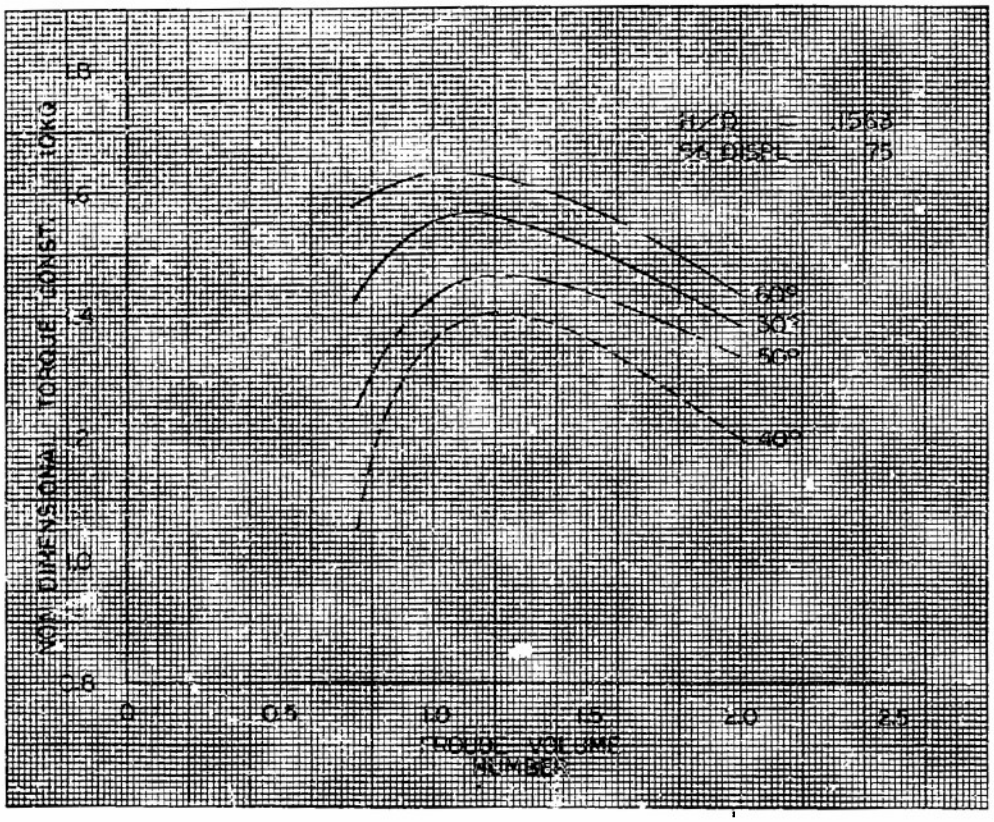

Figure 3-22 Non-Dimensional Torque Coefficient vs Froude Volume Number (H/D = 0.1563, 75 Percent Displacement)

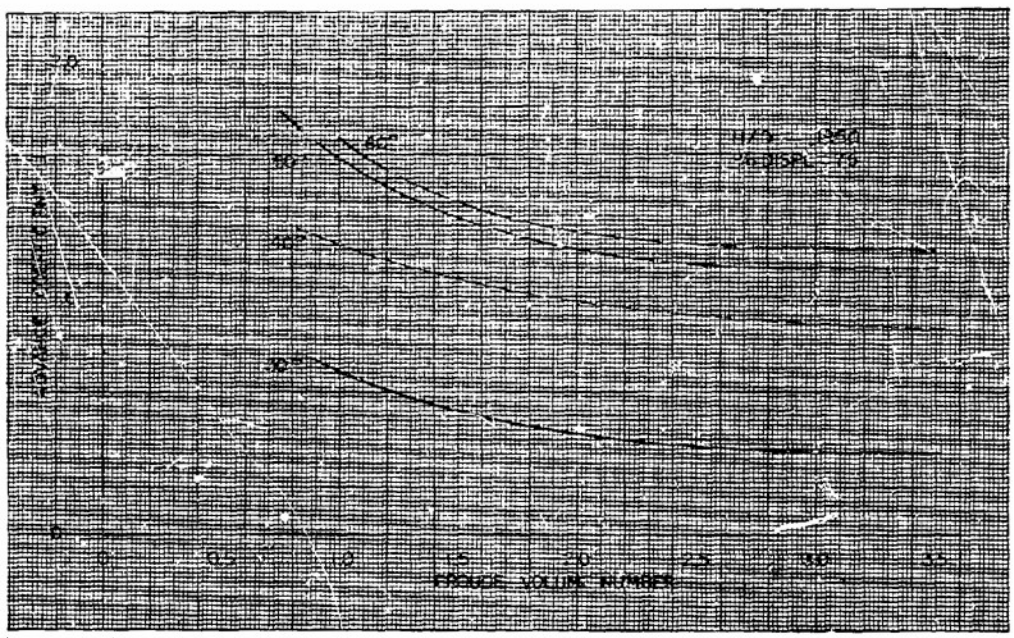

Figure 3-23 Advance Coefficient vs Froude Volume Number
(H/D = 0.1950, 75 Percent Displacement)

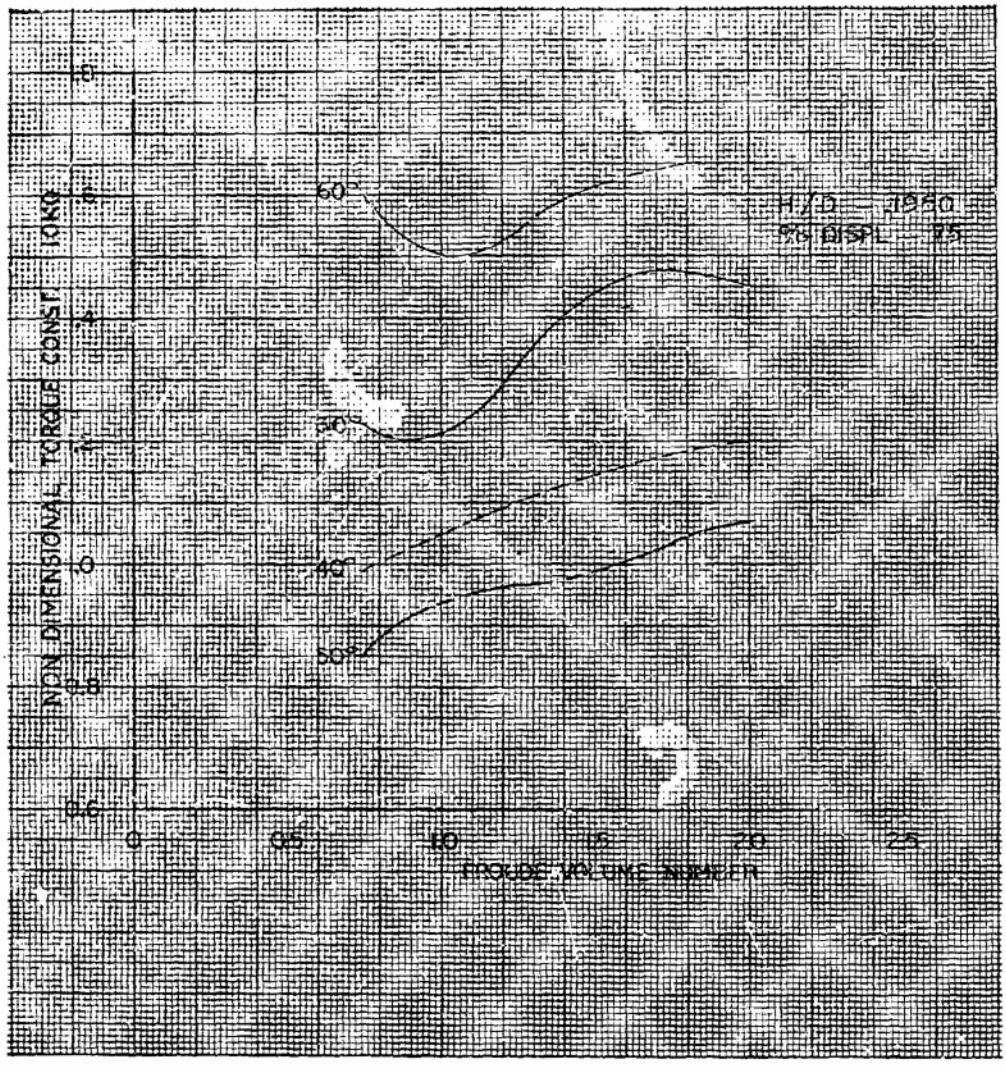

Figure 3-24 Non-Dimensional Torque Coefficient vs Froude Volume Number (H/D = 0.1950, 75 Percent Displacement)

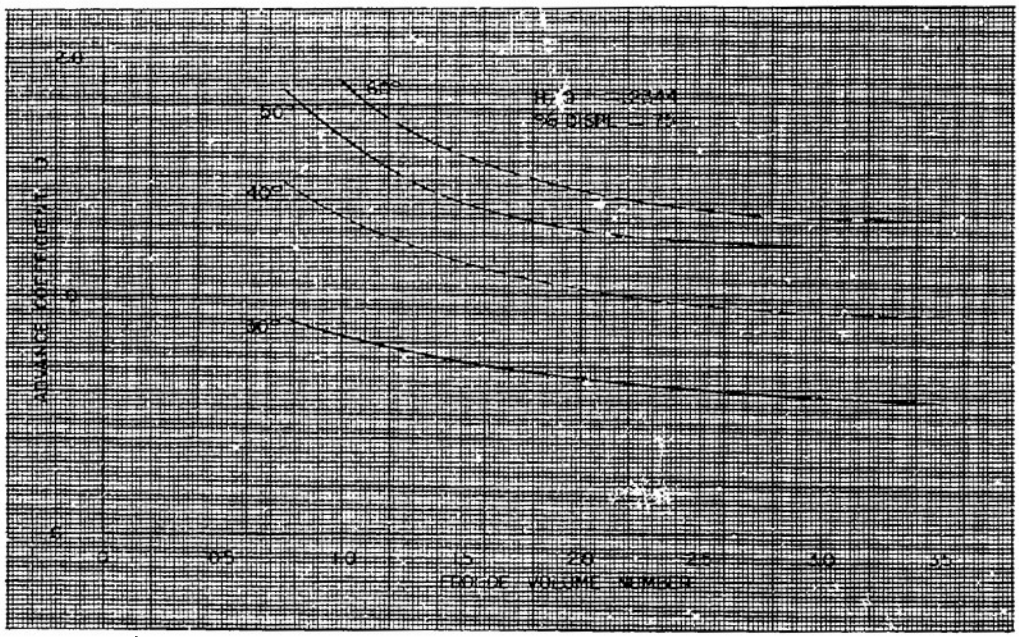

Figure 3-25 Advance Coefficient vs Froude Volume Number (H/D = 0.2344, 75 Percent Displacement)

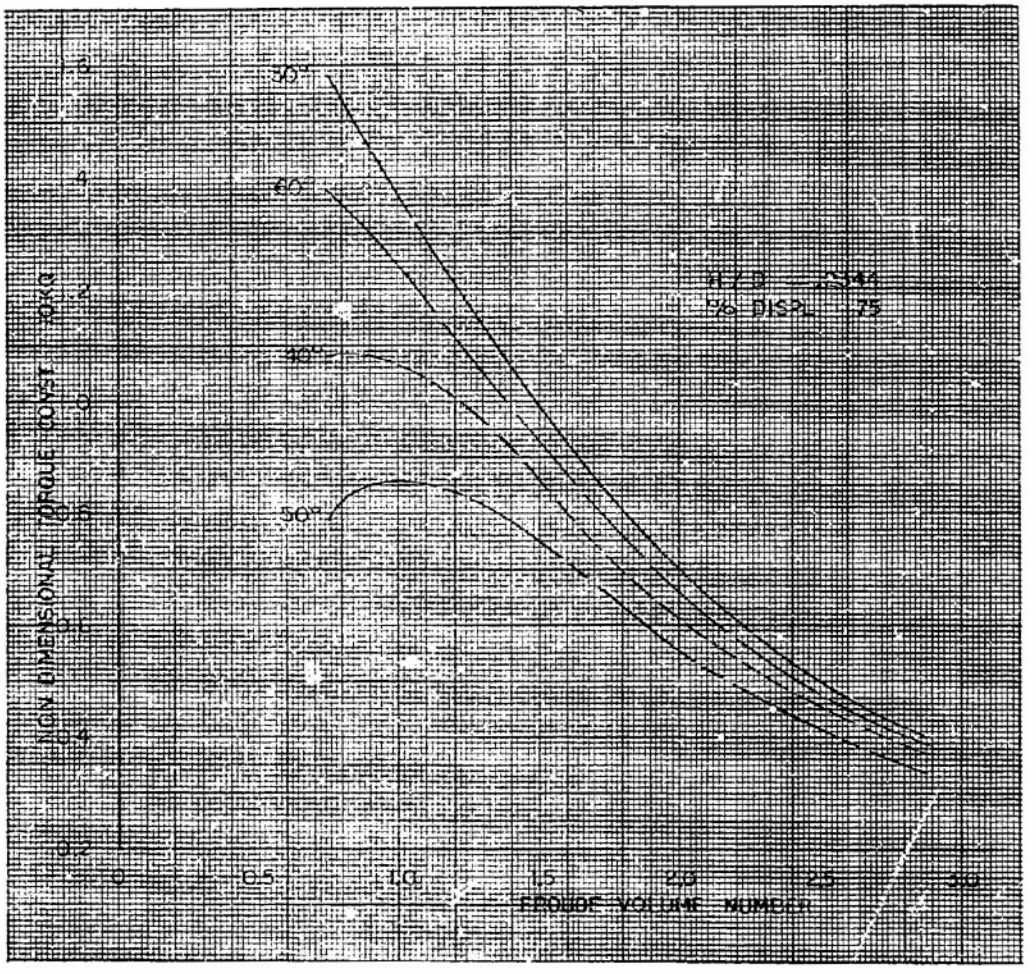

Figure 3-26 Non-Dimensional Torque Coefficient vs Froude Volume Number (H/D = 0.2344, 75 Percent Displacement)

LEGEND FOR FIGURES 3-27 AND 3-28

Curve	Helix Angle	H/D	Percent Displacement
1	50°	0.1950	75%
2	40°	0.1563	50%
3	60°	0.1950	50%
4	50°	0.1950	50%
5	30°	0.1150	25%
6	50°	0.1563	25%
7	50°	0.1950	25%

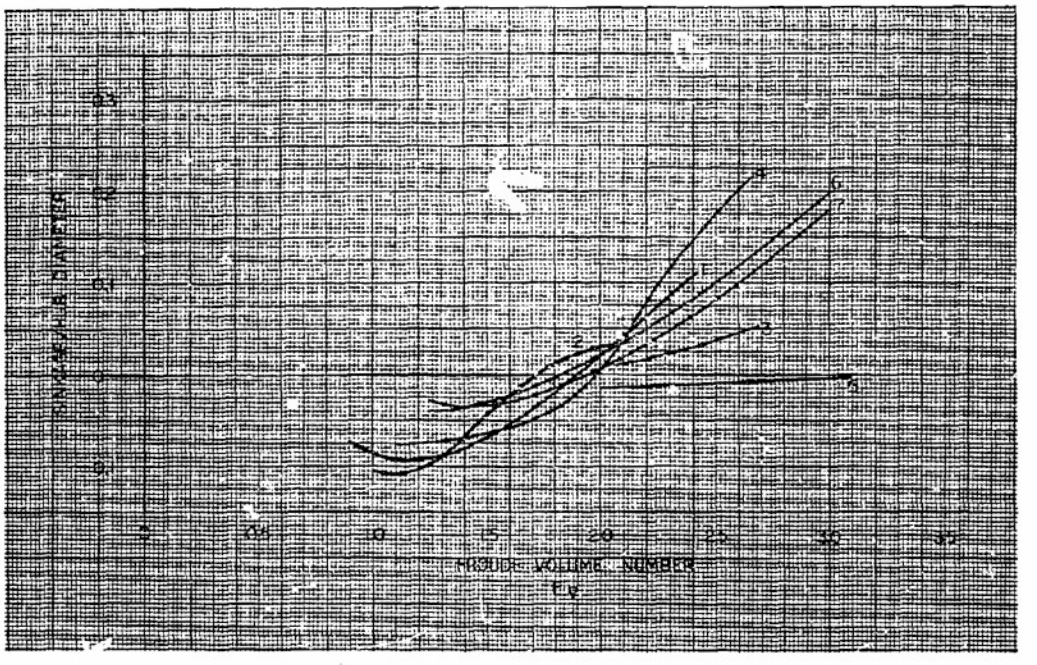

Figure 3-27 Sinkage/Hub Radius vs Froude Volume Number

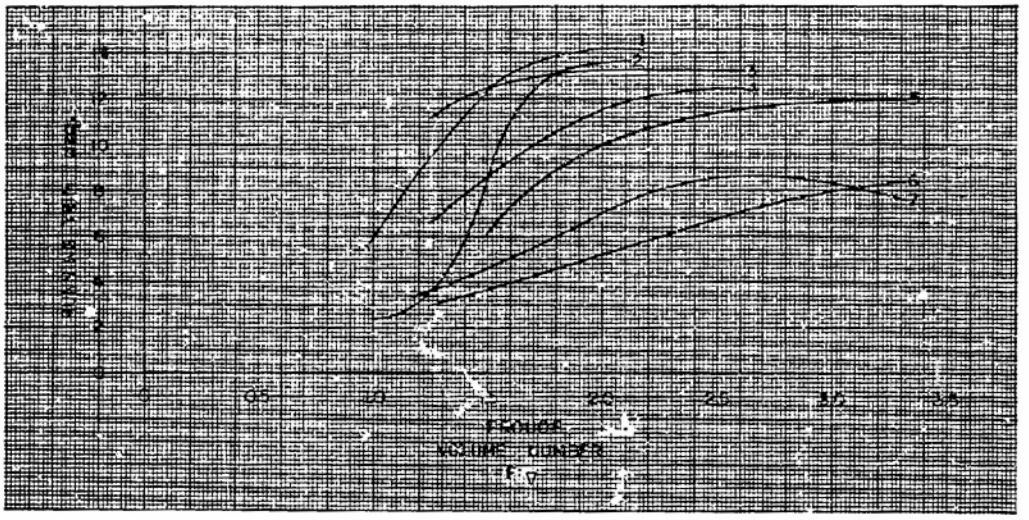

Figure 3-28 Running Trim vs Froude Volume Number

Section III

MISCELLANEOUS CONFIGURATIONS

The results presented in this section are of a limited investigation of the effects of various features and configurations. These tests were not intended to thoroughly explore any particular aspect, but merely to indicate trends in horsepower requirements which would be useful in the preliminary design of a specific vehicle. The different tests run were:

- Effect of initial trimming angle
- Effect of length-diameter ratio
- Effect of number of blades
- Effect of rotor stern shape
- Effect of a progressive helix angle
- Effect of a varying hub diameter
- Effect of blade cross sections
- Interaction effects between two ratios
- Effect of shrouds
- Effect of chain housing drag
- Drawbar pull tests

Since no particular aspect was thoroughly investigated, these sections will include additional explanations and conclusions which will be useful in understanding overall water performance. Throughout this section actual test data and results will be distinguished from pure con-

jecture. Since only one particular rotor configuration was used to investigate certain aspects, no specific horsepower requirements for configurations different from that tested can be specified, and only a trend can be established. Horsepower requirements are based on a scale ratio of three. It is important to realize that these trends may be either conclusively desirable or not, and the possibility of arriving at misleading conclusions is introduced. Certain aspects investigated may provide adverse results, but complete abandonment of the original idea is not necessarily warranted.

The test parameters and conditions pertaining to each investigation will be explained with the results noted on the graphs. Horsepower requirements and revolutions per second are presented either as a percentage of full scale values, or full scale values depending on what seemed appropriate.

3-1. EFFECT OF INITIAL TRIMMING ANGLE

One of the first series of tests was conducted in order to determine the optimum initial static trim. These tests were performed because it was anticipated that torque and RPM would be influenced by the position of the initial longitudinal center of gravity. This sequence of tests was conducted on a limited number of rotors of various configurations and various displacements, over a range of static trim angles from two degrees bow down to four degrees bow up.

The results are presented as percent incremental torque - vs - static trim angle for various speeds and percent displacements (Figures 3-29 through 3-36). The RPM data was plotted in a similar manner. The percent incremental torque is the ratio of torque at various trim angles compared to that value at one degree bow up static trim. Obviously the base torque varies for various configurations, displacements, and speeds. For certain sets of conditions, one degree initial trim is not the optimum and the graph indicates a negative percent change in torque. Since the same procedure was followed when plotting percent change in RPM - vs - initial trim the results are similar. The figures show that the optimum trim angle is a function of displacement, speed, and rotor configuration but generally one degree bow up static trim gives the least horsepower absorbed.

This value, one degree bow up static trim, was adopted for all the tests of the systematic series of rotors and for the remainder of the miscellaneous investigations. This corresponds to a vehicle with a longitudinal center of gravity somewhat aft of the mid-length of the rotors; the exact location is dependent on displacement. For vehicles with a center of gravity position different than that corresponding to the optimum static trim angle, estimates of incremental horsepower required can be made from the graphs in this section.

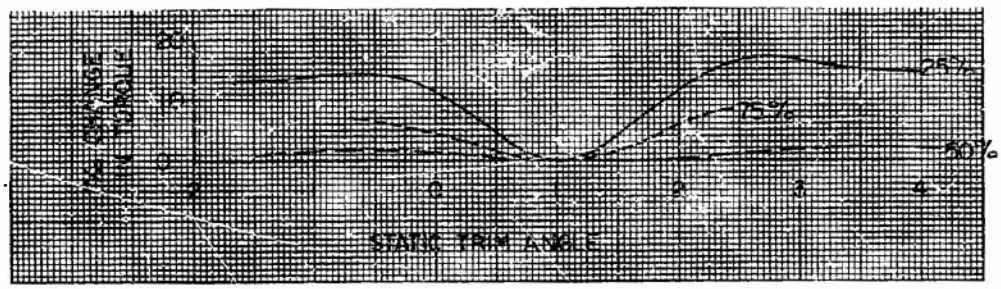

Figure 3-29 Percent Change in Torque vs Static Trim Angle, 40 Degree Helix Angle (H/D = 0.1950, V = 5 MPH)

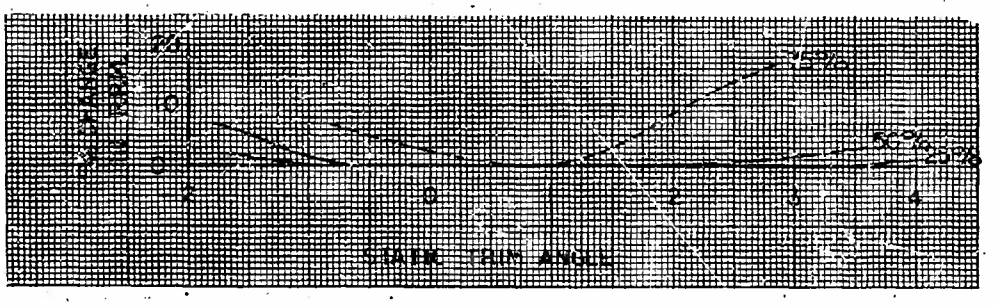

Figure 3-30 Percent Change in RPM vs Static Trim Angle, 40 Degree Helix Angle (H/D = 0.1950, V = 5 MPH)

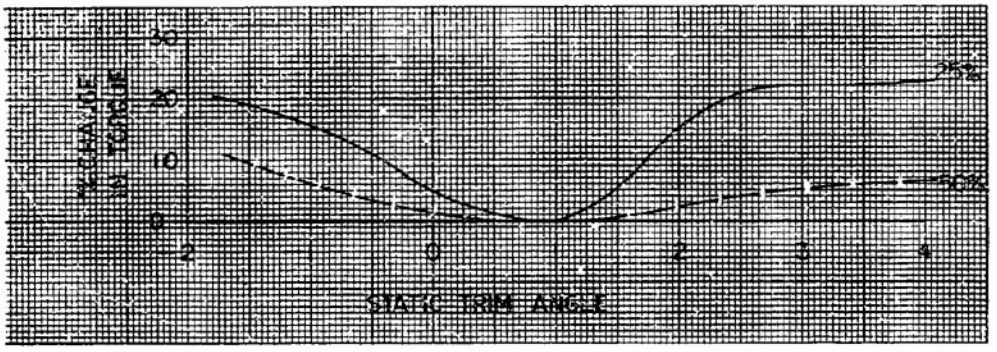

Figure 3-31 Percent Change in Torque vs Static Trim Angle, 40 Degree Helix Angle (H/D = 0.1950, V = 10 MPH)

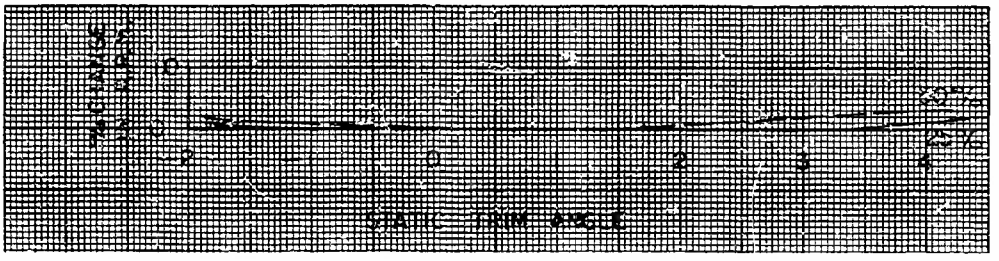

Figure 3-32 Percent Change in RPM vs Static Trim Angle, 40 Degree Helix Angle (H/D = 0.1950, V = 10 MPH)

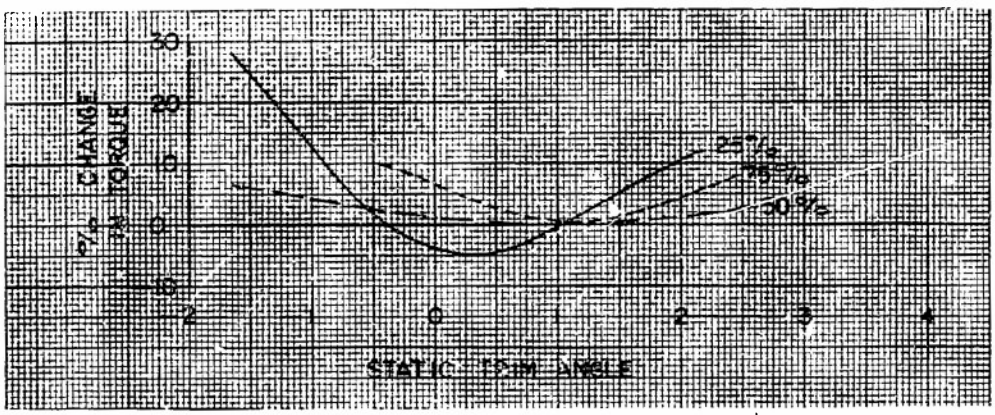

Figure 3-33 Percent Change in Torque vs Static Trim Angle, 40 Degree Helix Angle (H/D = 0.2344, V = 5 MPH)

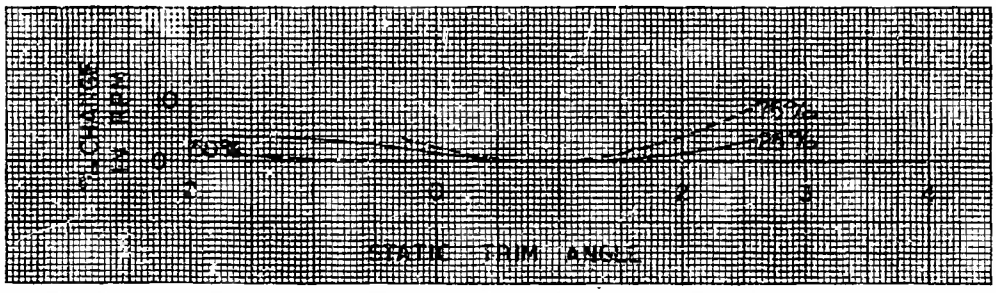

Figure 3-34 Percent Change in RPM vs Static Trim Angle, 40 Degree Helix Angle (H/D = 0.2344, V = 5 MPH)

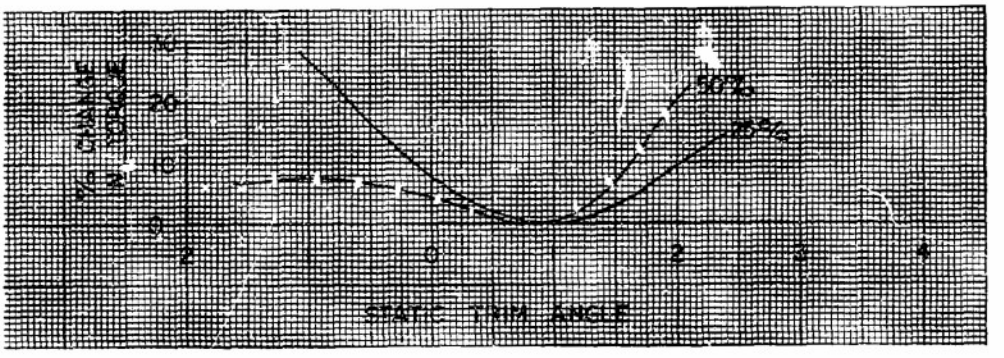

Figure 3-35 Percent Change in Torque vs Static Trim Angle, 40 Degree Helix Angle (H/D = 0.2344, V = 10 MPH)

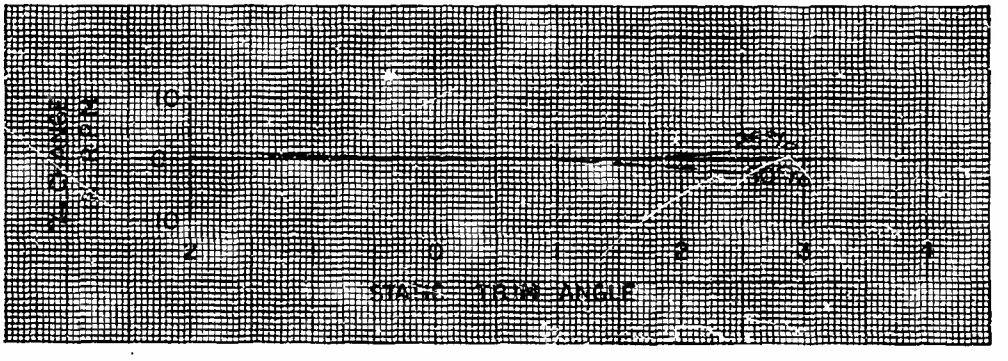

Figure 3-36 Percent Change in RPM vs Static Trim Angle, 40 Degree Helix Angle (H/D = 0.2344, V = 10 MPH)

3-2. EFFECT OF LENGTH-DIAMETER RATIO

All 1/3 scale rotors, with the exception of this particular investigation, were 48 inches long and had a hub diameter of 8 inches. One set of configurations was designed to investigate the effect of various length-diameter ratios (Figures 3-37 through 3-41). In this case the length was held constant and the diameter varied since the same test apparatus was used. The "parent" model in this series of 40 variations was the 50 degrees helix angle, 1.875-inch blade height rotor. In addition to the model mentioned above whose length to diameter (L/D) ratio equals six, three additional models were tested with hub diameters of 4.75, 6.00, and 12.00 inches. Blade heights were such that the blade height to dimater (H/D) ratio was the same for all models in the series. All rotors were tested in two displacement conditions 40 and 60 percent of the total hub volume. Adoption of a constant percentage displacement meant that actual volume displacement varied from one rotor to another. Because of this, the accompanying graph (Figure 3-37) shows specific horsepower - vs - length-diameter ratio based on a scale ratio of three. The graph indicates an optimum L/D of about 5.8, which is dependent on speed and loading to some extent.

However, this is only one method of determining optimum rotor proportions. Other considerations need to be taken into account in any specific design case. For instance, the most efficient rotor configuration may be defined as that which will transport any weight for the least power. Neither the weight nor the power

need be specified in the general case. Alternatively, in a specific design the weight to be transported would be known, fairly closely, such that the configuration yielding the minimum horsepower to transport that weight would be sought. Conceivably these two concepts may not be completely compatible. That is, another load may be transported more efficiently than that dictated by the specific design. In practice, however, the least possible vehicle weight would be sought and then the minimum horsepower configuration. Therefore, the optimum L/D ratio is first a function of design parameters which are unknown at this time, and the accompanying graph may be of only academic interest.

Another factor influencing the results presented herein was the manner in which the blade heights tests were determined. For all rotors H/D was held constant at 0.2433 which meant that the blade heights were not constant. In fact the blades on the rotor of highest L/D were quite small compared to those on the rotor of lowest L/D. For instance, since less horsepower is absorbed as blade height increases on the same rotor, had all blades been of the same height the optimum L/D on the accompanying plot would have been of a higher value. The correct choice of blade height parameter is difficult to judge. Perhaps blade area divided by $\nabla^{2/3}$ would be a good choice since blade loading might then tend to be constant. In this case blade height would be proportional to $D^{4/3}$. However, viewed this way the optimum L/D would be less than 5.8.

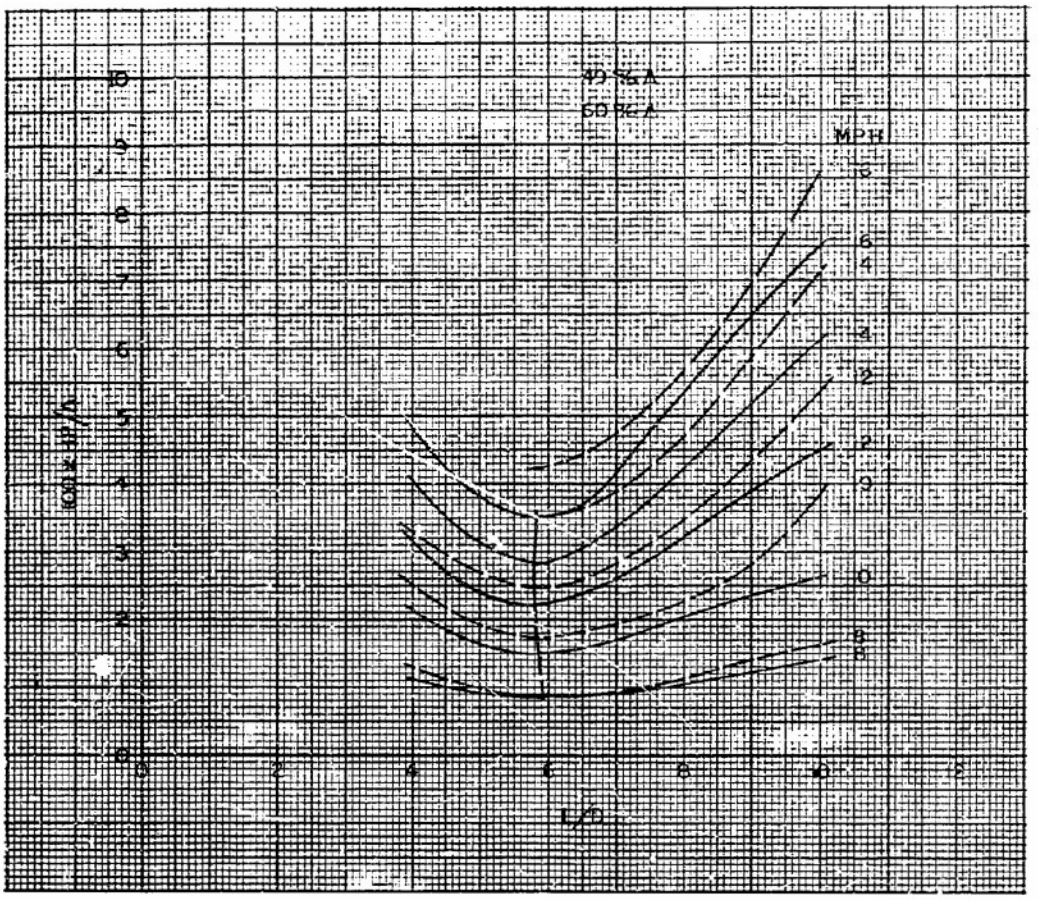

Figure 3-37 Specific Horsepower vs Length-Diameter Ratio

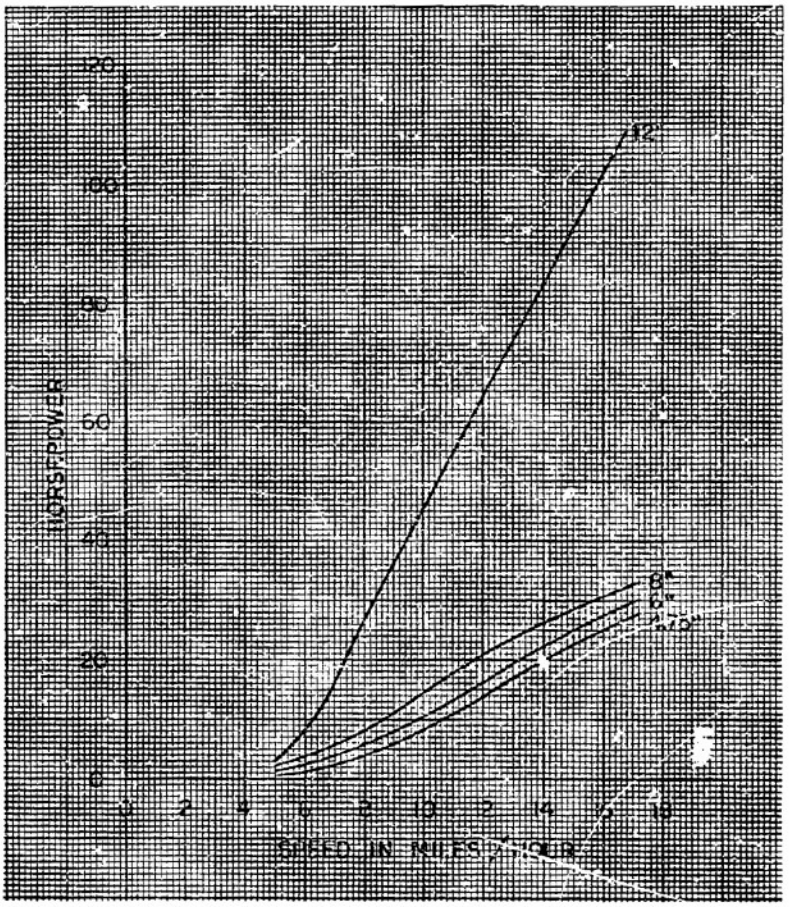

Figure 3-38 Horsepower vs Speed, 40 Percent Displacement

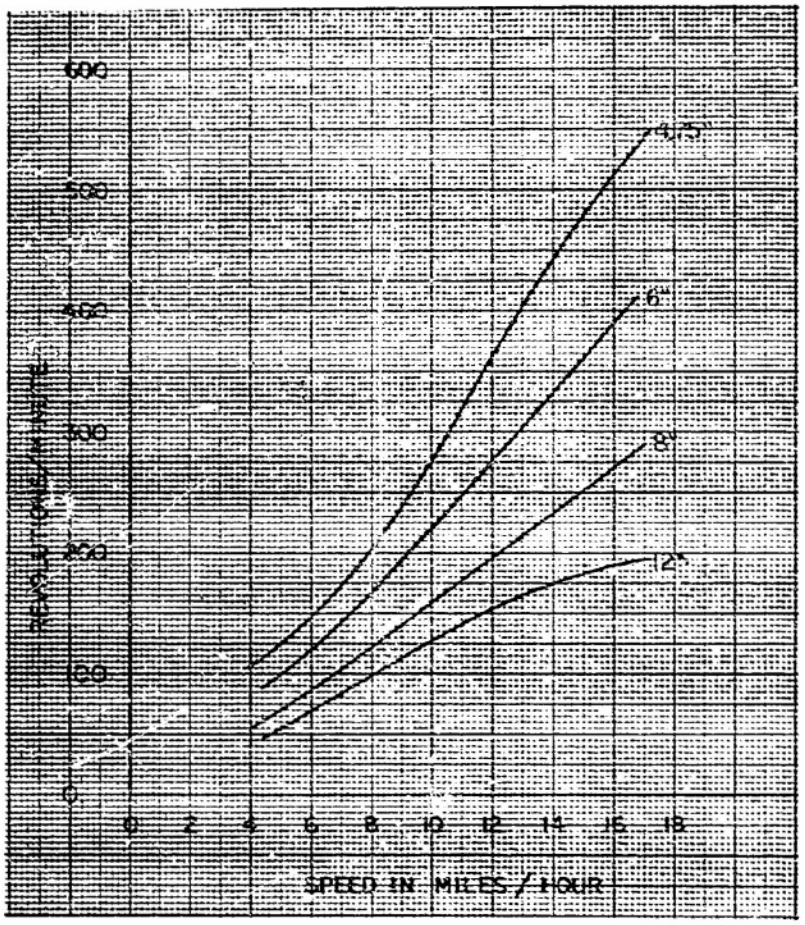

Figure 3-39 RPM vs Speed, 40 Percent Displacement

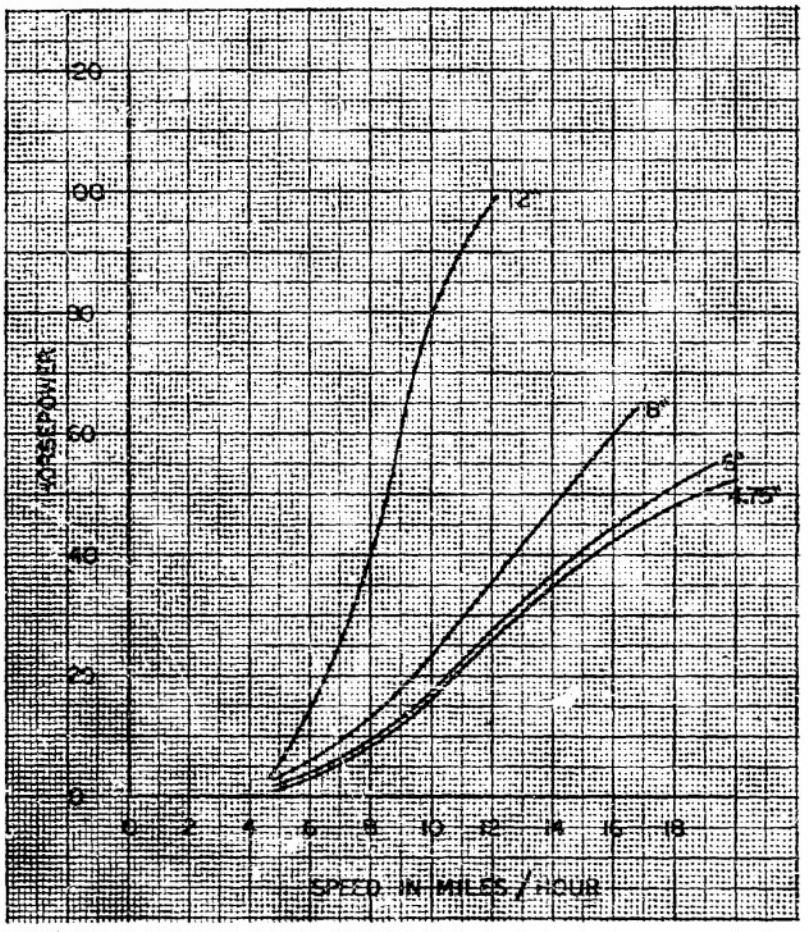

Figure 3-40 Horsepower vs Speed, 60 Percent Displacement

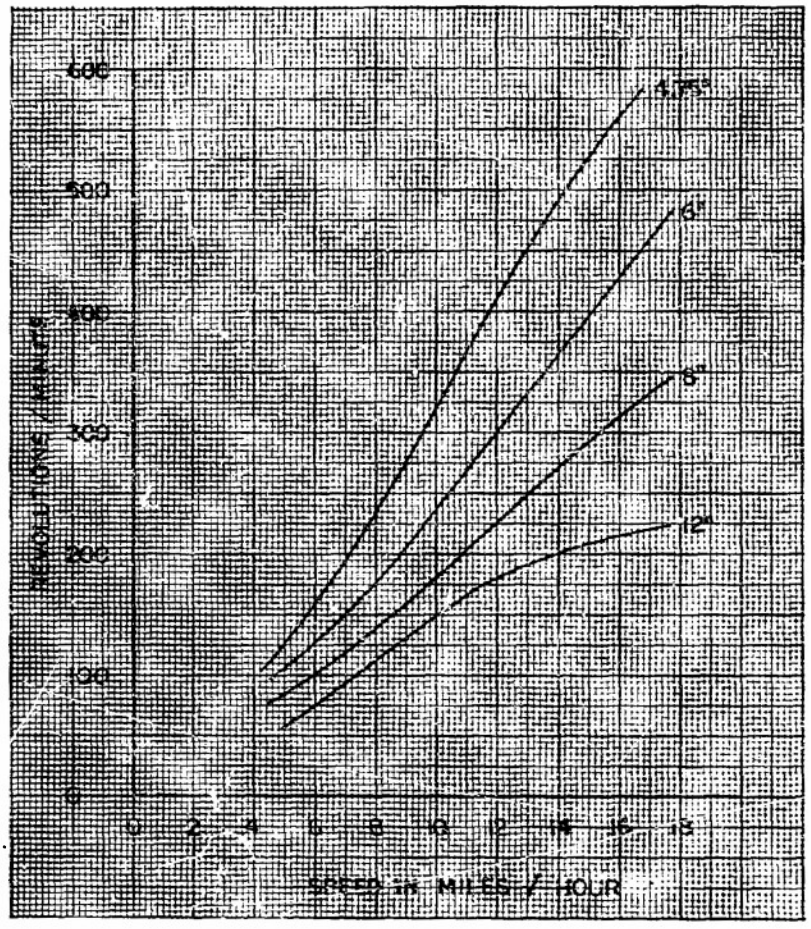

Figure 3-41 RPM vs Speed, 60 Percent Displacement

3-3. EFFECT OF NUMBER OF BLADES

Testing for the effect of the number of blades was conducted with a two bladed rotor and a single blade rotor with 40 degree helix angles and 1.875 model blade height. Results of these tests are shown in figures 3-42 and 3-43. Data and results from a previous program testing a three bladed rotor are reported for the sake of completeness (figure 3-44). Since the rotor configurations and conditions for the three blade rotor and the one blade rotor are different, the data are plotted separately. This aspect has not been investigated rigorously but is sufficient to establish a trend.

Comparison between the two and three bladed rotors indicates that the presence of three blades is detrimental to the thrust developed even though the total blade area is increased. A comparison between the one and two bladed rotor, which was conducted in the current test program, indicates that for the heavier displacements reducing the number of blades to one reduces the blade area to an insufficient level. It can be concluded that two blades provide the greatest thrust and with a minimum impediment of flow.

The tests conducted under a previous contract were run at a fixed linkage and trim since the test-rig was not as sophisticated as the present fixture. The data obtained from the one lead 40-degree helix, 1.875-inch model blade height rotor indicated that at 25 percent displacement it might be possible that less horsepower would be required than for the identical rotor with two leads.

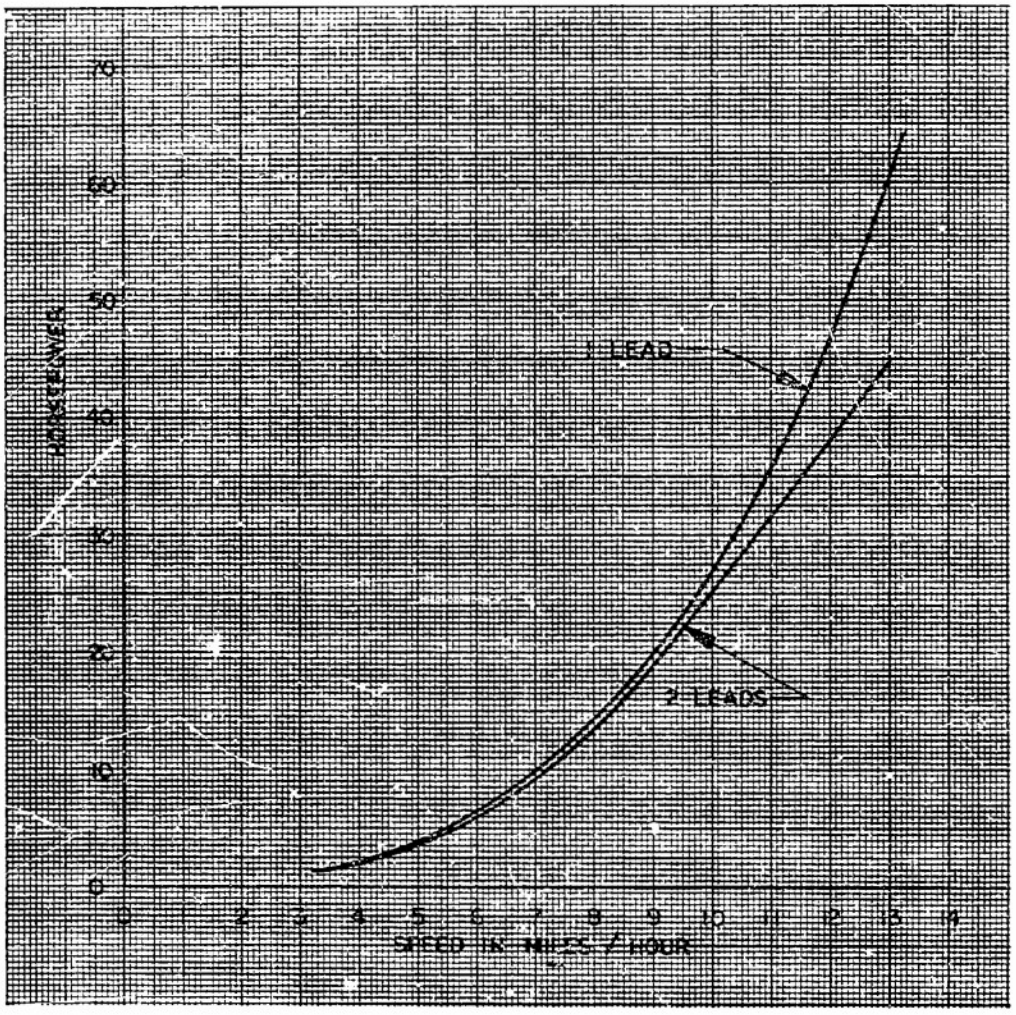

Figure 3-42 One Lead vs. Two Leads (40 Degree Helix, H/D = 0.2344, and 50 Percent Displacement)

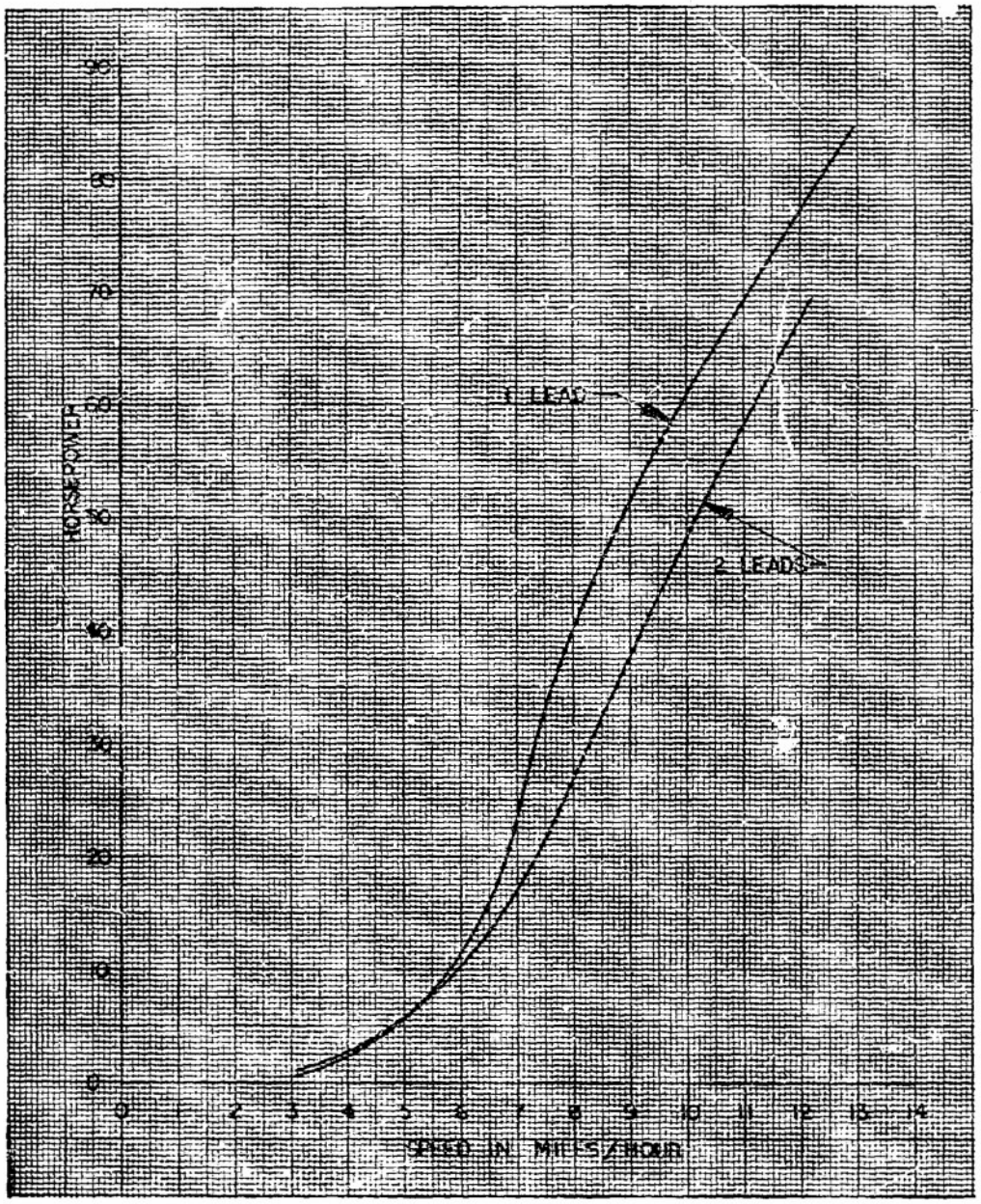

Figure 3-43 One Lead vs. Two Leads 140 Degree Helix, H/D = 0.2344, and 75 Percent Displacement

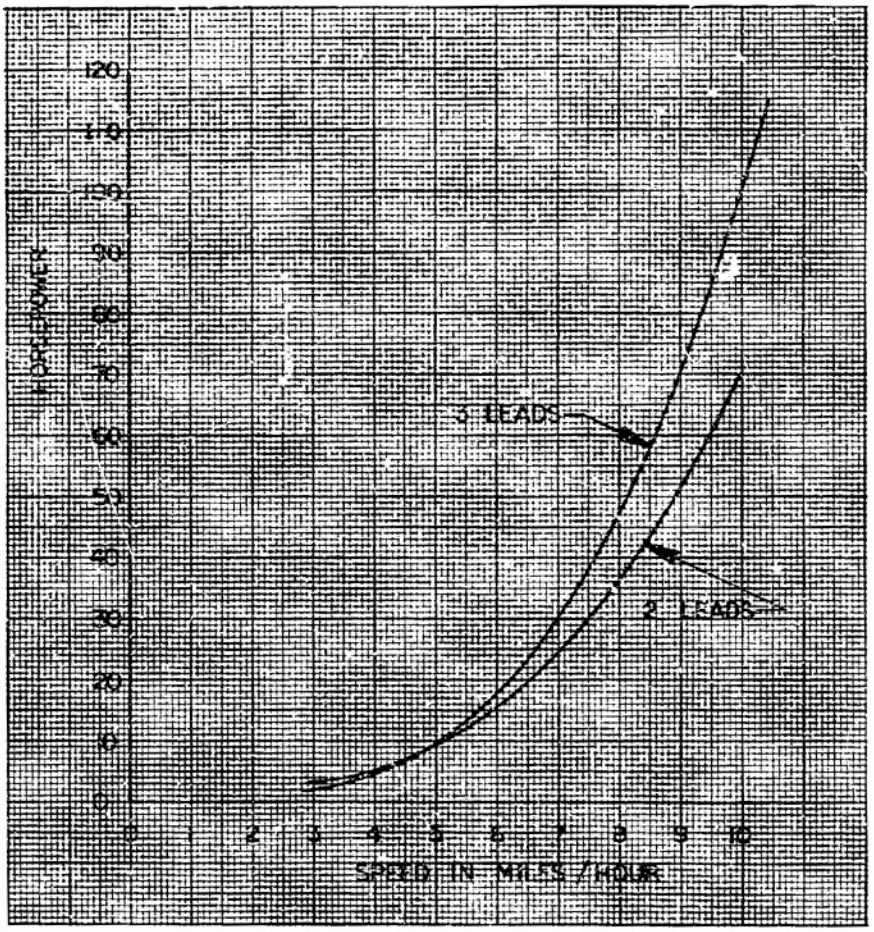

Figure 3-44 Three Leads vs. Two Leads 130 Degree Helix, H/D = 0.1150, and 75 Percent Displacement

3-4. EFFECT OF ROTOR STERN SHAPE

The shape of the rotor hub was investigated with the intention that form drag could be minimized at the higher speeds. As seen in figure 3-45 one rotor completed the cylindrical shape rather than tapering the end similar to the forward portion of the rotor. The reduction in horsepower is rather dramatic and is attributable to a lower trim angle and improved dynamic lift. Improved dynamic lift is indicated by reduced sinkage. (See figures 3-46 through 3-49.)

At lighter displacements than tested, the point at which the horsepower required for the tapered stern and blunt stern are equivalent would occur at a lower speed than indicated on the plot. The opposite would be true at a displacement higher than that tested.

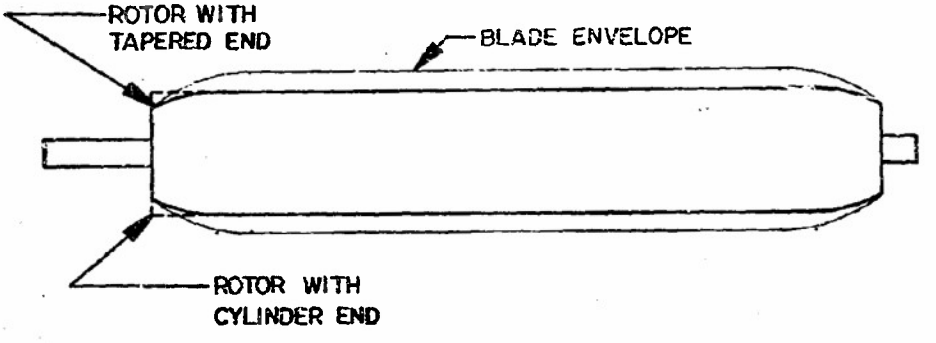

Figure 3-45 Rotor Stern Shapes

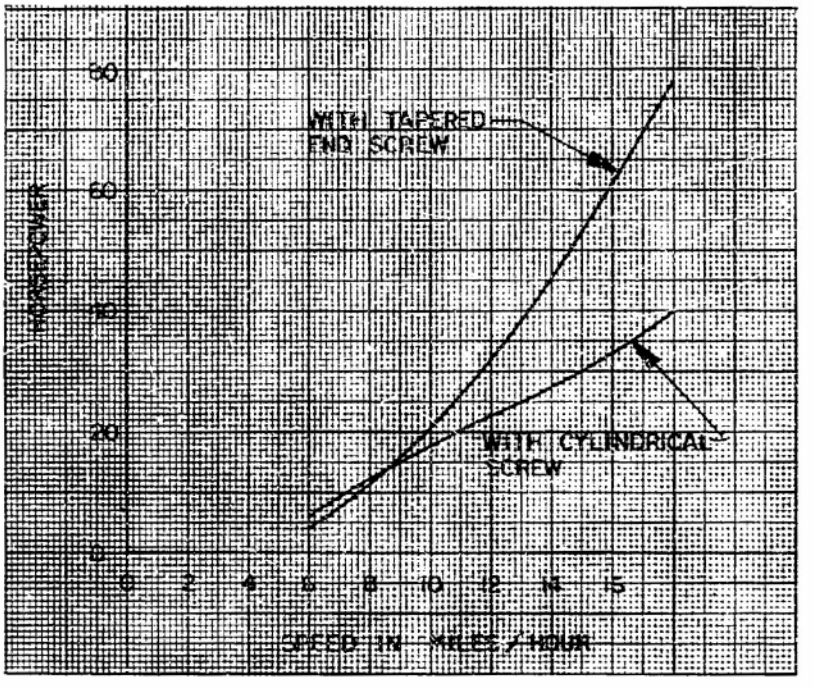

Figure 3-46 Stern Shape Effect, Horsepower vs Speed

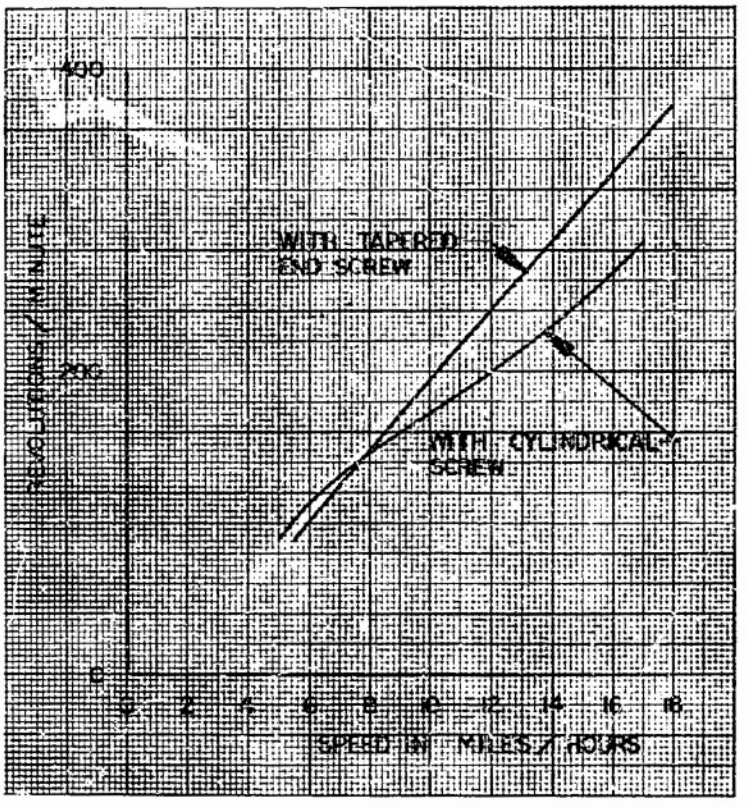

Figure 3-47 Stern Shape Effect, RPM vs Speed

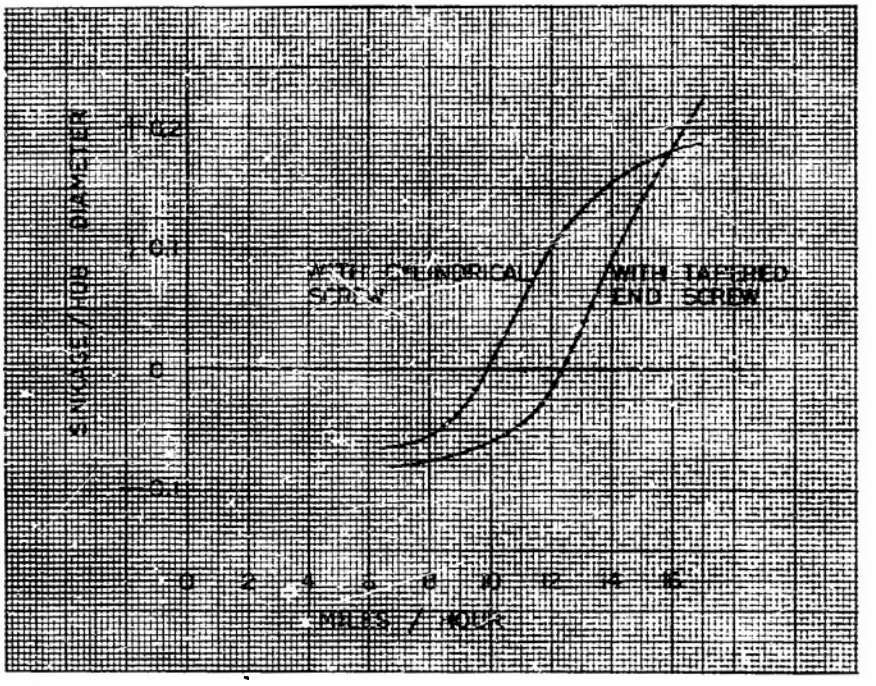

Figure 3-48 Stern Shape Effect, Sinkage/Hub Diameter vs Speed

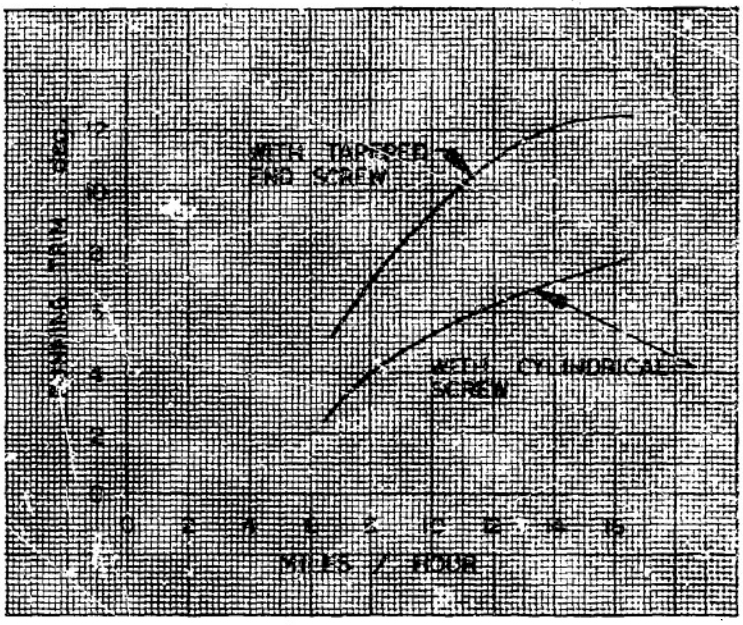

Figure 3-49 Stern Shape Effect, Running Trim vs Speed

3-5. EFFECT OF A PROGRESSIVE HELIX ANGLE

It would seem plausible that the most efficient rotor would be one that consistently accelerates the flow towards the stern of the rotor instead of one where the flow is initially accelerated at the bow and then carried along the remaining length of the rotor. This reasoning was investigated with a rotor with a helix angle that varied linearly from 35 degrees at the bow to 50 degrees at the stern. The blade height was 1.56 inches and tests were conducted at three displacements.

Reviewing the results, it is difficult to say what rotor would be comparible, if any, to the progressive pitch rotor. From figures 3-50 through 3-55, the only adverse effects of the varying helix angle are shown at the higher speeds. At the lower speeds conclusions are not easily reached. While these particular tests show adverse effects, certainly abandonment of this idea is not necessarily warranted since helix angle variations other than linear may be recommendable in a specific design.

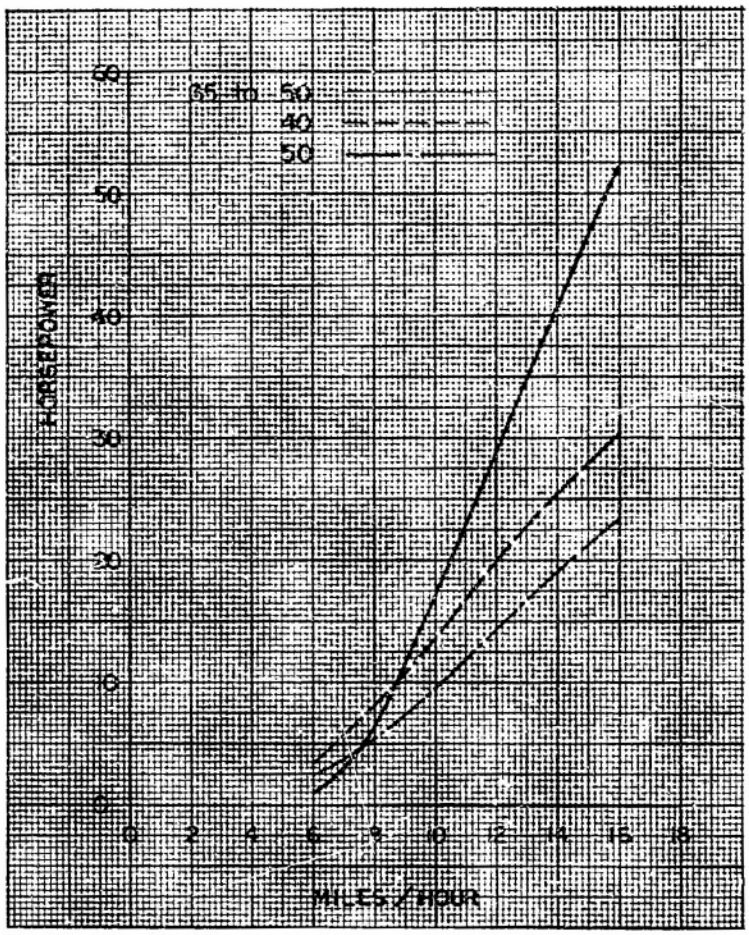

Figure 3-50 Progressive Helix Angle,
Horsepower vs. Speed (25 Percent Displacement)

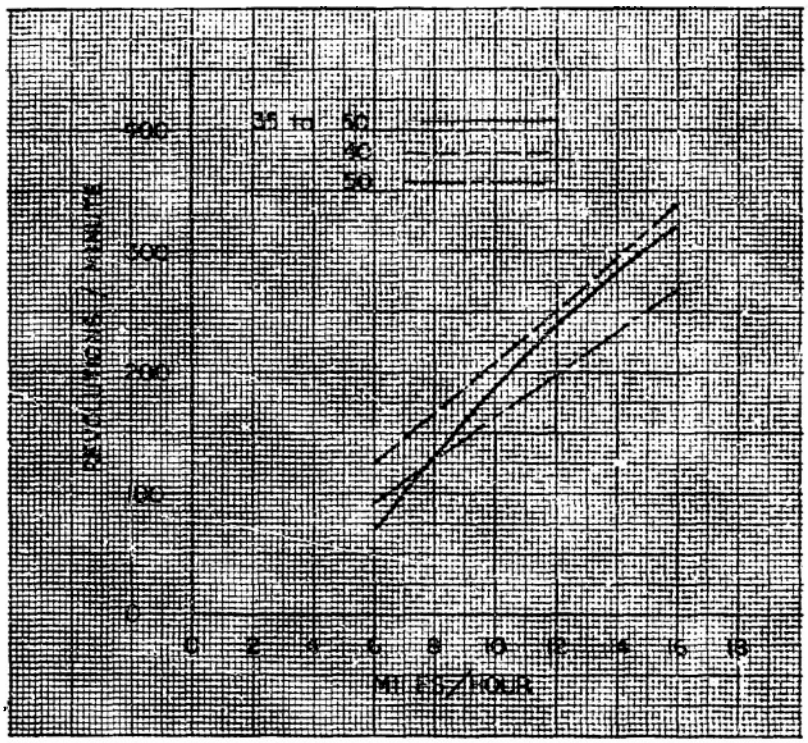

Figure 3-51 Progressive Helix Angle, RPM vs Speed
(25 Percent Displacement)

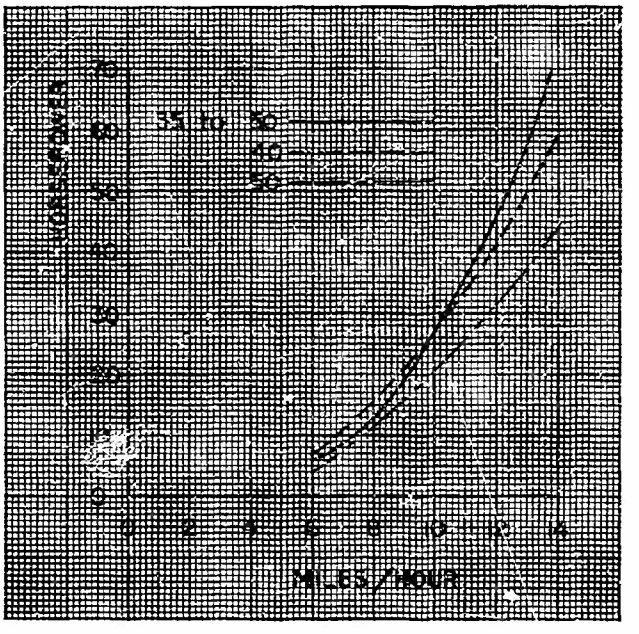

Figure 3-52 Progressive Helix Angle, Horsepower vs. Speed (50 Percent Displacement)

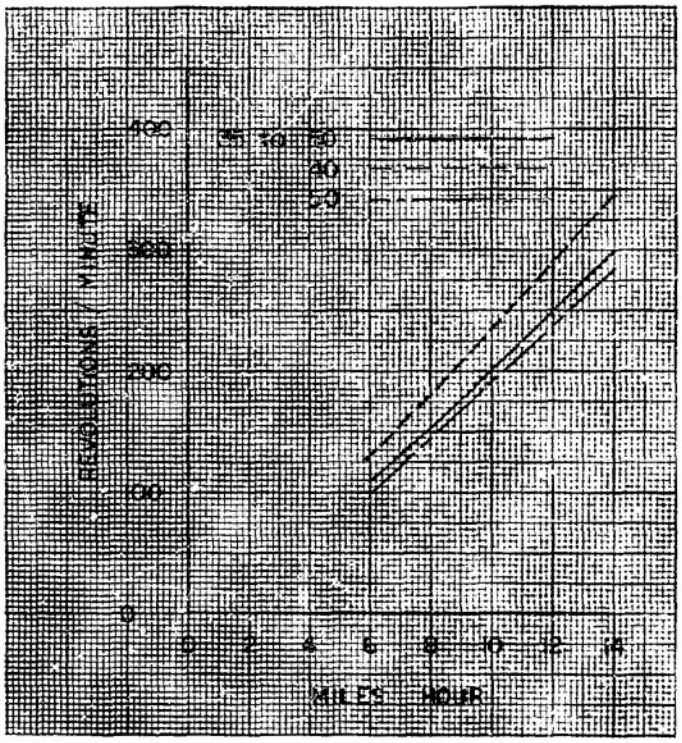

Figure 3-53 Progressive Helix Angle, RPM vs Speed (50 Percent Displacement)

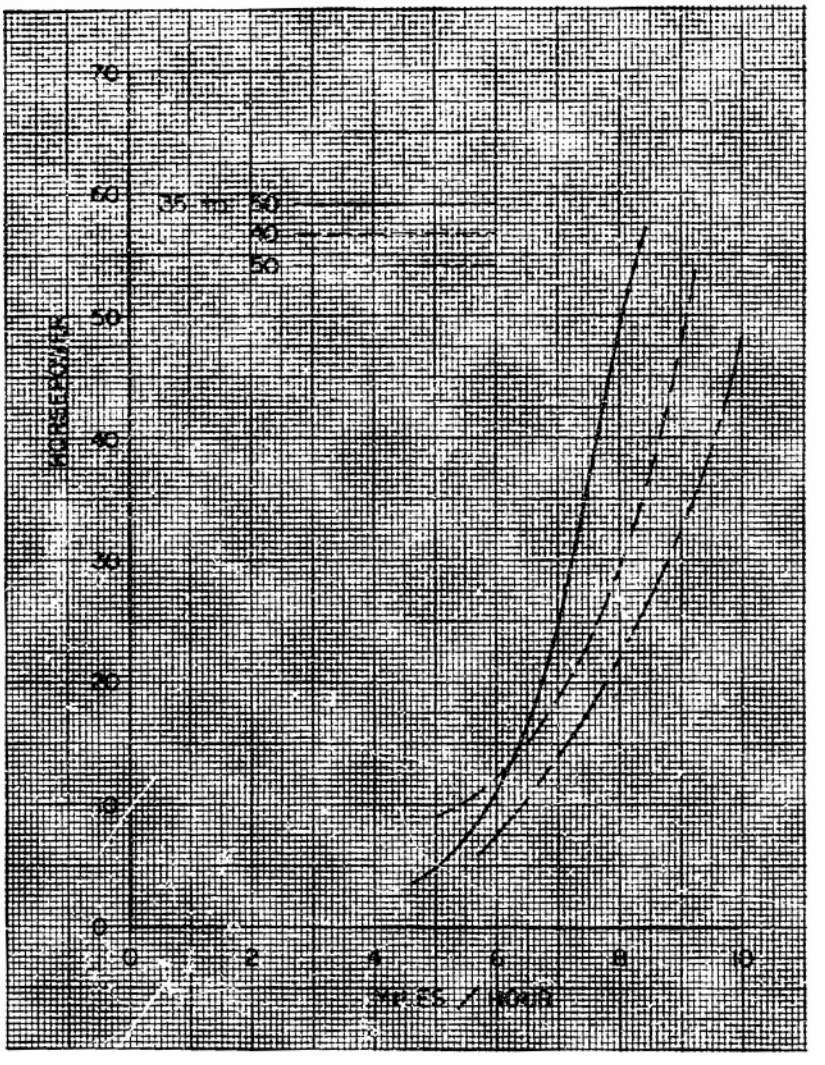

Figure 3-54 Progressive Helix Angle,
Horsepower vs. Speed (75 Percent Displacement)

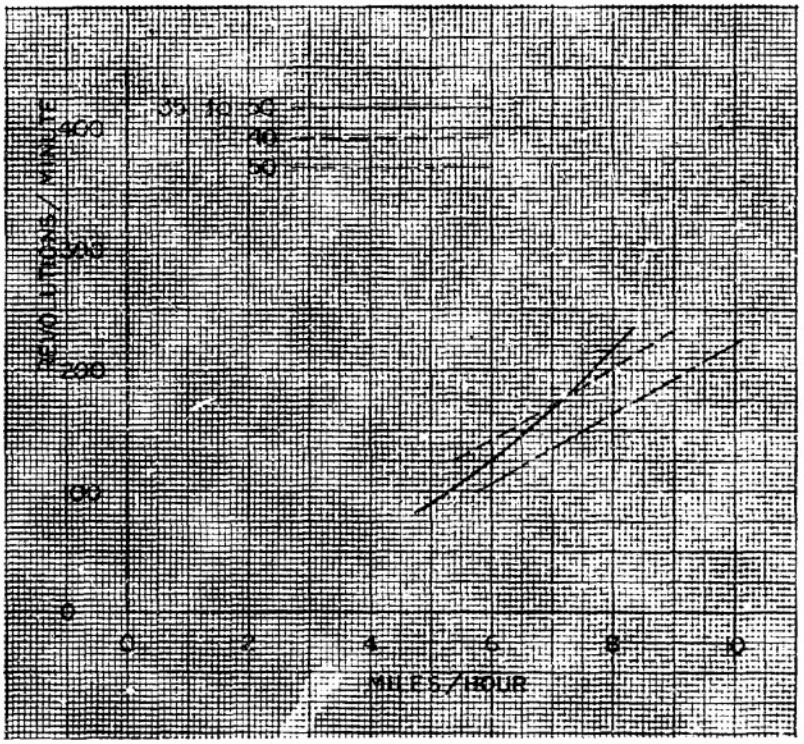

Figure 3-55 Progressive Helix Angle, RPM vs Speed (75 Percent Displacement)

3-6. EFFECT OF A TAPERING HUB DIAMETER

Another configuration tested was a model with a linearly varying diameter. The hub middlebody was a truncated right cone 36 inches long with a seven-inch diameter at the bow and a nine-inch diameter near the stern. The blade height was 1.56 inches with a constant helix angle at the surface of 50 degrees. The tests were run at two percentage displacements, 40 and 60 percent.

The following table is a comparison of the tapered hub rotor with a 50 degree, 1.56-inch blade height, 8-inch diameter rotor. The table shows the result of horsepower per pound displacement for the two models. A scale ratio of three was assumed. The table indicates that the tapered hub rotor of the configuration used offers no advantage over the cylindrical hub rotor.

	100 HP/$_\Delta$		
VELOCITY-MPH	CONICAL HUB		CYLINDRICAL HUB
	40%	60%	50%
5	.50	.47	.18
6	1.00	.90	.38
7	1.39	2.41	.65
8	3.65	—	.99

3-7. EFFECT OF BLADE CROSS-SECTION

The results presented in this section are taken from a previous program and are presented for completeness. All models had blade cross-sections which were rectangular with the exception of this particular investigation where cupped blades were used. For details of the blade cross-section, refer to Figure 3-56.

The original test apparatus did not allow for freedom in heave and trim. For the first test the sinkage and trim were fixed at zero; the second was run with sinkage at zero and trim at four degrees bow up. The results (Figure 3-57) show that for optimum water performance, cupped blades are more efficient at high trim angles and high speeds.

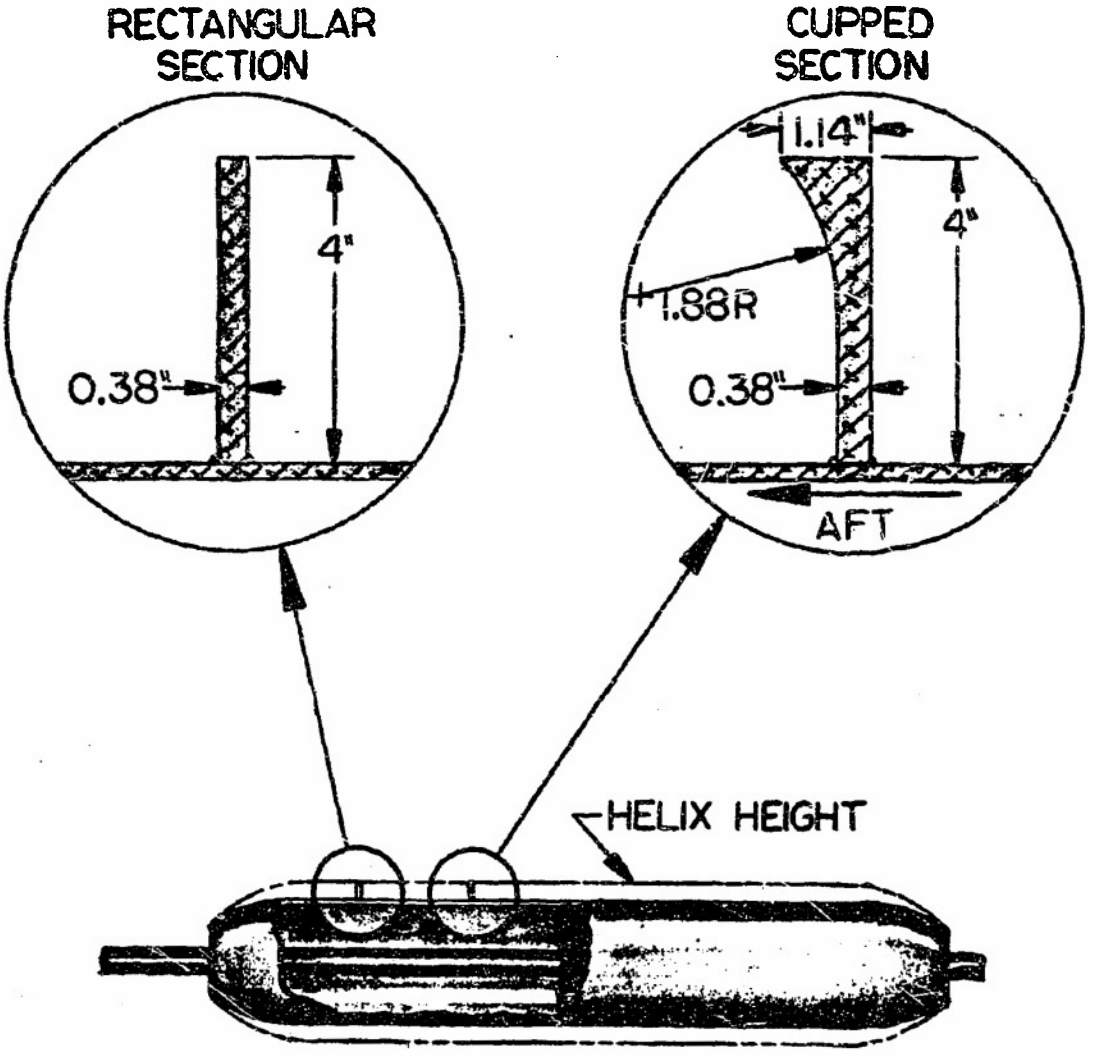

Figure 3-56 Blade Cross-Sections

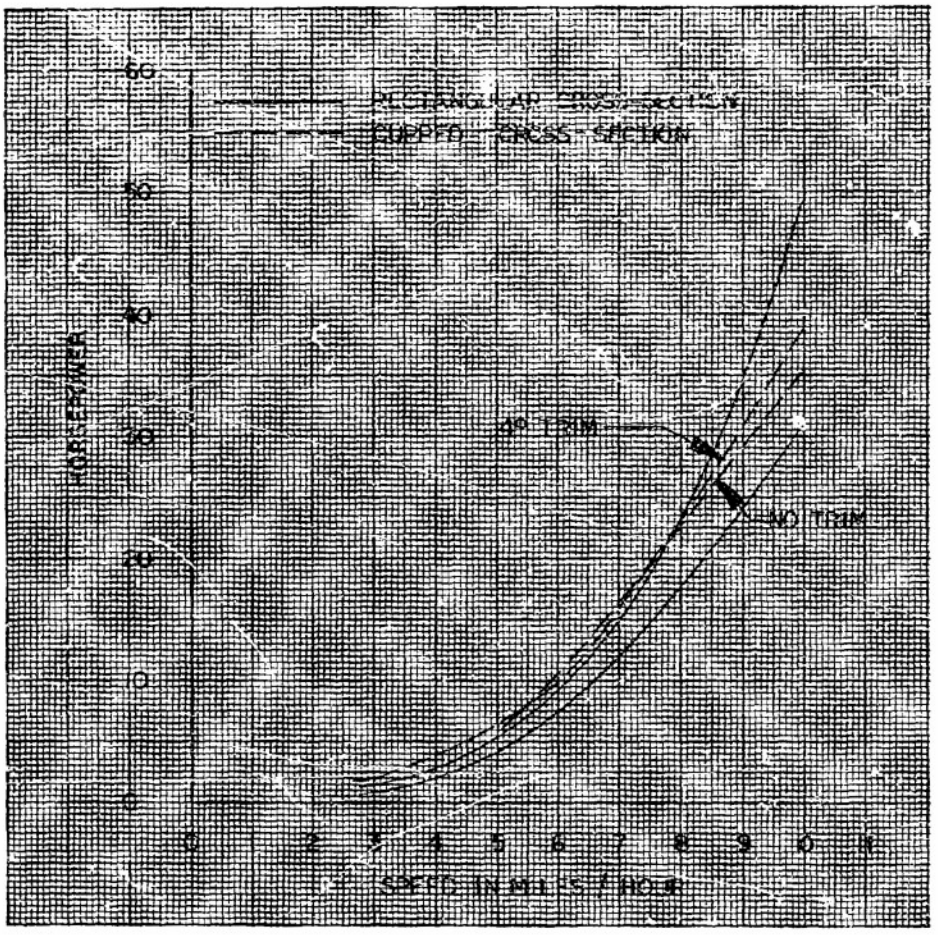

Figure 3-57 Blade Shape Effect, Horsepower vs. Speed

3-8. INTERACTION EFFECTS BETWEEN TWO ROTORS

In order to investigate the interference between two rotors running parallel to each other at a particular spacing, the testing apparatus was modified. A right and left-handed 50-degree helix angle, 1.560-inch blade height model was used. The transverse centerline spacing was selected as mutlitples of hub diameters. The actual model spacings are given in the table below.

ROTOR SPACING

Centerline Spacing In Diameters	Model Spacing In Inches
2	16
4	32
6	48

All configurations were run inboard turning except at one particular spacing, a centerline spacing equivalent to two hub diameters, where both inboard and outboard turning conditions were run. All tests were run in the 50 percent displacement condition. At displacements other than 50 percent, the optimum spacing should not change radically. It is important to realize that the results of this section are only important if there is no hull between the rotors. The paragraph that follows provided an estimate of additional horsepower required for a shrouded rotor.

The results are shown in Figures 3-58 and 3-59 as percentages of horsepower and RPM compared to two rotors at infinite spacing. Horsepower requirements at infinite spacing were calculated from the results of the systematic series rotor data. Small spacings are to be avoided owing to the adverse effects. There is an optimum range of spacings, near four diameters, where the horsepower for two rotors is less than that for twice a single rotor. In these graphs, the percentages are plotted as a family of curves of speed in KPH based on a linear scale ratio of three. This data can be used for a rotor of a different linear scale ratio by converting the speeds by Froude's law since the percentages will remain the same.

The differences found between inboard and outboard turning rotors was never more than one or two percent; outboard being slightly favorable. This result was for one particular spacing as mentioned previously.

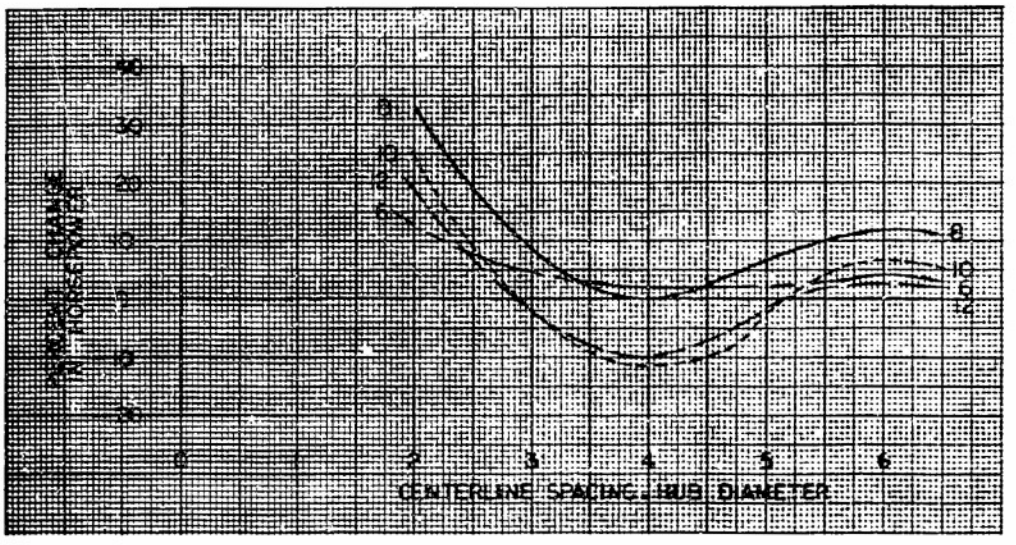

Figure 3-58 Percent Change in Horsepower vs Centerline Spacing, Hub Diameter

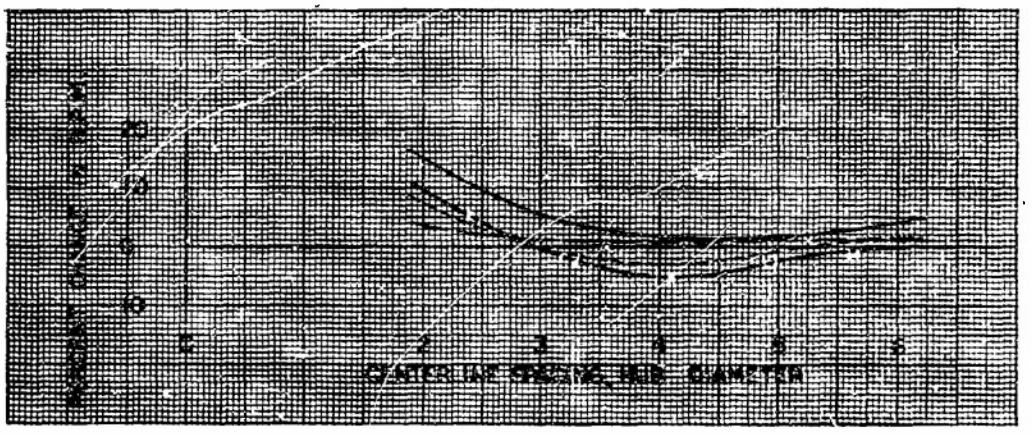

Figure 3-59 Percent Change in RPM vs Centerline Spacing, Hub Diameter

3-9. EFFECT OF SHROUDS

Continuously mentioned throughout this report is the fact that the data pertains to rotors only and not a particular vehicle. Therefore, one attempt at determining changes in required horsepower due to the proximity of a vehicle's hull was made to investigate the effect of shrouds. Of course, shrouds are only a portion of any proposed vehicle's hull. The rotor configurations used for this test had a 50 degree helix angle and a 1.560-inch blade height. Tests were conducted at 50 percent displacement.

Two shrouds were tested in various positions relative to the rotor as indicated in the following table. The rotors revolved clockwise looking forward from the stern. The shrouds were longitudinal segments of cylinders of the same length as the rotor.

Position	Included Angle (in degrees)	Spacing (measured from blade tips to shroud)
1	180	1
2	180	2
3	90 (port)	2
4	90 (starboard)	2

Initially, an error in evaluation of rough data was made and, for this reason, a shroud with an included angle of 90 degrees and a one inch spacing was not tested. This would have been the most desirable since the results indicate that the smaller spacing, as well as the shrouds of smaller included angles, require the

least additional horsepower. Obviously, the additional horsepower required due to shrouds would decrease with a decrease in displacement. The inboard turning rotation is more desirable compared to outboard turning for this particular rotor.

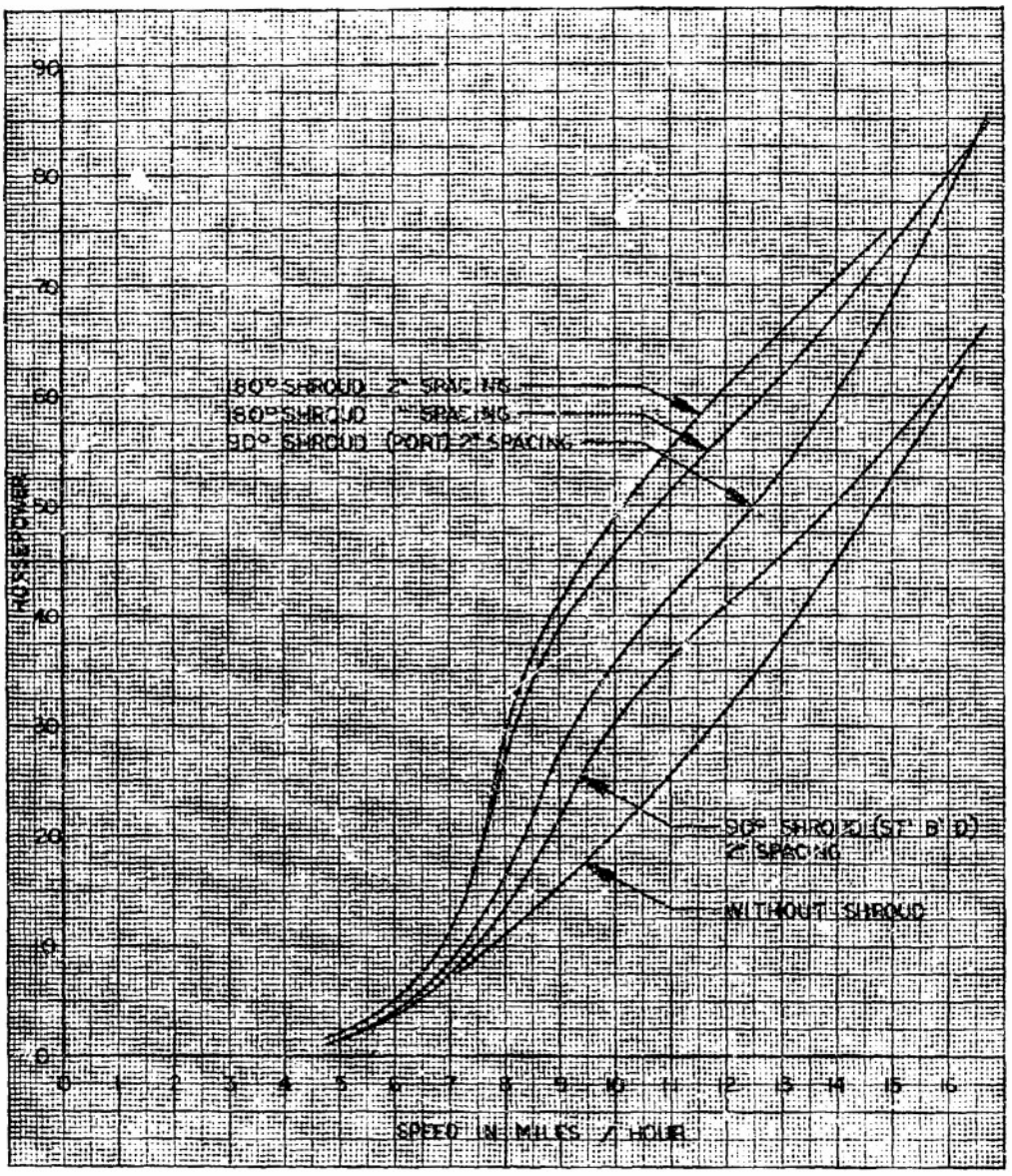

Figure 3-60 Shroud Effect, Horsepower vs Speed

3-10. EFFECT OF CHAIN HOUSING DRAG

During testing it became apparent that the impingement of spray on the leading surface of the chain drive housing represented a significant amount of drag which the rotor had to overcome. A series of tests was designed which lead to an estimate of the power required to balance the drag of the housing.

The frontal area of the aft strut was approximately 4.5 inches wide and the height upon which the spray impinged approximately 10.5 inches above the interface of the rotors and housing. This frontal area is dependent upon speed and displacement. Flat plates which extended the width, but held the height constant, were attached to increase the frontal area. The range of widths were chosen such that the same proportion of area would be affected by the spray over the speed range of interest. One plate was 16.5 inches wide the other 27.5 inches wide. The resulting full scale horsepower and rpm curves using a linear scale ratio of three are shown in figures 3-61 through 3-63.

Figure 3-63, representing the change in horsepower versus the change in aft strut frontal area, indicates an estimate of the induced horsepower for the chain housing. This method ignores the interaction between the plates and rotor, but does point out the desirability of maintaining the chain housing front area as small as practicable.

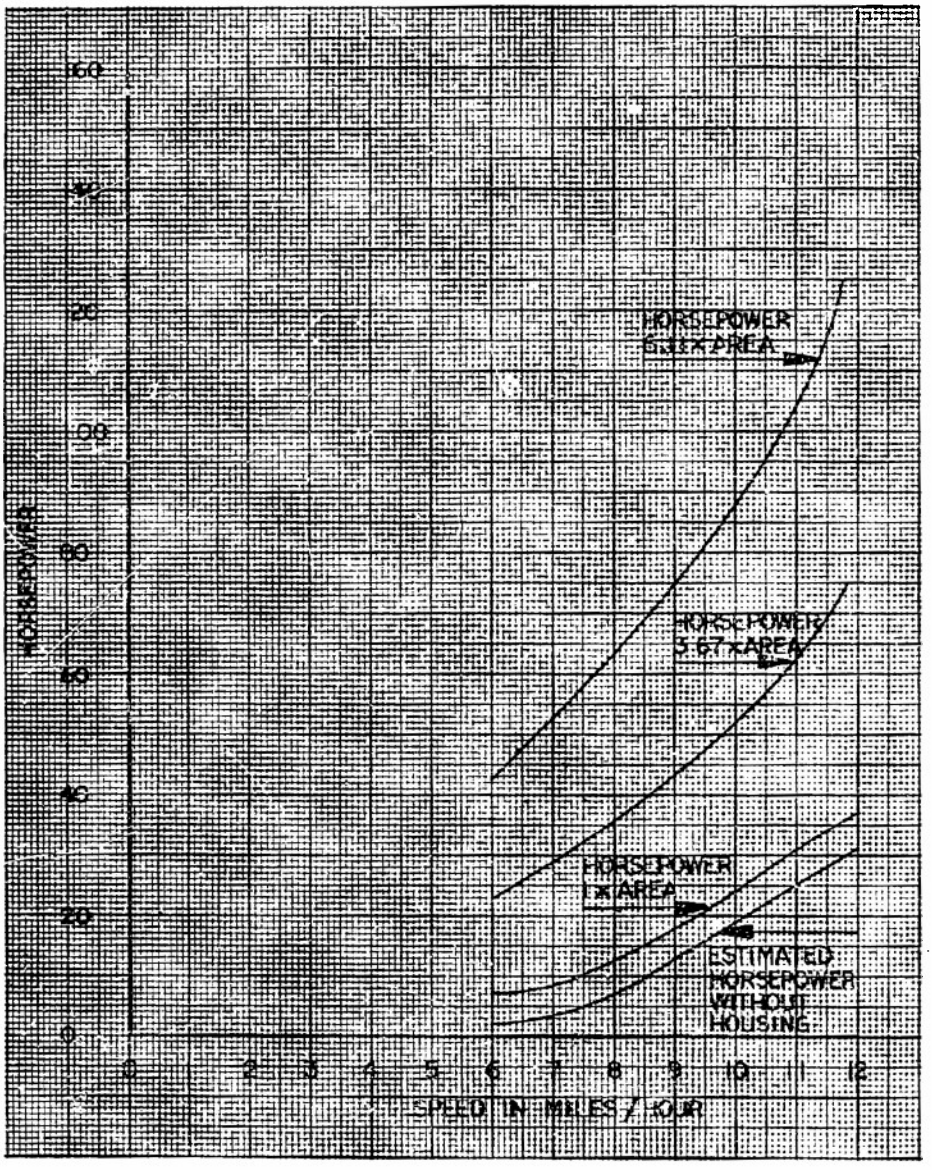

Figure 3-61 Chain Housing Drag Effect, Horsepower vs Speed

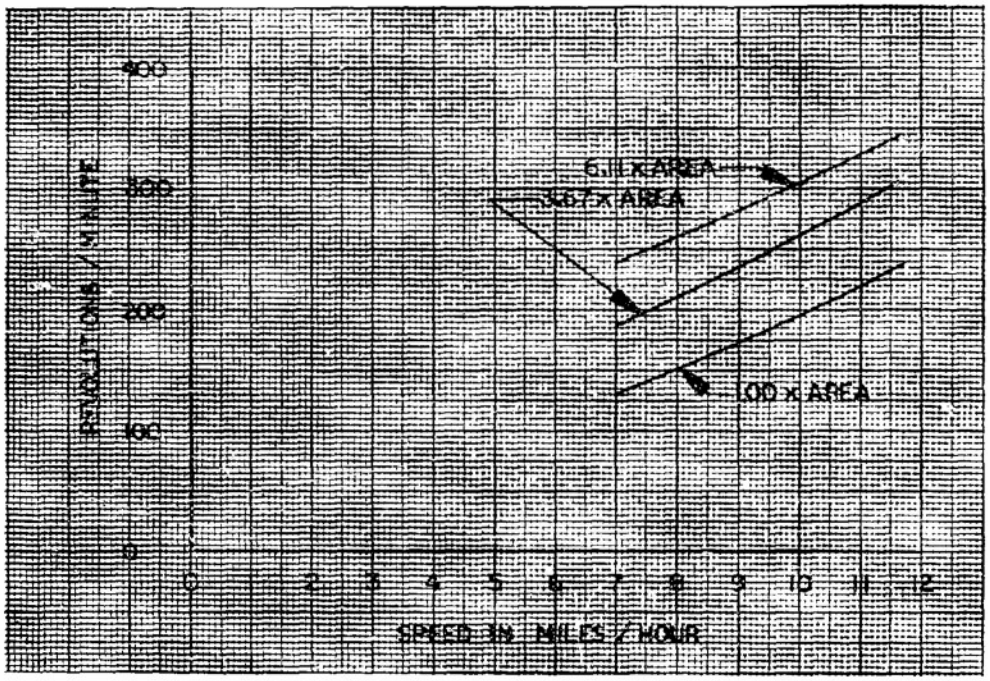

Figure 3-62 Chain Housing Drag Effect, RPM vs Speed

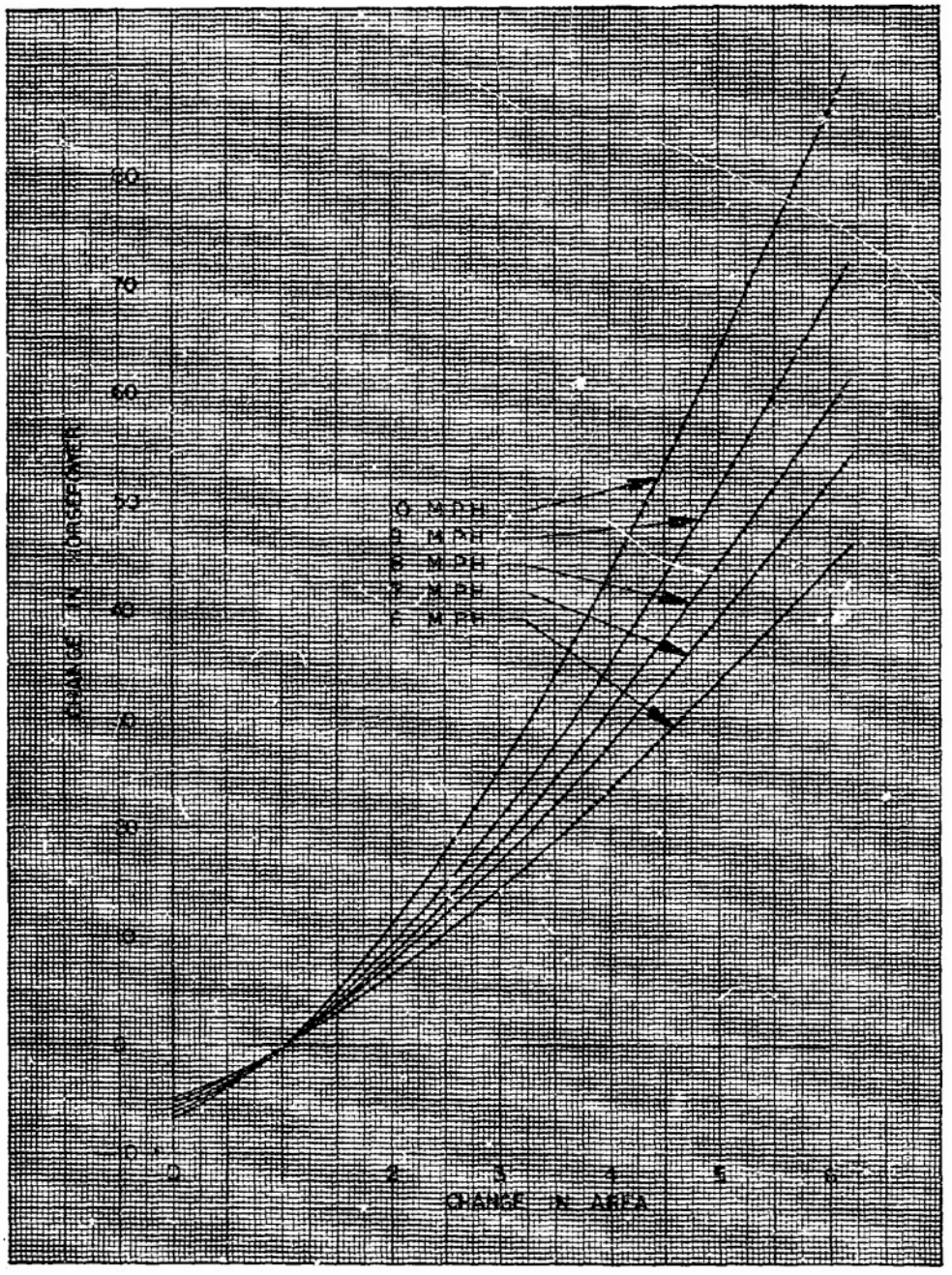

Figure 3-63 Chain Housing Draft Effect, Change in Horsepower vs Change in Area

3-11. DRAWBAR PULL TESTS

A simple drawbar pull test was run on the model with a 50-degree helix angle and 1.56-inch blade height, at a displacement of 50 percent of the hub volume and initial trim of one degree bow up. The results are presented in figure 3-64 and indicate towbar force and rpm versus horsepower absorbed. Knowing the horsepower available, one can determine the rpm and force for one rotor as indicated by the broken line. A linear scale factor of three was assumed for this rotor. The results can be converted to any size rotor by adhering to Froudes similitude.

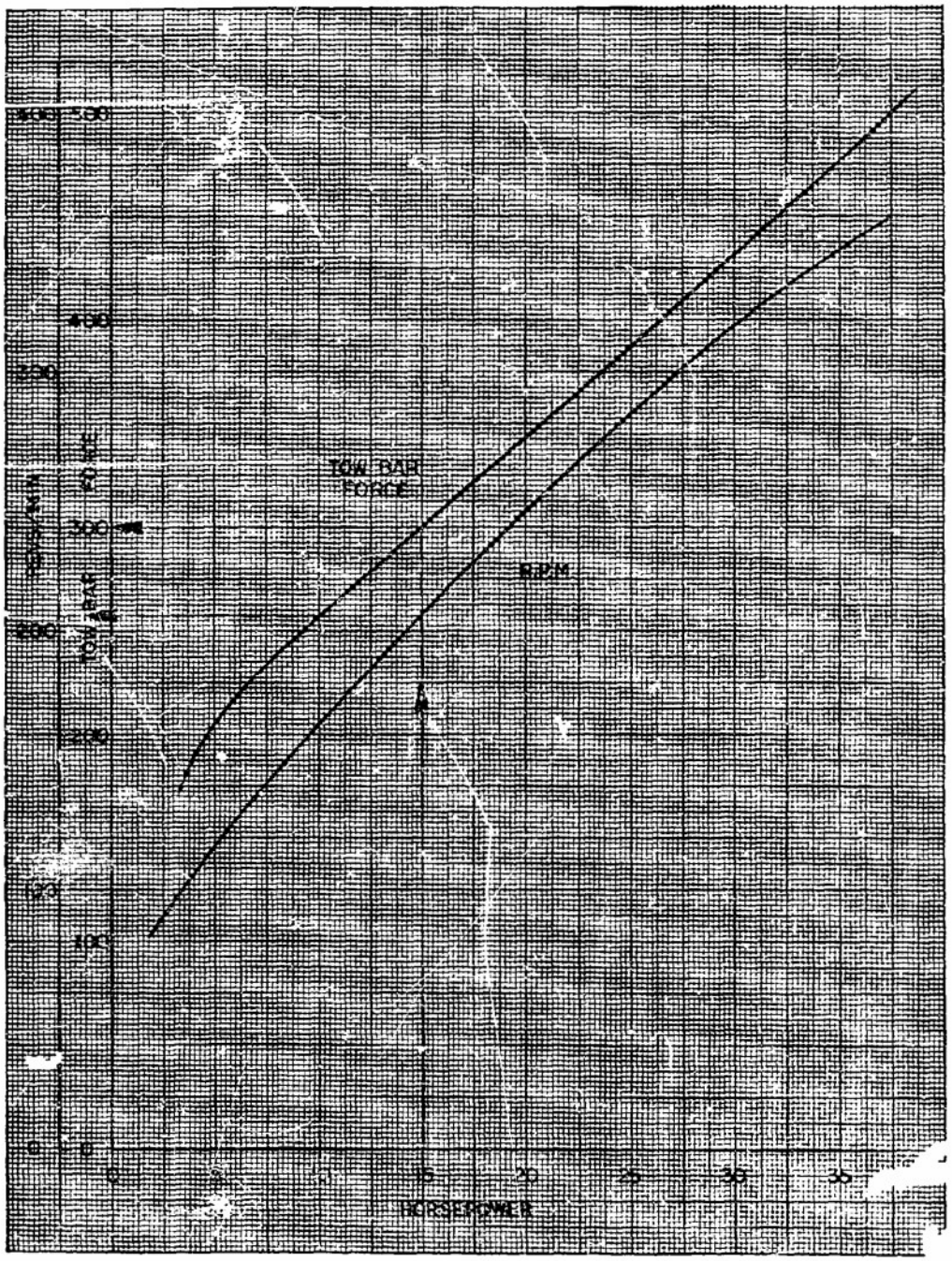

Figure 3-64 RPM and Tow Bar Force vs Horsepower

Section IV

FULL SCALE VEHICLE DATA

Tests of the Marsh Screw Amphibian were conducted at a water-filled gravel pit at the Chrysler Proving Grounds, Chelsea, Michigan. The vehicle was instrumented to measure torque and RPM at the output shaft of the transmission, and vehicle inclination. These values and the time required for the vehicle to travel over a 300-foot-long course were recorded on a CEC recording oscillograph. Tare values for torque at various RPMs were subtracted from the above readings. Thus, the method of obtaining the data was consitent with that used for obtaining the corresponding model values. The vehicle was tested with two different rotor configurations, a 30-degree helix angle with a 3-inch blade height, and a 40-degree helix angle with a 4-inch blade height. The basic vehicle characteristics are given in Figure 3-65. The vehicle with each rotor configuration was tested at two displacements; light condition - 3348 pounds and heavy condition 3880 pounds. Vehicle tests were conducted in both directions.

In Figure 3-66 predicted horsepower was inconsistent with actual vehicle results. As previously discussed, the apparatus used for the model tests allowed the rotors to seek their equilibrium trim angle and vertical position. Trim angles as high as 14 degrees were experienced with certain models. Again, it is emphasized and certainly apparent that all the model tests were of rotors and the effect of the

hull of any supposed vehicle was not introduced. Certainly a vehicle's equilibrium condition is very different from that of a single rotor, since the hull provides buoyancy and possibly some dynamic lift.

In Figure 3-66 correlation of vehicle data at equivalent angles of trim is consistent. But accuracy of predicting horsepower based on the systematic series data will degenerate with the higher displacement data being less accurate. (Refer to Figure 3-67 for RPM data and Figure 3-68 for vehicle trim data.) This is primarily due to difference in trim and is illustrated in Figure 3-69 where model data from a previous research program for a 30-degree, 3-inch rotor at constant zero trim was plotted with the predicted data obtained from the systematic series.

Figure 3-69 shows that a rotor performs better at lower angles of trim and that a hull is beneficial when considering overall efficiency, since it places a trim constraint on the rotor. It is probable that the horsepower required to overcome the drag of a hull is insignificant when compared to the horsepower expended due to operating at high trim angles. Certainly this is an area for further research. In no way does the above result discredit the data already obtained since optimum rotor configurations can be determined for any given condition.

The mission of the Chrysler designed and built Marsh Screw Amphibian is to economically transport six combat equipped troops plus driver through fresh and salt water, over sandy beaches, rice paddies, swamps, mudbanks, earthworks, bogs, and occasionally cross hard surface roads.

GENERAL

Weight	2,335 Lbs.
Crew (one driver)	175 Lbs.
Fuel and Oil	175 Lbs.
Passengers (6) or Cargo	1,050 Lbs.
Gross Vehicle Weight	3,735 Lbs.
Ground Pressure is 0.9 P.S.I. at 2-1/2 inches penetration at 3,735 Lbs. weight	
Fuel Capacity	45 Gallons

DIMENSIONS

Length Over-All	13 Ft. 8 In.
Width Over-All	8 Ft. 2 In.
Height Over-All	57 In.
Rotor Spacing (center to center)	66 In.
Rotor Diameter (over drum)	26 In.
Rotor Diameter (over helix)	32 In.
Ground Clearance Under Hull	20 In.

PERFORMANCE (Maximum Speed, Vehicle Loaded)

Mud	10 to 20 Mph
Water	7.5 Mph
Deep Snow	20 Mph

ENGINE

Make: Chrysler	Model: RG Special	Type:	Spark Ignition, Slant 6, Water Cooled OHV
Bore and Stroke	3.40 x 4.25 Inches		
Displacement	225 Cubic Inches		
Governed Speed	3600 Rpm		
Net Horsepower	116 HP at 3600 Rpm		

POWER TRAIN

Transmission: Chrysler Torqueflite Model A-727, 3-speed transmission with electric clutch/brake controlled by a steering wheel through a chain driven, double reduction final drive, ratio 6.55:1

ELECTRICAL SYSTEM

12 Volt w/Alternator

MATERIALS

Body and Rotor - 6061 T6 Aluminum
Engine Block, Transmission Housing, and Final Drive Housing are Aluminum

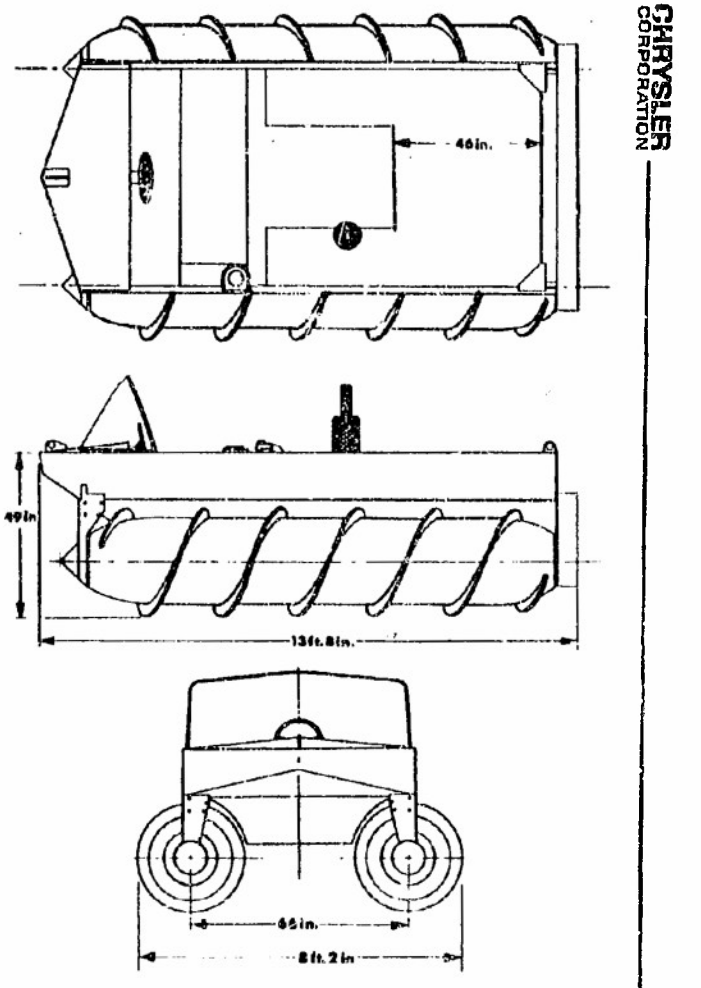

Figure 5-65 Marsh Screw Amphibian Characteristics

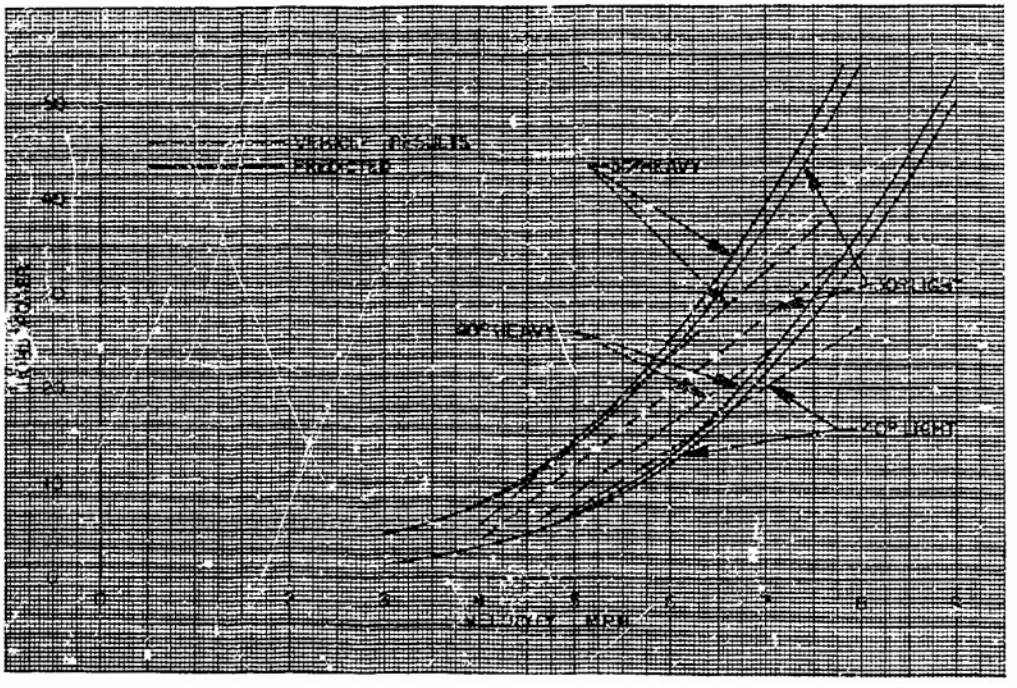

Figure 3-66 Full Scale Vehicle, Horsepower vs. Velocity

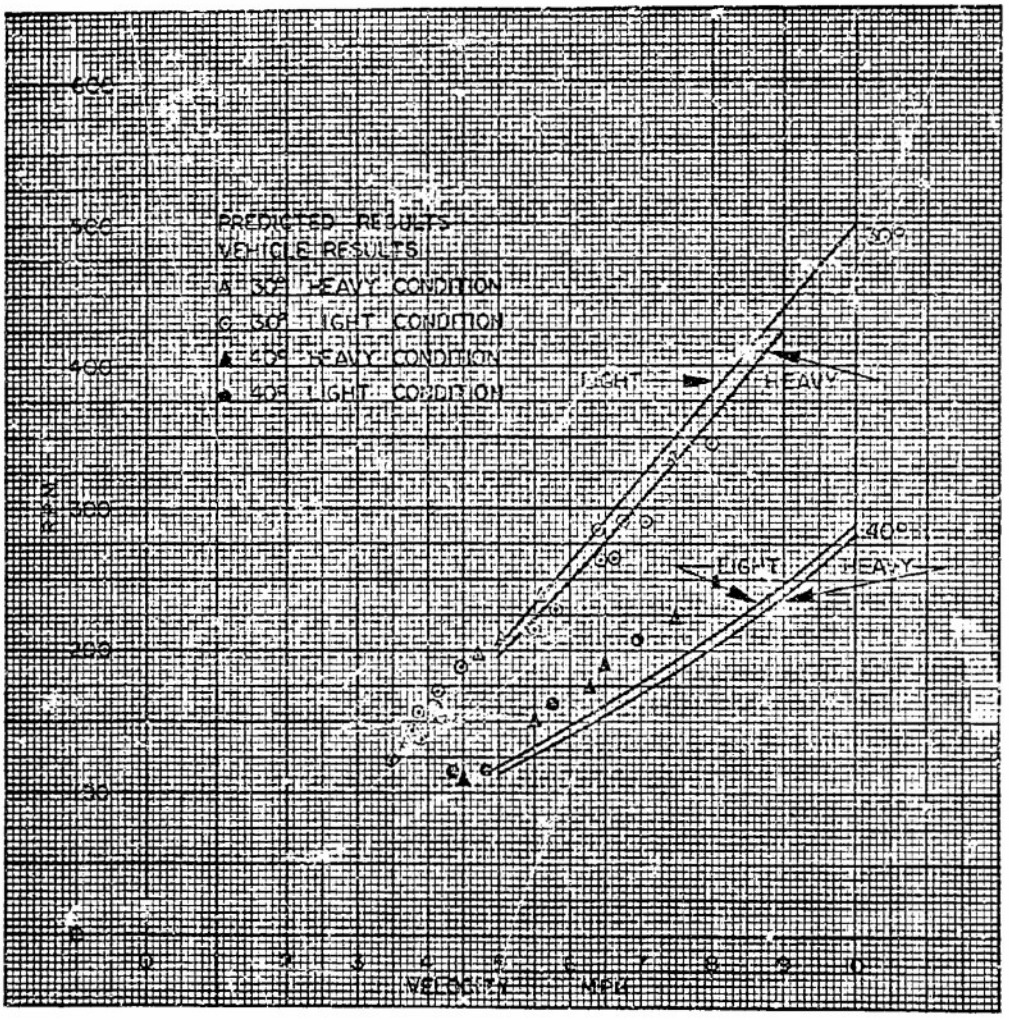

Figure 3-67 Full Scale Vehicle, RPM vs. Velocity

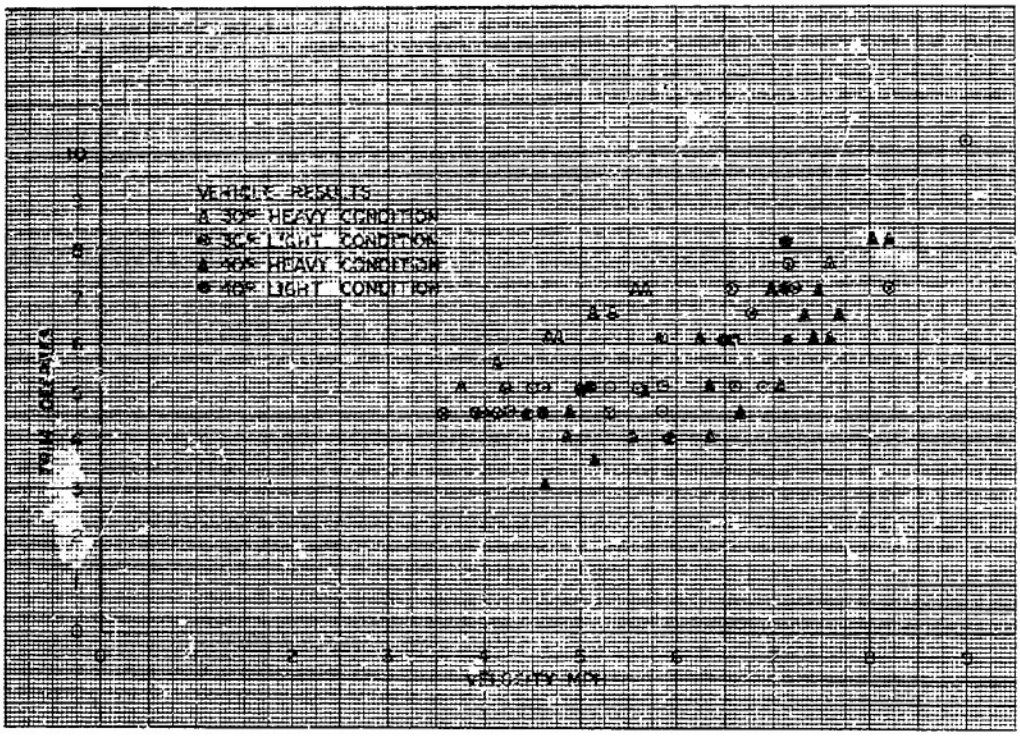

Figure 3-68 Full Scale Vehicle, Trim Degress vs. Velocity

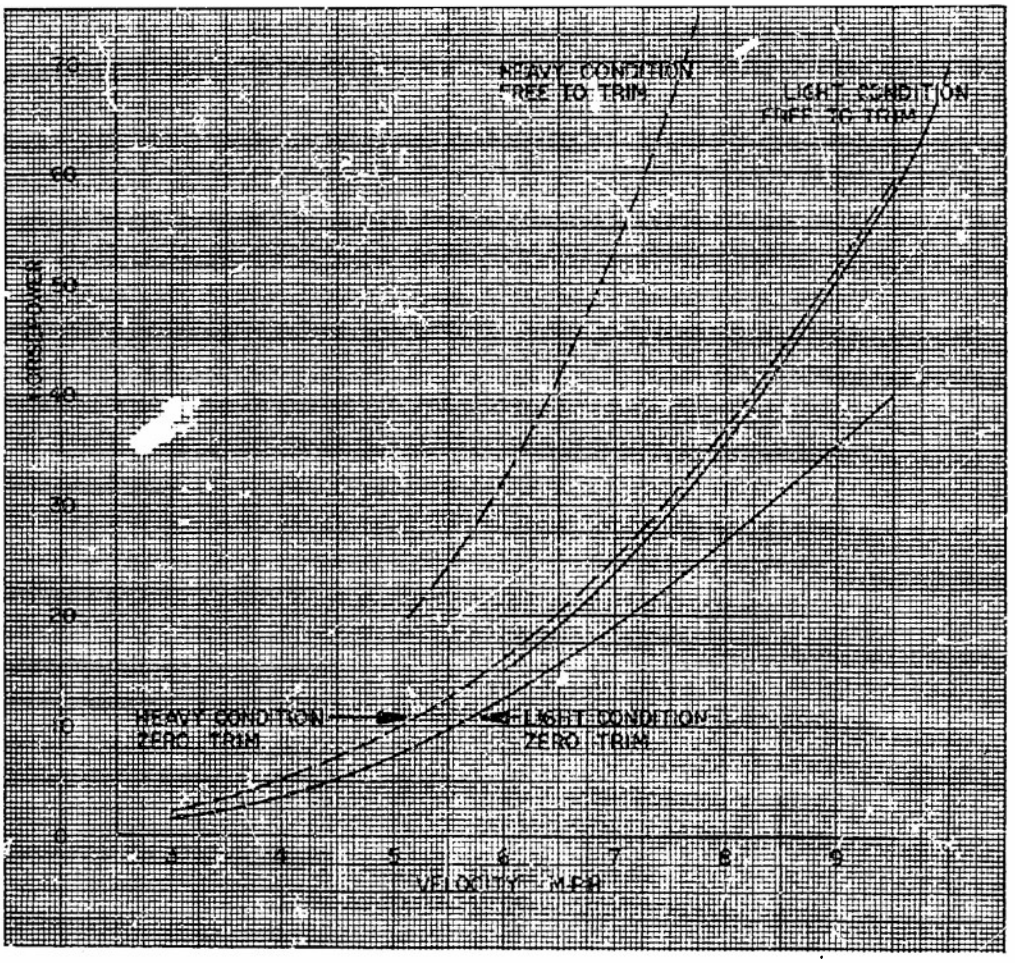

Figure 3-69 Effect of Trim on Model Data

CHAPTER 4

SOIL TESTS

The soil tests were conducted at Davidson Laboratory of Stevens Institute of Technology under contract to Chrysler Corporation Defense Engineering. The tests consisted of two phases:

- The testing of systematically varied buoyant screw rotors.
- The testing of miscellaneous configurations of buoyant screw rotors.

The following sections describe the test apparatus and procedures and presents testresults graphically. Full scale vehicle performance for various soil conditions are included at the end of the chapter for comparison with model test results.

Section I

DESCRIPTION OF APPARATUS

The experiments conducted at Davidson Laboratory were run in the soil bin at Tank 4. A rather detailed description of this fixture is presented since scatter of data resulted throughout testing.

The apparatus for the soil tests was comprised of a rotor and a dynamometer. A view of the soil bin fixture is shown in Figure 4-1. Attached to the main carriage was a rigid parallelogram-load cell arrangement for measuring drawbar pull. Attached to this was a mounting block holding two rods upon which the rotor and frame was allowed to heave and pitch. All other motions were constrained relative to the carriage. A strain gage balance was mounted at the final stage of the power input to measure the driving torque exclusive of mechanical losses. Extraneous forces and moments imposed by the input shaft were assumed to be negligible. The rotor drive motor was fitted with a tach-generator to measure rotor speed. Linear potentiometers measured sinkage at front and rear stations. This apparatus is similar to that used for the water tests.

Tests were made in both sand and mud. The sand was an air dry mason sand and the latter a fine organic silt procured from a marshy area in Michigan. The soils were tilled prior to each run by a modified rototiller to a depth of approximately six inches below the surface. This was done to assure uniformity of test conditions. Thus, the mud represented a completely worked soil. Periodic bearing strength

measurements were made in the sand with a cone penetrometer (30° cone, 3/4-inch maximum diameter). These gave a one, three, and five-inch penetration average of 26. The bearing capacity of the mud was so low that no meaningful readings could be established with the penetrometer. In this case, periodic moisture content readings were taken. The repeated measurements yielded a mean value for the moisture content present of 77 percent with a RMS deviation of 25 percent. Quick shear tests with representative samples yielded values of the soil properties, cohesion, c, and angle of internal friction, ϕ of

$$c = 0.3 \pm 0.1$$

$$\phi = 0 \text{ degree to } 7 \text{ degrees}$$

Obviously the frictional forces in comparison with the cohesive forces are negligible in this mud. The extreme opposite is apparent for the sand.

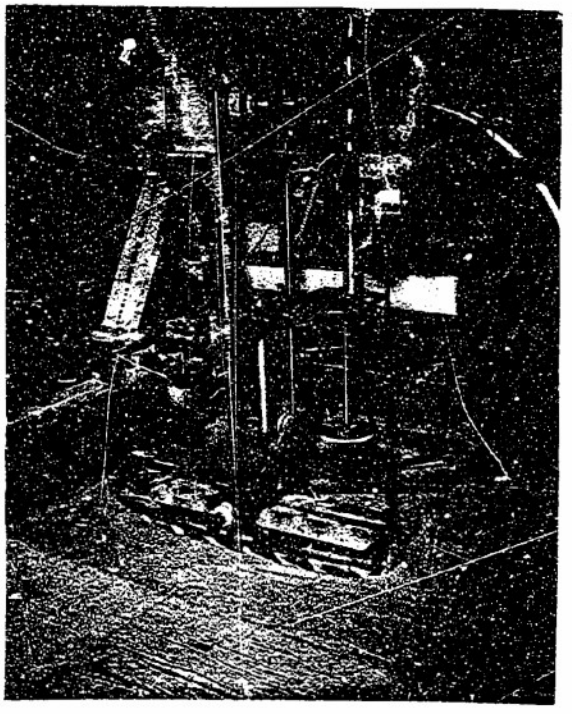

Figure 4-1 Soil Test Apparatus

Section II

SYSTEMATIC SERIES OF BUOYANT SCREW

An investigation of soil performance for a systematic series of rotors was conducted. The matrix of models tested is indicated in the following table.

BLADE HEIGHT Inches	HELIX ANGLE, degrees 30	40	50
0.460	X	X	X
0.625		X	
0.780		X	

Other model characteristics were:

Length	24.0 inches
Hub Diameter	4.0 inches
Hub Volume	0.1657 cubic feet

Each rotor was tested at a loading equivalent to 25, 50, and 75 percent of the total hub volume. This procedure was consistent with that used during the water tests. All data is contingent on a midpoint center of gravity location.

The model data was non-dimensionalized, with slip as the controlling parameter. The data did not always establish consistent trends and a complete matrix of buoyant screw configurations could not be represented because of the inability to cross plot the data. The non-dimensional parameters selected were:

Drawbar Pull/Weight, DBP/W

Specific Torque, T/Wr

Percent Slip, $1 - \frac{V}{Pn}$

V = Advance velocity ft/sec

r = Revolutions per second

p = pitch ft

T = Torque ft/lbs - Soil data is usually presented with this notation as opposed to "Q" for water performance

W = Weight - lbs

DBP = Drawbar Pull - lbs

r = Hub Radius - ft

Test results are shown in Figures 4-2 through 4-21.

Since scatter of data points is characteristics of model tests in soils, the actual data is shown. In most instances the curves are representative of the data they denote and representative of the trends established by the data obtained from other models in the matrix. A few curves require additional data points to justify the particular trend. Certain curves representing sufficient data are inconsistent with the trends established by other models within the matrix. This phenomenon can not be rationalized but the very nature of its existence must be accepted as gaps exist in the present state of the art and caution should be used in quantifying parameters in these performance areas.

A particular rotor configuration must experience positive drawbar pull if forward motion is to result. Any drawbar pull greater than zero provides motion in excess of the ability to transverse level terrain. Thus, the slope climbing capability of a vehicle is quantified by the magnitude of the positive drawbar pull/weight ratio. The specific torque, T/Wr, is only significant at values of slip greater than that required for zero drawbar pull.

No conclusions as to an optimum rotor configuration are made in this section, since such conclusions are dependent upon the design criteria. This will be further explained in Chapter 5.

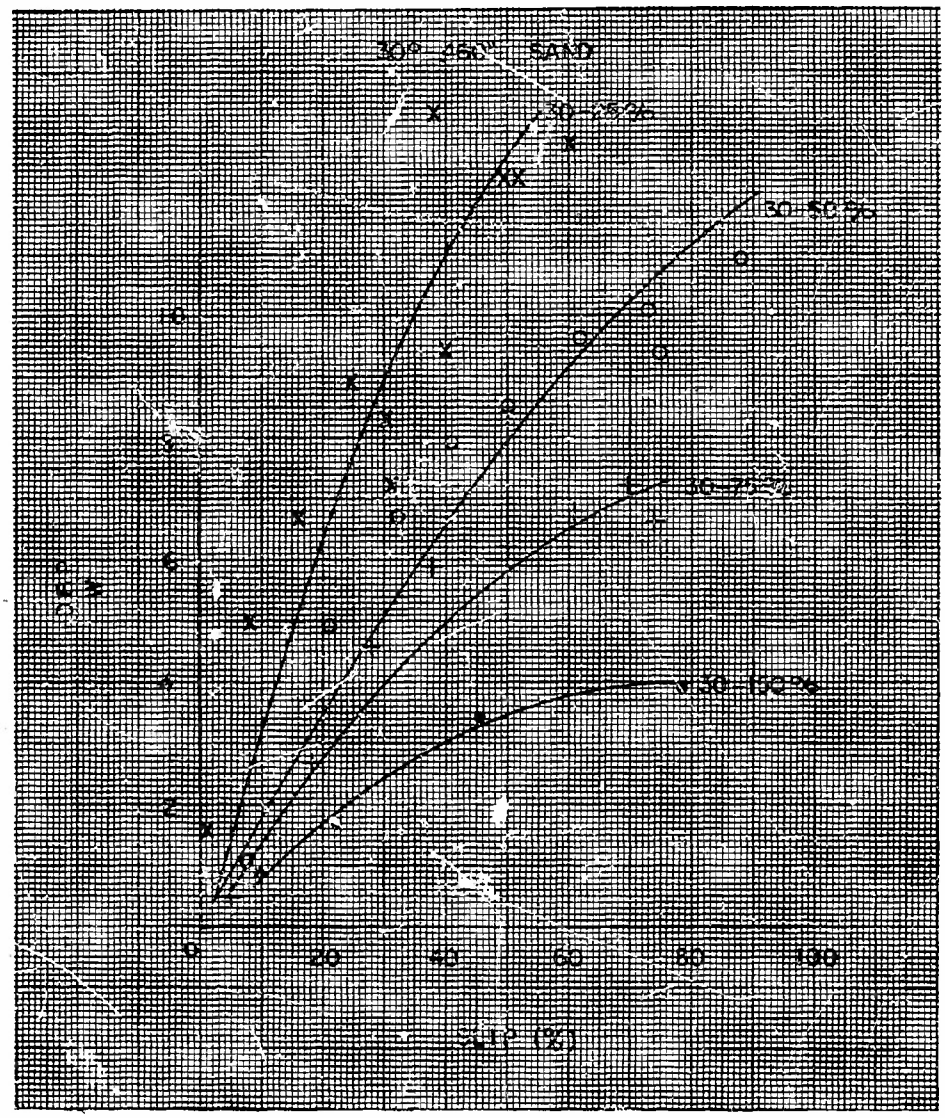

Figure 4-2 Drawbar Pull/Weight Ratio vs. Slip - Sand
(30 Degree Helix, 0.460 Inch Blade Height)

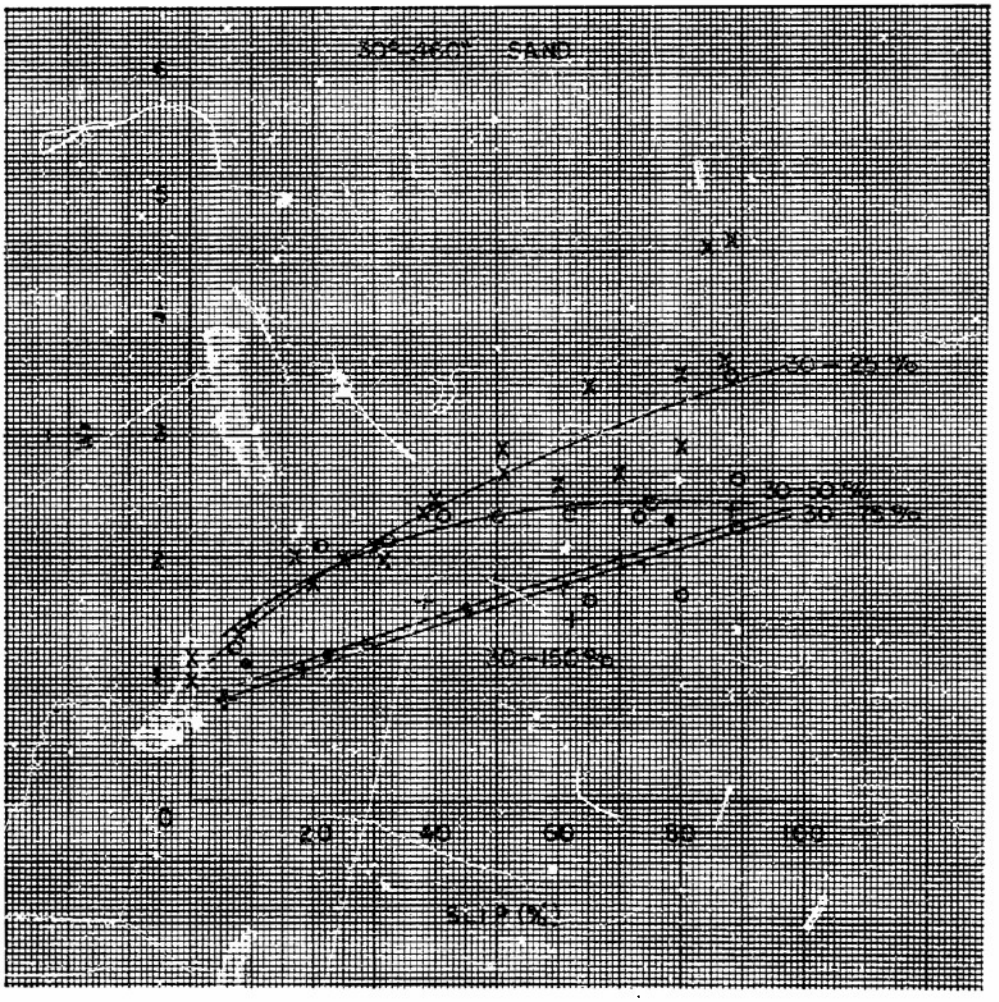

Figure 4-3 Specific Torque vs. Slip - Sand (30 Degree Helix, 0.460 Inch Blade Height)

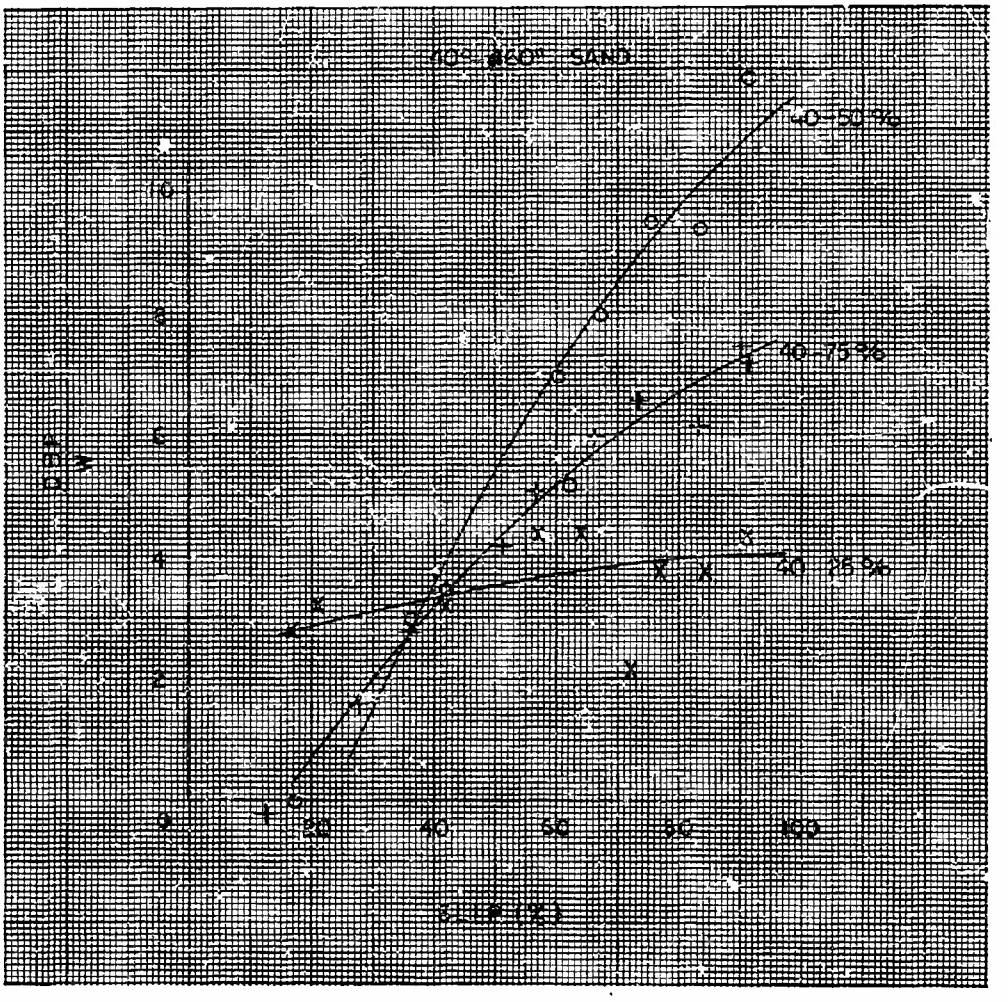

Figure 4-4 Drawbar Pull/Weight Ratio vs. Slip - Sand
(40 Degree Helix, 0.460 Inch Blade Height)

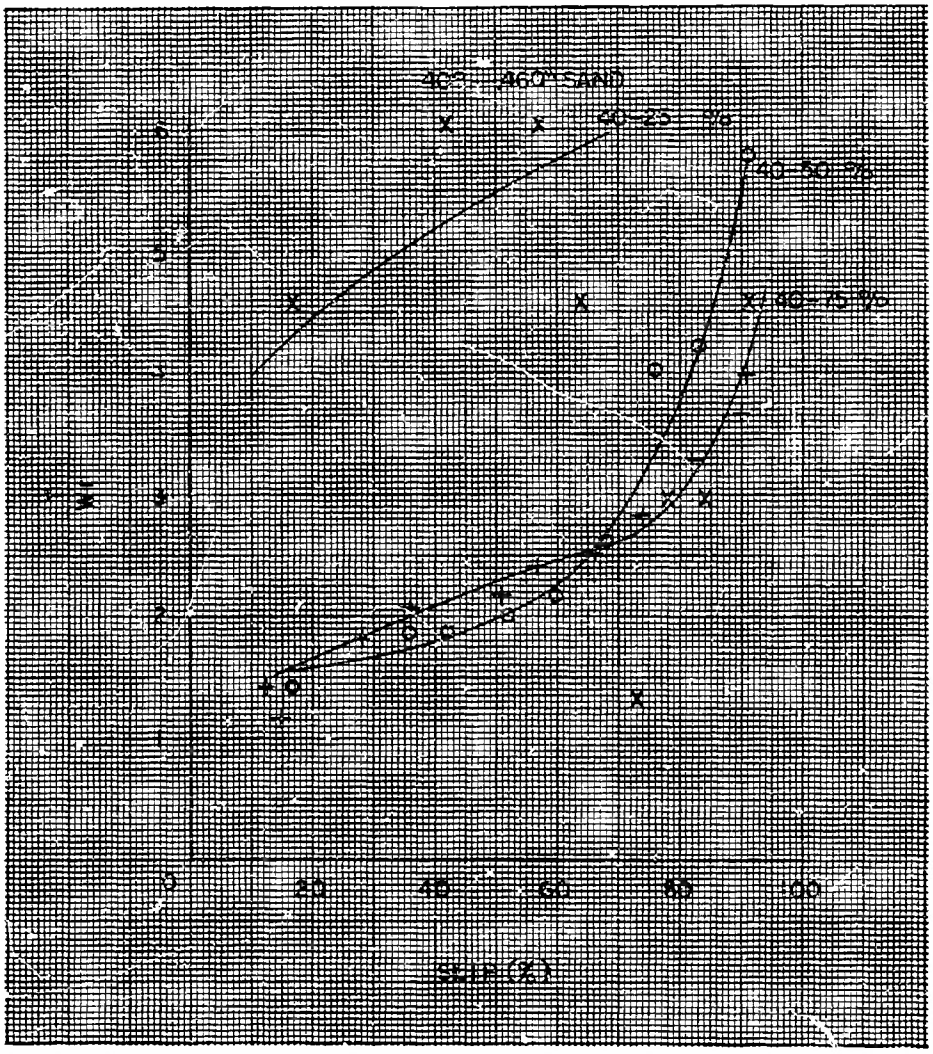

Figure 4-5 Specific Torque vs. Slip - Sand (40 Degree Helix, 0.460 Inch Blade Height)

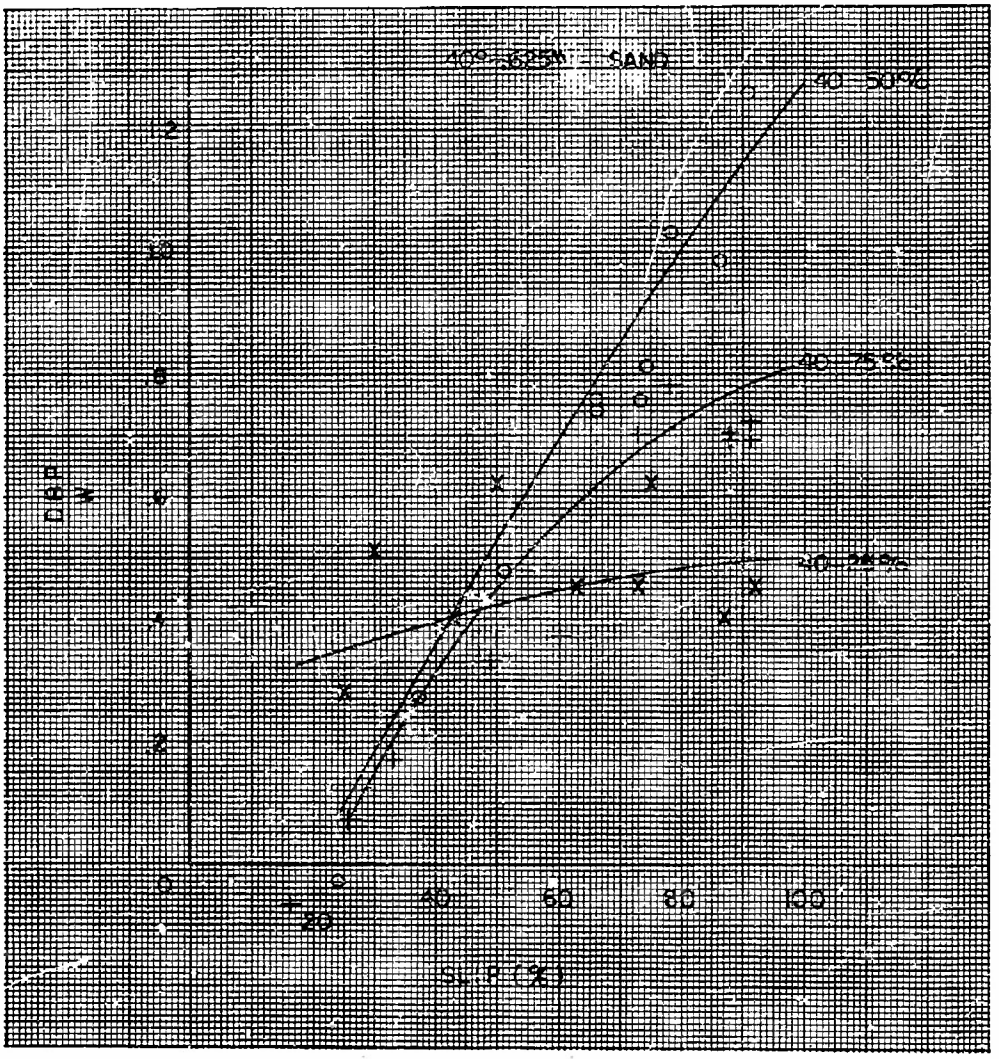

Figure 4-6 Drawbar Pull/Weight Ratio vs. Slip - Sand
(40 Degree Helix, 0.625 Inch Blade Height)

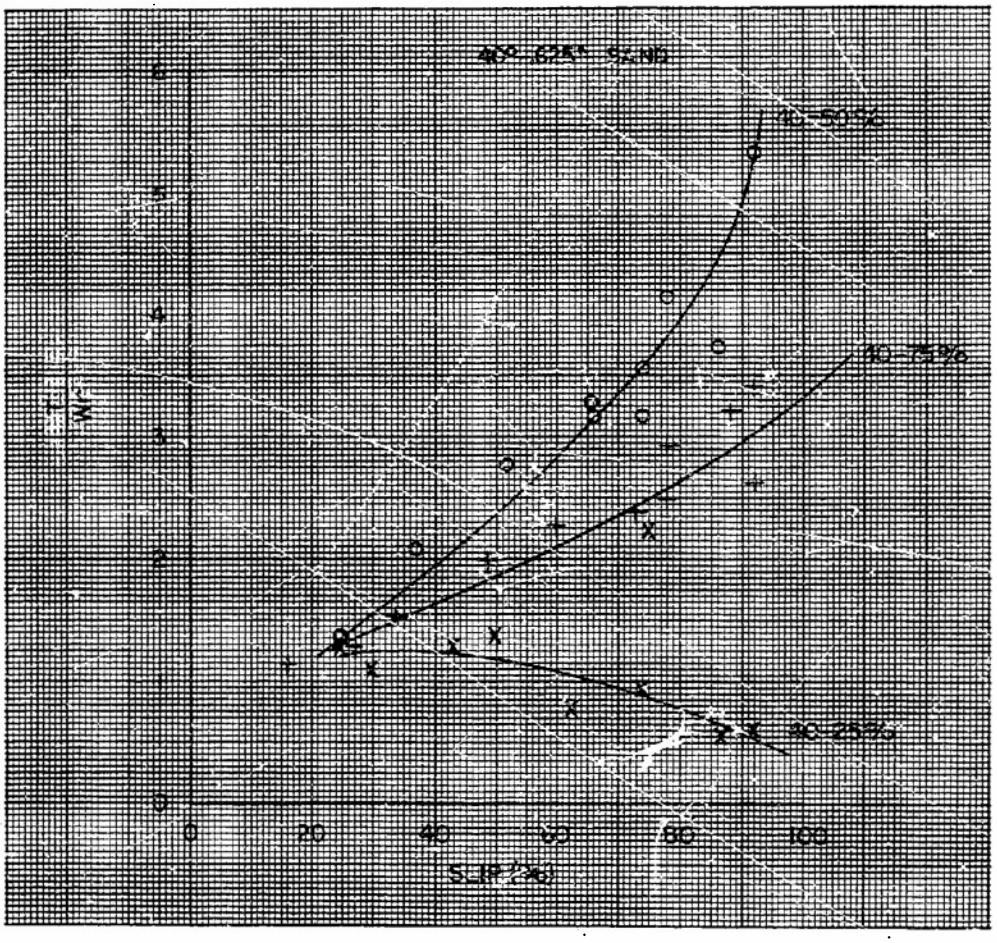

Figure 4-7 Specific Torque vs. Slip - Sand (40 Degree Helix, 0.625 Inch Blade Height)

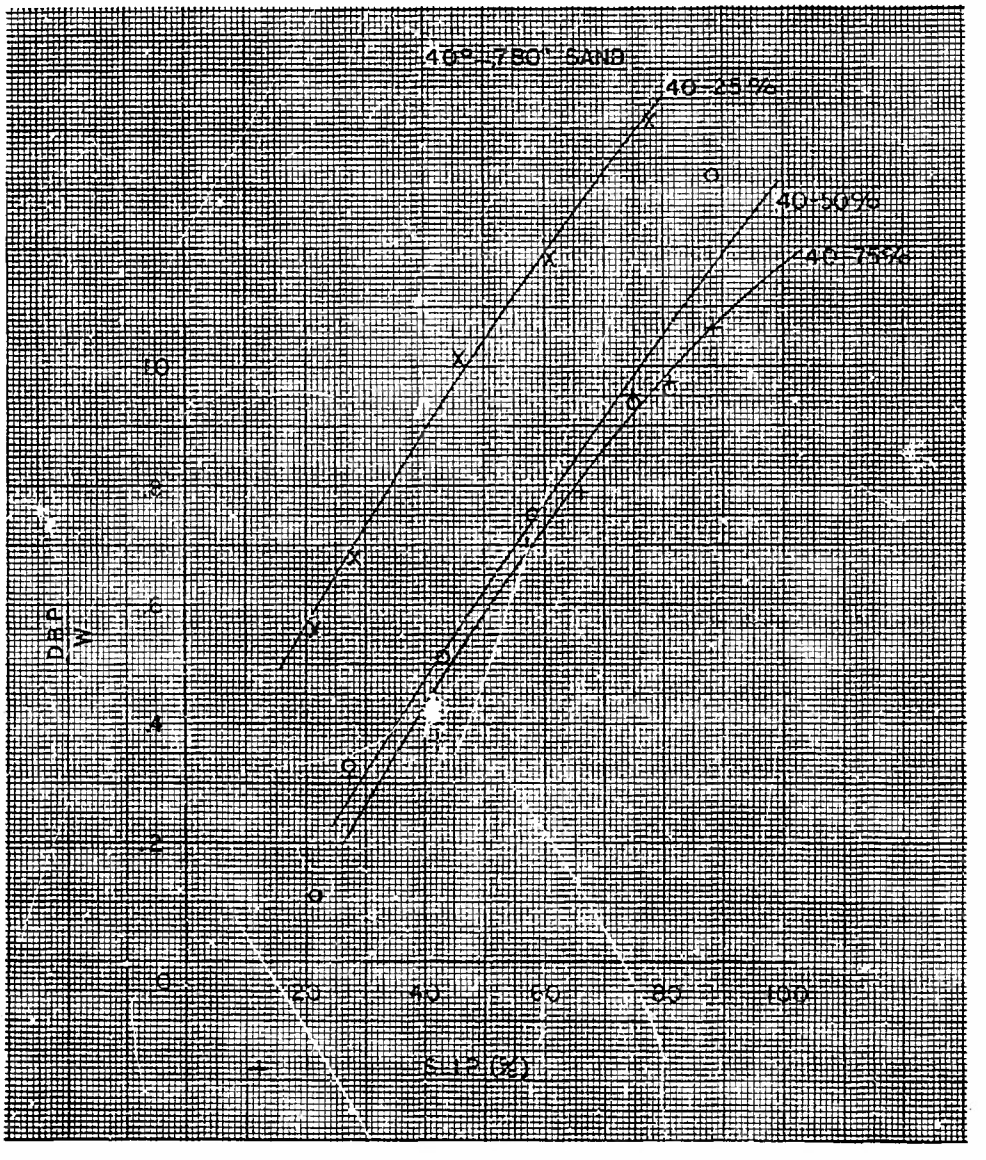

Figure 4-8 Drawbar Pull/Weight Ratio vs. Slip - Sand
(40 Degree Helix, 0.780 Inch Blade Height)

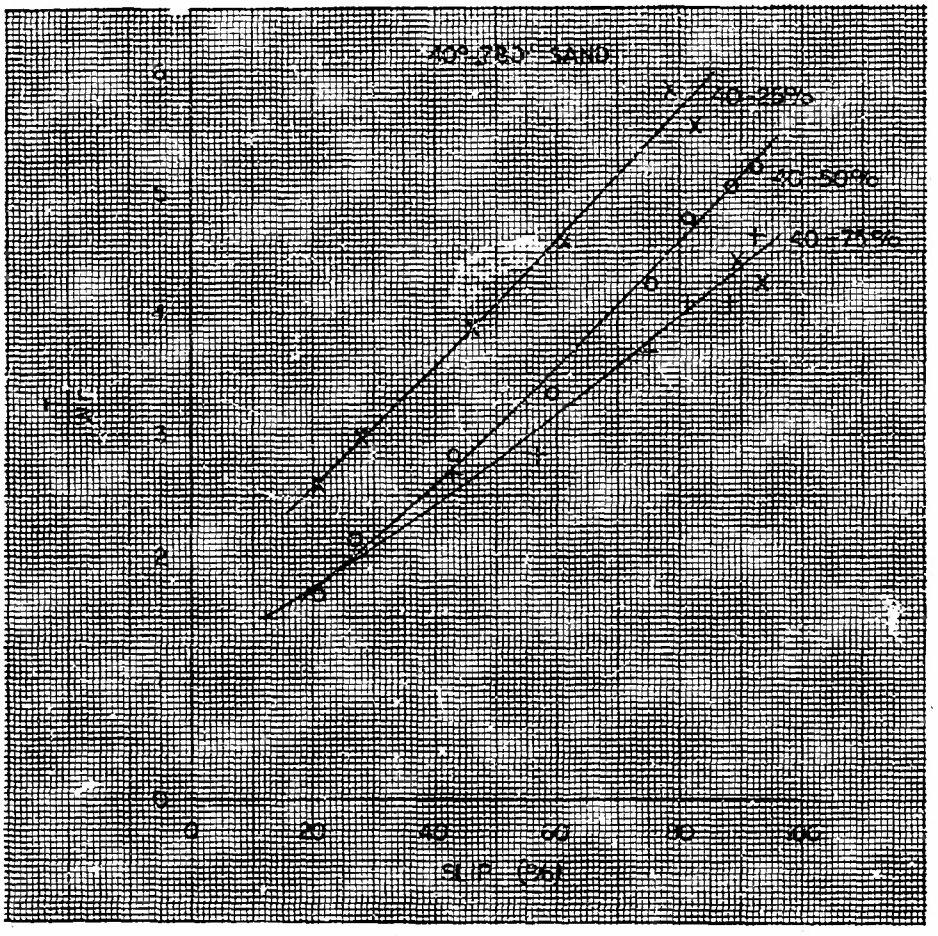

Figure 4-9 Specific Torque vs. Slip - Sand - (40 Degree Helix, 0.780 Inch Blade Height)

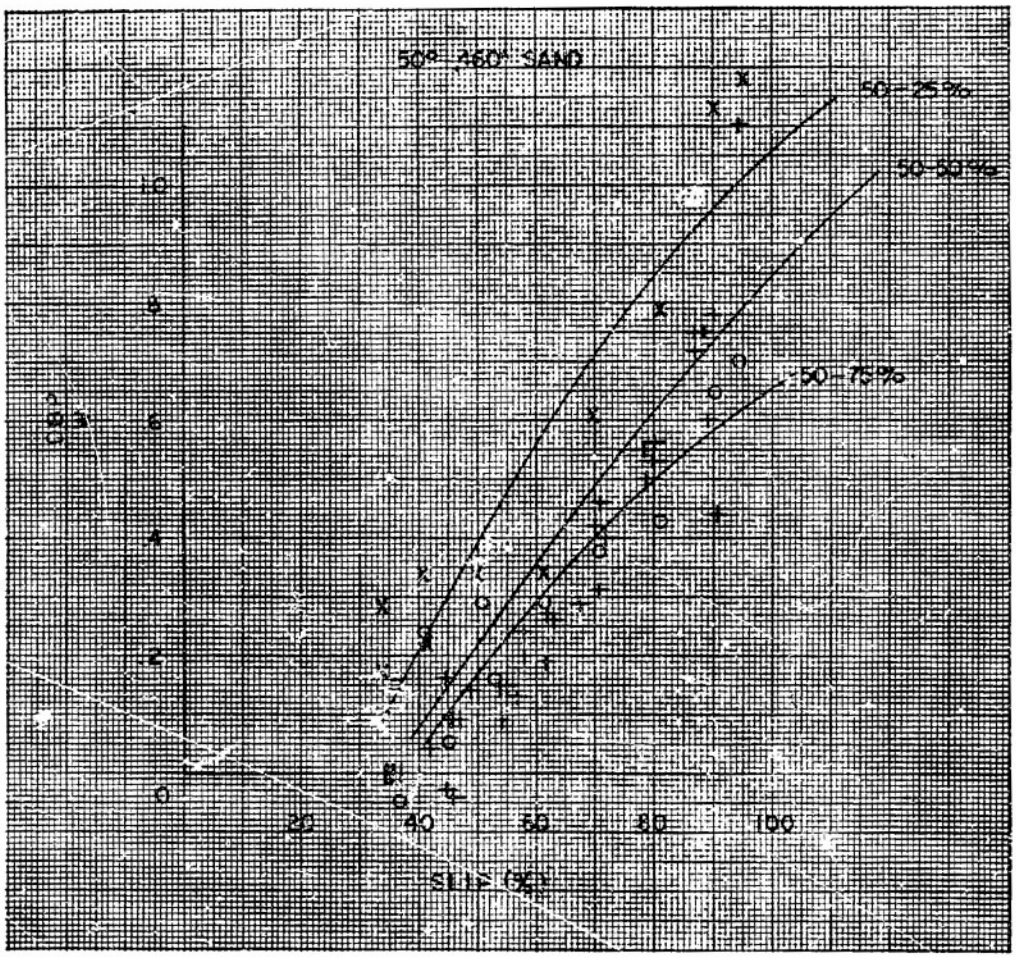

Figure 4-10 Drawbar Pull/Weight Ratio vs. Slip - Sand (50 Degree Helix, 0.460 Inch Blade Height)

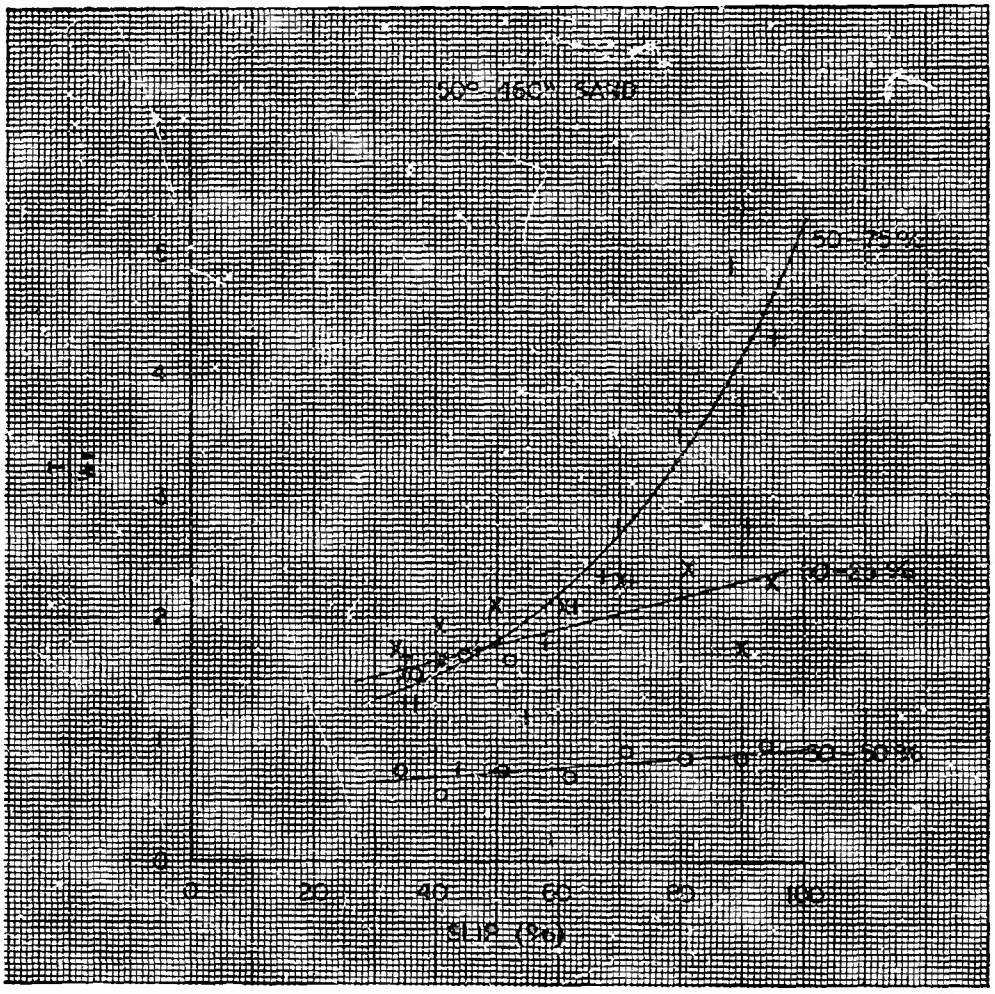

Figure 4-11 Specific Torque vs. Slip - Sand (50 Degree Helix, 0.460 Inch Blade Height)

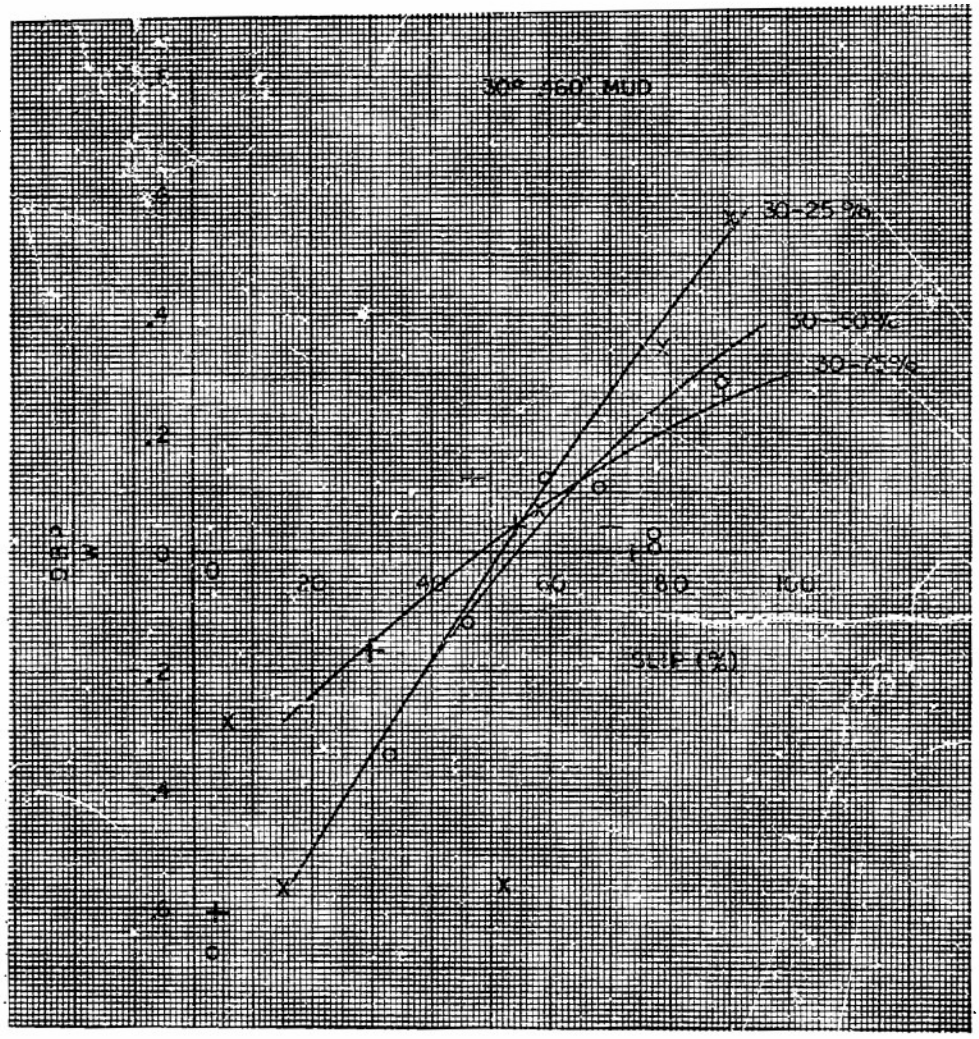

Figure 4-12 Drawbar Pull/Weight Ratio vs. Slip - Mud
(30 Degree Helix, 0.460 inch Blade Height)

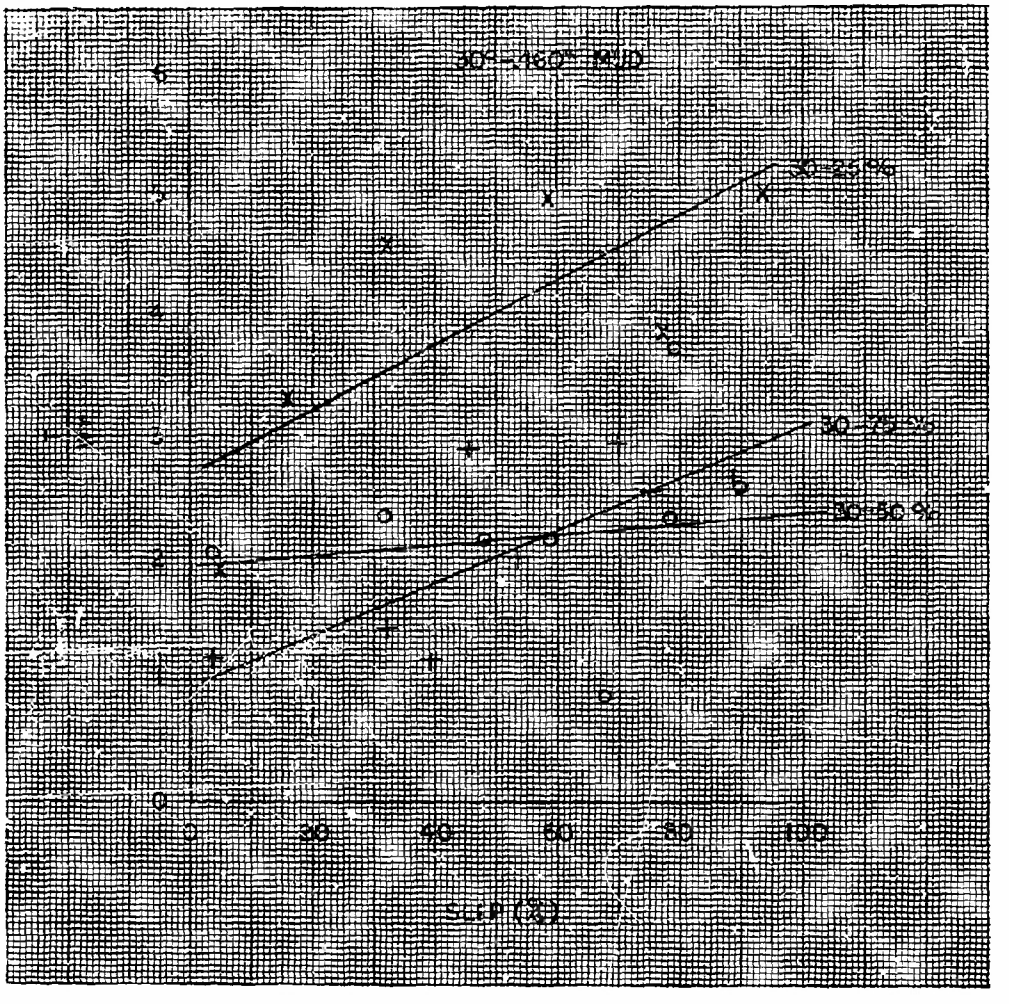

Figure 4-13 Specific Torque vs: Slip - Mud (30 Degree Helix, 0.460 Inch Blade Height)

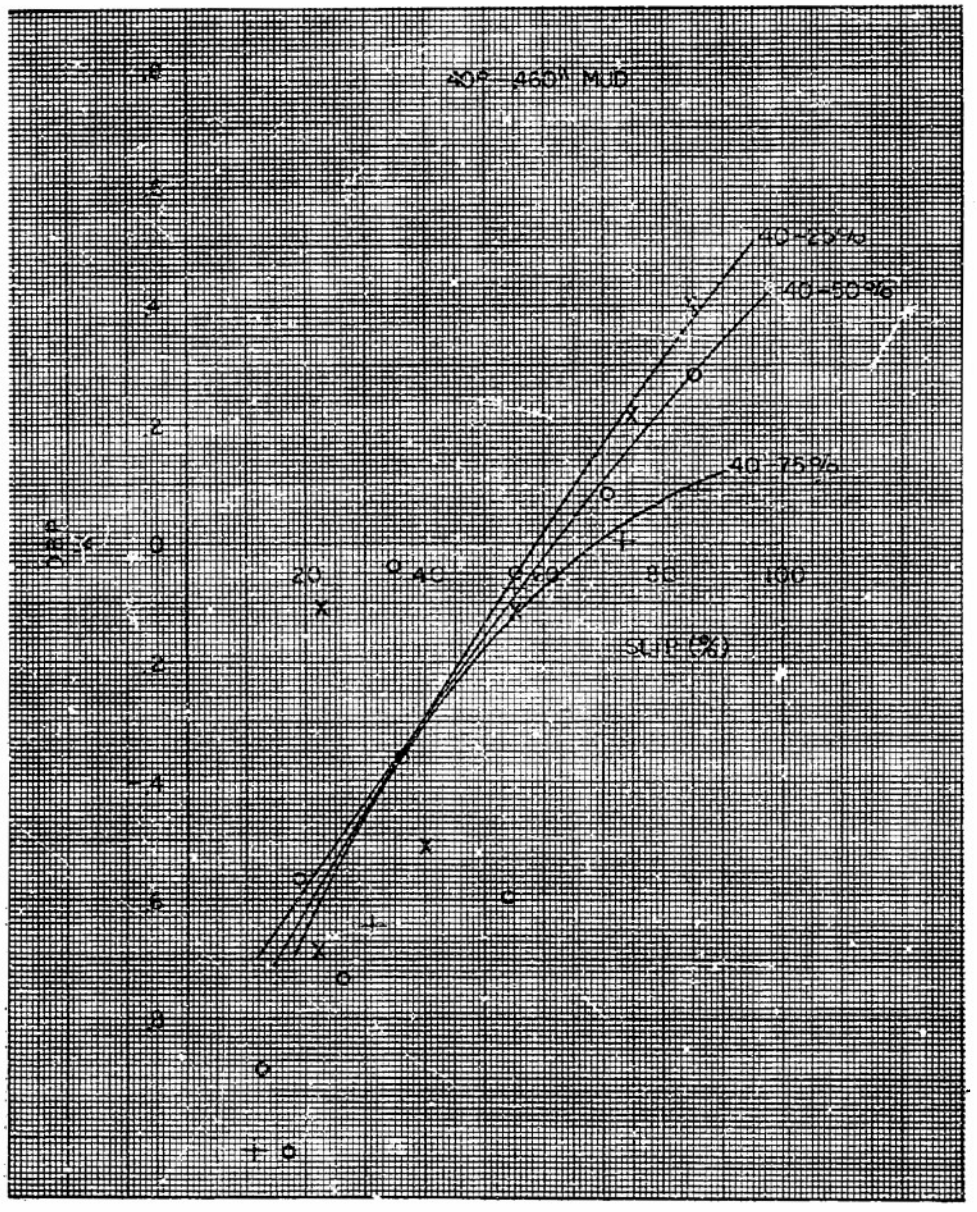

Figure 4-14 Drawbar Pull/Weight Ratio vs. Slip – Mud
(40 Degree Helix, 0.460 Inch Blade Height)

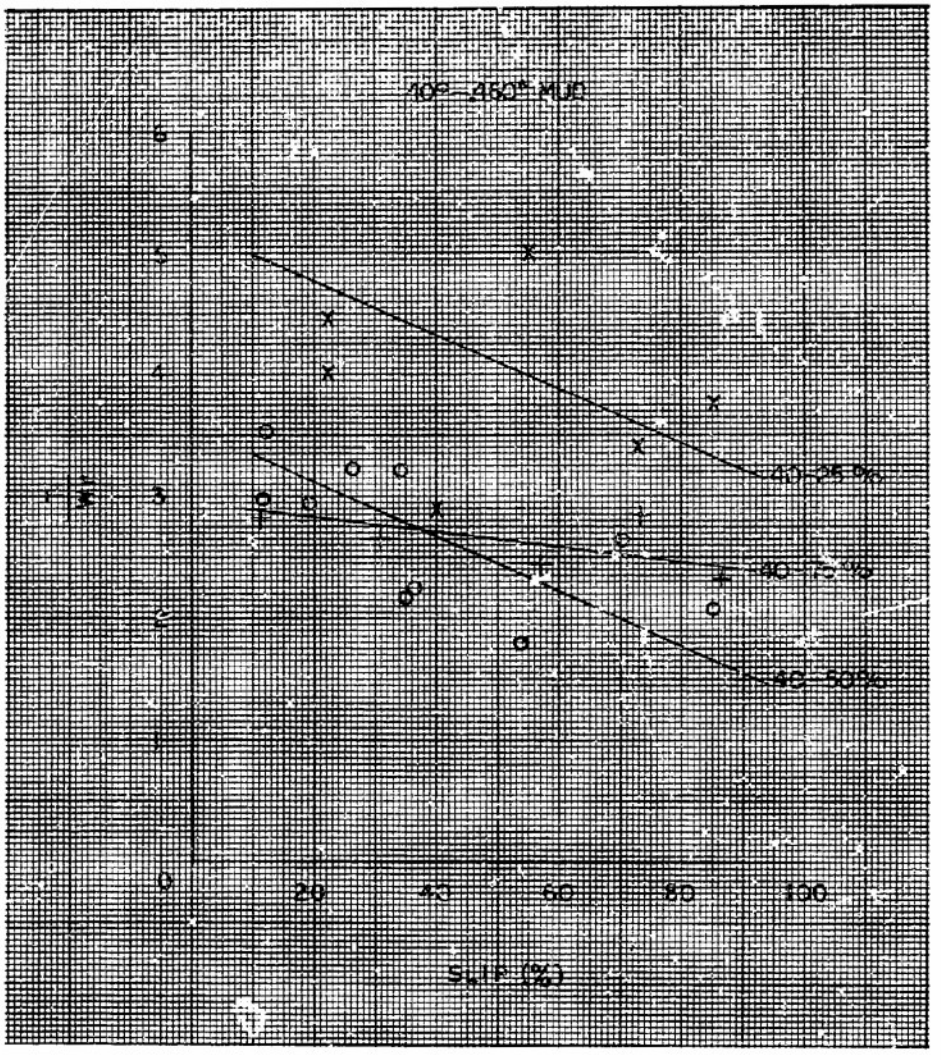

Figure 4-15 Specific Torque vs. Slip - Mud (40 Degree Helix, 0.460 Inch Blade Height)

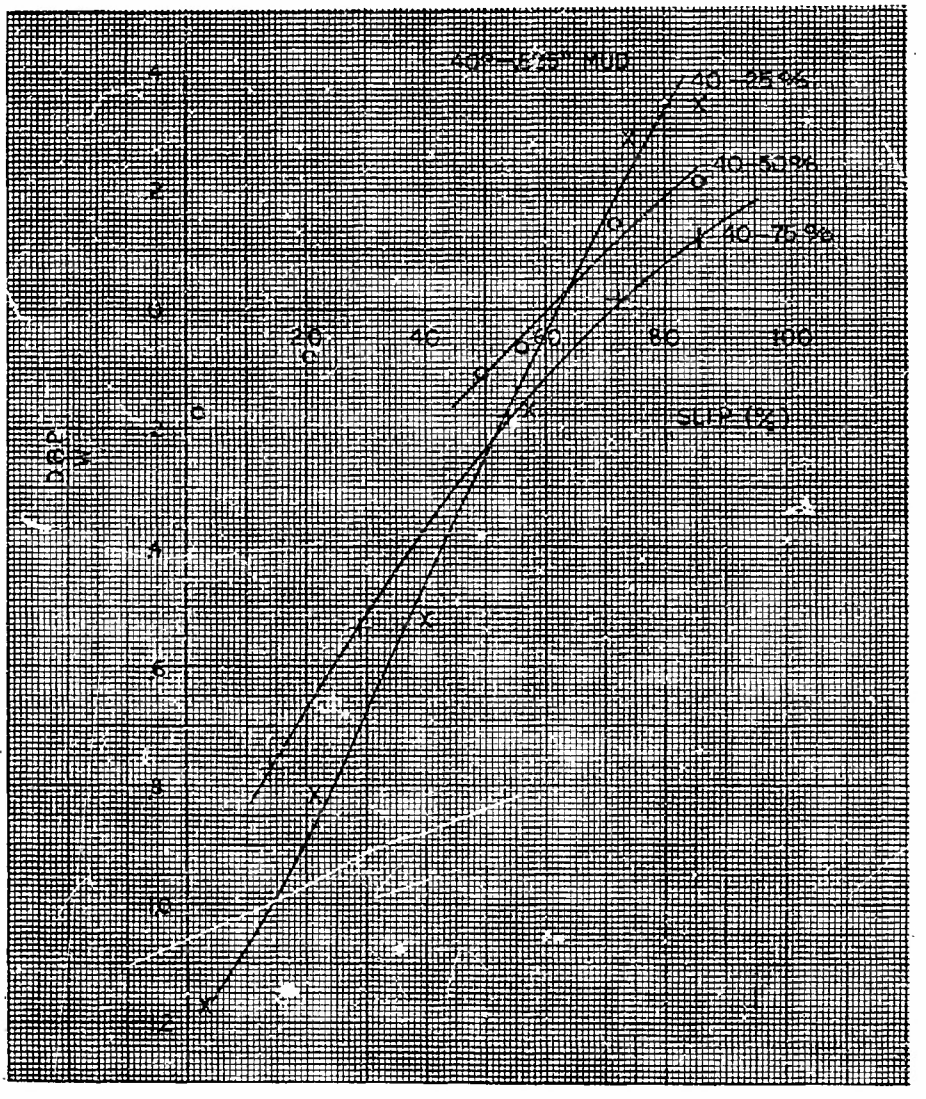

Figure 4-16 Drawbar Pull/Weight Ratio vs. Slip - Mud
(40 Degree Helix, 0.625 Inch Blade Height)

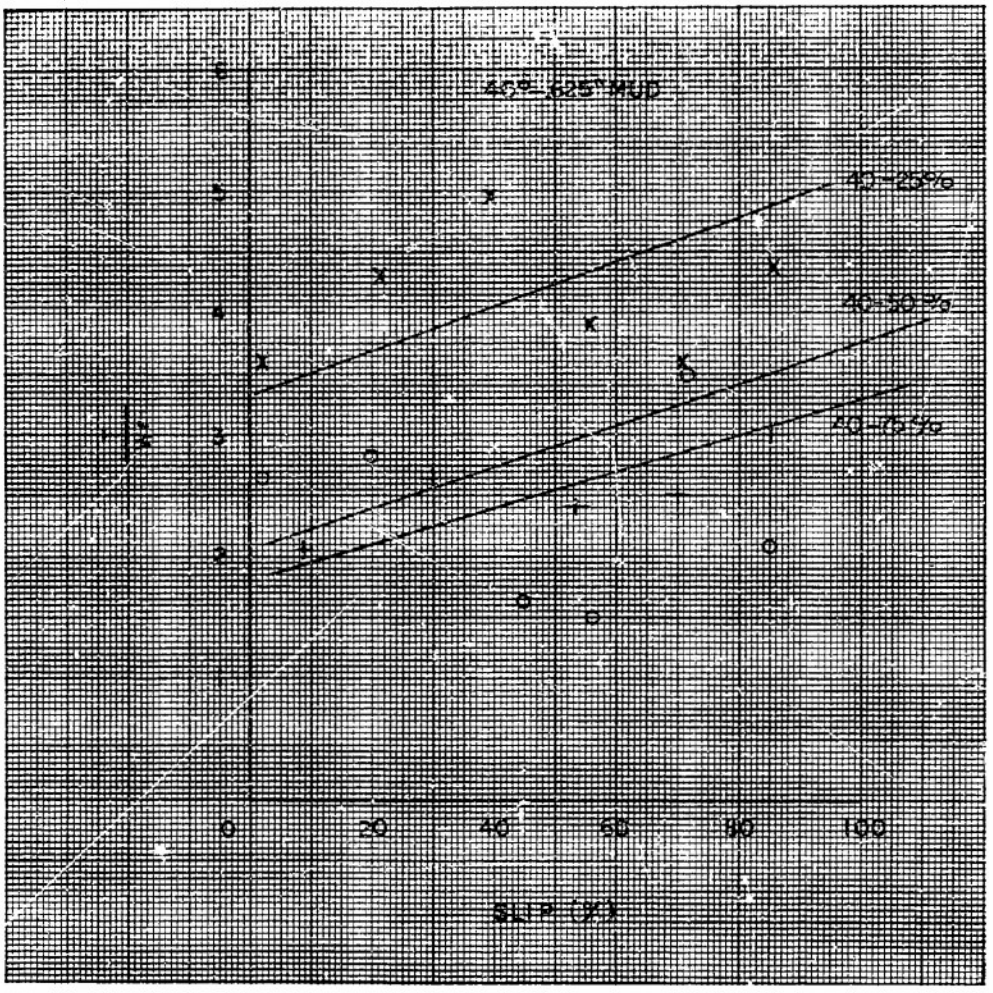

Figure 4-17 Specific Torque vs. Slip - Mud (40 Degree Helix, 0.625 Inch Blade Height)

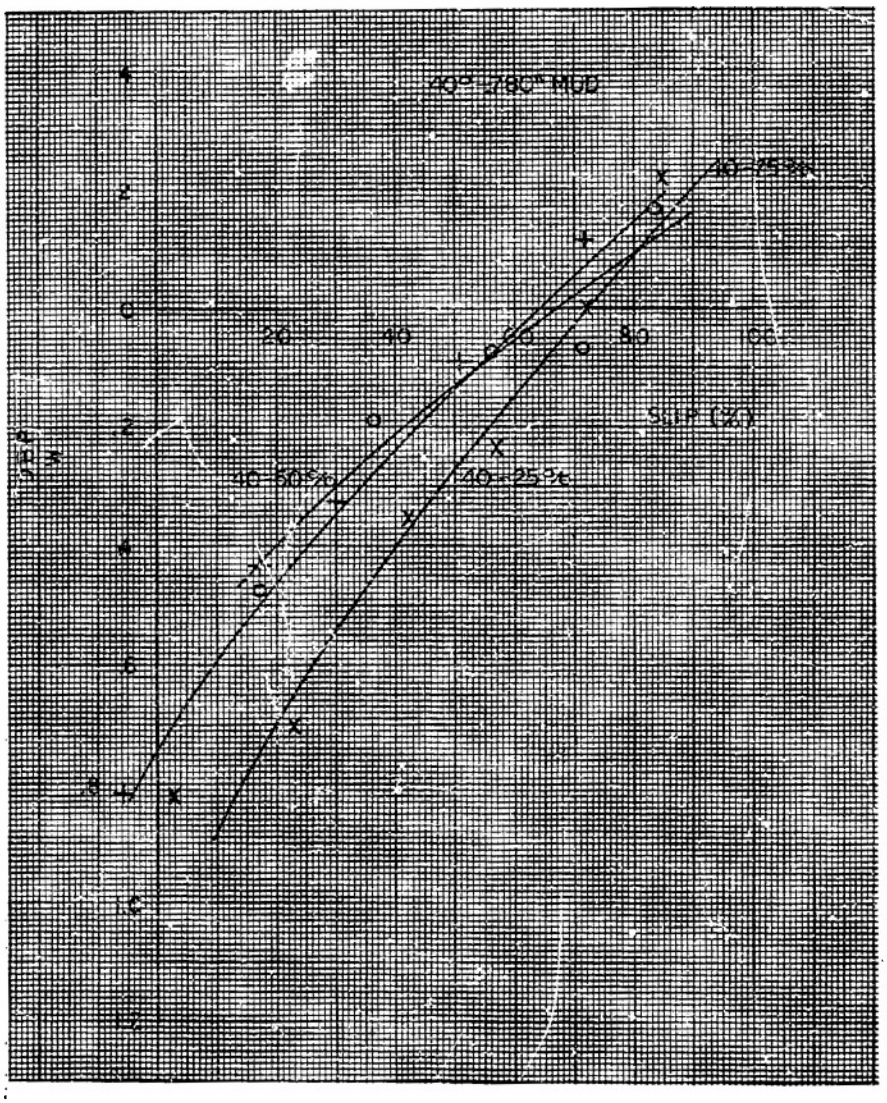

Figure 4-18 Drawbar Pull/Weight Ratio vs. Slip - Mud
(40 Degree Helix, 0.780 Inch Blade Height)

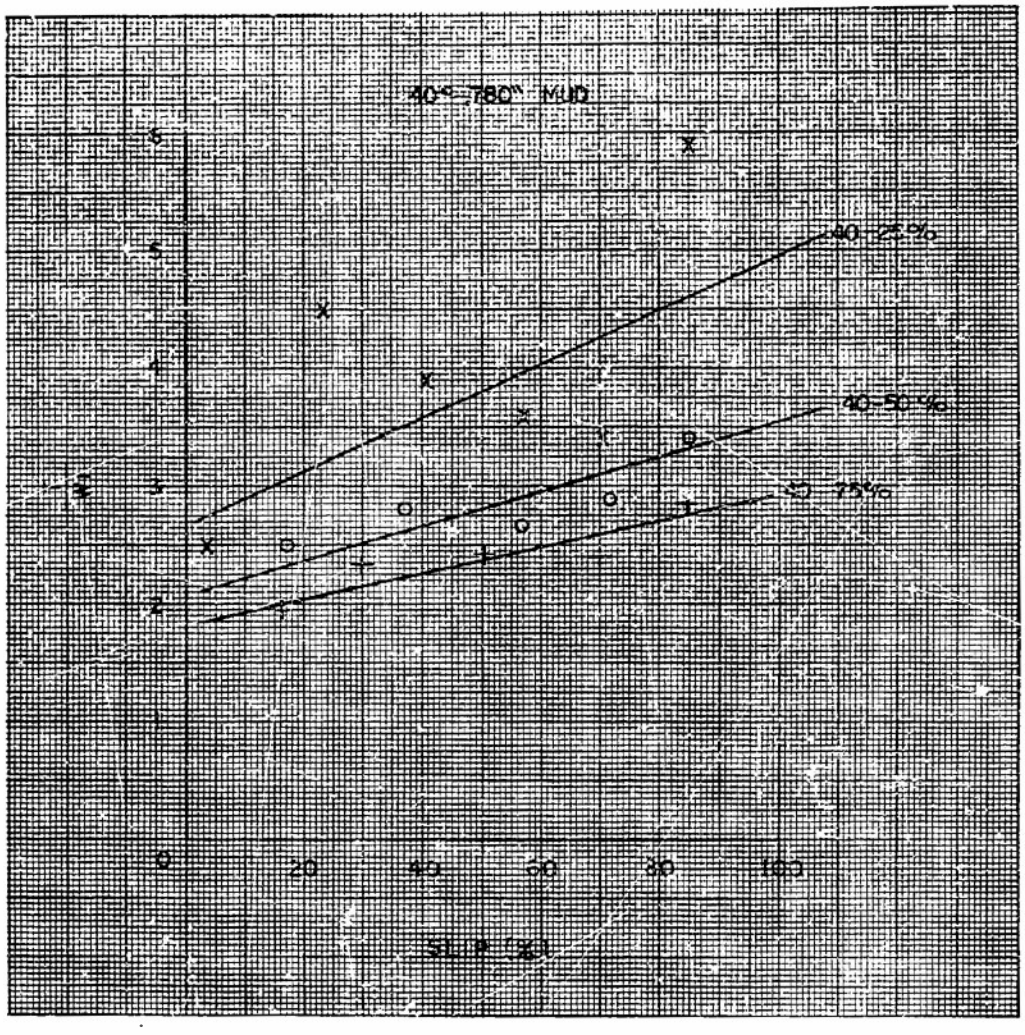

Figure 4-19 Specific Torque vs. Slip - Mud (40 Degree Helix, 0.780 Inch Blade Height)

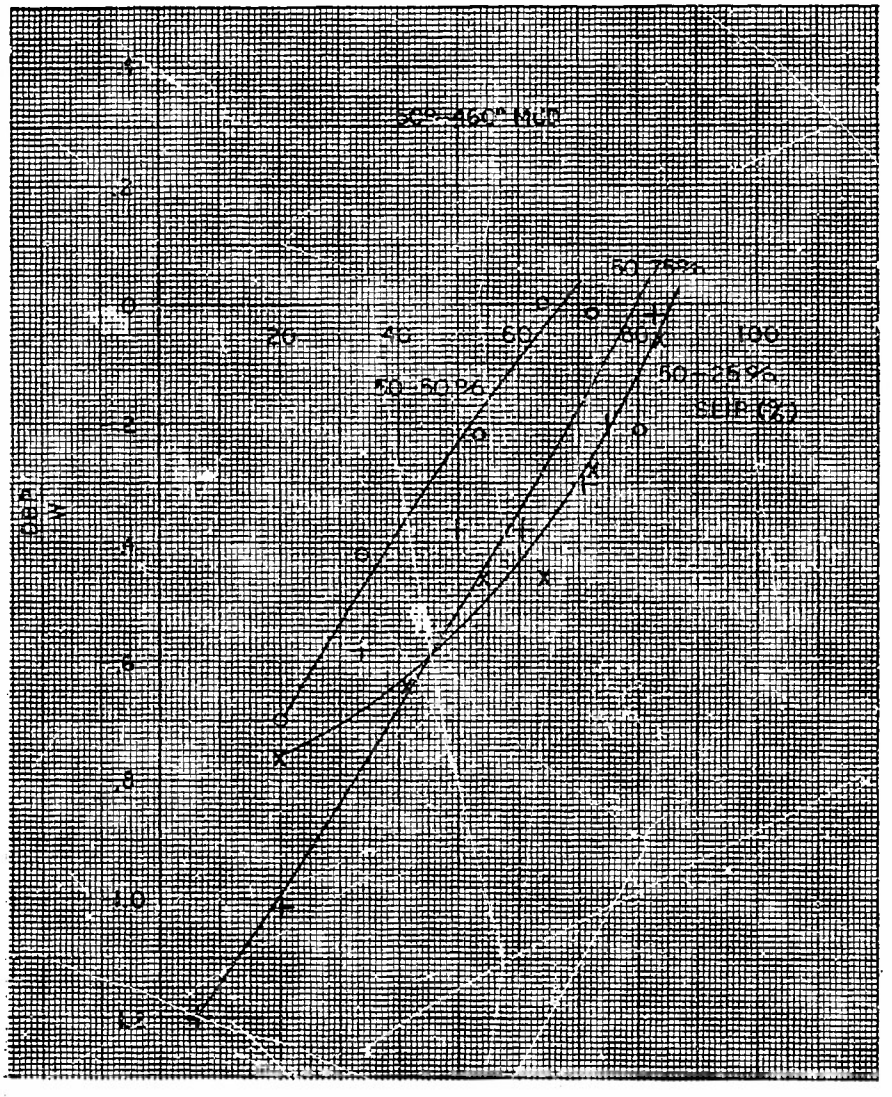

Figure 4-20 Drawbar Pull/Weight Ratio vs. Slip - Mud
(50 Degree Helix, 0.460 Inch Blade Height)

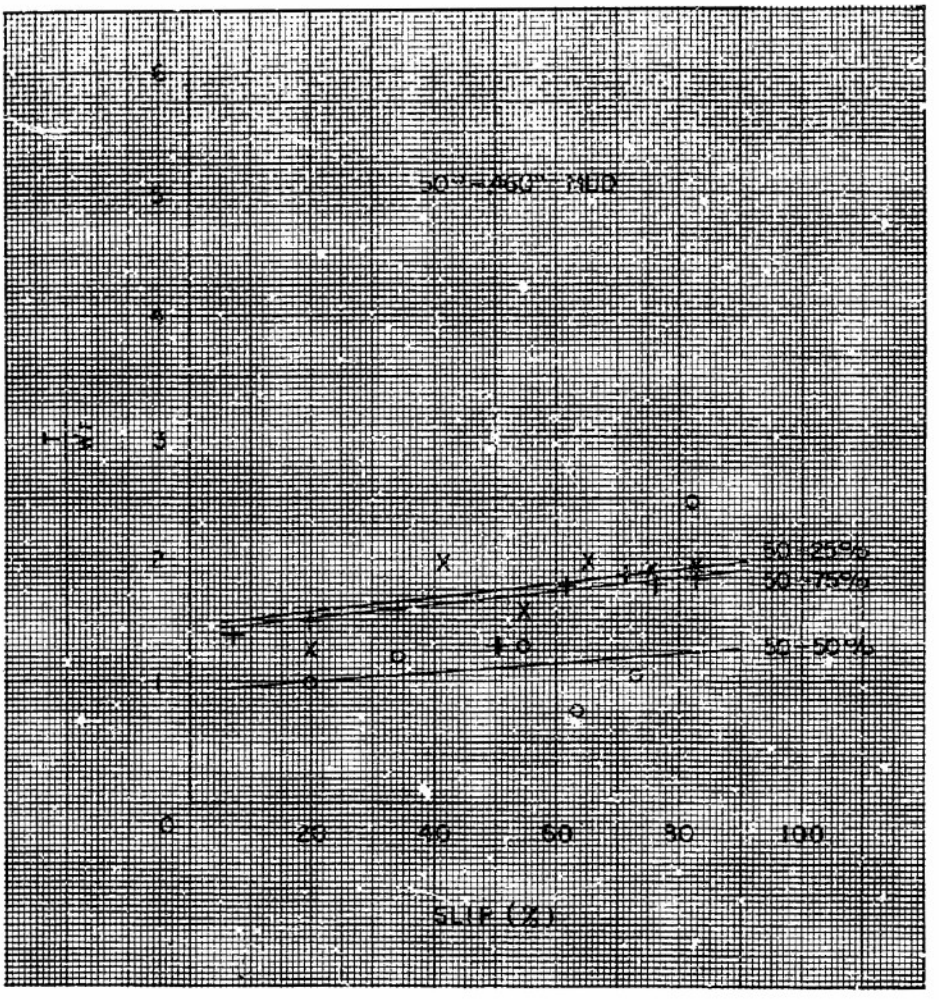

Figure 4-21 Specific Torque vs. Slip – Mud (50 Degree Helix, 0.460 Inch Blade Height)

Section III

MISCELLANEOUS CONFIGURATIONS

The results presented in this section are the effects of varying two characteristics to indicate trends in rotor performance. The tests conducted established the:

- Effect of center of gravity position.
- Effect of length/diameter ratio.

These tests were run in sand and extremely wet mud. One rotor configuration was used to investigate these characteristics, but similar results can be reasonably expected for other rotor configurations.

4-1. EFFECT OF CENTER OF GRAVITY POSITION

One of the first series of tests was conducted in order to determine the optimum center of gravity position. A model with a 30-degree helix angle and a 0.46-inch blade height was used for this investigation. The particulars are denoted on the Figures 4-22 through 4-25.

In sand the maximum drawbar pull is obtained with the center of gravity forward of midpoint, Figure 4-22. This assumes that the major concern is mobility on relatively flat sand beaches. A problem is encountered with the selection of this CG location since at high slips excessive forward sinkage results. But a vehicle does not experience these high slip values on relatively flat sand beaches. From Figure 4-23 the torque

required for positive drawbar pull is minimum for the forward CG location. Thus, the forward CG location is the most efficient for practical operation.

If a different approach is taken and the maximum drawbar pull obtainable, independent of slip is desired, then a CG located at midpoint would be best in sand. The torque required to obtain this drawbar pull at the high slip would be significantly large.

In the extremely wet mud, the tests were conducted at different displacements than the previous tests. The staff at Stevens decided against testing the forward CG location since it apparently was impractical based on the latter approach discussed above. On the basis of the available data, Figure 4-24, a CG located at midpoint is optimum since only in this position is positive drawbar pull generated at a reasonable slip. The torque required for positive drawbar pull is less for the midpoint CG location as observed from Figure 4-25.

Again, the data is inconsistent in its trends and the tests in mud were performed with soil in the completely worked condition. These results may not be valid if the buoyant screw was operating on natural soil.

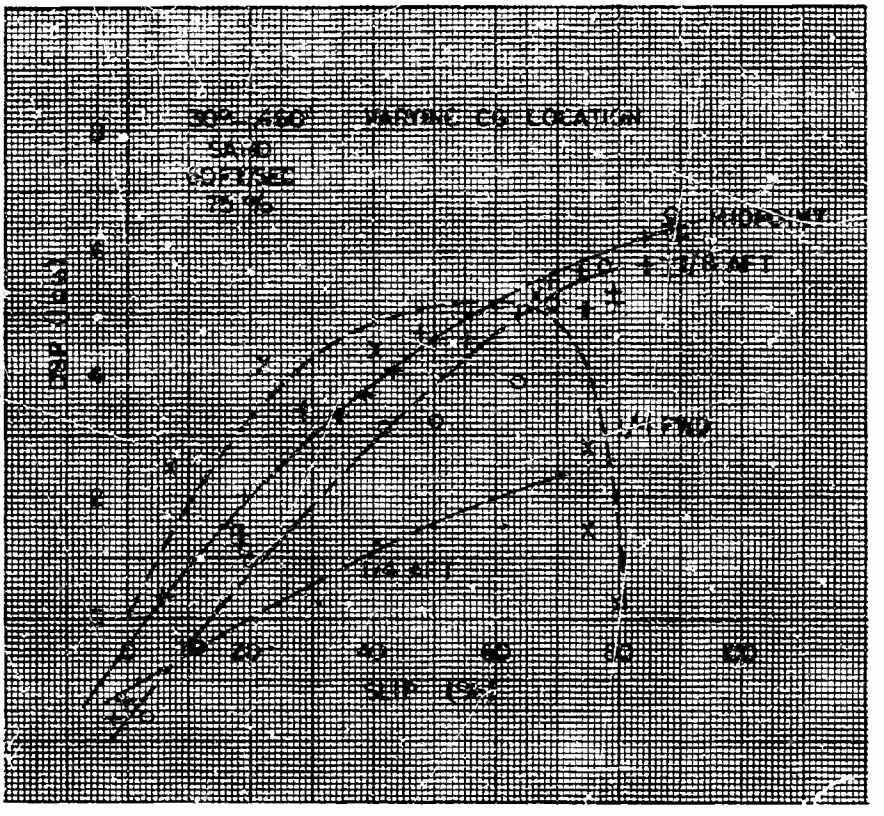

Figure 4-22 Effect of Varying CG in Sand, Drawbar Pull vs. Slip

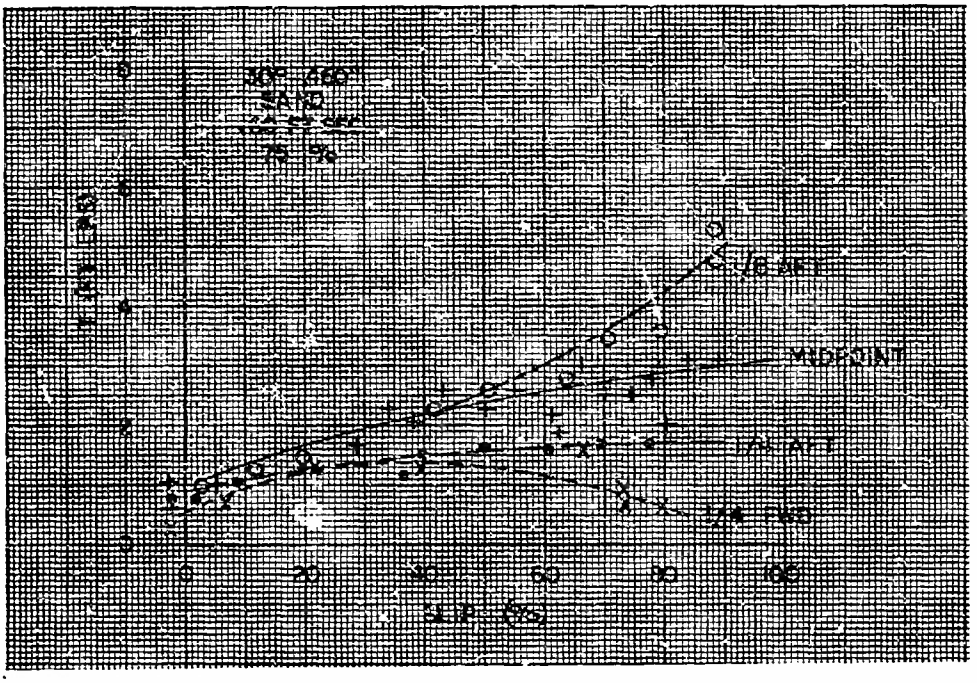

Figure 4-23 Effect of Varying CG in Sand, Torque vs. Slip

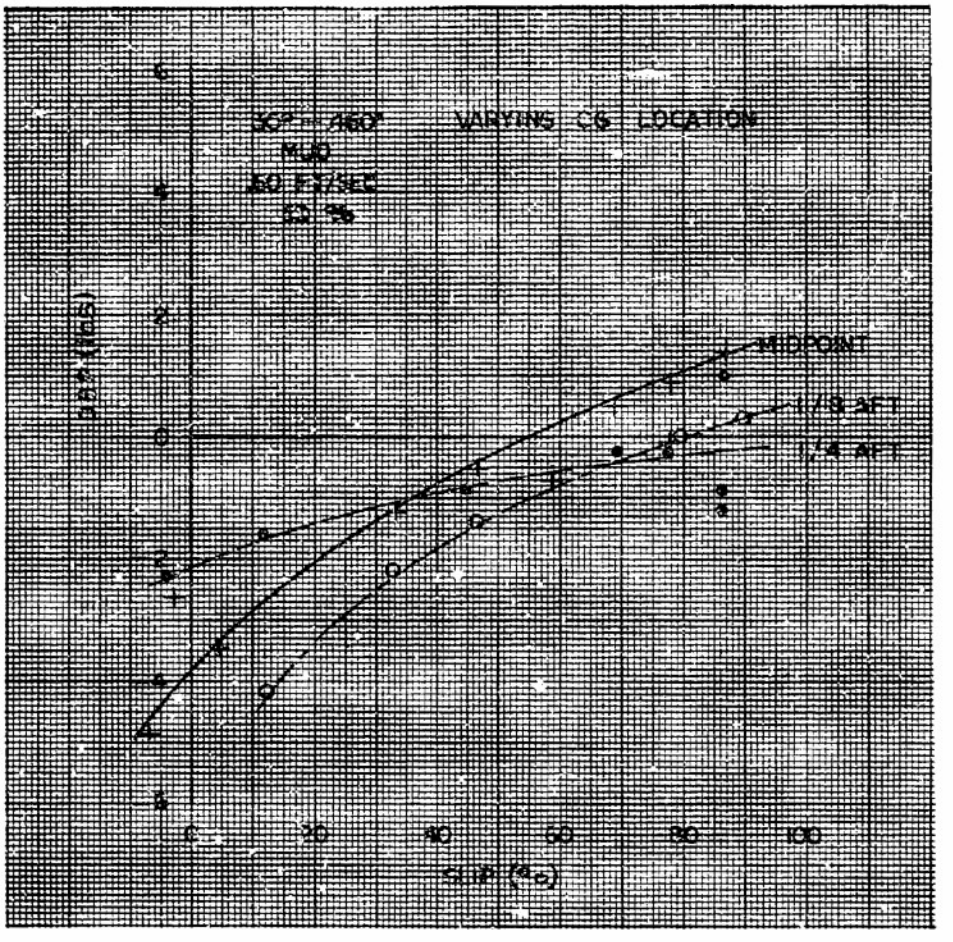

Figure 4-24 Effect of Varying CG in Mud, Drawbar Pull vs. Slip

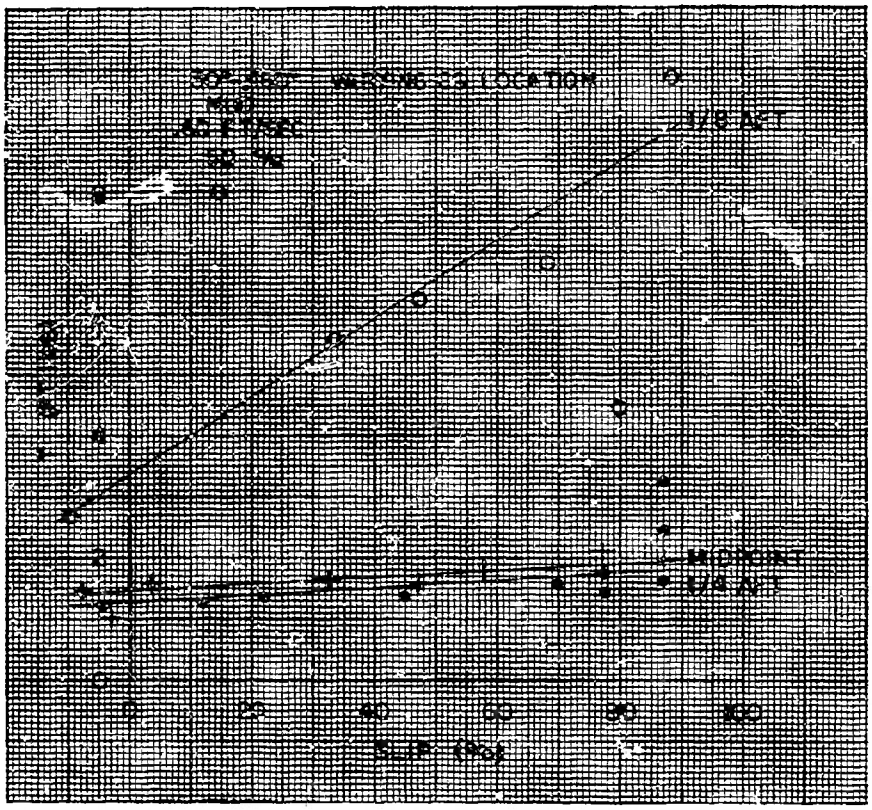

Figure 4-25 Effect of Varying CG in Mud, Torque vs. Slip

4-2. EFFECT OF LENGTH/DIAMETER RATIO

All 1/6 scale rotors used in the soil tests, with the exception of this particular investigation, were 24 inches long and had a hub diameter of four inches providing a length/diameter ratio of six. Two additional rotors with the same diameter but different lengths provide data for length/diameter ratios of four and eight. The blade/heights were constant on all rotors, 0.625 inches, and all rotors had a 40-degree helix angle. These length-diameter variations were tested at three loadings equivalent to percent displacements. Thus, the actual volume displacement varied from one rotor to another. Test results are shown in Figures 4-26 through 4-33.

A length diameter ratio of four was superior in comparison with the other two ratios tested in sand. This conclusion is not only based on the maximum drawbar pull ratio at equivalent loadings, but also on maximum efficiency. Efficiency is a function of the maximum drawbar pull/weight ratio divided by the specific torque measured for a particular increment of slip. This procedure was followed since zero drawbar pull is obtained at different slips for the different length-diameter variations and loading conditions.

In mud a length/diameter ratio of six was best when evaluated in a similar manner as described above. The graphs at the end of this section must be compared with those for the 40-degree helix angle, 0.625-inch blade height rotor with a length/diameter ratio of six found in the systematic series, Section II, Chapter 4.

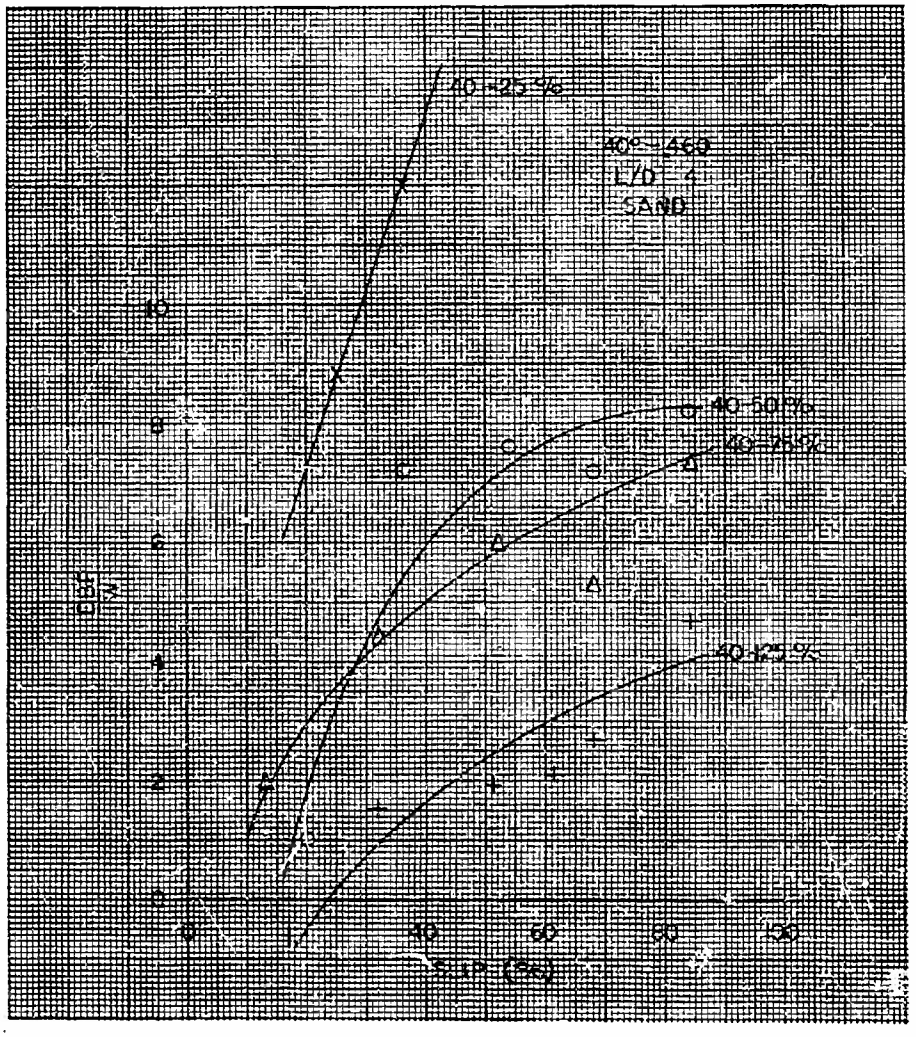

Figure 4-26 Effect ofVarying Length/Diameter Ratio in Sand, Drawbar Pull Weight Ratio vs. Slip (L/D = 4)

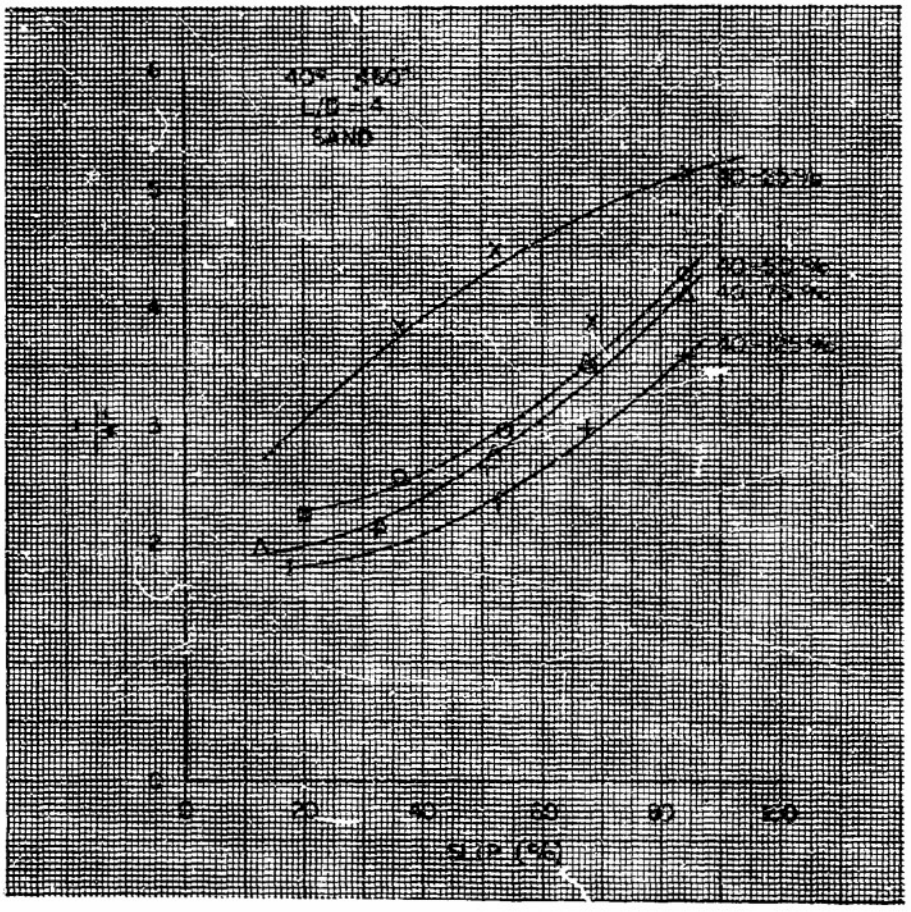

Figure 4-27 Effect of Varying Length/Diameter Ratio in Sand, Specific Torque vs. Slip (L/D = 4)

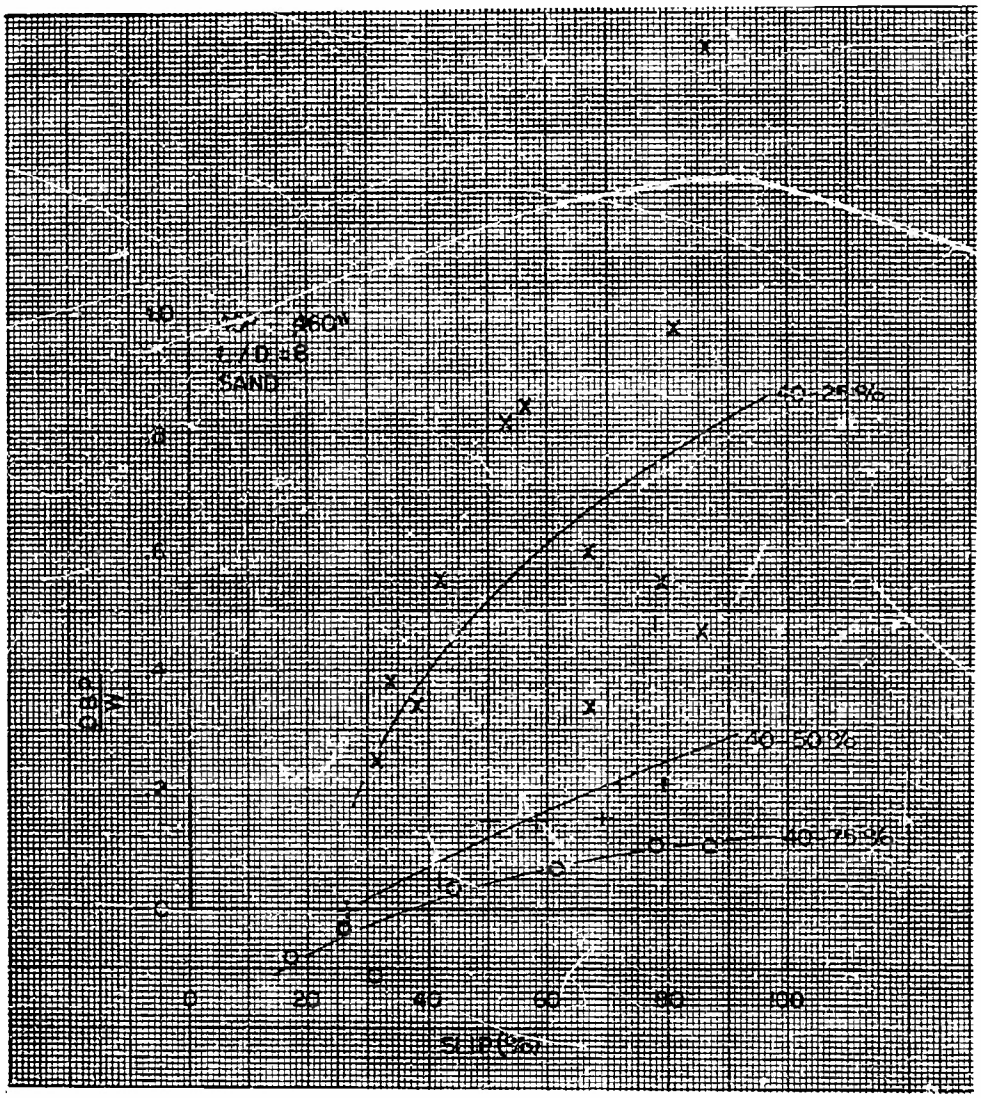

Figure 4-28 Effect of Varying Length/Diameter Ratio in Sand, Drawbar Pull Weight Ratio vs. Slip (L/D = 8)

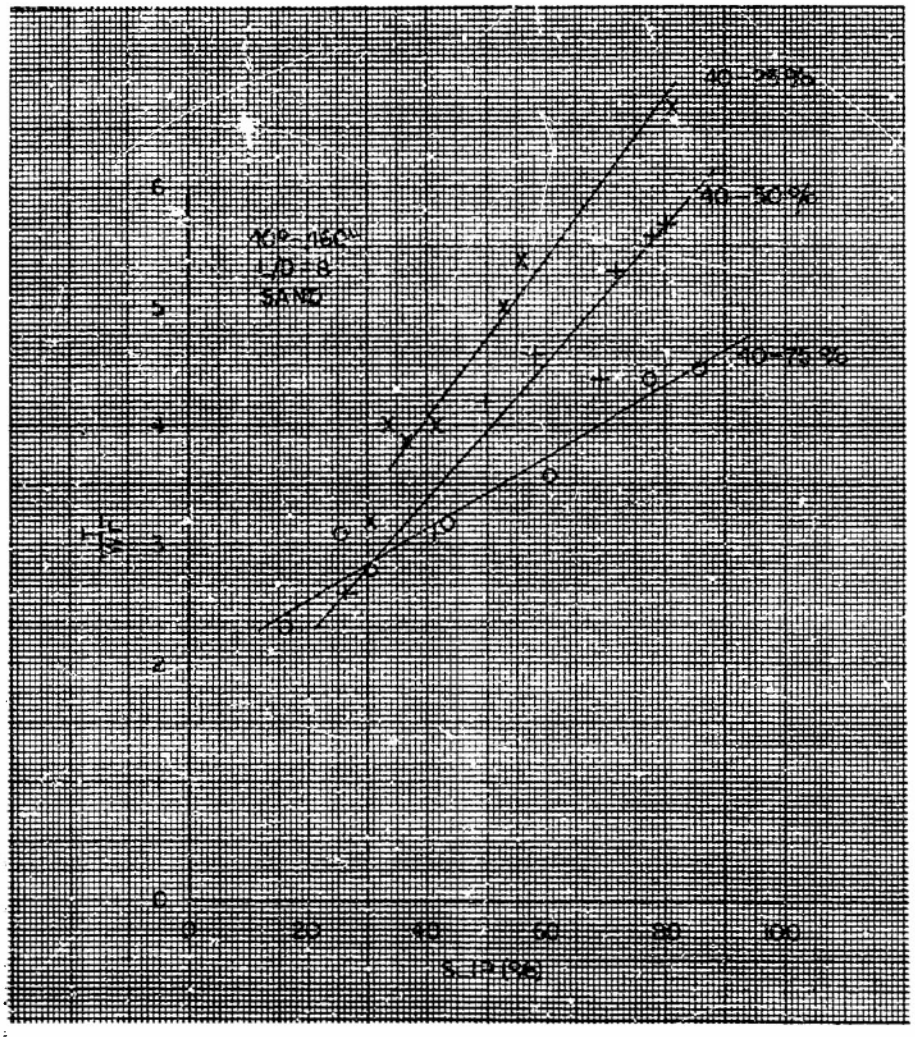

Figure 4-29 Effect of Varying Length/Diameter Ratio in Sand, Specific Torque vs. Slip (L/D = 8)

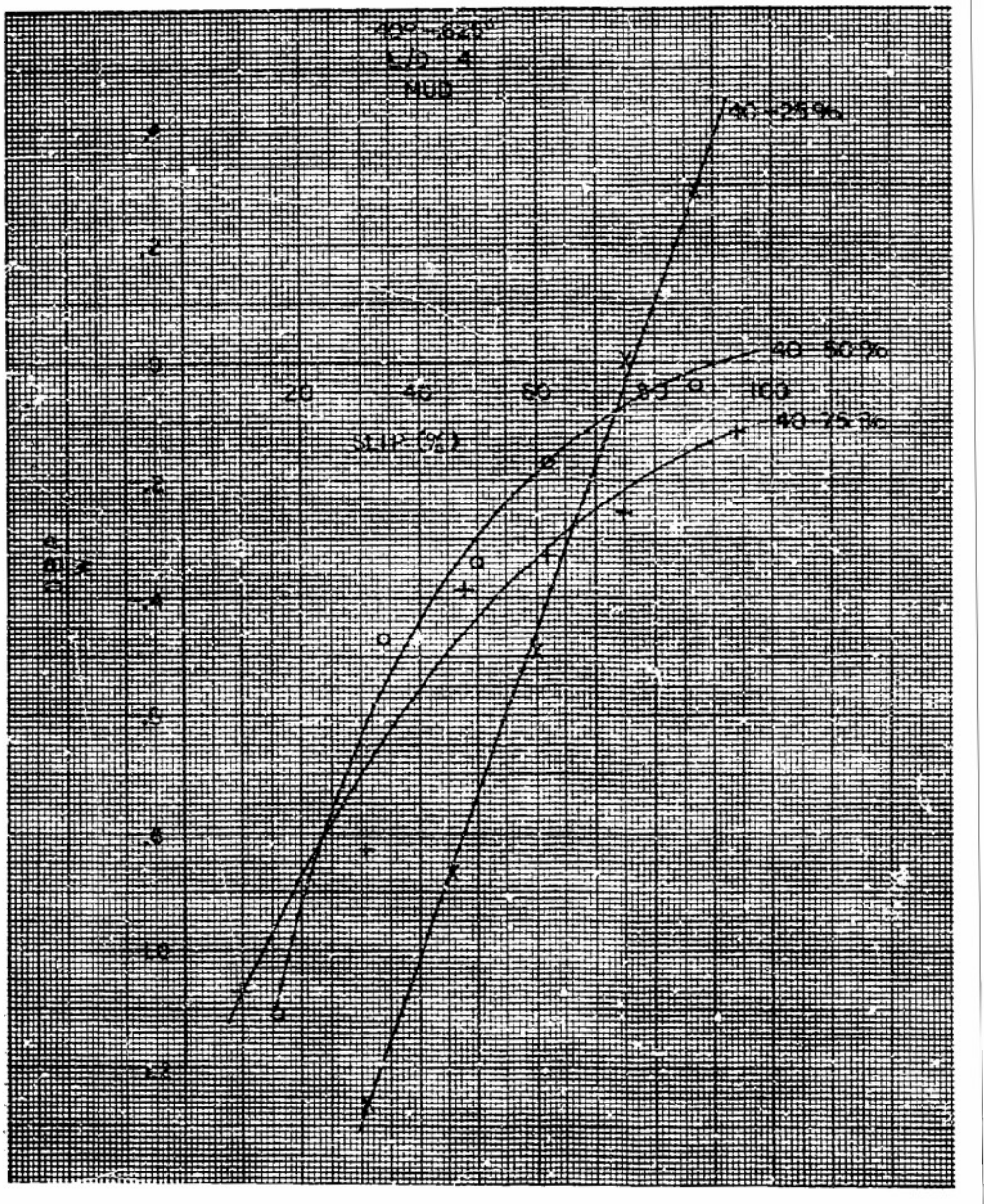

Figure 4-30 Effect of Varying Length/Diameter Ratio in Mud, Drawbar Pull Weight Ratio vs. Slip (L/D = 4)

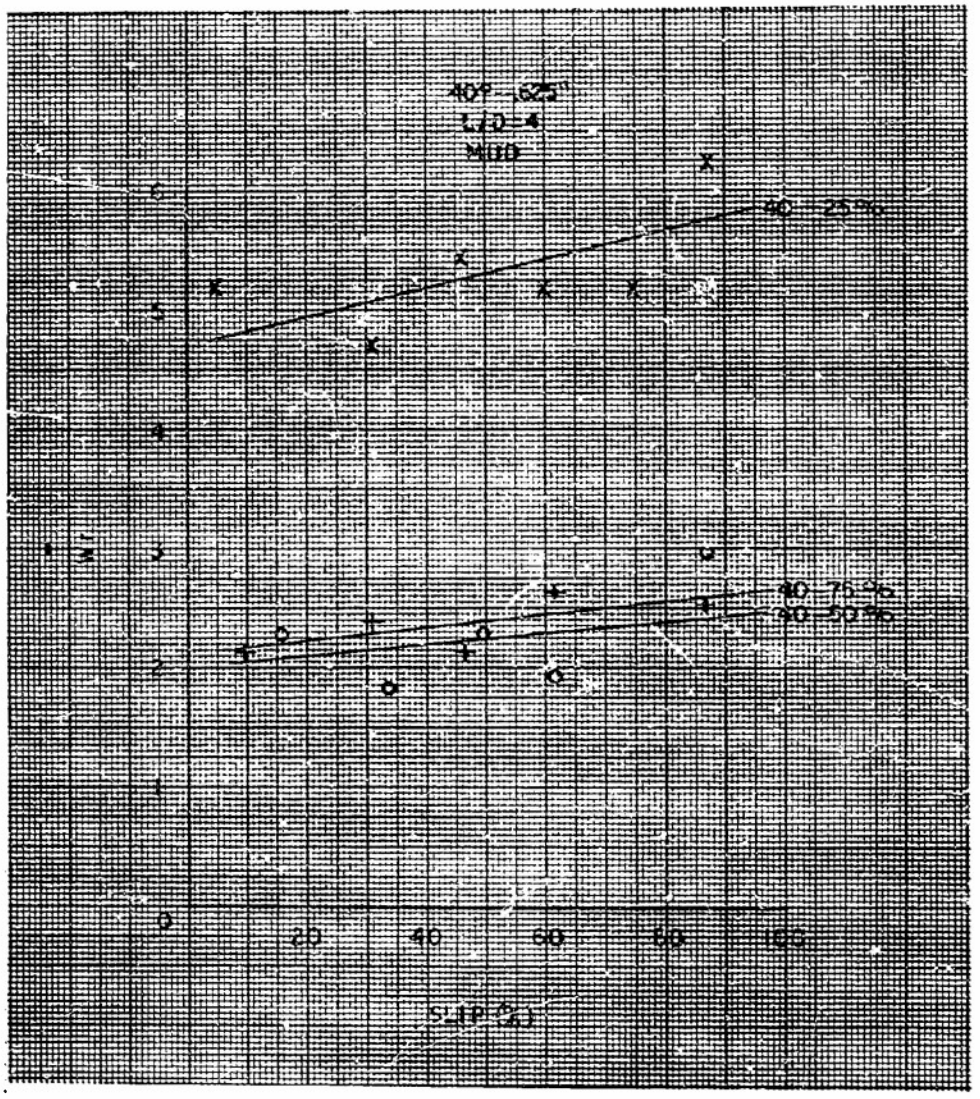

Figure 4-31 Effect of Varying Length/Diameter Ratio in Mud, Specific Torque vs. Slip (L/D = 4)

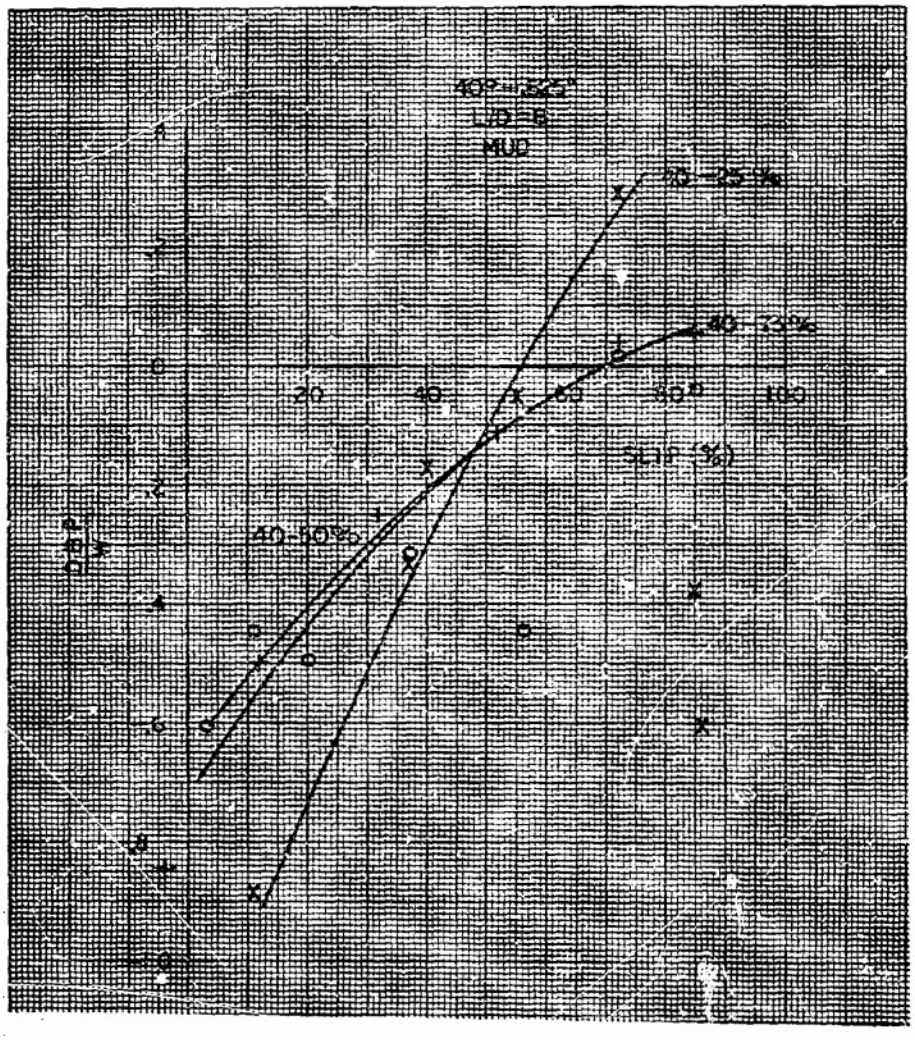

Figure 4-32 Effect of Varying Length/Diameter Ratio in Mud, Drawbar Pull Weight Ratio vs. Slip (L/D = 8)

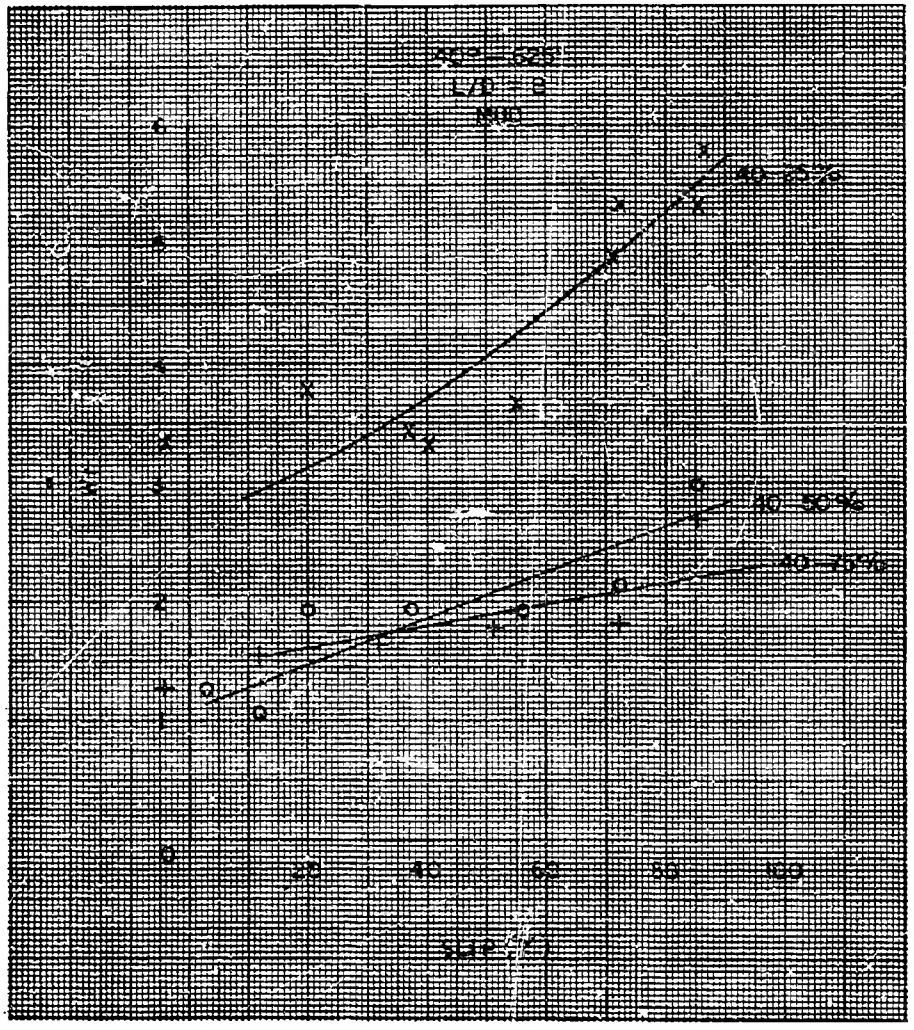

Figure 4-33 Effect of Varying Length/Diameter Ratio in Mud, Specific Torque vs. Slip (L/D = 8)

Section IV

FULL SCALE VEHICLE DATA

Unfortunately the 1/3 scale model test data provided inconclusive results and quantitative estimates of any correction factor as a result of scale effects was not established. Therefore, the full-scale data should be used in conjunction with the data presented to develop the required correction factors. The model and vehicle could not, however, be tested under identical conditions complicating such an approach still further. The model data can not be scaled quantitatively with confidence without further studying the scaling factors even though the relative performance between the various buoyant screw configurations was established from the data.

Tests of the Marsh Screw Amphibian were conducted on a sand beach at Lakeport, Michigan, with the vehicle instrumented in an identical manner to that of the water tests. The sand tests were conducted in the light condition, 3348 pounds,with a course length of 50 feet. Data was obtained for dry sand and wet sand. (Refer to Figures 4-34 and 4-35.)

The data obtained for model and vehicle in sand should scale fairly accurately by Froude's law or the λ^3 relationship. The full scale data indicates slips similar to those predicted for positive drawbar pull to exist. The values of specific torque are somewhat lower than predicted. This may be due to the fact that the sand used for both tests was not identical. The angle of internal friction

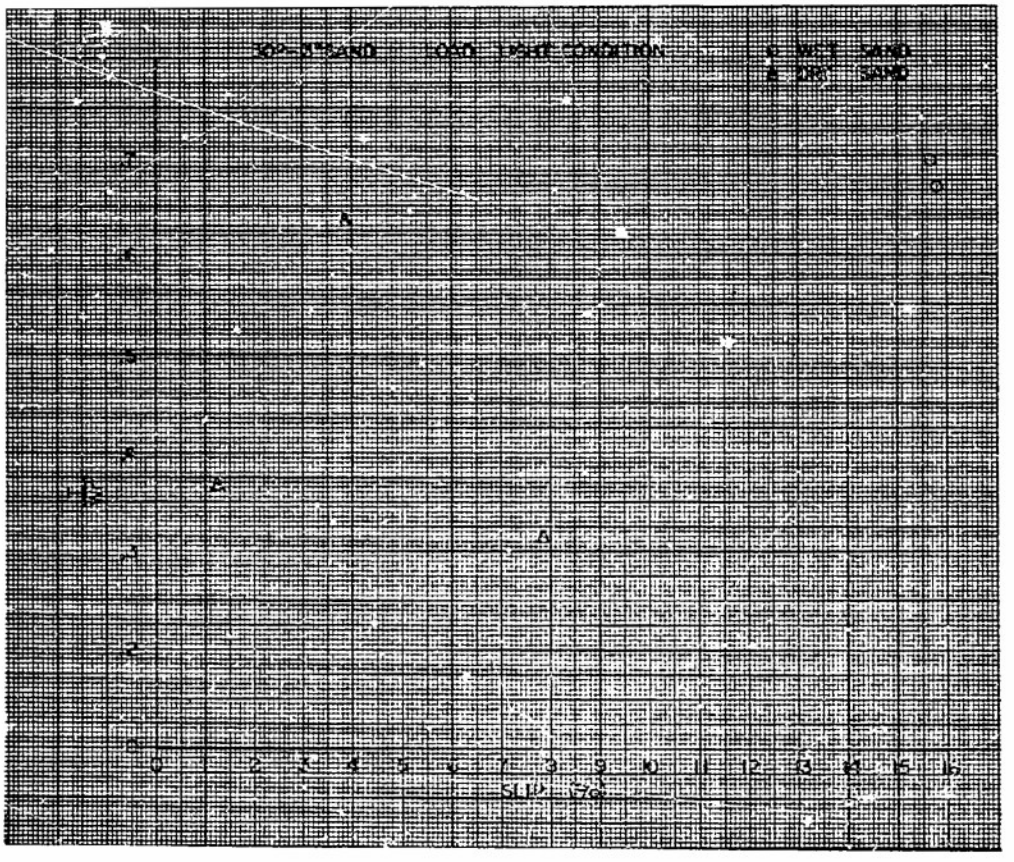

Figure 4-34 Full Size Vehicle Data, Specific Torque vs. Slip, Wet and Dry Sand

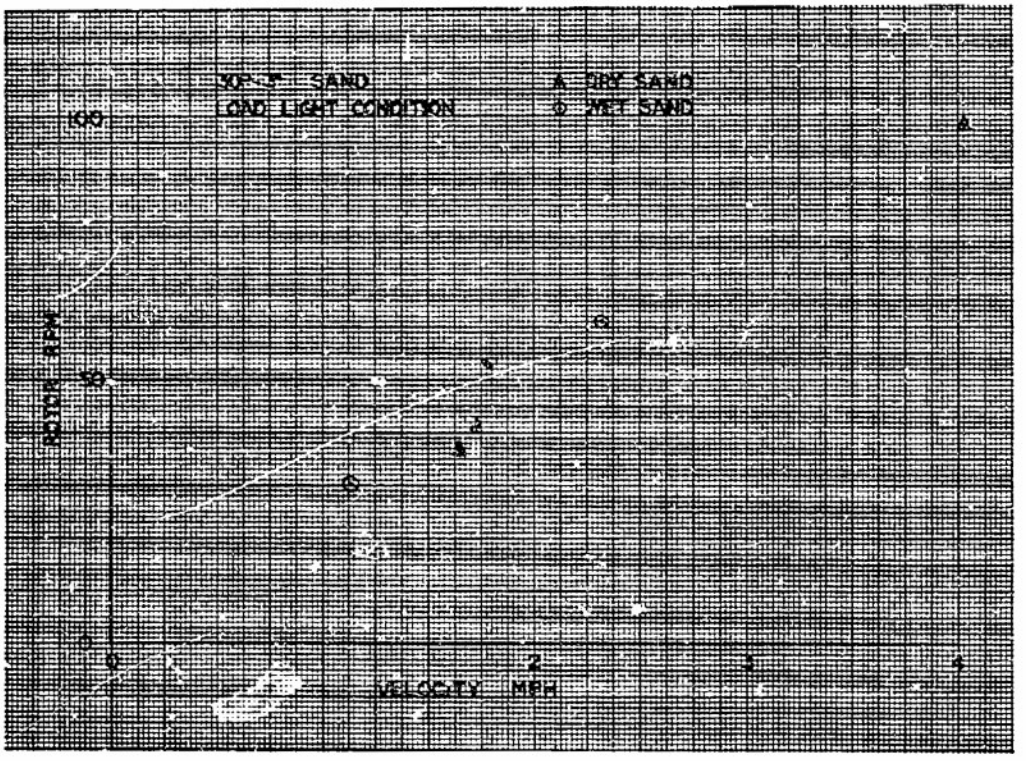

Figure 4-35 Full Size Vehicle Data, Rotor RPM vs. Velocity, Wet and Dry Sand

for the beach sand would be somewhat different than the sand in which the models were tested. This, in conjunction with inexact similitude, would cause such a discrepancy, making the model data somewhat conservative. Insufficient full scale data makes it difficult to establish the required correction factors.

Vehicle tests were also conducted on mud flats south of Monroe, Michigan. A 100 foot course was used at light and heavy load conditions of 3413 pounds and 3945 pounds respectively. (Refer to Figures 4-36 through 4-39 for test results.)

In mud correlation is not expected since the cohesive components of thrust scale by the λ^2 relationship. This was discussed in Section II of Chapter 2.

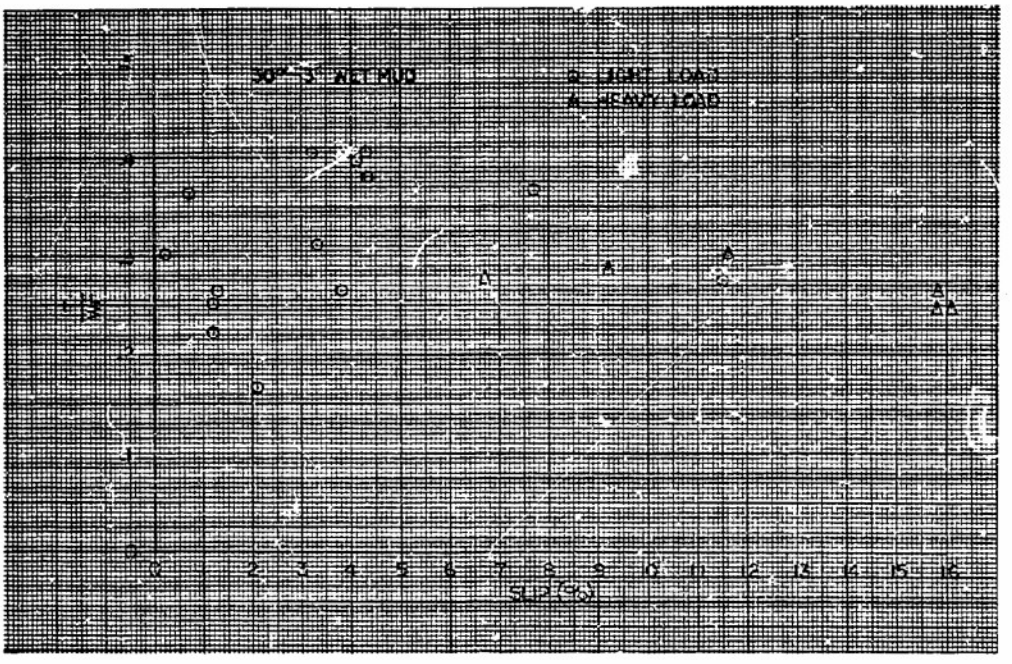

Figure 4-36 Full Size Vehicle Data, Specific Torque vs. Slip, Wet Mud (30 Degree Helix, 3 Inch Blade Height)

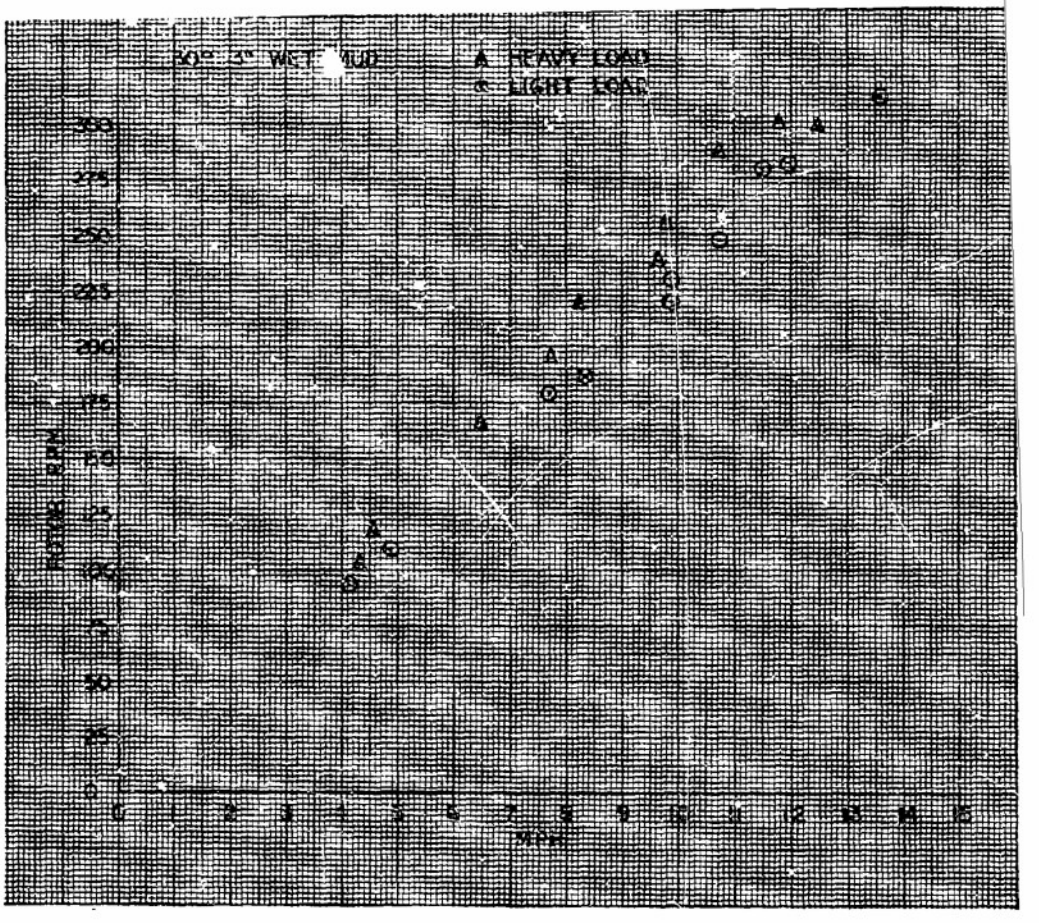

Figure 4-37 Full Size Vehicle Data, Rotor RPM vs. Velocity, Wet Mud (30 Degree Helix, 3 Inch Blade Height)

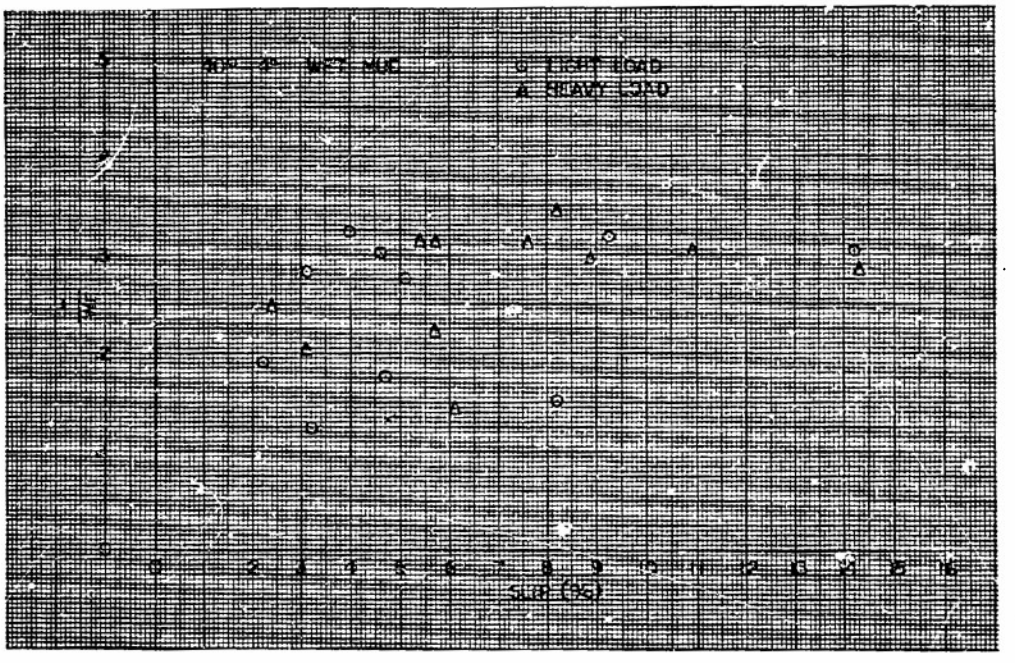

Figure 4-39 Full Size Vehicle Data, Specific Torque vs. Slip, Wet Mud (40 Degree Helix, 4 Inch Blade Height)

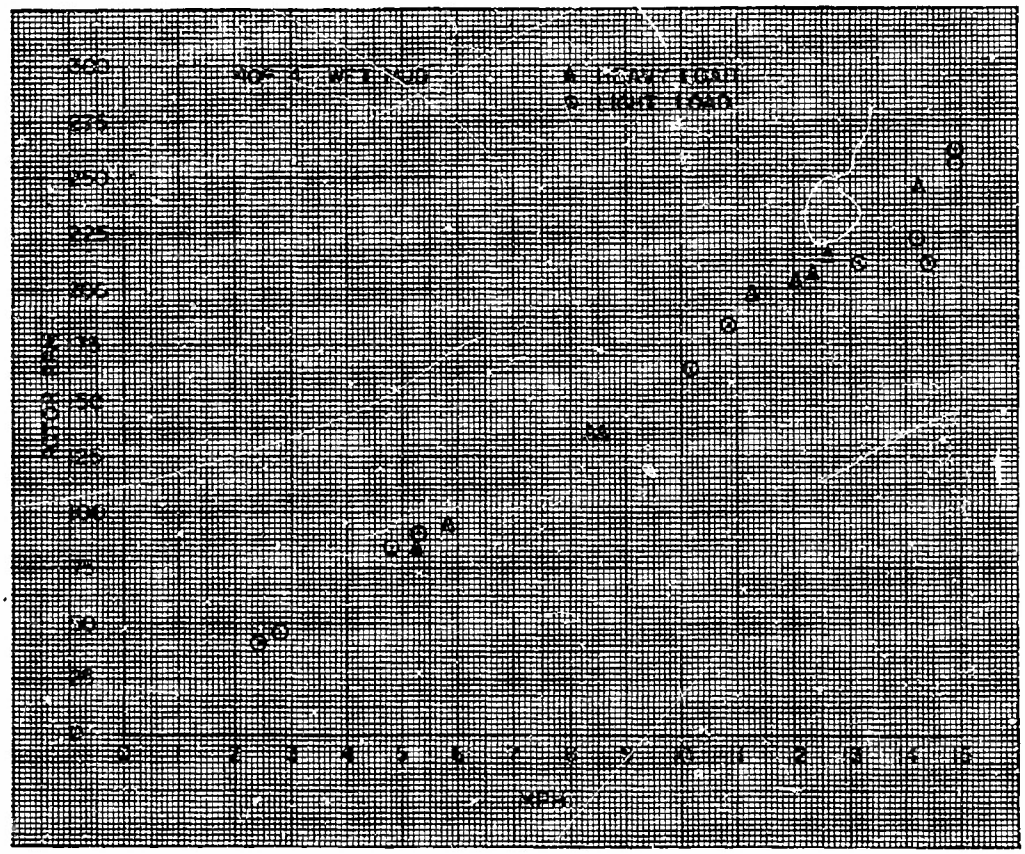

Figure 4-39 Full Size Vehicle Data, Rotor RPM vs. Velocity, Wet Mud (40 Degree Helix, 4 Inch Blade Height)

CHAPTER 5

DESIGN GUIDES AND EXAMPLES

The purpose of this manual is to provide a design technique for this unique means of propulsion. The data derived from the systematic series of bucyant screws provides adequate information useful for future designs. A criteria of performance must first be established before evaluating model data. This criteria is determined by the specific functional requirements of the proposed design. It is for this reason that conclusions from the systematic series data were not mentioned previously. This then leaves the evaluation up to the designer. Three examples are presented as guides only to such an evaluation.

Section I

EXAMPLE I - AMPHIBIOUS LOGISTIC VEHICLE

DESCRIPTION:

Amphibious Logistic Vehicle

Gross weight 6000 pounds

Emphasis on

- Maximum water speed
- Mobility over marginal terrains

Vehicle description is vague since the purpose of this example and those to follow is to establish design guides rather than a complete preliminary design.

WATER PERFORMANCE:

The most efficient rotor in water is one with a length/diameter ratio of six. The weight displacement of each rotor is half the gross weight, assuming all the buoyancy was contributed by the rotor. Rotor displacement was selected as 50 percent of the weight displacement

$$\nabla = 3000 \text{ lbs}/(62.4 \text{ lbs/ft}^3) = 48.125 \text{ ft}^3$$

from figure 5-1, a 17-foot, 6-inch rotor is selected since a rotor displacement of 50 percent was specified. Horsepower calculations for numerous configurations for a particular speed range are tabulated on the calculation sheets. These calculations were compiled by an IBM 1401 computer and the computer output is listed in Appendix D. The values for the advance coefficient, J, and the

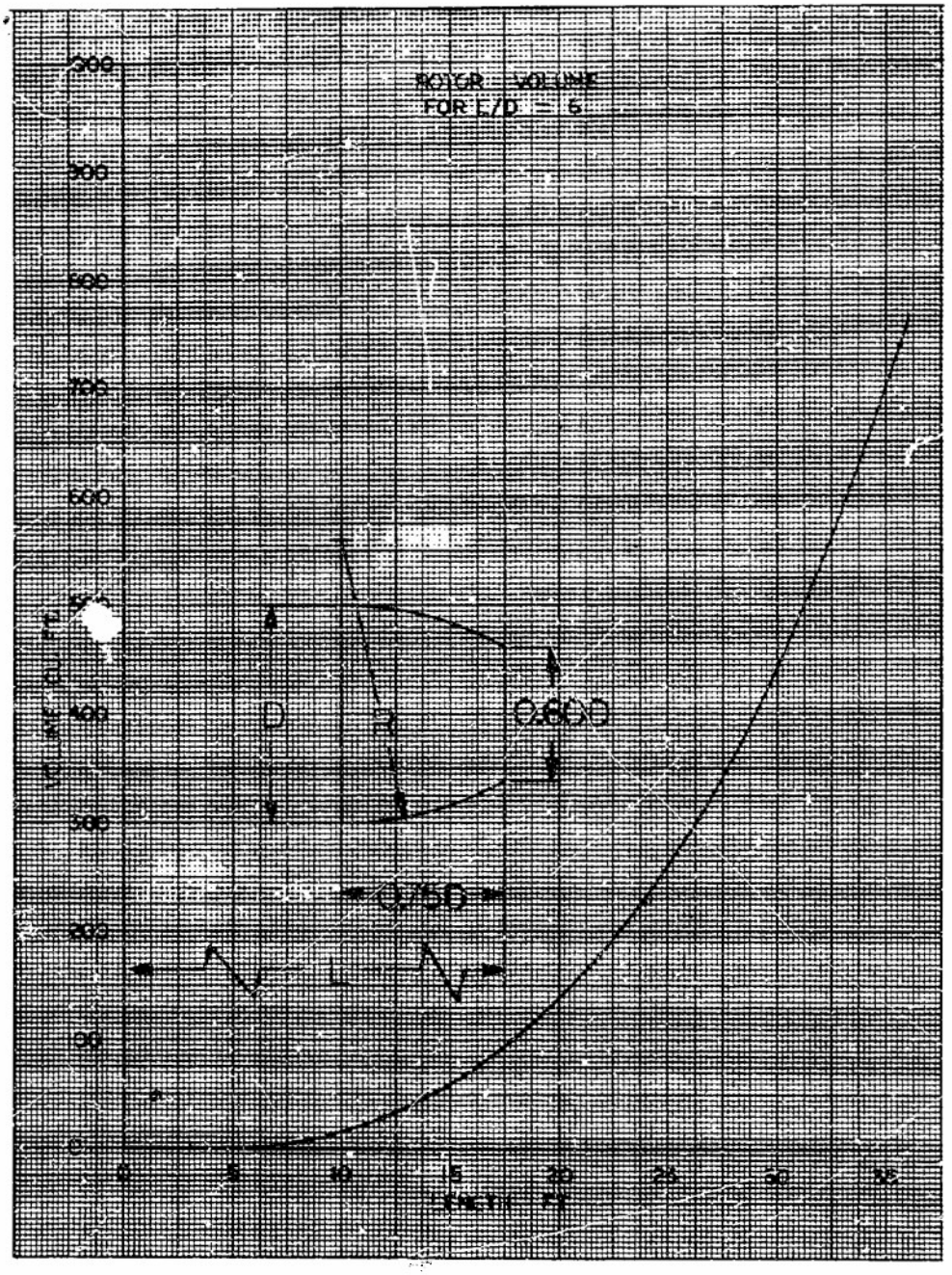

Figure 5-1 Volume vs. Length for Rotor with Length/Diameter Ratio of Six

non-dimensional torque constant, $10K_Q$, for specific blade height/diameter ratios and Froude volume numbers are obtained from the appropriate figures in Section I of Chapter 3. Visual inspection of these calculations results in a blade height/diameter ratio selection of 0.2344. Horsepower for various helix angles was plotted as indicated in figure 5-2. Thus, a rotor with a 52 degree helix angle and a blade height diameter ratio of 0.2344 is the most efficient rotor configuration.

The rotor horsepower calculated is for a single rotor. If the rotor has a blunt stern the rotor horsepower is halved at 18 MPH as illustrated in figure 3-46. This posed a trade-off consideration since reverse operation of the vehicle in soil would be penalized, but it will be assumed that such performance degradation is acceptable. Other power corrections can be estimated for various rotor spacings, shrouding, and reduced rear strut frontal area. The latter has a significant affect upon horsepower requirements. For this reason the drive train will be positioned at the forward strut. A non-rotating cylindrical fairing would house the bearings and drive shaft.

Therefore, neglecting hull effects, 130 rotor horsepower is required at 18 MPH for the rotor configuration selected above. At 18 MPH the rotor speed is 233 RPM as obtained from calculation sheet 4. Assuming a drive train efficient of 85 percent results in 153 net horsepower being required.

V MPH	V^1 FPS	F_{rj}	$V^{1\,2}$	% DISPLACEMENT = 50				H/D = .1150											
				J				$10K_Q$				n				Q			
				30°	40°	50°	60°	30°	40°	50°	60°	30°	40°	50°	60°	30°	40°	50°	60°
8.0	11.74	1.085	137.73	.73	1.05	1.32	1.48	1.10	1.0	1.1	1.37	4.42	3.07	2.44	2.18	1451	1320	1452	1806
10.0	14.67	1.356	215.21	.70	1.00	1.18	1.32	.93	.94	1.02	1.21	5.76	4.03	3.82	3.06	2041	1839	2104	2495
12.0	17.60	1.627	309.90	.66	.95	1.11	1.24	.89	.86	.92	1.07	7.33	5.09	4.36	3.90	2643	2554	2732	3178
14.0	20.54	1.898	421.81	.64	.91	1.08	1.20	.79	.77	.82	.95	8.82	6.21	5.23	4.71	3193	3112	3314	3840
16.0	23.47	2.169	550.93	.62	.89	1.06	1.17	.71	.70	.74	.84	10.40	7.25	6.09	5.52	3748	3496	3907	4435
18.0	26.41	2.440	697.28	.61	.88	1.05	1.15	.64	.63	.67	.74	11.90	8.25	6.91	6.31	4276	4210	4477	4945

V MPH	Qn				RHP			
	30°	40°	50°	60°	30°	40°	50°	60°
8.0					73.3	46.3	40.5	45.0
10.0					134.	89.3	82.1	87.1
12.0					221	149	136	142
14.0					322	221	198	206
16.0					446	306	272	279
18.0					581	397	354	357

PRINCIPAL CHARACTERISTICS

L = 17.5 FT.

D = 2.92 FT.

Δ = 3000# PER ROTOR LBS.

∇ = 48.13 $FT.^3$

e = 1.991 $\frac{LB\text{-}SEC^2}{FT.^4}$

$$J = \frac{V^1}{n\nabla^{1/3}}$$

$$K_Q = \frac{Q}{eV^{1\,2}\nabla}$$

V MPH	V' FPS	F_∇	V'^2	% DISPLACEMENT = 50 H/D=.1563															
				J				$10K_Q$				n				Q			
				30°	40°	50°	60°	30°	40°	50°	60°	30°	40°	50°	60°	30°	40°	50°	60°
8.0	11.74	1.085	137.73	.91	1.36	1.70	1.97	1.08	.99	.86	1.16	3.55	2.37	1.90	1.64	1425	1307	1135	1531
10.0	14.67	1.356	215.21	.86	1.29	1.57	1.84	1.03	.98	.88	1.06	4.69	3.13	2.57	2.19	2124	2021	1815	2186
12.0	17.60	1.627	309.90	.82	1.23	1.50	1.75	.95	.93	.86	.98	5.90	3.94	3.23	2.77	2821	2762	2554	2910
14.0	20.54	1.898	421.81	.79	1.19	1.46	1.70	.86	.84	.80	.89	7.15	4.75	3.87	3.32	3476	3395	3234	3597
16.0	23.47	2.169	550.93	.76	1.16	1.42	1.66	.76	.74	.71	.80	8.49	5.56	4.54	3.89	4012	3907	3748	4224
18.0	26.41	2.440	697.28	.74	1.14	1.40	1.64	.66	.64	.62	.70	9.81	6.37	5.19	4.43	4410	4276	4143	4677

5-6

V MPH	Qn				RHP			
	30°	40°	50°	60°	30°	40°	50°	60°
8.0					57.7	35.4	24.6	28.7
10.0					114	72.2	53.3	54.7
12.0					190	124	94.1	91.9
14.0					284	184	143	136
16.0					389	248	195	188
18.0					494	311	245	237

PRINCIPAL CHARACTERISTICS

L = 17.5 FT.

D = 2.92 FT.

Δ = 3000# PER ROTOR. LBS.

∇ = 48.13 $FT.^3$

e = 1.991 $\frac{LB\text{-}SEC^2}{FT.^4}$

$$J = \frac{V'}{n\nabla^{1/3}}$$

$$K_Q = \frac{Q}{eV'^2\nabla}$$

CHRYSLER DEFENSE ENGINEERING

DESIGN CALCULATIONS - BUOYANT SCREW

SHEET 2 OF 4

V MPH	V^1 FPS	F_∇	$V^{1\,2}$	% DISPLACEMENT = .50				H/D = .1950											
				J				$10K_Q$				n				Q			
				30°	40°	50°	60°	30°	40°	50°	60°	30°	40°	50°	60°	30°	40°	50°	60°
8.0	11.74	1.089	137.73	1.00	1.53	1.96	2.05	1.02	.94	.86	1.13	3.23	2.11	1.47	1.57	1346	1241	1135	1491
10.0	14.67	1356	215.21	.94	1.48	1.82	1.92	.94	.87	.81	1.03	4.29	2.73	2.22	2.10	1939	1794	1670	2124
12.0	17.60	1627	309.90	.90	1.43	1.73	1.84	.85	.77	.72	.92	5.38	3.38	2.80	2.63	2524	2287	2138	2732
14.0	20.54	1898	421.81	.86	1.40	1.68	1.80	.76	.69	.64	.82	6.57	4.03	3.36	3.14	3072	2789	2587	3314
16.0	23.47	2169	550.93	.83	1.36	1.63	1.78	.67	.62	.58	.72	7.77	4.75	3.96	3.63	3537	3273	3062	3801
18.0	26.41	2.440	697.28	.81	1.34	1.65	1.74	.60	.55	.52	.64	8.96	5.42	4.68	4.17	4009	3675	3475	4276

5-7

V MPH	Qn				RHP			
	30°	40°	50°	60°	30°	40°	50°	60°
8.0					49.6	29.9	21.4	26.8
10.0					95.0	55.9	42.3	51.0
12.0					155	88.4	68.3	82.1
14.0					230	129	99.3	119
16.0					314	177	138	157
18.0					410	227	186	204

PRINCIPAL CHARACTERISTICS

L = 17.5 FT.

D = 2.92 FT.

Δ = 3200# PER ROTOR LBS.

∇ = 48.13 $FT.^3$

e = 1.991 $\frac{LB\text{-}SEC^2}{FT.^4}$

$$J = \frac{V^1}{n\nabla^{1/3}}$$

$$K_Q = \frac{Q}{eV^{1\,2}\nabla}$$

CHRYSLER DEFENSE ENGINEERING

DESIGN CALCULATIONS - BUOYANT SCREW

SHEET 3 OF 4

V MPH	V' FPS	F_∇	V'^2	% DISPLACEMENT = .50 H/D = .2344															
				J				$10K_Q$				n				Q			
				30°	40°	50°	60°	30°	40°	50°	60°	30°	40°	50°	60°	30°	40°	50°	60°
8.0	11.74	1.085	137.73	1.14	1.68	2.12	2.50	.121	1.01	.91	1.33	2.83	1.92	1.52	1.29	1597	1333	1201	1755
10.0	14.67	1.356	215.21	1.07	1.62	2.02	2.42	1.08	.93	.85	1.17	3.78	2.49	2.00	1.67	2227	1918	1753	2413
12.0	17.60	1.627	309.90	1.02	1.56	1.95	2.34	.92	.80	.73	.97	4.75	3.10	2.48	2.07	2732	2376	2168	2881
14.0	20.54	1.898	421.81	.98	1.51	1.91	2.30	.78	.68	.62	.81	5.76	3.74	2.96	2.46	3153	2749	2506	3274
16.0	23.47	2.169	550.93	.95	1.48	1.89	2.25	.65	.58	.52	.68	6.79	4.36	3.41	2.87	3432	3062	2745	3590
18.0	26.41	2.440	697.28	.93	1.45	1.87	2.21	.55	.48	.44	.58	7.81	5.00	3.88	3.29	3675	3207	2940	3875

V MPH	Qn				RHP			
	30°	40°	50°	60°	30°	40°	50°	60°
8.0					51.6	25.3	20.9	25.9
10.0					95.9	54.8	40.0	45.9
12.0					148	84.2	61.5	68.1
14.0					208	117	84.6	91.8
16.0					266	153	107	118
18.0					328	183	130	145

PRINCIPAL CHARACTERISTICS

L = 17.5 FT.

D = 2.92 FT.

Δ = 30002# PER ROTOR LBS.

∇ = 48.13 FT^3

e = 1.991 $\frac{LB\text{-}SEC^2}{FT.^4}$

$$J = \frac{V'}{n\nabla^{1/3}}$$

$$K_Q = \frac{Q}{eV'^2\nabla}$$

CHRYSLER DEFENSE ENGINEERING

DESIGN CALCULATIONS - BUOYANT SCREW

SHEET 4 OF 4

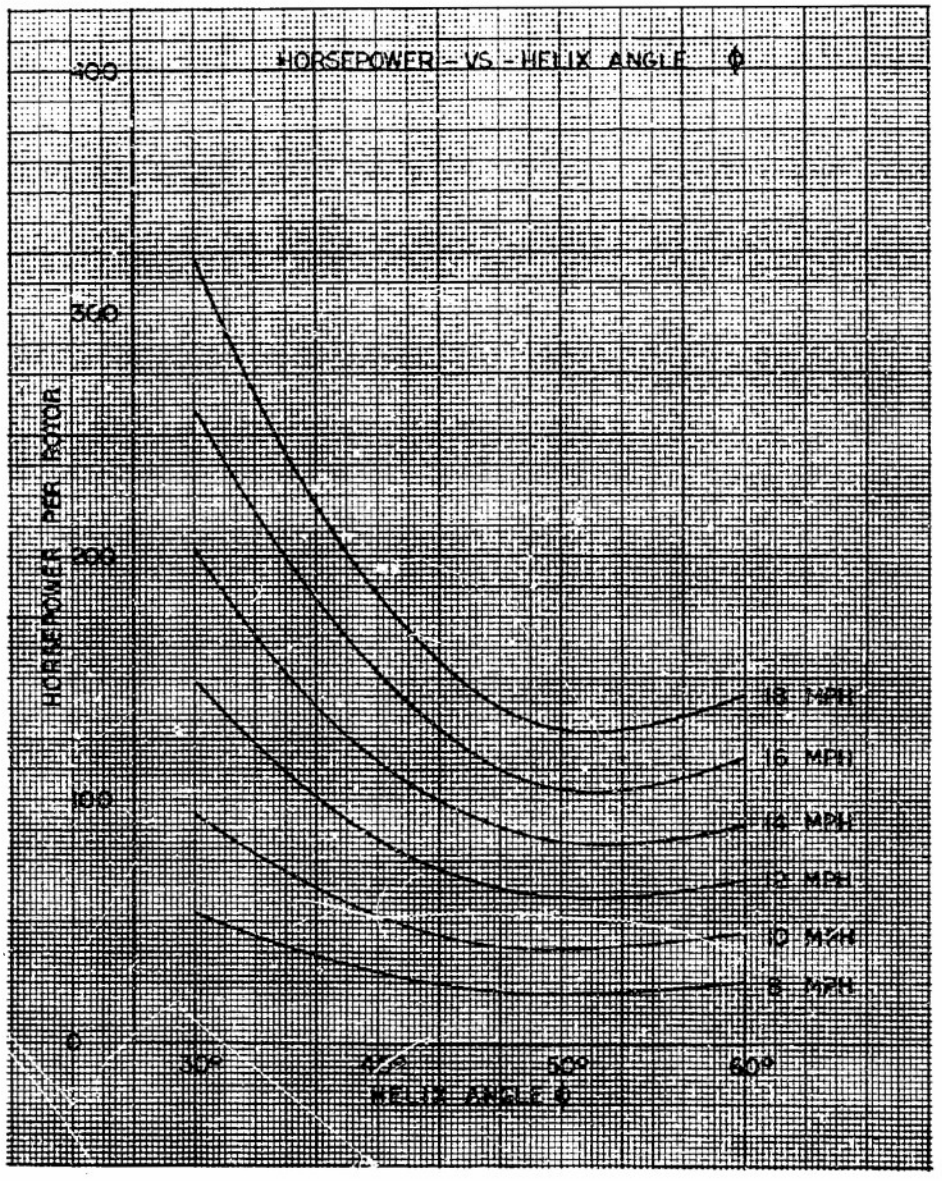

Figure 5-2 Horsepower vs. Helix Angle

Selection of an engine with at least the required net horsepower at 3600 RPM dictates a gear reduction of 15.5:1 for water performance.

SOIL PERFORMANCE:

In general, land vehicles designed for high mobility use drawbar pull or a drawbar pull/weight ratio for comparison. This is important because, in order to experience forward motion, the drawbar pull must be greater than zero and for it to maneuver adequately the DBP/W ratio must be in excess of 5 percent. The DBP/W is a measure of the vehicle's slope climbing capability. In sand, due to the angle of repose, grades in excess of 40 percent most likely would be considered as impractical. In extremely soft mud, slopes would not be expected and only maneuverability would be important. Hence, this amphibious vehicle must have a DBP/W ratio in excess of 0.05 for sufficient mobility over flat sandy beaches and mud flats. In order to guarantee that the vehicle does not become immobile a DBP/w ratio of 0.40 for sand will also be investigated.

Highest torque requirements occur for mobility over sand and therefore sand data will establish the low gear ratio. Examining the values of specific torque, T/Wr, for the various rotor configuration and the actual Marsh Screw Amphibian data in sand, a T/Wr = 1.3 appears to cover all conditions of operation with a satisfactory performance margin.

TABLE 5-I.

SPECIFIC TORQUE VALUES

ROTOR CONFIGURATION	% SLIP @ .05 $\frac{DBP}{W}$	$\frac{T}{Wr}$ @ % SLIP FOR .05 $\frac{DBP}{W}$
30° -0.460"	0.5%	0.90
40° -0.460"	25.0%	1.50
40° -0.625"	25.0%	1.25
40° -0.780"	22.5%	1.75

ALL VALUES WERE TAKEN AT 50% DISPLACEMENT

The torque requirement at the rotor is,

$T = 1.8(6000 \text{ lbs})(1.457 \text{ ft})$

$T = 15{,}750$ ft-lbs

It is assumed that the power plant selected has 360 FT-LBS of available torque from 1200 to 2900 RPM. The low gear ratio becomes

15,750 ft-lbs/360 ft-lbs

or a gear reduction of 43.8:1

The transmission gear spread then is

43.8/15.5 or 2.82 minimum

This is well within the range of standard automotive transmissions.

Thus for a rotor with a 50 degree helix angle, the pitch

$P = 2\pi r \tan \phi$

$P = 2(3.1416)(1.457)(1.1917) = 10.9$ ft

2900 RPM/43.8 = 66.2 RPM at rotor or 1.105 RPS at rotor

[% SLIP - 1.0] Pn = -V

.50(10.9 ft)(1.105 RPS) = 6.025 ft/sec

SPEED IN SAND, 4.1 MPH

If the vehicle is to climb grades up to 40% the gear ratio requirements are different. Again examination of values of specific torque, T/Wr, for various rotor configurations is made.

TABLE 5-2.

SPECIFIC TORQUE VALUES

ROTOR CONFIGURATION	% SLIP @ .40 $\frac{DBP}{W}$	$\frac{T}{Wr}$ @ % SLIP FOR .40 $\frac{DBP}{W}$
30° - .460"	20%	1.1
40° - .460"	40%	1.8
40° - .625"	40%	2.0
40° - .780	40%	2.3
50° - .460"	70%	0.8

ALL VALUES TAKEN AT 50% DISPLACEMENT

A specific torque of 2.5 appears to cover all conditions of operation and assumes an adequate performance margin. Thus the torque requirement at the rotor is,

T = 2.5(6000 lbs) (1.457 ft)

T = 21,800 ft lbs

again the same power plant is assumed and the low gear ratio becomes

21,800 ft-lbs/360 ft-lbs

or a gear reduction of 60.5:1

The required transmission gear spread is

60.5/15.5 or 3.9 minimum

This also is well within the range of a standard automotive transmission. For example, a Chrysler torque flight transmission has a 2.45:1 gear spread plus a 2:1 torque converter ratio with a net spread of 4.9:1.

2900 RPM/60.5 = 48.0 RPM at rotor

or 0.8 RPS at rotor

[% SLIP - 1.0] Pn - -V

0.30(10.9 ft)(1.105 RPS) = 3.6 ft/sec

SPEED UP a 40% grade in sand 2.45 MPH

Any significant increase in sand performance would require an engine with a comparable increase in power. Whether increased sand performance is necessary is dependent on a more specific functional requirement.

Mud performance is difficult to predict from the model test data because of the completely remolded condition of the soil used. Experience with the test vehicle in the same mud under natural conditions showed a very low level of specific torque and therefore it is logical to assume that torque and power requirements will fall between the water and sand requirements and are not an important consideration in the drive ratio selections.

Based on the above calculations a vehicle was conceived and is shown on figure 5-3.

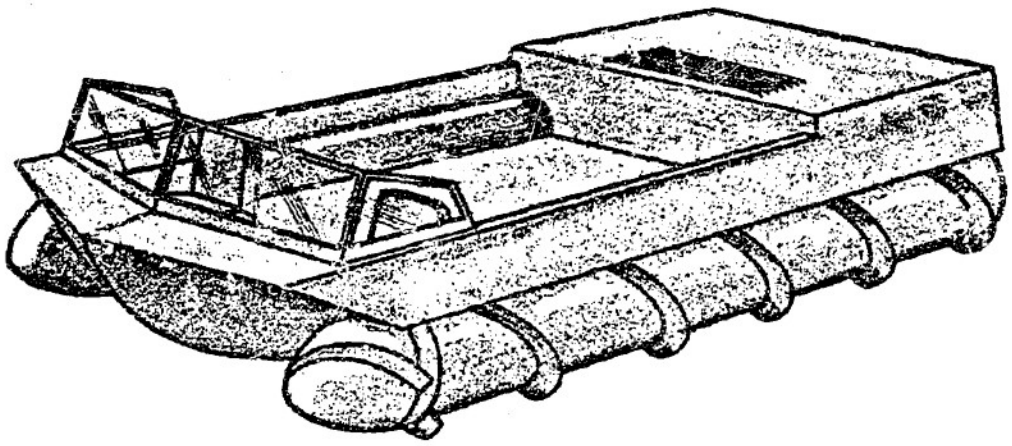

LENGTH	17'-6"
BEAM	10'-6"
ROTOR DIAMETER	2'-11"
BLADE HEIGHT	7"
NET WEIGHT	4000 LBS
GROSS WEIGHT	6000 LBS
HORSEPOWER	153 NET ENGINE
SPEED WATER	18.0 MPH
SAND	4.1 MPH

Figure 5-3 6000 Pound Logistic Vehicle

Section II

EXAMPLE II - GENERAL PURPOSE AMPHIBIAN

DESCRIPTION:

General Purpose Amphibian

- Payload capacity 5000 pounds
- Mobility over marginal terrains

SOIL PERFORMANCE:

Since all performance parameters are related to the gross weight of a vehicle, the designer is immediately faced with the problem of an appropriate payload/net weight ratio. A ratio of .5 will be used for this initial investigation. Thus the gross weight of the vehicle is 15,000 pounds. The validity of this assumption can only be proven after the vehicle design has progressed to a point where a valid weight analysis can be performed.

As stated in the previous example, mobility in sand results in the highest torque requirements. A 50 degree helix angle is selected based upon the available data and the blade height/diameter ratio of .1150 is selected. From Figure 4-10 a DBP/W = .05 is experienced at 35 percent slip. From Figure 4-11 the specific torque at 35 percent slip is .70. These values are based on a loading equivalent to 50 percent of the rotor hub. For a length diameter ratio of six

$$\forall = 7500 \text{ lbs}/62.4 \text{ lbs/ft}^3$$

$$\forall = 120 \text{ ft}^3$$

Therefore the rotor length of approximately 24.0 feet is required, and the rotor diameter is 4.0 feet. The torque required at the rotor is

$$T = .70\ (15{,}000\ \text{lbs})\ (2.063\ \text{ft})$$

$$T = 21700\text{-ft lbs}$$

A speed required in sand is assumed to be 5 MPH or 7.33 FPS. The pitch of the rotor is

$$p = 2\pi r \tan\phi$$

$$p = 2(3.1416)\ (2.063)\ (1.1917) = 15.5\ \text{ft}$$

$$[\%\ \text{Slip} - 1.0]\ pn = -V$$

$$(.35 - 1.0)\ 15.5n = -7.33$$

$$n = 7.33/(.65)\ (15.5)$$

$$n = .73\ \text{RPS} \quad \text{or} \quad 43.75\ \text{RPM}$$

HORSEPOWER REQUIRED

$$RHP = \frac{2\pi\ Qn}{550}$$

$$RHP = \frac{2(3.1416)\ (21700\ \text{ft-lbs})\ (.73/\text{sec})}{550\ \text{ft-lbs/sec/HP}}$$

$$RHP = 181$$

NET HORSEPOWER = 213

Based upon the above calculations a review of suitable power plants resulted in an engine which provides the required horsepower at 3600 RPM. The gear reduction required is

3600 RPM/43.75 RPM

or 82.4 : 1

The engine torque required at this RPM

$$T = 21{,}700 \text{ ft lbs}/82.4$$

$$T = 264 \text{ ft-lbs}$$

This provides mobility only over relatively flat ground. If we assume that the vehicle will frequently encounter slopes somewhat less than 40 percent then a DBP/W ratio of .40 is required. From Figure 4-10 the required DPB/W ratio is experienced at 70 percent slip. At this slip the specific torque is .80 as obtained from Figure 4-11. Therefore the torque required at the rotor is

$$T = .80\ (15{,}000 \text{ lbs})\ (2063 \text{ ft})$$

$$T = 24{,}800 \text{ ft-lbs}$$

A speed required for traversing sandy slopes is assumed to be 2 MPH or 2.94 FPX. The pitch of the rotor remains the same and the required rotor RPM is,

$$[\% \text{ Slip} - 1.0]\ pn = -V$$

$$[.70 - 1.0]\ 15.5 \text{ ft} = -2.94 \text{ ft/sec}$$

$$n = 2.94/(15.5)\ (.30)$$

$$n = .632 \text{ RPS} \quad \text{or} \quad 88 \text{ RPM}$$

HORSEPOWER REQUIRED

$$RHP = \frac{2\pi Qn}{550}$$

$$RHP = \frac{2(3.1416)\ (24{,}800 \text{ ft lbs})\ (.632/\text{sec})}{550 \text{ ft-lbs/sec/HP}}$$

$$RHP = 179$$

This is approximately the same power requirement as that for speed of 5 MPH on level sandy beaches. Since the engine selected provides the horsepower at 3600 RPM the gear reduction required is

3600 RPM/38 RPM

or 94.8 : 1

The engine torque required at this RPM is

$T = 24{,}800/94.3$

$T = 262$ ft-lbs

WATER PERFORMANCE:

Since a 50 degree helix angle and a blade height/diameter ratio of .1150 was specified, the water speed is desired for the previously specified horsepower. The horsepower calculations are figured for a 50 percent displacement condition. Inspection of the calculation sheet indicates that for a blunt end rotor a water speed of approximately 10.5 MPH will be met with 181 rotor horsepower. The calculations also indicate that 2.56 RPS at the rotor is required.

3600 RPM/2.56 RPS (60 min/sec)

23.4 : /1

The transmission gear spread is

94.8/23.4

4.05 Minimum

V MPH	V^1 FPS	F_∇	$V^{1\,2}$	% DISPLACEMENT = 50 H/D = .2344															
				J				$10K_Q$				n				Q			
				30°	40°	50°	60°	30°	40°	50°	60°	30°	40°	50°	60°	30°	40°	50°	60°
	10.0	.723	100.0			2.4				.85				.70				361	
	15.0	1.08	225.0			2.12				.91				1.19				870	
	20.0	1.445	400.0			2.0				.81				1.68				1375	
	25.0	1.81	625.0			1.93				.65				2.17				1725	
	15.0	1.08	225.0			1.6*				0.86*				1.57				940	

2 — APPROXIMATELY 9 KNOTS

* VALUES AT 75% Δ FOR A ROTOR WITH A DECREASED L&D BUT WITH A L/D = 6

V MPH	Qn				RHP			
	30°	40°	50°	60°	30°	40°	50°	60°
							29	
							118	
							264	
							428	
							169	

PRINCIPAL CHARACTERISTICS

L =	29.0	FT.
D =	4.84	FT.
Δ =	13,300	LBS.
∇ =	213.0	$FT.^3$
e =	1.991	$\frac{LB\text{-}SEC^2}{FT.^4}$

$$J = \frac{V^1}{n\nabla^{1/3}}$$

$$K_Q = \frac{Q}{\rho V^{1\,2}\nabla}$$

CHRYSLER DEFENSE ENGINEERING

DESIGN CALCULATIONS - BUOYANT SCREW

SHEET 1 OF 1

The gear spread is within the range of most standard automotive transmissions. Actually the horsepower requirements would be greater in water due to an unfavorable rotor spacing dictated by practical size limitations.

Section III

EXAMPLE III - LCVP TYPE CRAFT

DESCRIPTION:

LCVP type craft with emphasis placed on water performance.

WATER PERFORMANCE:

From the previous examples it is apparent that approximately 50 degrees helix angle and a blade height/diameter ratio of 0.2344 results in the most efficient rotor. This particular configuration was chosen to investigate the power requirements for this buoyant screw LCVP. The characteristics of the LCVP are described in the following table.

TABLE 5-3

CHARACTERISTICS OF LCVP

LENGTH	35' 9"
BEAM	10' 6-1/4"
DRAFT	3' 5"
FULL LOAD DISPLACEMENT	26,600 lbs
HOISTING WEIGHT	18,500 lbs
POWER - CONTINUOUS	165 HP
POWER - EMERGENCY	225 HP
SPEED AT FULL DISPLACEMENT	9 knots

Assuming a rotor displacement of 50 percent of the weight displacement and the latter being:

$$\nabla = 13{,}300 \text{ lbs}/(62.4 \text{ lbs/ft}^3) = 213 \text{ ft}^3$$

From Figure 5-1 a 29 foot rotor is selected and the diameter would be 4.84 feet. Horsepower calculations for this one configuration are tabulated on the calculation sheet. Assuming an optimum rotor spacing from rotor centerline to centerline of four diameters and considering allowances for a blunt end rotor the horsepower requirements would be approximately the same for the two vehicles.

The beam of the buoyant screw LCVP is not practical. At the expense of additional power requirements and reduced steering control the beam could be reduced further by using a rotor with a different L/D ratio and by reducing the rotor spacing.

If a rotor with a L/D = 10 is selected which we will assume is loaded to 75 percent of the rotor hub volume then the rotor length is approximately 35 feet long and 3.5 foot in diameter. The last row of calculations on the calculation sheet indicates values for a rotor at 75 percent rotor displacement and an L/D = 6 that the power required is about 50 percent greater than the larger rotor at 50 percent rotor displacement. These calculations are adjusted based upon Figure 3-37 for an L/D = 10. Extrapolation from this graph at 75 percent rotor displacement and at 10 MPH (approximately 9 knots) indicates a 100 percent additional horsepower penalty.

With a length/diameter ratio of 10 the rotor spacing is reduced to 14 feet. If a beam of 10.5 feet is desired a further horsepower penalty is realized. The rotor centerline spacing would be approximately two diameters and from Figure 3-58 a 30 percent additional horsepower penalty results.

This feasibility investigation has illustrated the limitation of applying the buoyant screw propulsion to an LCVP. Since the power requirements for the buoyant screw version are double that for the LCVP (the overall dimensions being similar for both vehicles) it remains for the military tacticians to decide whether the increased power requirements are offset by the increased mobility, that is the ability to cross sand bars, climb beaches, negotiate mud, and to operate in vegetation infested waters.

V MPH	V' FPS	F_∇	V'^2	% DISPLACEMENT = 50 H/D .1150															
				J				$10K_Q$				n				$Q10^{-2}$			
				30°	40°	50°	60°	30°	40°	50°	60°	30°	40°	50°	60°	30°	40°	50°	60°
8	11.7	922	138			1.48				1.08				1.601				348	
10	14.7	1.158	216			1.27				1.10				2.364				555	
12	17.6	1.386	310			1.17				1.01				3.055				733	
14	20.5	1.614	421			1.12				.93				3.705				916	
16	23.5	1.846	549			1.08				.84				4.41				1075	
18	26.5	2087	701			1.06				.77				5.07				1261	

V MPH	Qn				RHP			
	30°	40°	50°	60°	30°	40°	50°	60°
8							63.6	
10							150	
12							255	
14							398	
16							541	
18							704	

PRINCIPAL CHARACTERISTICS

L = 24.75 FT.

D = 4.125 FT.

Δ = 15,000 LBS.

∇ = 120.5 $FT.^3$

e = 1.936 $\frac{LB\text{-}SEC^2}{FT.^4}$

$$J = \frac{V'}{n\nabla^{1/3}}$$

$$K_Q = \frac{Q}{eV'^2\nabla}$$

CHRYSLER DEFENSE ENGINEERING

SHEET 1 OF 1

DESIGN CALCULATIONS - BUOYANT SCREW

APPENDIX A

LIST OF SYMBOLS

APPENDIX A

LIST OF SYMBOLS

c	COHESION COEFFICIENT
D	DIAMETER
DBP	DRAW BAR PULL
f	COEFFICIENT OF FRICTION
F_∇	FROUDE VOLUME NUMBER
g	ACCELERATION OF GRAVITY
J	ADVANCE COEFFICIENT
K_Q	NONDIMENSIONAL TORQUE CONSTANT
L	LENGTH
M	MASS
m	AS A SUBSCRIPT DENOTES QUANTITY PERTAINING TO A MODEL
n	NUMBER OF REVOLUTIONS PER SECOND
p	PITCH - ft
p	AS A SUBSCRIPT DENOTES QUANTITY PERTAINING TO A PROTOTYPE
Q	TORQUE - ft lbs
r	HUB RADIUS-ft
R	REYNOLDS NUMBER
RHP	THE TERM HORSEPOWER USED THROUGHOUT THE TEXT FOR BOTH PREDICTED AND ACTUAL VEHICLE HORSEPOWER IS A DELIVERED HORSEPOWER TO THE ROTOR EXCLUSIVE OF ALL INTERMEDIATE LOSSES, RHP, AND IS DEFINED AS FOLLOWS:

$$RHP = \frac{2\pi Qn}{550}$$

WHERE Q = TORQUE IN ft lbs AT THE ROTOR

n = ROTOR REVOLUTIONS PER SECOND

THE HORSEPOWER DELIVERED TO THE ROTOR WILL BE LESS THAN THE SHAFT HORSEPOWER DUE TO DRIVE TRAIN INEFFICIENCY, n = DRIVE TRAIN EFFICIENCY, THEREFORE

THE NET ENGINE HORSEPOWER EQUALS $\frac{RHP}{n}$

T	TORQUE - ft lbs
V	VELOCITY
W	WEBER NUMBER
W	WEIGHT
π_i	DENOTES DIMENSIONLESS PARAMETERS
Δ	DISPLACEMENT pounds
∇	DISPLACEMENT cubic feet
ρ	DENSITY
μ	VISCOSITY
ν	KINEMATIC VISCOSITY
ϕ	ANGLE OF INTERNAL FRICTION
θ	HELIX ANGLE
σ	SURFACE TENSION COEFFICIENT
λ	SCALE FACTOR

APPENDIX B

DIMENSIONAL ANALYSIS

APPENDIX B

DIMENSIONAL ANALYSIS

MARSH SCREW ROTOR IN WATER

The following variables are considered to be influential whe.. performing a dimensional analysis on torque. The M, L, T system of units is used.

VARIABLES	UNITS
D	L
n	L^{-1}
V	LT^{-1}
ν	L^2T^{-1}
ρ	ML^{-3}
σ	MT^{-2}
g	LT^{-2}

$$Q = f(D,n,V,\nu,\rho,\sigma,g)$$

$$\text{i.e., } \pi_1 = D^{x_1} V^{y_1} \rho^{z_1} n$$

$$M^oL^oT^o = (L)^{x_1}(LT^{-1})^{y_1}(ML^{-3})^{z_1}T^{-1}$$

$$M: z_1 = 0$$

$$L: x_1 + y_1 - 3z_1 = 0;\ x_1 + y_1 = 0$$

$$T: 0 = +y_1 + 1;\ y_1 = -1 \therefore x_1 = +1$$

$$\pi_1 = \frac{DN}{V} : \text{ Advance Coefficient}$$

$$\pi_2 = D^{x_2} V^{y_2} p^{z_2} \nu$$

$$M^{\circ}L^{\circ}T^{\circ} = (L)^{x_2} (LT^{-1})^{y_2} (ML^{-3})^{z_2} L^2T^{-1}$$

M: $0 = z_2$

L: $0 = x_2 + y_2 + 2 = 0$; $x_2 + y_2 + 2 = 0$

T: $0 = -y_2^{-1}$, $y_2 = -1$; $x_2 = -1$

$0 = -y_2 - 1$

$\pi_2 = \frac{\nu}{DV}$ Reynolds Number

$$\pi_3 = D^{x_3} V^{y_3} p^{z_3} \sigma$$

$$M^{\circ}L^{\circ}T^{\circ} = (L)^{x_3} (LT^{-1})^{y_3} (ML^{-3})^{z_3} MT^{-2}$$

M: $0 = z_3 + 1$; $z_3 = -1$

L: $0 = x_3 + y_3 - 3z_3$; $x_3 + y_3 + 3 = 0$

T: $0 = -y_3 - 2$; $y_3 = -2$ $x_3 = -1$

$\pi_3 = \frac{\sigma}{DV^2 p}$ Weber Number

$$\pi_4 = D^{x_4} V^{y_4} \rho^{z_4} Q$$

$$M^\circ L^\circ T^\circ = (L)^{x_4} (LT^{-1})^{y_4} (ML^{-3})^{z_4} ML^2T^{-2}$$

M: $0 = z_4 + 1$; $z_4 = -1$

L: $0 = x_4 + y_4 - 3z_4 + 2$; $x_4 + y_4 + 5 = 0$

T: $0 = -y_4 - 2$; $y_4 = -2$; $x_4 = -3$

$$\pi_4 = \frac{Q}{D^3V^2\rho} \quad \text{But } (nD)^2 = V^2$$

$$\therefore \pi_4 = \frac{Q}{\rho n^2 D^5} = K_Q \quad \text{Torque Parameter}$$

$$\pi_5 = D^{x_5} V^{y_5} \rho^{z_5} g$$

$$M^\circ L^\circ T^\circ = (L)^{x_5} (LT^{-1})^{y_5} (ML^{-3})^{z_5} LT^{-2}$$

M: $0 = z_5$

L: $0 = x_5 + y_5 + 1$

T: $0 = -y_5 - 2$: $y_5 = -2$ $\therefore x_5 = 1$

$$\pi_5 = \frac{Dg}{V^2} \quad \text{Froude Number}$$

MARSH SCREW ROTOR IN SOILS

The following variables are considered to be influential when performing a dimensional analysis on drawbar pull. The M, L, T, system of units is used

VARIABLES	UNITS
D	L
n	T^{-1}
V	LT^{-1}
c	$ML^{-1}T^{-2}$
W	MLT^{-2}
f	-
ϕ	-
g	LT^{-2}

$$DBP = f(D,n,V,c,W,f,\phi,g)$$

$$\pi_1 = n^{x_1} V^{y_1} W^{z_1} c$$

$$M^oL^oT^o = (T^{-1})^{x_1} (LT^{-1})^{y_1} (MLT^{-2})^{z_1} ML^{-1}T^{-2}$$

$$M: \quad 0 = z_1 + 1 \qquad z_1 = -1$$

$$L: \quad 0 = y_1 + z_1 - 1 \qquad y_1 = z$$

$$T: \quad 0 = -x_1 - y_1 - 2z_1 - 2$$

$$-x_1 - (2) - 2(-1) - 2$$

$$-x_1 - 2 \qquad \therefore x_1 = -2$$

$$\pi_1 = \frac{\sigma V^2}{Wn^2} \times \pi_2 = \frac{cD^2}{W}$$

$$\pi_2 = n^{x_2} V^{y_2} W^{z_2} D$$

$$M^oL^oT^o = (T^{-1})^{x_2} (LT^{-1})^{y_2} (MLT^{-2})^{z_2} L$$

M: $0 = z_1$ $z_1 = 0$

L: $y_2 + z_1 + 1$ $y_2 = -1$

T: $-x_2 - y_2 - 2z_2 = x_2 - (-1) - 2(0)$

$x_2 = +1$

$$\pi_2 = \frac{Dn}{V}$$ Advance Coefficient

$$\pi_3 = n^{x_3} V^{y_3} W^{z_3} g$$

$$M^oL^oT^o = (T^{-1})^{x_3} (LT^{-1})^{y_3} (MLT^{-2})^{z_3} LT^{-2}$$

M: $0 = z_3 = 0$

L: $0 = y_3 + z_3 + 1$ $y_3 = -1$

T: $0 = -x_3 - y_3 - 2z_3 - 2$

$-x_3 - (-1) - 2$

$-x_3 - 1$ $x_3 = -1$

$$\pi_3 = \frac{g}{nV} \times \pi_2 = \frac{Dg}{V2}$$: Froude Number

$$\pi_4 = \phi$$

$$\pi_5 = f$$

$$\pi_6 = n^{x_6} V^{y_6} W^{z_6} DBP$$

$$M^oL^oT^o = (T^{-1})^{x_6} (LT^{-1})^{y_6} (MLT^{-2})^{z_6} MLT^{-2}$$

M: $0 = z_6 + 1$ $z_6 = -1$

L: $0 = y_6 + z_6 + 1$ $y_6 = 1 + 1 = 0$

T: $0 = -x_6 - y_6 - 2z_6 - 2$ $-y_6 - 2(-1) - 2 = 0$

$$\pi_6 = \frac{DBP}{W}$$

APPENDIX C

DEFINITION OF A FRICTIONAL TORQUE LINE

APPENDIX C

DEFINITION OF A FRICTIONAL TORQUE LINE

As stated previously if it were possible to define a frictional torque line analogous to a flat plate friction line as used for extrapolation in the ship model case as well as properly determining the spray scale effect, expansion of rotor torque might be handled in the same manner as ship model resistance expansion. Flat plate friction lines characteristically have high negative slope at low Reynolds numbers with decreasing slope as Reynolds number increases. At high enough Reynold number, the change in friction coefficient becomes a small percentage of the total resistance coefficient. The slope of the friction line, rather than the magnitude, is the predominant factor. With this in mind simplifying assumptions were made in order to estimate an equivalent frictional torque line.

1. The flow follows a helical path, guided by the blades.
2. In the case chosen, 50 percent displacement, the effective length for computing Reynolds number is half the helical distance from one end of the rotor to the other.
3. The velocity for computing Reynolds number is the vector summation of the rotary and advance velocities.
4. At the Reynolds number computed by second and third assumptions the flat plate friction coefficient, using the 1947 A.T.T.C. line, may be multiplied by the hub

radius and the cosine of the helix angle to obtain the equivalent frictional torque coefficient.

The computations were made for a 50-degree helix angle, 1.56-inch blade height rotor and the resulting line is shown in the following figure. The slope of the line is extremely flat at the higher Reynolds numbers so that, under the above assumptions, one can assume very little frictional scale effect in going from the model data to full scale.

Since the possibility of scale effect on the spray component still exists, an analysis of the scaling of the spray drag is desirable. Unfortunately, there is no direct method analogous to the ship case as there was for the frictional component. It can be reasoned that less frictional scale effect and more spray scale effect exist at the high helix angles and the reverse exists at low helix angles. Certainly the exact percentage would be dependent upon trim, speed, blade height, etc. Since the nondimensional torque constant is approximately, independent of the Weber number, then we are justified in relaying the condition of complete similarity and extrapolating the model data by Froudes Law.

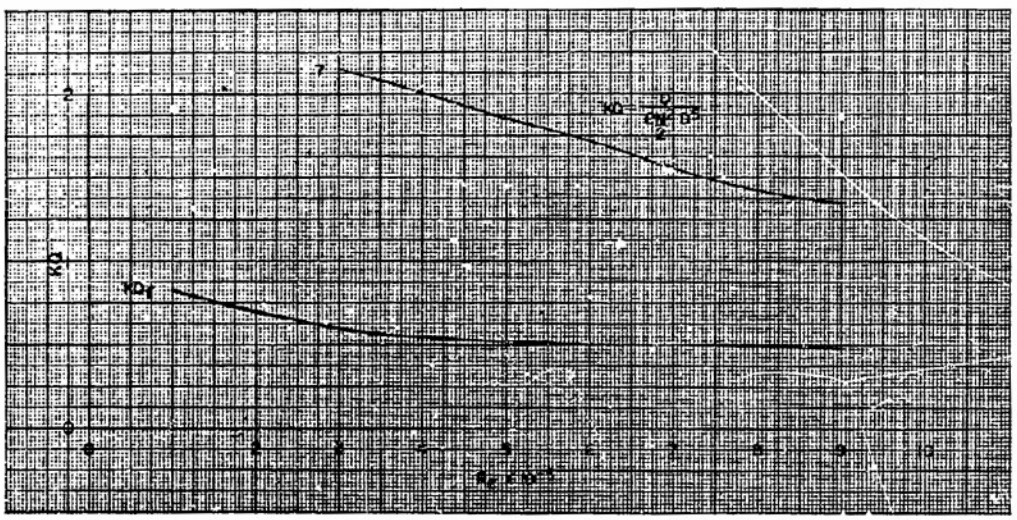

Figure C-1 Non-Dimensional Torque Constant vs Reynolds Number

APPENDIX D

COMPUTER CALCULATIONS

APPENDIX D

COMPUTER CALCULATIONS

The following velocities and Froude volume numbers were used to determine the data listed in this appendix.

VELOCITY MPH	VELOCITY FPS	VELOCITY FPS^2	FROUDE VOL NUMBER
8.000	11.736	137.73	1.085
10.000	14.670	215.21	1.356
12.000	17.604	309.90	1.627
14.000	20.538	421.81	1.898
16.000	23.472	550.93	2.169
18.000	26.406	697.28	2.440

HELIX ANGLE = 30°

DISPLACEMENT CUBIC FEET		BLADE HEIGHT DIAMETER RATIO		
48.1300			0.1150	
VELOCITY FPS	RPS	RPM	Q	SHP
11.736	4.420	265.18	1451.84	73.30
14.670	5.761	345.68	2041.66	134.38
17.604	7.333	439.96	2643.02	221.40
20.538	8.822	529.33	3193.23	321.83
23.472	10.408	624.46	3748.40	445.67
26.406	11.901	714.03	4276.34	581.38

HELIX ANGLE = 40°

DISPLACEMENT CUBIC FEET		BLADE HEIGHT DIAMETER RATIO		
48.1300			0.1150	
VELOCITY FPS	RPS	RPM	Q	SHP
11.736	3.073	184.36	1319.86	46.33
14.670	4.033	241.98	1938.54	89.31
17.604	5.094	305.66	2553.93	148.63
20.538	6.205	372.27	3112.39	220.61
23.472	7.250	435.02	3695.60	306.10
26.406	8.249	494.96	4209.52	396.70

HELIX ANGLE = 50°

DISPLACEMENT CUBIC FEET		BLADE HEIGHT DIAMETER RATIO		
48.1300			0.1150	
VELOCITY FPS	RPS	RPM	Q	SHP
11.736	2.444	146.65	1451.84	40.54
14.670	3.418	205.07	2103.52	82.13
17.604	4.360	261.60	2732.11	136.08
20.538	5.228	313.68	3314.49	197.95
23.472	6.087	365.25	3906.78	271.69
26.406	6.914	414.82	4476.79	353.58

HELIX ANGLE = 60°

DISPLACEMENT CUBIC FEET		BLADE HEIGHT DIAMETER RATIO		
48.1300			0.1150	
VELOCITY FPS	RPS	RPM	Q	SHP
11.736	2.180	130.80	1808.21	45.03
14.670	3.055	183.32	2495.36	87.10
17.604	3.903	234.17	3177.56	141.68
20.538	4.705	282.31	3839.96	206.40
23.472	5.515	330.91	4434.72	279.41
26.406	6.312	378.75	4944.52	356.57

HELIX ANGLE = 30°

DISPLACEMENT CUBIC FEET		BLADE HEIGHT DIAMETER RATIO		
48.1300			0.1563	
VELOCITY FPS	RPS	RPM	Q	SHP
11.736	3.545	212.73	1425.45	57.74
14.670	4.689	281.37	2124.15	113.80
17.604	5.902	354.11	2821.20	190.21
20.538	7.147	428.82	3476.18	283.82
23.472	8.490	509.43	4012.37	389.18
26.406	9.810	588.60	4409.98	494.22

HELIX ANGLE = 40°

DISPLACEMENT CUBIC FEET		BLADE HEIGHT DIAMETER RATIO		
48.1300			0.1563	
VELOCITY FPS	RPS	RPM	Q	SHP
11.736	2.372	142.34	1306.66	35.41
14.670	3.126	187.58	2021.03	72.18
17.604	3.935	236.08	2761.80	124.14
20.538	4.745	284.68	3395.34	184.04
23.472	5.563	333.76	3906.78	248.27
26.406	6.368	382.07	4276.34	311.09

HELIX ANGLE = 50°

DISPLACEMENT CUBIC FEET		BLADE HEIGHT DIAMETER RATIO		
48.1300			0.1563	
VELOCITY FPS	RPS	RPM	Q	SHP
11.736	1.898	113.87	1135.08	24.61
14.670	2.569	154.13	1814.81	53.26
17.604	3.226	193.58	2553.93	94.13
20.538	3.867	232.03	3233.65	142.86
23.472	4.544	272.65	3748.40	194.59
26.406	5.185	311.11	4142.71	245.40

HELIX ANGLE = 60°

DISPLACEMENT CUBIC FEET		BLADE HEIGHT DIAMETER RATIO		
48.1300			0.1563	
VELOCITY FPS	RPS	RPM	Q	SHP
11.736	1.638	98.27	1531.04	28.65
14.670	2.192	131.51	2186.02	54.74
17.604	2.765	165.93	2910.29	91.94
20.538	3.321	199.28	3597.44	136.49
23.472	3.887	233.23	4223.55	187.56
26.406	4.426	265.59	4677.25	236.52

HELIX ANGLE = 30°

DISPLACEMENT CUBIC FEET		BLADE HEIGHT DIAMETER RATIO		
48.1300			0.1950	
VELOCITY FPS	RPS	RPM	Q	SHP
11.736	3.226	193.58	1346.26	49.62
14.670	4.290	257.42	1938.54	95.01
17.604	5.377	322.64	2524.23	155.06
20.538	6.565	393.92	3071.97	230.40
23.472	7.774	466.46	3537.22	314.16
26.406	8.962	537.73	4009.07	410.46

HELIX ANGLE = 40°

DISPLACEMENT CUBIC FEET		BLADE HEIGHT DIAMETER RATIO		
48.1300			0.1950	
VELOCITY FPS	RPS	RPM	Q	SHP
11.736	2.109	126.52	1240.67	29.89
14.670	2.725	163.50	1794.18	55.85
17.604	3.384	203.06	2286.65	88.41
20.538	4.033	241.98	2789.03	128.50
23.472	4.745	284.68	3273.25	177.42
26.406	5.417	325.05	3674.98	227.44

HELIX ANGLE = 50°

DISPLACEMENT CUBIC FEET		BLADE HEIGHT DIAMETER RATIO		
48.1300			0.1950	
VELOCITY FPS	RPS	RPM	Q	SHP
11.736	1.646	98.77	1135.08	21.35
14.670	2.216	132.96	1670.45	42.29
17.604	2.797	167.85	2138.17	68.33
20.538	3.361	201.65	2586.92	99.32
23.472	3.959	237.52	3062.07	138.48
26.406	4.683	281.01	3474.53	185.90

HELIX ANGLE = 60°

DISPLACEMENT CUBIC FEET		BLADE HEIGHT DIAMETER RATIO		
48.1300			0.1950	
VELOCITY FPS	RPS	RPM	Q	SHP
11.736	1.574	94.43	1491.44	26.82
14.670	2.101	126.03	2124.15	50.97
17.604	2.630	157.81	2732.11	82.09
20.538	3.137	188.21	3314.49	118.77
23.472	3.625	217.51	3801.19	157.42
26.406	4.172	250.32	4276.34	203.82

HELIX ANGLE = 30°

DISPLACEMENT CUBIC FEET		BLADE HEIGHT DIAMETER RATIO		
48.1300			0.2344	
VELOCITY FPS	RPS	RPM	Q	SHP
11.736	2.830	169.81	1597.03	51.63
14.670	3.769	226.15	2227.26	95.90
17.604	4.745	284.68	2732.11	148.09
20.538	5.761	345.68	3152.81	207.51
23.472	6.792	407.54	3431.63	266.28
26.406	7.806	468.34	3674.98	327.71

HELIX ANGLE = 40°

DISPLACEMENT CUBIC FEET		BLADE HEIGHT DIAMETER RATIO		
48.1300			0.2344	
VELOCITY FPS	RPS	RPM	Q	SHP
11.736	1.920	115.23	1333.06	29.25
14.670	2.489	149.37	1917.92	54.55
17.604	3.102	186.14	2375.75	84.20
20.538	3.739	224.35	2748.61	117.41
23.472	4.360	261.60	3062.07	152.52
26.406	5.006	300.39	3207.26	183.43

HELIX ANGLE = 50°

DISPLACEMENT CUBIC FEET		BLADE HEIGHT DIAMETER RATIO		
48.1300			0.2344	
VELOCITY FPS	RPS	RPM	C	SHP
11.736	1.522	91.31	1201.07	20.88
14.670	1.997	119.79	1752.94	39.98
17.604	2.482	148.91	2167.87	61.46
20.538	2.956	177.37	2506.08	84.63
23.472	3.414	204.85	2745.31	107.08
26.406	3.882	232.92	2939.98	130.38

HELIX ANGLE = 60°

DISPLACEMENT CUBIC FEET		BLADE HEIGHT DIAMETER RATIO		
48.1300			0.2344	
VELOCITY FPS	RPS	RPM	C	SHP
11.736	1.291	77.43	1755.41	25.88
14.670	1.667	99.99	2412.87	45.94
17.604	2.068	124.09	2880.59	68.06
20.538	2.455	147.29	3274.07	91.82
23.472	2.868	172.07	3590.91	117.62
26.406	3.285	197.09	3875.43	145.43

APPENDIX E

REFERENCES

APPENDIX E

REFERENCES

WATER PERFORMANCE

L. B. Chapman & H. E. Possell, Principles of Naval Architecture, Vol II, published by the Society of Navel Architects and Marine Engineers, New York, New York 1939, 12th printing 1962.

H. L. Langhaar, Dimensional Analysis and Theory of Models , John Wiley & Sons Inc 1951

J. L. Moss, "Marsh Screw Vehicle Rotor Model Test Results" Office or Research Administration, University of Michigan, January, 1964.

J. L. Moss, "Systematic Investigation of Marsh Screw Rotor Water Propulsion" Office of Research Administration, University of Michigan, March, 1965.

Harold E. Saunders, Hydrodynamics in Ship Design, published by the Society of Naval Architects and Marine Engineers, New York, New York.

F. H. Todd "The Fundamentals of Ship Model Testing" TSNAME, 1951.

SOIL PERFORMANCE

M. G. Bekker, Theory of Land Locomotion, the Univeristy of Michigan Press, 1956, Chapter II.

I. R. Erhlich & H. Dugoff "Systematic Test of Marsh Screw Rotors in Soil" Davidson Laboratory, Stevens Institute of Technology.

C. J. Nuttail Jr., R. P. McGowan, "Scale Models of Vehicles in Soils and Snows", Proceedings of the 1st International Conference on the Mechanics of Soil-Vehicle Systems, 1961.

E. T. Vincent et All "Rigid Wheel Studies by Means of Dimensional Analysis". Report No. 7841 Land Locomotion Laboratory, US Arm Tank-Automotive Center.